**Meandering in Gravel-Bed Rivers**

By

Christian Arthur Braudrick

A dissertation submitted in partial satisfaction of the
requirements for the degree of
Doctor of Philosophy

in

Earth and Planetary Science

in the

Graduate Division

of the

University of California, Berkeley

Committee in charge:

Professor William E. Dietrich, Chair
Professor Michael Manga
Professor Leonard Sklar
Professor Mark Stacey

Fall 2013

# Meandering in Gravel-Bed Rivers



by

Christian Arthur Braudrick

# Abstract

Meandering in Gravel-Bed Rivers

By

Christian Arthur Braudrick

Doctor of Philosophy in Earth and Planetary Science

University of California, Berkeley

William E. Dietrich, Chair

It is surprising that gravel-bed rivers meander. In laboratory settings using cohesionless sediment transported as bedload, braiding inevitably emerges. The easily entrained outer bank sediments lead to relatively rapid bank erosion, the inner bank bar reaches it shallowest depth towards the center of the channel, the flow diverges, and braiding arises. These observations have led to the inference that meandering requires some bank strength to slow outer bank erosion and allow the inner bank to keep pace with outer bank retreat. Commonly it has been suggested that vegetation can provide that outer bank strength. While this view has led recently to numerical modeling incorporating vegetation strength, no studies had successfully created meandering rivers in the laboratory such that controlling mechanisms could be explored. Nor has there been an effort to delineate under what general conditions gravel bedded meanders are found in the field. These knowledge gaps are particularly important to stream restoration work because the creation of morphologically-stable gravel-bedded meanders is a common goal.

This dissertation uses flume experiments and a compilation of field data to explore the conditions that support meandering in gravel-bed rivers. Using alfalfa sprouts as model vegetation, sand as scaled-down gravel, and a lightweight plastic as scaled-down sand, I created for the first time a self-maintaining, laterally migrating meandering river with cutoff loops in a 6.1-m wide, 17-m long laboratory flume. The channel, 0.4 m wide, had a sinuosity of 1.1-1.2 and transported sediment with a median size of 0.78 mm. The sinuosity of the channel increased as bends grew, decreased as the channel cut off, and was regenerated while the channel maintained a steady width. In this experiment, we found that a steady bankfull flow was sufficient to sustain a meandering planform, and that application of higher peak flows caused the channel to widen because bank erosion outpaced bar growth. Coarse sediment was exchanged between eroding banks and the next bar downstream with little net downstream flux, consequently to prevent aggradation and avulsion at the upstream end of the experimental reach required turning off the coarse sediment feed. The input of fine sediment was crucial for blocking chute channels (a locus for braiding), filling point bars downstream of the bend apex, and plugging abandoned channels following cutoff. Hence, sustained growth of bends and development of meandering requires more than just sufficient bank strength to slow the outer bank erosion rate.

A compilation of 166 gravel-bedded meanders from the literature shows that gravel meanders primarily occur in lower gradient reaches extending from mountain ranges, high-elevation valleys, and in humid areas influenced by glaciation or glacio-fluvial outwash.

Unexpectedly, analysis of Google Earth imagery showed that about 1/3 of the dataset lacked cutoff scars and other evidence of active migration. Gravel bedded meanders with median surface grain size> 10 mm had low Shields stress, particularly for meanders with cutoffs and without islands. Gravel bedded meanders with median surface grain sizes < 10 mm had higher Shields stresses that were transitional between coarser gravel bedded meanders and finer sand bedded meanders. Calculation of potential sediment transport rates show that for 16 of the 18 gravel bedded meanders with migration rate data, the sediment flux from bank erosion exceeds this transport capacity, suggesting that bank erosion is a primary source of sediment. Collectively this shows that gravel bedded meanders can be classed into different types that reflect the relative migration rates and associated Shield stress and that generally gravel-bedded meanders are associated with low Shield stresses and relatively low sediment supply.

Because of the importance of sediment supply in meandering rivers, I also investigated the morphological effects of doubling supply to a self-formed sinuous channel with 9 bends that was fixed in place. Five of these bends developed bar-pool topography. The doubling of supply caused the channel to steepen by 33%, and the topographic response of bars was limited to shoaling of two pools as they filled with coarse sediment. One of the bars also extended upstream. Three other bends had limited changes to an increase in supply, likely due to the fixed walls that supported wide bars and narrow, deep pools. The maximum aggradation was greater than a channel depth, indicating that for a similar supply increase in a freely migrating channel would lead to avulsion. This experiment supports further the interpretation that gravel-bedded meanders are associated with relatively low sediment supply.

The final experiment replicated our first alfalfa experiment but used a constant discharge and sediment supply with much denser alfalfa, in order to explore the effect of increased bank strength on channel morphodynamics. The denser alfalfa led to a narrower channel, but the migration rate was similar to our first experiment. As the channel migrated, associated decreases in the water surface slope caused the style of migration to change from focused on the entire bend to focus at the bend apex, creating skewed bends. As the bend skewness increased, the sediment flux at the flume outlet decreased, and most of the sediment flux out of the experimental reach was the lightweight plastic (model sand) rather than the coarse sediment supply. This created a channel with a sinuosity of 1.6, but then the channel aggraded and cut off, decreasing the sinuosity (to 1.2) and a corresponding increased slope. Following the cutoffs, the sediment transport rates and channel migration rates increased. The steady flow discharge and dense alfalfa limited cutoffs until aggradation altered floodplain hydrology to suppress alfalfa growth and create relatively weak paths through the floodplain.

Taken together these studies show that for gravel bedded rivers to meander three conditions are needed: 1) additional bank strength (here from vegetation) to slow erosion rates' 2) low sediment supply and correspondingly low Shields stresses to prevent aggradation and avulsion as sinuosity increases; and 3) fine sediment to fill chutes and the downstream end of bars. Variable peak discharges are not necessary but may contribute to cutoffs that maintain a steeper slope able to transport the sediment supplied to the reach. These observations suggest that creating a self-maintaining laterally migrating gravel-bedded river as a restoration outcome will require an assessment of likely coarse and fine sediment supply as well as the ability of vegetation to provide sufficient bank strength.

# Contents

List of Figures ..... ii

List of Tables ..... iv

Acknowledgements ..... iv

1 Introduction ..... 1

2 Necessary conditions for sustained meandering in coarse bedded rivers: experimental evidence ..... 6

2.1 Abstract ..... 6
2.2 Introduction ..... 6
2.3 Experimental methods ..... 7
2.4 Results ..... 9
2.5 Discussion ..... 11
2.6 Conclusions ..... 14
2.7 Acknowledgements ..... 14
2.8 Tables ..... 15
2.9 Figures ..... 16

3 Where do gravel bedded rivers meander? ..... 22

3.1 Abstract ..... 22
3.2 Introduction ..... 22
3.3 Methods ..... 26
3.3.1 Characteristics of gravel meanders database ..... 26
3.3.2 Data Analysis ..... 27
3.4 Results ..... **Error! Bookmark not defined.**
3.4.1 Geographic Distribution of Gravel Meanders ..... 29
3.4.2 Slope, discharge, and sinuosity of gravel meanders ..... 29
3.4.3 Bank vegetation and channel width-depth ratio ..... 30
3.4.4 Sediment supply ..... 31
3.5 Discussion ..... 34
3.5.1 Spatial bias in river databases ..... 34
3.5.2 Sediment supply and channel migration ..... 34
3.5.3 Channel planform, width to depth ratio, and bankfull $\tau^*$ ..... 36
3.6 Conclusions ..... 37
3.7 Acknowledgements ..... 39
3.8 Tables ..... 40
3.9 Figures ..... 42

4 The response of fixed-wall meandering channel to increased sediment supply ..... 60

4.1 Abstract ..... 60
4.2 Introduction ..... 60
4.3 Methods ..... 63

4.4 Results ..... 65
4.4.1 Low (6 kg/hr) feed rate (-27.5 to 0 hrs) ..... 65
4.4.2 Increased supply ..... 66
4.5 Discussion ..... 69
4.5.1 Topographic change in response to increased supply ..... 69
4.5.2 Slope and depth changes to the sediment transport rate ..... 70
4.5.3 Comparison with previous experiments ..... 71
4.5.4 Bank erosion and sediment supply ..... 72
4.6 Conclusions ..... 73
4.7 Acknowledgements ..... 73
4.8 Tables ..... 74
4.9 Figures ..... 75

5 Meandering river dynamics under constant boundary conditions ..... 95

5.1 Introduction ..... 95
5.2 Methods ..... 97
5.2.1 Differences with the previous experiment ..... 99
5.3 Results ..... 100
5.3.1 Description of bar growth and bank erosion ..... 100
5.3.2 Morphologic evolution ..... 101
Sediment Flux ..... 102
5.3.4 Water surface slope and sinuosity ..... 103
5.3.5 Channel geometry ..... 103
5.3.6 Migration Rates ..... 104
5.3.7 Summary of results ..... 105
5.4 Discussion ..... 105
5.4.1 Comparison with 2009 experiment ..... 106
5.4.2 Revised time scaling and comparison of migration rates ..... 106
5.4.3 Controls on the change in the pattern of migration ..... 107
5.4.4 Comparison with field channels ..... 107
5.5 Conclusions ..... 108
5.6 Tables ..... 110
5.7 Figures ..... 112

6 Bibliography ..... 129

Appendix A-Supplemental Video 1 ..... 143

Appendix B-Morphologic river data used in Chapter 3 ..... 144

Appendix C-Enlarged Depth and Facies maps from Chapter 4 ..... 167

Appendix D-Enlarged Topographic maps and videos from Chapter 5 ..... 185

Appendix E-References used in the apendices ..... 204

## List of Figures

Figure 2.1. Map of channel position through time. 16
Figure 2.2. Discharge, channel width, and sinuosity change with time. 17
Figure 2.3. Cumulative sediment feed for coarse (black) and fine (gray) sediment. 18
Figure 2.4. Overhead photograph and shaded topographic image 103 hours after the beginning of the experiment. 19
Figure 2.5. Sediment facies in of second and third bars downstream from the flume inlet. 20
Figure 2.6. Photograph of cutoff channel and fine sediment filling the former channel. 21
Figure 3.1. Google Earth aerial photographs of meanders with cutoffs 42
Figure 3.2. Google Earth aerial photographs of meanders with cutoffs and islands. 43
Figure 3.3. Google Earth aerial photographs of meanders without cutoffs. 44
Figure 3.4. A. Location and morphology of rivers in the gravel meander database. 45
Figure 3.5. Cumulative distribution function of elevation for each river morphology. 46
Figure 3.6. Plot of bankfull discharge versus channel slope and valley slope for different channel morphologies. 47
Figure 3.7. Cumulative density function of sinuosity for each channel morphology. 48
Figure 3.8. A. Distribution of vegetation classes by channel morphology. B. Distribution of land use classes by channel morphology. 49
Figure 3.9. Bankfull discharge and width-depth ratio of the river datasets. 50
Figure 3.10. Bankfull discharge and width depth ratio by vegetation class for gravel bed meanders of all morphologies. 51
Figure 3.11. Particle Reynolds number and Shields stress for rivers in the dataset. 52
Figure 3.12. Map of Shields stress for rivers with D50>8mm in North America, Great Britain, and New Zealand. 53
Figure 3.13. Particle Reynolds number versus Shields stress for gravel bedded meanders in the database grouped by vegetation class. 54
Figure 3.14. Schematic illustration of bank erosion parameters and areas of deposition and erosion during migration. 55
Figure 3.15. Photograph of channel bank in Bear Valley Creek, ID 56
Figure 3.16. Bankfull width and bend wavelength. 57
Figure 3.17. Rates of channel migration. 58
Figure 3.18. Shields stress versus relative supply of sediment from bank erosion. 59
Figure 4.1. Bed topography comparing low and high sediment feeds for the Outdoor Stream Lab experiments from Erwin [2012]. 75
Figure 4.2. Overhead images of A. the self-formed channel using alfalfa to provide bank strength similar to Braudrick et al. [2009] prior to channel infilling due to a feeder malfunction and B. The fixed wall channel used in the RFS experiments. 76
Figure 4.3. Grain size distribution of the sediment feed. 77
Figure 4.4. A. Channel depth, sediment facies, and centerline coordinates at 0 hrs 78
Figure 4.5. The minimum radius of curvature for a bend scaled by the flume width (45 cm) ($R_c$/B) relative to the maximum pool depth in the bend f scaled by the average depth for the flume for a given time step ($H_{max}$/H) .. 79
Figure 4.6. Water surface profile measurements through time. 80
Figure 4.7. Sediment flux measured at the flume outlet. 81

Figure 4.8. Water surface elevation maps for -3 and 80 hours. ..... 82
Figure 4.9. Map of sediment facies through time. ..... 83
Figure 4.10. Percent of the bed area occupied by each of the sediment facies through time. ..... 84
Figure 4.11. Changes in the extent of each facies by bend ..... 85
Figure 4.12. Change in hydraulic variables used to calculate the transport capacity for the RFS experiment through time. ..... 86
Figure 4.13. Mean bed elevation through time. ..... 87
Figure 4.14 Average boundary shear stress for the entire flume length calculated using equation 4.2. ..... 88
Figure 4.15. Variation in mean depth, water surface slope, and active width in the flume.. 89
Figure 4.16. Maps of flow depth through time. ..... 90
Figure 4.17. Maps of flow depth changes through time. ..... 91
Figure 4.18. Maximum depth ($H_{max}$) divided by the mean depth (H)..... 92
Figure 4.19. Depth and facies maps of Bend 4 at 0 and 20 hours and Bend 8 at 55 and 80 hrs..... 93
Figure 4.20. Overhead time series of experiments conducted immediately after the RFS experiments. ..... 94
Figure 5.1. Initial channel morphology for the 2012 and 2009 experiments.. .....112
Figure 5.2. Mean basin slope at 0 hours .....113
Figure 5.3. Grain size distribution of the coarse sediment feed.....114
Figure 5.4. Overhead images of experiment through time.....115
Figure 5.5. Topographic maps of the channel through time.....116
Figure 5.6. Channel centerline locations through time for all 18 topographic surveys. .....117
Figure 5.7. Comparison of the 2012 and 2009 experiments. .....118
Figure 5.8. Rapid deposition of fine sediment downstream of the bend apex as the downstream limb of the bend. .....119
Figure 5.9. Reach-Average hydraulic characteristics from 6-15.9 m.....120
Figure 5.10. Evolution of channel from 8-15 at 52-77.5 hrs. .....121
Figure 5.11. Submerged sediment flux measured at the flume outlet.. .....122
Figure 5.12. The density of sediment measured at the flume outlet and the fraction of the flux at the outlet that is lightweight plastic.....123
Figure 5.13 Water surface profiles through time.. .....124
Figure 5.14. Water surface slope and sinuosity of Bends 1-4 through time.....125
Figure 5.15. Mean width for each bend through time. The location of the bends at 39 hours is shown in the bottom panel. .....126
Figure 5.16. Average migration rate and through time downstream of x =6 m. .....127
Figure 5.17. Comparison of migration rates for gravel-bed meanders with scaled migration rates from the experiment.....128

## List of Tables

Table 2.1. Experimental conditions..... 15
Table 2.2. Comparison of conditions for the two runs..... 15

Table 3.1. Summary statistics for sand meanders, gravel braided, and gravel bed meanders. ..... 40
Table 3.2. Summary statistics for gravel bed meandering rivers for all grain sizes. ..... 40
Table 3.3. Summary statistics of bankfull discharge width depth ratio for each vegetation type. ..... 41
Table 3.4. Summary statistics for gravel bed meandering rivers coarser than 8 mm..... 41
Table 4.1. Experimental conditions for the initial sediment feed ..... 74
Table 4.2. Length and minimum radius of curvature relative to width ($R_c$/B) of experimental bends with point bars. ..... 74
Table 5.1. Comparison of the 2012 experimental methods with the 2009 experiment [Chapter 2]..... 110
Table 5.2. Channel cutoffs during the 2012 experiment. ..... 110
Table 5.3. Comparison of the 2012 experimental results with the 2009 experiment [Chapter 2]. ..... 111
Table 5.4. Comparison of average conditions in the 2012 experiment with the inner quartile range of gravel meanders in the field from Appendix B. ..... 111

## Acknowledgements

Although my name is on the cover of this dissertation, it represents collaborative work and ideas and it would not have been possible with all of the support I've received academically and personally from the people listed below. I've feel exceptionally lucky to have such a wonderful network of support. First, I would like to thank Bill Dietrich. To me, Bill epitomizes what a professor should be. He combines tirelessness and thoughtfulness to his support and education of graduate students, our field, and undergraduate education. He always challenges you to be sure you understand your results, moves onto the next question when you've answered the last, and provides endless options when things don't work. I often find myself asking "what would Bill do?" The answer is nearly always "work harder" and "think". Bill was also a good friend, and sent the first congratulatory email after the Giants won the World Series in 2010. I will miss our conversations about how to approach teaching, research, and being a scientist.

I've been lucky to work with Leonard Sklar throughout my time at Berkeley. Leonard has been a tireless advocate for me, first strongly encouraging me to leave my consulting job and to come back to school, and later helping to design the experiments and helping to address experimental hiccups and intellectual challenges associated with this research. Although I was not his student he always found time to help when I needed it and his advice was insightful and crucial to nearly every thought on these pages. Michael Manga and Mark Stacey were both gracious about the inevitable last minute rush of to get finished. They both read things with alarming speed and their dedication is appreciated. I would also like to thank the other members of my orals committee (Jim Kirchner and Roland Burgmann) for their keen questions and patience while I searched for the correct answer. Any discussion of mentors would be incomplete without also thanking Bob Anderson for introducing me to geomorphology in 1991, and Gordon Grant for nurturing me as a scientist during my MS degree.

It is hard to imagine a better group of fellow students and postdocs than the geomorphology group at Berkeley. There are too many great people to list, but you have all been great. They

were great friends, and it was inspiring to be surrounded by such gifted people, all of whom were willing to lend a helping hand before talks, oral exams, or whenever I encountered problems in the lab. I particularly want to thank Joel Rowland and Leslie Hsu, my fellow Richmond Field Station lifers. Joel and I spent endless hours in adjacent flumes and he provided essential help on my experiments (and inspired me to use plastic sediment) and an occasional wise-crack. Leslie Hsu kept the group humming along while she was at Berkeley, and continues in that role long after she left. Sharing an office with Peter Nelson and Mike Lamb was among the luckiest things to happen in graduate school. Our discussions about each other's research and rivers and landscapes, in general were always enlightening, and I still think about them today. Peter's patience with my Matlab questions is deeply appreciated. Toby Minear helped me conduct some experiments we still need to write up, and was always a great friend. I'd also like to thank Daniella Rempe for being the world's greatest GSI and putting up with me while I taught Geomorphology in 2012. I'd also like to thank the office staff here in Earth and Planetary Science. Their doors were always open and they made dealing with Berkeley logistics much, much easier. In particular, Margie Winn would always answer my pesky questions. Without Margie, navigating graduate school here would have been much more difficult.

The early days at the Richmond Field Station were happily spent with Glen Leverich. While he was working on his Master's thesis, he was designing the flume, testing our measurement apparatuses, and reading books on Origami to learn how to fold a tarp. He was also remodeling his kitchen at night. Glen was always positive, always thoughtful, and many of our early observations in a smaller flume formed the basis for the rest of my PhD. It was really a lucky treat to have him working with me.

Several colleagues from outside of Berkeley have also been a constant help. Gary Parker always took time out during meetings to check in on my research and it was his suggestion that guided us toward using alfalfa sprouts. Peter Wilcock invited me to join the Barflys –Susannah Erwin, Chuck Podolak, and Andreas Krause—to digest papers on alternate bars and tubular meat. Peter and Susannah welcomed me to participate in their experiments at the Outdoor Stream Lab with open arms. Those experiments were only tangentially included in this dissertation, but our observations greatly helped interpret the results of similar experiments I conducted at the Richmond Field Station.

The experiments reported in the following pages wouldn't have been possible without help from many people. First, I'd like to thank Stuart Foster, John Potter, and Neto Santana for their help building the flume. Without their expertise and hard work, we'd still be building the large basin. Stuart Foster was there throughout my time at the Richmond Field Station even after he retired. He taught me how to use power tools, how to build things, and how to seal them once they were built. For the rest of my life whenever I use caulk or PVC cement, I will think of Stuart. Many SF State students provided needed labor and great advice. Peter Polito and Skye Corbett always seemed to be around when we needed some help and always provided guilt-free. I was also lucky to have several undergraduates come through the lab. Most notable were Sumner Collins and Russell McArthur who sieved without complaint and who's care in data measurement was always appreciated. I also got a lot of help from members of the National Center for Earth-Surface Dynamics. In particular, Jim Mullin and Chris Ellis dealt with my panicked phone calls

with calm and helpful advice. Thanks also to Michal Tal for her helpful advice in getting our alfalfa sprouts up and running.

I'd also like to thank my parents and the rest of my family. My parents never blinked when I told them I was thinking of leaving my consulting job and going back to school. They strongly supported this decision, as they have supported me throughout my life. I have been lucky to have been raised by such open-minded people, who worried less about my financial security and more about my happiness. They always told me I would like college better than high school, but I don't think they knew it would go on for so long. I've been lucky to have such great friends in the Bay Area and elsewhere. You know who you are, and you are awesome. My friends kept me going during the doldrums with cocktails, Sunday night mysteries, good conversation, and wonderful humor.

Lastly I'd like to thank my two favorite people in the world. Maya Hayden encouraged me to start this wonderful journey and then later decided she wanted to come to school. Maya put up with working weekends and late nights throughout my time here, but more importantly she was always there when times were hard or research just wasn't going well with encouragement, laughter, and love. Meeting Maya was the luckiest day of my life. Finally, in her 18 month-long life (which started one week after the experiment in Chapter 5 ended), Fiona Braudrick has seen me teach Geomorphology, lose a gall bladder, and write up a dissertation. She's made every day a joy since she arrived. Her smile warms my heart and a hug from her makes all the bad things go away. This dissertation is of course dedicated to them. I love you both! Banana!

# 1 Introduction

Meandering rivers migrate across their floodplains through erosion of their outer banks and growth of point bars on their inner banks. If bank erosion and point bar growth are balanced, the channel will maintain a steady width and maintain a meandering morphology. If bank erosion exceeds bar growth the channel will widen and braid, while if bank erosion is less than the rate of bar growth the channel will narrow, and aggradation may cause the channel to avulse. Qualitative models of channel form emphasize that meandering requires strong banks and low sediment supply [Schumm, 1985; Church, 2006]. Strong banks limit the bank erosion while lower sediment supply is thought to limit the tendency towards braid bar development. Until very recently, theoretical models of river meandering [e.g., Ikeda et al., 1981; Blondeaux and Seminara, 1985; Howard, 1992; Sun et al., 2001; Seminara, 2005] assumed that the inner and outer banks migrate at the same rate regardless of the bank strength and sediment supply. Models are now being developed that can assess inner bank deposition and outer bank erosion independently [e.g., Parker et al., 2011; Asahi et al., 2013], but have yet to be extensively tested. The processes by which inner bank deposition keeps pace with outer bank erosion, and how erosion as the channel evolves are poorly known and are a fundamental gap in our understanding of meandering rivers.

Migration poses several challenges to balancing bank erosion and bar deposition because as channels migrate their sinuosity and curvature continuously change. Because the curvature strongly affects the migration rate [e.g., Hickin and Nanson, 1984; Hooke, 2003], the migration rate should vary through space and time. Moreover, migration causes bends to grow, increasing the sinuosity and decreasing the channel slope. Migration can also induce cutoffs, which increase the local slope and sediment supply to downstream reaches. The adjustments to slope are particularly problematic for gravel bedded meanders because they are often close to their transport threshold [e.g., Parker et al., 2007; Metivier and Barrier, 2012] where small slope changes can have a large effect on sediment transport. In contrast, sand bed channels typically have Shields stresses well above their critical transport threshold [Parker et al., 2003; Wilkerson and Parker, 2011], and are able to accommodate changes in sediment supply through changes in the morphology of bedforms as well as slope [Dietrich and Whiting, 1989]. The spatial and temporal variability in slope, curvature, and sediment supply should have profound effects on the ability of the river to transmit its load and maintain a sinuous, single-thread channel.

This dissertation focuses on gravel bedded meanders because they are an important source of aquatic habitat [e.g., Trush et al., 2000; McKean et al., 2008] and consequently have become an important in stream restoration design [Kondolf et al., 2001; Smith and Prestegaard, 2005; Kondolf, 2006; Harrison et al., 2011]. Our inability to define the necessary conditions for meandering in gravel bedded rivers hinders their success in stream restoration. Additionally, gravel bedded meanders can also be scaled to the laboratory, which allowed me to explore their formation and dynamics in a controlled setting where the boundary conditions can be adjusted and are known.

Laboratory flume experiments using non-cohesive sediment show that without additional bank strength, the bank erosion rate will exceed the bar growth rate and the river will widen and braid [e.g., Wolman and Brush, 1961; Whiting and Dietrich, 1993a; Federici and Paola, 2003;

Eaton and Church, 2004]. In the field, banks can be strengthened when they are capped with cohesive material [e.g., Schumm, 1963; ASCE Task Committee, 1998; Constantine et al., 2009] or when banks are vegetated [e.g., Brice, 1964; Hickin, 1984; Millar, 2000; Micheli and Kirchner, 2002; Parker et al., 2011]. Vegetation also strengthens the floodplain, limiting cutoffs and promoting higher sinuosity [Smith, 2004; Braudrick et al., 2009; Kleinhans, 2010]. Given the ability of vegetation to strengthen banks and floodplains, it is perhaps not surprising that widespread meandering in the rock record is limited until after the rise of rooted plants and trees [Davies and Gibling, 2010]. The presence of ancient meandering channels on Mars [e.g., Moore et al., 2003] suggests that it is bank strength rather than vegetation that is a necessary component for meandering.

Bank strength alone is not sufficient to promote meandering. In flume experiments braiding can develop as flow is diverted down the chutes that form between the bar and the floodplain. Chutes occur because the area of maximum coarse sediment deposition is not located at the boundary between the bar and floodplain, but rather towards the center of the channel. These chutes are a locus for channel bifurcation and braiding [Bertoldi and Tubino, 2005]. In gravel meanders in the field, these chutes are often plugged with sand [McGowen and Garner, 1970]. Bedload measurements in gravel meanders show that 30-60% of the bedload trapped in gravel meanders is sand, even though it is not present on the bed surface [Leopold, 1992; Ferguson et al., 1996; Clayton and Pitlick, 2007]. Studies of coupled flow and sediment transport in meander bends show that bedload and suspended load follow separate paths, with bedload transported toward the outer bank downstream of the bar apex and suspended sediment transported toward the bar [Dietrich and Smith, 1984], and the downstream end of bars are therefore finer than upstream [Fisk, 1944; McGowen and Garner, 1970; Bluck, 1971; Nanson, 1980; Clayton and Pitlick, 2008]. Sand that transitions from bedload to suspended load may therefore be a crucial component of gravel bedded meanders. Vegetation encroachment across the chute and onto the bar promotes fine deposition further reducing the tendency to braid.

Although a low sediment supply is often cited as being characteristic of gravel bed meanders [Carson, 1984; Schumm, 1985; Ferguson, 1987; Metivier and Barrier, 2012], there are few measurements of sediment supply and transport that can be used to directly assess the role of sediment supply in channel patterns [e.g., Ferguson et al., 1995; Leopold and Emmett, 1997; Metivier and Barrier, 2012; Pitlick et al., 2012]. Instead compilations of field data use proxies for the sediment supply to explore the controls on channel planform. These proxies may include the bankfull discharge, channel (or valley) slope, median surface grain size, and Shields stress [Leopold and Wolman, 1957; Carson, 1984; Ferguson 1987; van den Berg, 1993; Kleinhans and van den Berg, 2010; Metivier and Barrier, 2012]. These proxies for sediment supply suggest that on average meandering rivers have lower slopes relative to discharge (and lower stream power) than braided channels, but the conditions that support gravel meanders and gravel braided channels can be similar. Although nearly everyone agrees that sediment supply has a large influence on channel planform, the mechanisms by which supply influences morphology and how sediment supply, channel slope, and bank strength interact are poorly understood.

One approach to understanding the how meanders develop and maintain their morphology meandering is to try to create meandering rivers in the laboratory. One of the challenges to creating meandering rivers in the laboratory has been scaling bank strength. The

addition of bank strength to laboratory channels can have a profound effect on channel form [Friedkin, 1945; Schumm and Khan, 1972; Smith, 1998; Gran and Paola, 2001; Peakall et al., 2007; Tal and Paola, 2007; Tal and Paola, 2010; van Dijk et al., 2012]. Adding cohesive sediment to banks can slow bank erosion leading to sinuous channels, but these channels either develop sinuosity and stop migrating [e.g., Smith, 1998] or cut off and straighten after developing curvature [e.g., Peakall et al., 2007]. Oscillating the upstream boundary condition can maintain migration in experimental channel with cohesive sediment [van Dijk et al., 2012], but this does not reveal how the dynamic balance of bank erosion and bar growth is maintained. Recently, alfalfa sprouts have been used to provide bank strength in experimental channels [Gran and Paola, 2001; Jang and Shimizu, 2007; Tal and Paola, 2007; Tal and Paola, 2010]. Adding alfalfa sprouts to braided channels transformed them into dynamic channels with characteristics of both single-thread and island-bar morphology [Tal and Paola, 2007; Tal and Paola, 2010]. The alfalfa experiments replicate many processes observed in the field including avulsions and cutoffs, but meandering was intermittent and limited to a relatively small portion of the flume [Tal and Paola, 2007].

This dissertation uses laboratory experiments and a compilation of field data to define the conditions that support gravel bed meanders, how they respond to an increase in sediment supply, and how channel morphology changes under constant boundary conditions as a river migrates. A detailed description of the relevant literature is provided at the beginning of each chapter. Chapter 2 tests the conditions necessary to create and sustain meandering in a gravel bed river (published as [Braudrick et al., 2009]). This study hypothesized that meandering required bank strength, a low Shields stress (and sediment transport rates), coarse and fine sediment, and variable flood flows to fill chutes and deposit sediment on bar tops. We used alfalfa sprouts as model vegetation to strengthen banks and floodplains. Sand was our model gravel, and we also fed a lightweight plastic as model sand. The discharge consisted of a bankfull flow and periodic large flood for the first 71 hours, and a steady bankfull flow for the last 65 hours of the experiment. Variable flood flows were not required for meandering as the channel maintained a meandering morphology under steady bankfull conditions. The model sand filled the chutes that were a locus for braiding in previous experiments, filled the downstream end of point bars, and rapidly plugged cut off channels. The channel maintained a constant width as it migrated across its floodplain. The sinuosity reached a maximum of 1.2, but after cutting off the channel regenerated curvature. Coarse sediment feed needed to be turned off periodically to limit aggradation at the upstream end of the channel. Nearly all of the fed coarse sediment was exchanged laterally from eroding banks to point bars. This experiment suggests that sustained gravel meanders require bank strength, coarse and fine sediment, and very low sediment supply. It demonstrates the first self- maintaining laterally migrating channel created in a laboratory flume.

Chapter 3 explores the conditions necessary for meanders in gravel bedded rivers using a compilation of field data from the literature to ask where and under what conditions gravel bedded rivers meander. In this chapter I compiled location and hydraulic information for 166 gravel bed meanders. I then used Google Earth to determine the vegetation and land use near the river, and describe channel planform. Most of the data set was from North America and Britain, and gravel meanders were primarily found in humid, formerly glaciated (or glacio-fluvial landscapes) and adjacent to mountain ranges. During the Google Earth analysis, I observed that

gravel bedded meanders could be grouped into 3 morphologies: meanders with cutoffs and without islands, meanders with islands and cutoffs, and meanders without cutoffs. Meanders without cutoffs were less steep for their bankfull discharge relative to the two other channel types. I found that gravel meanders have low bedload supply (as indicated by a median Shields stress of 0.044, less than half that of gravel braided channels), and generally transport coarse sand as bedload. Meanders with cutoffs and without islands had lower Shields stresses (median=0.038) than meanders without cutoffs and meanders with islands (median=0.045 and 0.047, respectively). Gravel meanders with median surface grain sizes < 10 mm had Shields stresses intermediate between sand meanders (>0.3) and coarser gravel meanders (typically <0.08). Furthermore, for the 18 gravel bedded meanders with migration data, and sufficient information to calculate the sediment transport rate, the annual volume of sediment derived from eroding the banks exceeded the long-term transport capacity of the channel. This suggests that gravel meanders are primarily exchanging sediment laterally from eroding banks to the next bar downstream.

Given the importance of sediment supply in meandering rivers, I then examined the effects of doubling the supply on a laboratory gravel meander that was fixed in place. In this experiment, I fixed channel walls along the boundary of a self-formed freely meandering channel with 4 bends. I ran the flume at a constant discharge and sediment supply until it equilibrated. I then doubled the sediment feed rate and monitored the evolution of bed topography, water surface topography, bed facies, and sediment transport. In response to the doubling of supply the channel steepened, and the depth decreased. Two of the bends shoaled as their pools filled with coarse sediment in response to the increased feed. One of the bars extended upstream creating a bend with two point bars. For 3 other bends, topographic adjustments to the doubling of feed were small, despite the bed aggrading by up to one channel depth. The responsive bends were longer with intermediate curvature and had relatively straight reaches upstream. Two of the bends which experienced limited topographic change due to the doubling of supply had higher curvature and shorter bend length. The response may be partially controlled by the immobile banks that created deep pools (the maximum depth was approximately 3.5 times the average depth) and wide bars, which likely limited the ability of the bed topography to adjust to the supply increase.

Finally, I conducted an experiment similar to Chapter 2, in which I again used alfalfa to provide bank strength and a lightweight plastic as model sand. There were some changes to the channel inlet, but the main adjustments were a steady (and slightly higher sediment feed) and a tripling of the amount of alfalfa seeds spread on the flume (expected to increase sinuosity). The increased supply and bank strength lead to a narrower channel than the experiments in Chapter 2, although the bank erosion rates were similar. The higher bank strength did lead to a more sinuous channel as sinuosity ranged between 1.2-1.6. Although the channel had constant boundary conditions, the hydraulics, sediment transport, and planform evolution varied through time. In particular, the pattern of erosion went from symmetric meanders, to asymmetric meanders as the slope declined. The slope declined as sinuosity increased which reduced the sediment transport rate and the channel aggraded and subsequently 3 bends cut off in relatively rapid succession.

Taken together these 4 chapters show that bedload dominated meandering rivers require bank strength to slow bank erosion, low gravel supply, and fine sediment (sand) to fill the downstream end of bars and plug chutes. The gravel supply must be low enough so that lateral exchange of sediment from bars to banks can accommodate the majority of the bedload. Meanders that are fixed in place respond to increased supply by steepening with variable (but limited) topographic response aside from the slope change. In this case, the elevated bed level at the upstream end of the channel would have promoted avulsion if the fixed bank heights were at the elevation of the floodplain. Higher bank strength leads to narrower channels that have similar erosion rates to channels with lower strength. Migration causes the slope to decline, decreasing the sediment transport rate, and if the sediment feed is constant, this leads to aggradation that makes cutoffs more likely.

# 2 Necessary conditions for sustained meandering in coarse bedded rivers: experimental evidence

## 2.1 Abstract

Meandering rivers are common on Earth and other planetary surfaces, yet the conditions necessary to maintain meandering channels are unclear. As a consequence, self-maintaining meandering channels with cutoffs have not been reproduced in the laboratory. Such experimental channels are needed to explore mechanisms controlling migration rate, sinuosity, floodplain formation, and planform morphodynamics and to test theories for wavelength and bend propagation. Here we report the first successful experiment in which meandering with near-constant width was maintained during repeated cutoff and regeneration of meander bends. We found that elevated bank strength (provided by alfalfa sprouts) relative to the cohesionless bed material and the blocking of troughs (chutes) in the lee of point bars via suspended sediment deposition were the necessary ingredients to successful meandering. Varying flood discharge was not necessary. Scaling analysis shows that the experimental meander migration was fast compared to most natural channels. This high migration rate caused nearly all the bedload sediment to exchange laterally, such that bar growth was primarily dependent on bank sediment supplied from upstream lateral migration. The high migration rate may have contributed to the relatively low sinuosity of 1.19, and this suggests that to obtain much higher sinuosity experiments at this scale may have to be conducted for several years. Although patience is required to evolve them, these experimental channels offer the opportunity to explore several fundamental issues about river morphodynamics. Our results also suggest that sand supply may be an essential control in restoring self-maintaining, actively shifting gravel-bedded meanders.

## 2.2 Introduction

River meandering --the lateral bank shifting that produces sinuous, single-thread channels-- is inherent to coupled flow and sediment transport in gravel- and sand-bedded channels within a broad range of channel width to depth ratios [Parker, 1976]. Channel planform classification based on field observations qualitatively suggests that meandering depends strongly on channel slope, grain size, bank strength, and sediment supply [e.g., Schumm 1985; Church, 2006]. Theoretical models of river meandering [Ikeda et al., 1981; Blondeaux and Seminara, 1985; Howard, 1992; Sun et al., 2001; Seminara, 2005], however, assume that the inner and outer banks migrate at the same rate during meandering no matter the bank strength and sediment supply. The processes by which inner bank deposition keeps pace with outer bank erosion are poorly known. This is a fundamental gap in our understanding of meandering rivers.

Laboratory experiments have demonstrated that channels with sand or gravel bed and banks will develop bars and planform curvature but will inevitably braid [e.g., Wolman and Brush, 1961; Whiting and Dietrich, 1993a; Eaton and Church, 2004] because the weak outer banks erode faster than bars can grow and accrete to the inner bank. Braiding often develops due to flow diversion down chutes that form between the bar and the floodplain. Chutes occur because the area of maximum coarse sediment deposition is not located at the boundary between the bar and floodplain, but rather towards the center of the channel. These chutes are a locus for channel bifurcation and braiding [Bertoldi and Tubino, 2005]. Experiments using clay and silt

materials to strengthen the banks have produced sinuous channels, and under some conditions, channels with high sinuosity, [e.g., Friedkin, 1945; Schumm and Khan, 1972; Smith, 1998; Peakall et al., 2007] but these experiments have not successfully created meandering channels with repeated cutoffs that both produce a floodplain and maintain their geometry. Instead, in such experiments the channel simplifies to a single bend following cutoffs [Peakall et al., 2007] or bank migration ceases once sinuosity develops [Smith, 1998]. Recently, alfalfa sprouts have been used to provide bank strength in experimental channels [Gran and Paola, 2001; Tal and Paola, 2007]. Adding alfalfa sprouts to braided flume channels transformed them into dynamic channels with characteristics of both single-thread and island-bar morphology. The alfalfa experiments replicate many processes observed in the field including avulsions and cutoffs, but meandering was intermittent and limited to a relatively small portion of the flume [Tal and Paola, 2007].

Although previous experiments were able to initiate channel meandering they have not been able to maintain channel migration once sinuosity developed. The inability to generate self-maintaining laterally migrating channels with cutoffs in the laboratory prevents us from conducting scaled-experiments which would be valuable in problems ranging from developing practical guidelines for stream restoration, to channel response to climate change, and to understand the conditions necessary to support meandering channels observed on Mars and Titan. These practical and theoretical issues prompted us to explore specifically how to make a scaled gravel-bed meandering river. We focus on gravel-bed meanders because of their importance to aquatic habitat [e.g., Trush et al., 2000] and stream restoration [Kondolf, 2006], and because they can be more readily scaled to laboratory dimensions and hydraulic conditions.

Here we report the successful experimental generation of a lateral migrating, bedload-dominated meandering channel with repeated cutoffs. The key challenges were to create conditions that allowed outer bank erosion and inner bank deposition (including up to the height of the adjacent floodplain) at the same rate, and that led to deposition in the bar-adjacent chute such that the incipient meandering was not rapidly cutoff by flow diversion down the chute. We hypothesized that in addition to hydraulic conditions that support meandering [see Parker, 1976] the necessary conditions to obtain successful experimental meandering were: 1) bank strength greater than that due to deposited bedload (to slow outer bank erosion rate), 2) the addition of suspended load (to both settle out in the chutes, reducing the tendency for a low sinuosity cut-off, and to become deposited on the bar top, raising the surface to floodplain level), and 3) periodic overbank flow (to raise the depositional surface of the point bar and to disperse suspended sediment into nearby low areas). Our experiment strongly supports the first two hypotheses, but surprisingly meandering was maintained without variable peaks. The experiment also suggests that sand supply and deposition should be included in the design of gravel bed meandering rivers for restoration projects and included in numerical models of gravel bar growth in meandering rivers.

### 2.3 Experimental methods

We carved a 40-cm wide, 1.9-cm deep channel in a 6.1-m wide, 17-m long flume set at a slope of 0.0046. The downstream 12 m of the flume were slightly steeper (0.0052) than the basin as a whole, this steeper reach was generally downstream of the first bend and the influence of the

flume inlet. The dimensions, slope, and discharge placed the channel well within the meandering regime defined by Parker [1976]. The flume was filled with sorted sand with median diameter of 0.8 mm (Table 2-1), and an initial bend was carved at the inlet to hasten the onset of meandering (Figure 2.1). Following Tal and Paola [2007], we used alfalfa sprouts to provide bank strength. We seeded approximately 2.6 kg of alfalfa (1.2 seeds/ $cm^2$) by hand throughout the flume basin, while a low flow irrigated the basin. We would then allow the alfalfa to grow for 7-10 days depending on the air temperature before we commenced the run. During this period, five 1000 Watt metal-halide grow lights were suspended over the channel to promote growth and water was supplied by an irrigation flow not sufficient to transport sediment. This caused the alfalfa on the margin of the basin to die off more quickly than the alfalfa near the channel. We typically ran the flume for 10-14 hours over the course of 2-3 days, by which time the alfalfa started to die because it had been submerged for an extensive period. We would then replant the alfalfa outside of the bankfull channel and allow an additional 7-10 days for the alfalfa to grow. During the course of this experiment, we seeded alfalfa 11 times. The alfalfa sprouts have one primary tap root, with very small secondary roots. The rooting network differs from mature riparian vegetation, which, typically has a broader rooting structure, but is similar to the rooting structure of young cottonwood (*Populus* sp.) and willow (*Salix* sp.) trees [Amlin and Rood, 2002]. The alfalfa was primarily used as a means to provide bank strength, but it also increased flow resistance along potential chute cutoffs, and thereby promoted fine sediment accretion along the inner bank.

The flume was run for 136 hours under two hydrologic regimes. For the first 71 hours we repeated a simple two-stage hydrograph consisting of 5.5-hours of bankfull flow (1.8 l/s) and a 1.5-hour flood flow (2.7 l/s). The discharge consisted of a steady bankfull flow for the remaining 65 hours (Figure 2.2, Table 2-2). In addition during the first 30 hours, we ran three short duration flood flows at much higher rates (3.7, 4.2, and 4.4 l/s) to test the effect of high flows on bank resistance, overbank sediment deposition, and persistence of channel form (Figure 2.2). The channel was in flood stage for about 25% of the first 71 hours of the experiment and 13 % of the total run time. During the last 65 hours, the discharge consisted of a steady 1.8 l/s bankfull flow. Although this flow was intended to be at bankfull stage, the channel shallowed so that the discharge during the final 65 hours was overbank with 2-5 mm-deep flows on the floodplain. As is typical of small experimental channels, the flow was in the hydraulically smooth rather than rough regime.

The sediment feed consisted of both a coarse (sand) and fine (lightweight plastic) sediment (Table 2-1) that were fed separately at the upstream end of the flume. The sand scales as gravel found in natural lowland gravel bedded rivers. The coarse feed was identical to the sediment in the basin, but was painted blue. The 0.8 mm diameter sorted coarse sediment had a standard deviation of 1.3 mm. The coarse feed rate was periodically reduced to limit aggradation upstream of the first bend. Of the 102 kg of coarse sediment fed during the experiment, 82% was fed during the first 71 hours (Figure 2.3). This is partially due to increased supply during high peaks, and also because we increased our efforts to eliminate aggradation at the upstream end of the flume as the experiments progressed. Aggradation upstream of the first bend forced water onto the floodplain and out of the channel and reduced in-channel discharge downstream. During the steady portion of the experiment, much of the coarse sediment was derived from erosion of the aggraded bed upstream of the first bend.

The fine sediment scaled as sand in gravel bedded streams, moving both as bedload and suspended load. The lightweight plastic was crucial for allowing this behavior by combining a low settling velocity (allowing for sediment to move in suspension), while reducing the critical stress relative to natural sediment with an equivalent settling velocity (e.g. silt). Because of excess Shields stress less than 2 for the majority of the bed sediment, the ratio of flow depth to median grain size less than 16, and the absence of depth-scaled bedforms (e.g. dunes and ripples), we consider this channel as representative of gravel bed streams passing fine sediment.

We varied the fine sediment feed rate at the beginning of the experiment with an averaged feed rate of 3.4 kg/hr over the entire experiment. During the final 65 hours, the fine feed rate was held constant at 3 kg/hr. In these experiments the lightweight sediment moved as both bedload and suspended load. The fine feed comprised approximately 82% of the total fed sediment, higher than portion of sand caught in bedload traps at gravel bed meandering rivers [Ferguson et al., 1996; Leopold and Emmett, 1997; Clayton and Pitlick, 2007], which ranges from 20 to 70% of the bedload (depending on the river, the stage, and location within the bend. Because the fines travel as both suspended and bedload, we set the portion of the fine feed to be higher than bedload traps in the field which do not trap sediment suspended in the water column. We used two-types of commercially available lightweight plastic sediment as model sand. Both types of plastic ranged between 0.25-0.42 mm in diameter and were not cohesive. We used two-types of commercially available lightweight plastic sediment as model sand. Both types of plastic ranged between 0.25-0.42 mm in diameter and were not cohesive. The lightweight plastic for the first 71 hours of the experiment was Urea Type II, which has specific gravity of 1.5. For the remainder of the experiment, we replaced it with a lighter plastic (Clear-cut), which had a specific gravity of 1.3. The fine feed rate during the steady bankfull portion of the experiment (3 kg/hr) is equivalent to 460 mg/l, which is within the range of suspended sediment concentrations during peak flows [Walling and Webb, 1987; Simon et al., 2004]. The average shear velocity (u*) in our experiment was 1.5 and 2.4 times the settling velocity ($W_s$) of the plastic sediment (as reported in Rowland, 2007]. The calculated critical shear stress was reduced by 66% (for Clear-cut) and 54% (for Urea Type II) relative to quartz sediment of equivalent settling velocity. The critical shear stress for the plastic sediment was calculated using the best-fit line to the Shields curve proposed by Parker et al., [2003].

Several measurements were made during the experiments. Overhead photographs were taken at 5-minute intervals during the experiment to record the position of the channel. Bed topography and water surface elevations were measured from a movable cart above the flume. Water surface elevations were measured with a point gauge and bed topography was measured using a laser sheet photographed by an oblique camera while the flume was dry. Velocity was measured using a dye tracer and overhead photographs taken every 10 seconds. Sediment discharge from the flume was not regularly monitored due to repeated equipment failure.

## 2.4 Results

During the course of the 136-hour experiment the channel migrated both laterally and downstream, developing five bends and experiencing five distinct cutoff events. At the end of the experiment, the channel was entirely self-formed (Figure 2.1 and Supplemental Video 1). The wavelength stabilized at approximately 14 channel widths, which is somewhat higher than

typically reported for meandering rives [e.g., Knighton, 1998]. Alternate bars were not present prior to the development of curvature despite conditions that should have favored alternate bar development. Bends grew through a combination of downstream and lateral translation, and on average the bends migrated about 2 channel widths laterally and about 5 channel widths downstream. Migration rates were fastest during initial bend development at the beginning of the experiment and immediately following cutoffs. These rapid periods of channel migration were associated with high rates of sediment deposition, which redirected flow and increase downstream bar migration rates (see Supplemental Video 1).

The channel width increased during the first 40 hours of the experiment before stabilizing and remaining within ±12% of the resulting channel width for the remainder of the experiment (Figure 2.2). The initial large increase in channel width corresponded to the high flow peaks, where bank erosion occurred faster than point bars could accrete vertically to create new floodplain deposits. For the remainder of experiment, the bar margin kept pace with bank erosion as the bar grew vertically to the elevation of the floodplain. The depth was more variable than the width, with local changes in depth due to changes in upstream bank erosion. At the conclusion of the experiments, the average depth was 1.3 cm.

The alfalfa sprouts increase the strength of the banks relative to sand without sprouts [e.g., Pollen and Simon, 2006], and thereby decreased the rate of bank erosion, giving time for inner bank sediment accretion to keep pace with outer bank erosion. Banks eroded by the entrainment of grains along the margin rather than by large-scale bank failure. The sprouts both roughened the near-bank region and increased the stress required to move particles. Bank erosion was not a steady process, and often occurred in pulses as flow was redirected due to upstream bar migration and cutoffs. Peak erosion rates occurred when the minimum radius of curvature of a bend was 1-3 times the average channel width, lower than generally reported in the literature [Hooke, 2003], but similar to the lower Mississippi River [Hudson and Kessel, 2000].

Bars were built by deposition of coarse sediment eroded from upstream banks and fine sediment fed from the upstream end of the flume. Little of the coarse fed sediment was observed downstream of the first bar until after the first cutoff (Figures 4 and 5, Supplemental Video 1). Prior to this time, deposition of fed sediment at the upstream-most bar caused erosion of the outer bank, which provided sediment to downstream reaches. When we reduced the coarse feed rates to prevent aggradation at the upstream end of the flume, erosion of the bed upstream of the first bar sent sediment downstream.

Fine sediment was crucial for connecting bars to the floodplain by filling the upstream end of chutes. Chute channel development between the bars and the floodplain was limited to rapid periods of migration at the beginning of the experiment and following cutoffs (see Supplemental Video 1). After their formation, the upstream end of chutes would at first be paths of weak inner bank flow which would carry in fine sediment. Here the sediment would settle, eventually blocking further inflow. Downstream of the bed apex coarse sediment would shift outward by rolling down the bar front, while fine sediment would be carried inward with the secondary circulation (as described by Dietrich and Smith [1984]). This fine sediment would tend to deposit on the downstream end of bars (mark F in Figure 2.4 and the white facies in Figure 2.5) and settle in the downstream end of chutes, further blocking this pathway. The

chutes for the two upstream-most bars were also sealed at their downstream end by deposition of fine sediment. The consequence of these processes, dominated by fine sedimentation, was that the chutes behind each bar were sealed at their upstream end and, at times, at the downstream end and the water within them was not flowing. Hence, the chute did not enlarge as the experiment progressed (which would lead to cutoff or braiding). Fine sediment also was deposited overbank, forming levee-like features along the right margin of the channel (looking downstream) (Figure 2.4 mark O). In natural meanders such processes would contribute to bank strengthening through the deposition of sediment (silt and clay) that have high critical shear stress upon re-entrainment.

The sinuosity increased throughout the experiment to a maximum value of 1.19 with dips during cutoff events, which limited the sinuosity of the channel (Figure 2.2). The water surface slope and bed slope ranged from 0.0044 to 0.0047 downstream of the first bend during the final 50 hours of the experiment. The channel straightened via chute cutoffs five times during the 136-hour experiment or an average of 1 cutoff every 25 hours (Figures 1 and 2). Of the five cutoffs, four were caused by channel migration into an abandoned and isolated chute, and in two of these cutoffs the channel switched back to its pre-cutoff location within a few hours (Figure 2.1). The fifth (and final) cutoff occurred when upstream bank erosion caused local aggradation increasing the flow depth over the floodplain deposits even though the discharge was steady. The overbank flow became concentrated, where vegetation growth was weakest, and carved a small channel, which eventually connected with the downstream chute and expanded into a cutoff. Following all of the cutoffs, the channel regenerated bars and the abandoned channels were quickly plugged with fine sediment (Figure 2.6).

## 2.5 Discussion

Although we expected that variable discharge would be required to promote the creation of new floodplain via point bar growth, we found that meandering was maintained during steady flows as well. This occurred because as the channel evolved, our designed bankfull flow became slightly overbank, which allowed overbank deposition during steady flow. Had the floodplain roughness been greater (through higher alfalfa density), the flow may have been may have forced the steady flow to be entirely contained within the bankfull channel as observed by [Tal and Paola, 2007]. High peak flow tests during the first 40 hours of the experiment caused the channel to widen progressively (Figure 2.2) as the bars did not have sufficient time to accrete vertically to the floodplain elevation and had we continued with these high peaks the channel likely would have braided. Our results imply that limiting bank erosion rate to the rate at which bars can grow is crucial for maintaining a meandering morphology. They also suggest that erosion during rare high events may control whether a channel has a braided or meandering morphology.

Comparing the experimental migration rates to the field requires scaling time between the experiment and the field. Additionally, because migration rates are often reported as a portion of the channel width per year, we must also account for the number of days per year during which bankfull flows or greater occur. Time scales differently than length in flume experiments, however, and the scaling procedure differs depending on the process of interest [Yalin, 1971; Peakall et al., 1996]. Here we use a Froude-scale approach common in laboratory experiments [Ashmore, 1998; Parker et al., 2003]. Extrapolating our experiments to the field requires scaling

our experiments to the field, and then estimating the data to years (the typical time unit of migration rates), by estimating the exceedance probability of bankfull floods. In Froude-scale models like this experiment, time is scaled by multiplying the experimental time by the square root of the scaling factor [Yalin, 1971; Peakall et al., 1996; Parker et al., 2003]. Field time is converted to experimental time by:

$$t_{flume} = \sqrt{\lambda} t_{field} \quad (2.1)$$

where $t_{flume}$ is the experimental duration, $\lambda$ is the scaling factor (and is less than 1) and $t_{field}$ is the equivalent time in the field.

The mean values of bed grain size (40 mm), bankfull width (43 m) and depth (1.5 m) of the gravel-bed meandering rivers analyzed by van den Berg [1995] suggest the length scale factor ($\lambda$) for our flume to be between 1/30 and 1/100. Assuming $\lambda$ ranges between 1/30 and 1/100, our 136-hour experiment corresponds to 31 to 57 days of bankfull or greater flow. Although there is significant variation, bankfull flow is exceeded approximately 8 days per year in Wyoming [Dunne and Leopold, 1979] and Colorado [Andrews and Nankervis, 1995]. Nixon [1959] found that bankfull discharge occurred 2.2 days per year for 29 rivers in England and Wales, but this was based on only five years of data at each river, whereas much of the data from Andrews and Nankervis [1995] is from gauges with at least 15 years of data. If we use the data from the Rocky Mountains and assume that most channel migration occurs during bankfull flows, which are typically equaled or exceeded 8 days per year [cf. Dunne and Leopold, 1979; Andrews and Nankervis, 1995], then our 136-hour experiment corresponds to 5-7 years of high flows. Excluding the rapid migration rates at the beginning of this experiment, the average basin-wide migration rate calculated following the procedure described in Micheli and Kirchner [2002] ranged between 0.5 to 0.7 channel widths per year, depending on the scaling factor. Migration rates reported in the literature for natural channels are often reported for individual bends and range from less than 0.01 to a maximum 0.18 channel widths per year with a clustering of data around 0.01 to 0.02 channel widths per year [Nanson and Hickin, 1986; Hooke, 2007]. Hence our rate is much faster than that typically found in natural channels. To reduce the migration, we could have grown alfalfa to a high density (bank strength is linearly related to alfalfa density [Pollen and Simon, 2006]). Decreasing our migration rates to typical field values would, however, require increasing the duration of experiments by about an order of magnitude, requiring several years to complete.

Maintaining a meandering morphology and steady width under such rapid migration rates requires an equally rapid bar growth rate. In our experiment, the fine sediment was critical to maintaining this rapid bar growth rate because fines deposited in areas where coarse sediment did not: at the upper elevation of the bars, the chute tops, and downstream of the bar apex. We note that in relatively sinuous gravel bed meanders with high migration rates sand makes up the majority of the sediment accreted along the inner bank [Leopold and Wolman, 1960; Hooke, 1995]. Without fine sediment deposition, the bars would not have grown to the elevation of the floodplain, and the chutes would be much larger.

If the migration rates were much slower there may have been sufficient time for bar growth to keep pace with bank erosion in the absence of fine sediment, but several lines of

evidence indicate that this may not be the case. As discussed above, studies of coupled flow and sediment transport in meander bends show that bedload and suspended load follow separate paths, with bedload transported toward the outer bank downstream of the bar apex and suspended sediment transported toward the bar [Dietrich and Smith, 1984], and the downstream end of the bars are therefore finer [Fisk, 1944; McGowen and Garner, 1970; Bluck, 1971; Nanson, 1980; Clayton and Pitlick, 2008]. Even at flood discharge, bedload transport over the top of the bar tends to travel towards the outer bank. Hence, in the absence of suspended bed material, which can travel with the secondary currents to the inner bank and deposit (elevating the bar along the inner bank and closing the back bar chutes), there is no mechanism to attach the bar to the bank and to prevent chute cutoff at high flow. Dense vegetation can contribute to surface stabilization and retard chute cutoff, but without fine sediment to infill the chute, flow can reoccupy this path (and promote island bars). Vegetation growth on exposed bar surfaces also slows the flow, traps fine sediment, and induces vertical accretion. In exceptional cases of slowly migrating meanders with abundant vegetation, organic detritus may collect and consolidate to retard chute cutoff and maintain meandering. These experiments show that models of bar growth in meandering streams should include both coarse and fine sediment to allow bars to create new floodplain deposits. The experiments also contradict the practice of limiting sand supply in many restoration projects in meandering rivers.

Although the migration rates in this experiment were high relative to natural rivers, the sinuosity was relatively low. Our maximum sinuosity downstream of the first bend was 1.19, which is considerably lower than most meandering gravel bedded channels, where sinuosities are often greater than 1.5 [Hickin and Nanson, 1984; Hooke, 2007]. Despite the low sinuosity, the processes of bar growth, bank erosion, and cutoff were similar to gravel bed meanders in the field. These processes resulted in a channel with a width-depth ratio and a bend wavelength to width ratio within the range of natural channels [Parker et al., 2007]. As also observed by Friedkin [1945], sinuosity was limited by the cutoff frequency. In our case the rapid migration (particularly downstream migration) increased the cutoff frequency by increasing the rate at which the channel migrated into open chutes. In addition, rapid migration during curvature development may limit chute filling because the main flow and high concentrations of sediment migrate away from the chutes. Filling the entire chute with sediment would decrease the cutoff frequency and consequently allow the sinuosity to increase but this would require either much higher sediment concentrations or limiting migration rates to increase the time for fine sediment to deposit in the chute. Based on these experiments, we would expect meandering channels in the field to have higher sinuosity where cutoffs are suppressed by rapid filling of chute channels during bar growth.

Taken together these results suggest that developing highly sinuous channels requires sufficient time for fine sediment to completely infill low areas along the inner bank such that chutes are essentially gone, and cannot be exploited during chute cutoffs. This would reduce the frequency of chute cutoffs and allow the channel to develop a greater sinuosity. Experimentally it may be difficult to achieve such high sinuosity channels through the method of bank strengthening with alfalfa sprouts because growth of the sprouts imposes significant time delays in running experiments. In our experiments we had to pause one week every for 15 to 20 hours of runtime to reseed the alfalfa and allow it to grow. Making self-maintaining, high-sinuosity laboratory meanders will be the next experimental challenge.

## 2.6 Conclusions

By increasing the bank strength relative to non-cohesive sediment and promoting deposition of fine sediment in troughs between point bars and the floodplain we created the first self-sustaining meandering channel in a laboratory flume. The initial sedimentologic and hydraulic conditions were sufficient for meandering as defined by Parker [1976]. The channel width stabilized after the first 40 hours of the experiment, indicating that bank erosion and bar growth occurred at about the same rate and there was little change in width as the channel migrated and cut off. Chutes remained behind bars, and bars were connected to the floodplain at their upstream end, and were either open or closed off at their downstream end. Chute cutoffs occurred when the channel migrated into open chutes or following local aggradation and incision along preferential flow paths. Our migration rates were very fast relative to natural channels, which allowed chutes to remain behind bars and likely increased the cutoff frequency. Given such rapid migration rates, fine sediment was critical for attaching chutes to bars, elevating the deposition rate downstream of the bar apex, and plugging cut off channel. Sinuosity was low relative to meandering rivers in the field, likely because of the frequent cutoffs caused by partially open chutes. Slowing the migration rates to typical field values would likely increase the amount of fine sediment deposited in the chutes (and decrease chute cutoff frequency) but would increase the time required for the experiments significantly. Meandering was maintained with a steady, slightly over bank flow, and variable discharge was not necessary.

These experiments suggest that bank strength and, surprisingly, sand are necessary components of restoration projects for gravel bed meanders. The results provide the first data on entirely self-formed meandering channels that can be used to test new theories of meandering that explicitly model inner bank sediment accretion, and thereby, predict channel width, rather than assume it is a fixed value. This should be a stepping stone towards a general mechanistic theory for channel width in river channels.

## 2.7 Acknowledgements

This project was funded by the CALFED Ecosystem Restoration Program (Grant No. ERP-02D-P55) and by the STC program of the National Science Foundation (NSF) via the National Center for Earth Surface Dynamics (NCED) under agreement EAR-0120914. G. Parker suggested using alfalfa sprouts and provided crucial input on experimental design. Without the assistance of S. Foster, N. Santana, J. Potter, J. Rowland, C. Ellis, M. Tal, J. Marr, and M. Hayden this flume experiment would not have been possible. G. Seminara, S. Lanzoni, and M. Pittaluga provided insightful observations regarding experimental results. R. Slingerland and J. Hooke provided thoughtful reviews of the manuscript.

## 2.8 Tables

Table 2.1. Experimental conditions

| Parameter | Value |
|---|---|
| Flume width | 6.7 m |
| Flume length | 17 m |
| Median coarse grain size | 0.8 mm |
| Median fine grain size | 0.3 mm |
| Initial channel width | 40 cm |
| Initial channel depth | 1.9 cm |
| Bankfull discharge | 1.8 l/s |
| Basin slope | 0.0046 |
| Froude number | 0.55 |
| Reynolds number | 4,500 |

Table 2.2. Comparison of conditions for the two runs.

| | Variable discharge | Steady discharge |
|---|---|---|
| Duration | 0-71 hours | 71-136 hours |
| Bankfull discharge | 1.8 l/s | 1.8 l/s |
| Overbank discharge | 2.6 l/s | n/a |
| Plastic sediment specific gravity | 1.5 | 1.3 |
| Basin slope | 0.0046 | 0.0046 |

## 2.9 Figures

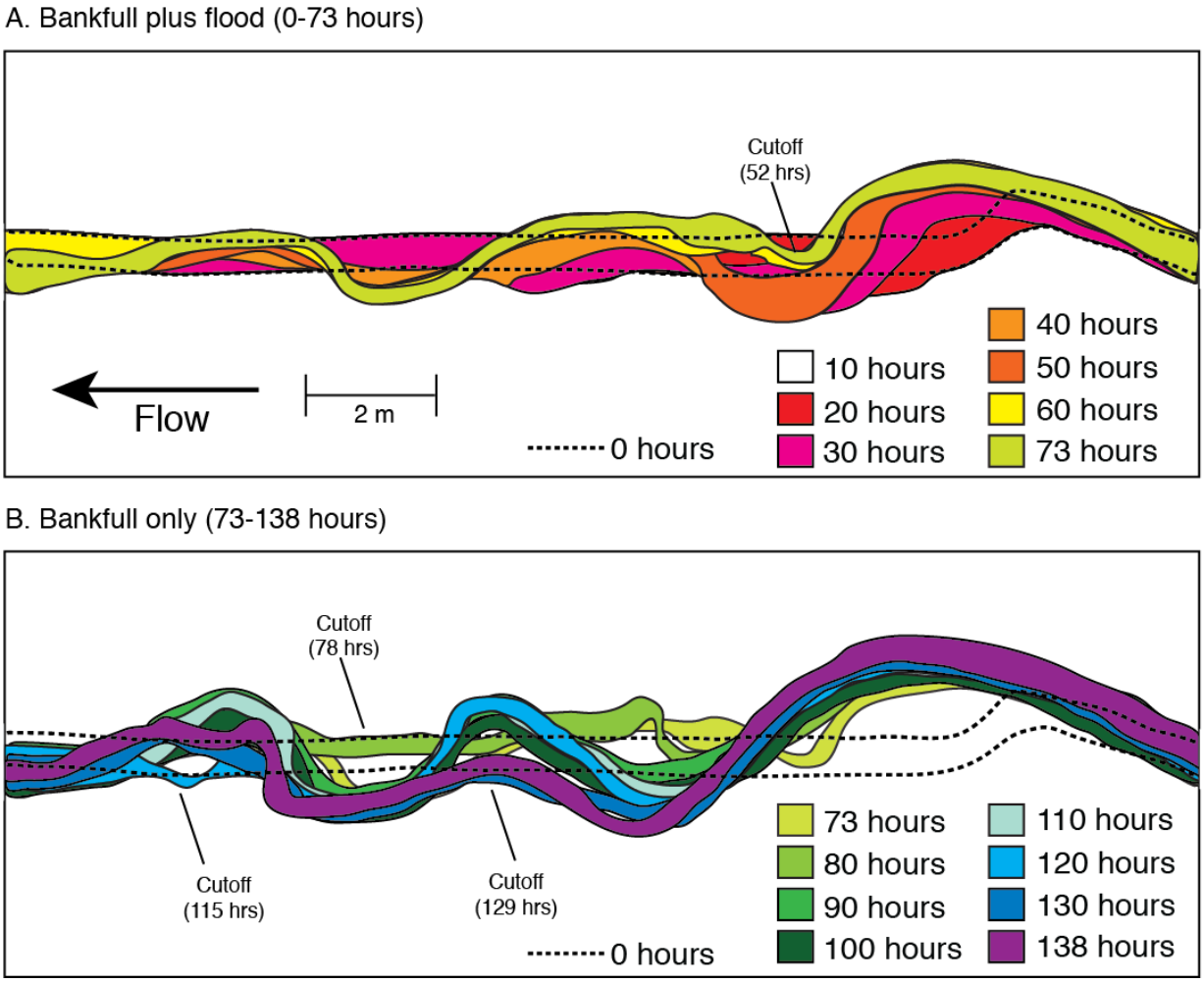


Figure 2.1. Map of channel position through time. Panel A shows the channel position during the first 71 hours of the experiment when discharge included both a bankfull and flood flow, while panel B shows channel evolution from 71-136 hours when the discharge was a steady bankfull flow. The original carved channel boundary is represented by the dashed lines, and the channel margin at 10 hours is not visible beneath the boundary at 20 hours, when the channel width was expanding. The short-lived cutoff at 29 hours is not visible in this figure. Chutes have not been included in the figure for clarity, but the morphology of chutes is shown in Figure 3.

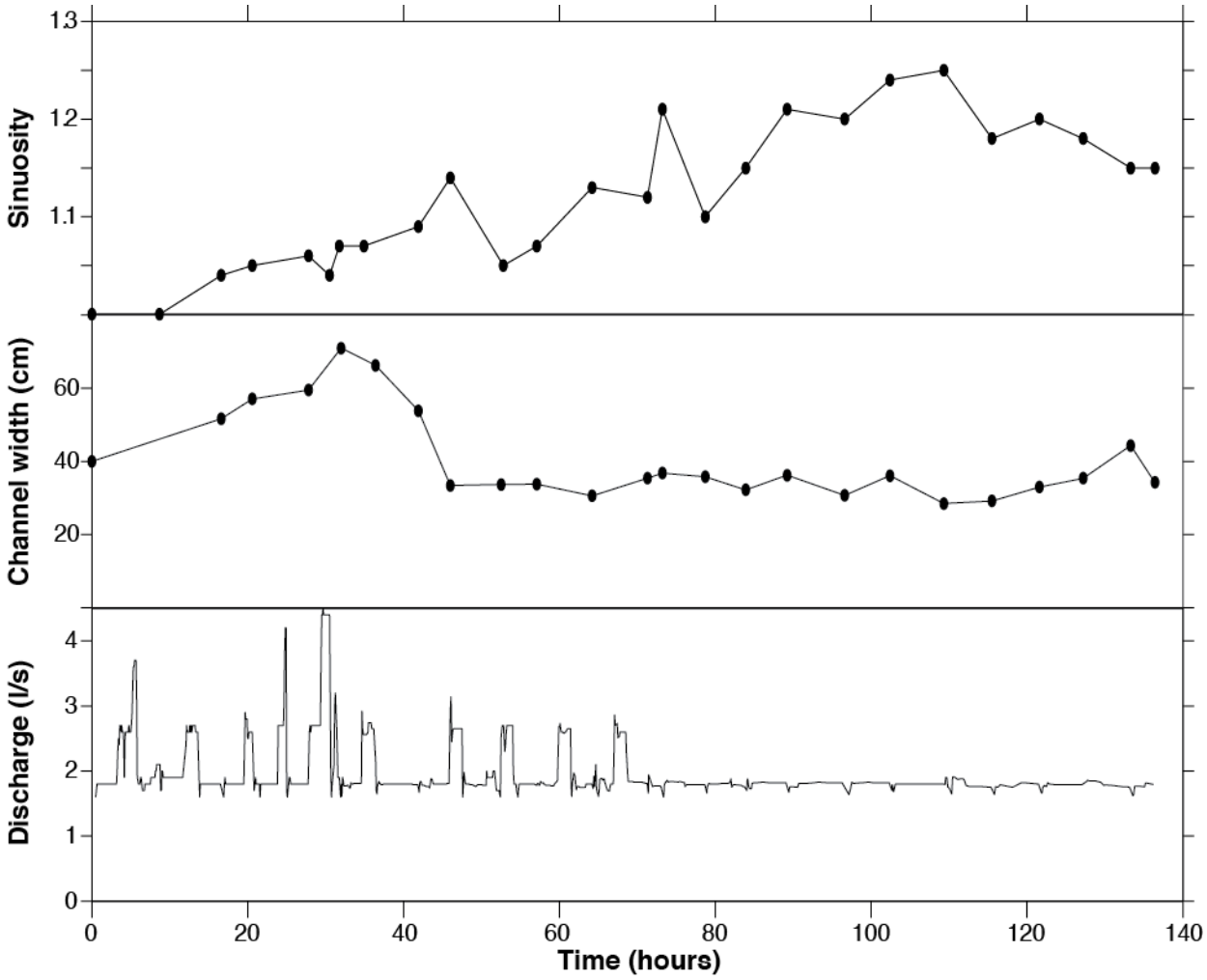


Figure 2.2. Discharge, channel width, and sinuosity change with time. The channel width is the average of 10 measurements downstream of the upper 5 m, the straight reach influenced by the input conditions. The sinuosity is measured downstream of the first bend and does not include the straight section immediately downstream of the inlet. Dips in the sinuosity are associated with cutoffs.

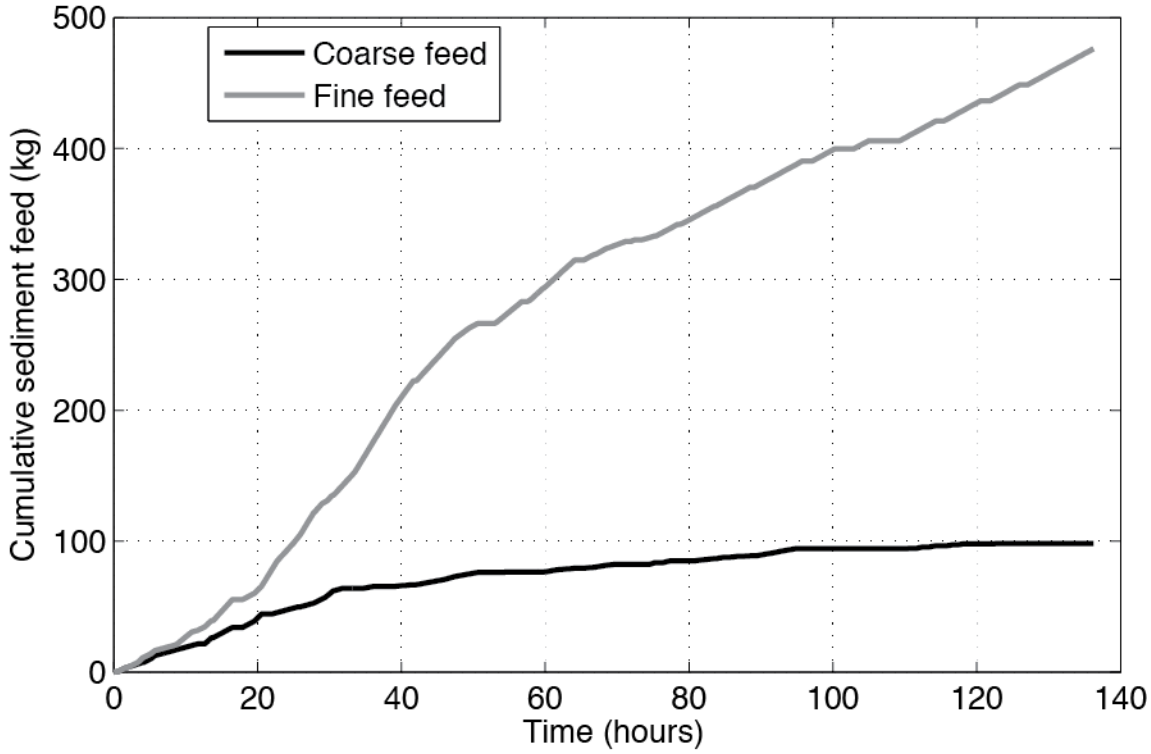


Figure 2.3. Cumulative sediment feed for coarse (black) and fine (gray) sediment. The coarse feed was adjusted to prevent aggradation upstream of the first bend, and the majority of the coarse feed was supplied in the beginning of the experiment.

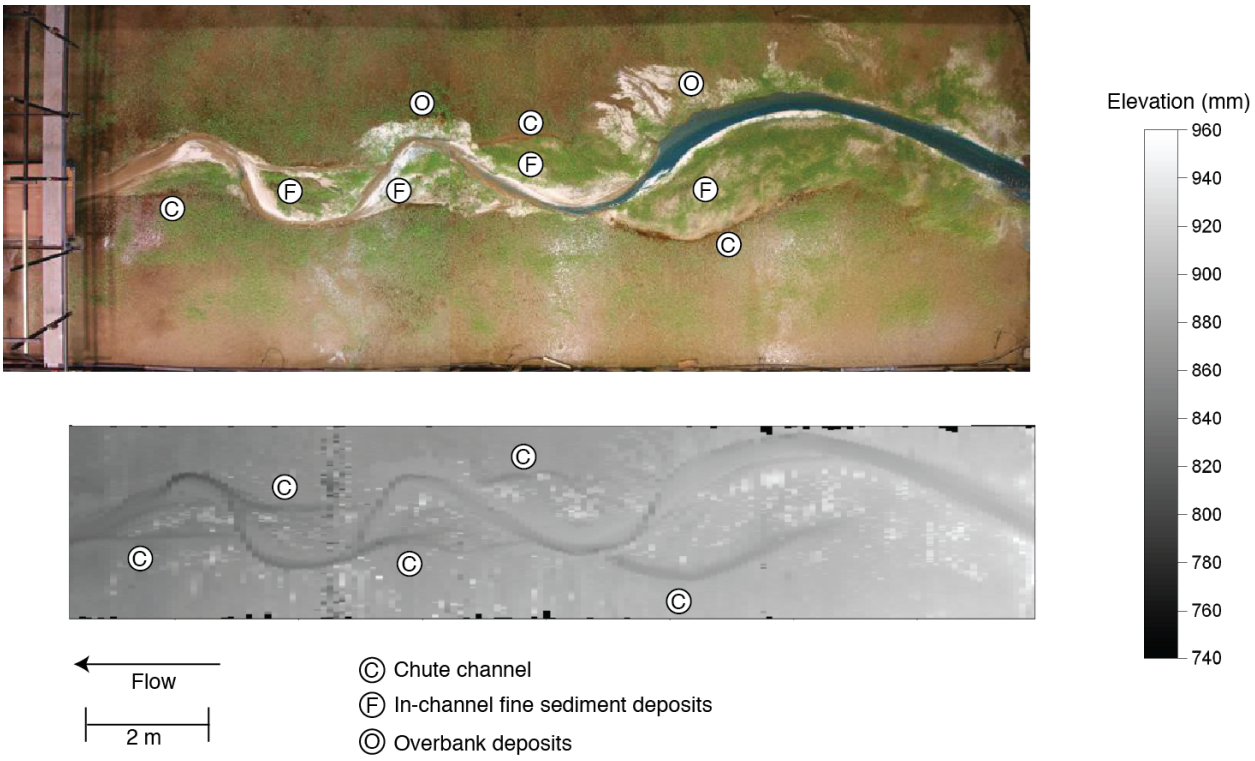


Figure 2.4. Overhead photograph and shaded topographic image 103 hours after the beginning of the experiment. The topographic image does not extend the length or entire width of the flume. In the topographic image, darker areas are lower elevation. Labels indicate chute channels, fine sediment deposits at the downstream end of bars, and areas of overbank deposition. In the photograph, the blue sediment is sand fed from upstream, the brown sediment is derived from the bed and banks of the channel, and the white sediment is fine sediment fed from upstream. The right bank was slightly lower than the left bank. A feature similar to a breakout channel formed during periods of aggradation at the upstream end of the flume on the lower elevation right bank.

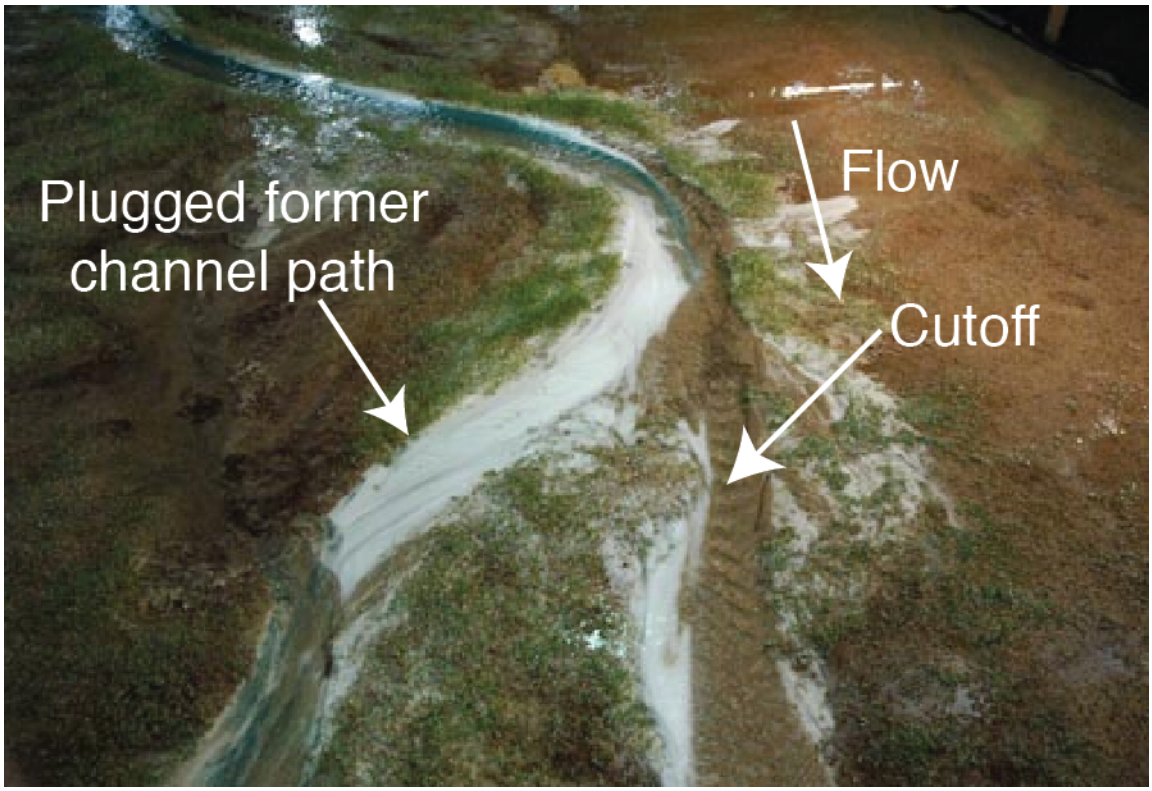


Figure 2.5. Sediment facies in of second and third bars downstream from the flume inlet. Fine sediment facies are mapped where the majority of the floodplain thickness was fine sediment. Accumulation of organic matter from dead alfalfa makes some of the bar appear brown where it is primarily fine sediment.

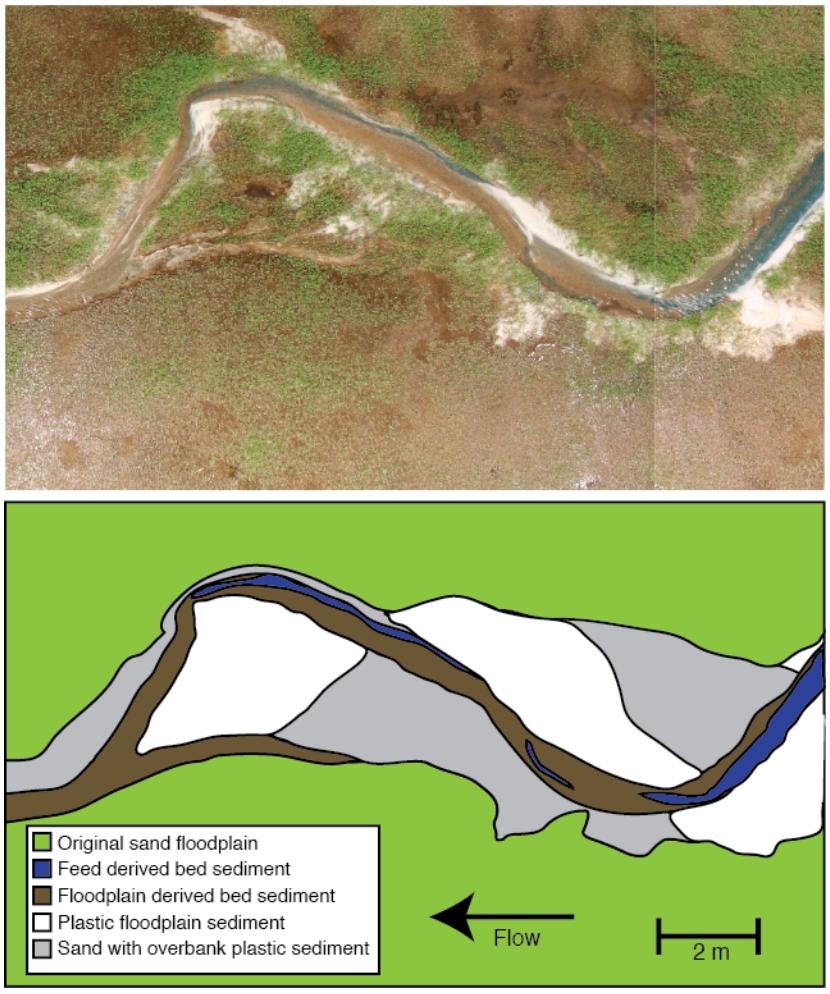


Figure 2.6. Photograph of cutoff channel and fine sediment filling the former channel. Sediment colors are the same as Figure 4. Fines also comprised the downstream end of the bar visible in the photograph. This was the final cutoff of the experiments and was caused by headward erosion rather than bar migration into a chute.

# 3 Where do gravel bedded rivers meander?

## 3.1 Abstract

The conditions which support meandering in gravel bed rivers are poorly understood, challenging theory, impairing stream restoration, and reducing our ability to infer environmental conditions where gravel meanders are present. We assembled a database of 166 gravel bedded meanders (and a smaller set of data for gravel braided and sand bedded meanders) to explore their morphology and the conditions that control their planform. Only meanders bounded by floodplains for at least 90% of their length with ample room for meander growth and cutoff were included in this analysis. The available dataset is strongly biased toward North America and Britain. We subdivided gravel bed meanders into three groups: meanders with cutoffs, meanders with islands (but with cutoffs), and meanders without cutoffs. This third meander type, though not widely discussed, is relatively common, especially in the British dataset. Meanders lacking associated cutoffs also lack scroll bars and appear to record stabilized channel forms. In general, meanders with cutoffs have lower channel and valley slopes relative to their discharge than meanders with islands and meanders without cutoffs. For meanders with median surface grain sizes > 8 mm, meanders with cutoffs had median bankfull Shields stress of 0.037, while meanders with islands and meanders without cutoffs had higher, but still relatively low Shields stresses (~0.044). In contrast, Shields stresses were 2-5 times higher for channels with median grain sizes ≤ 8 mm, likely due to the presence of sand dunes on the bed. Low Shields stresses for all gravel bedded meanders relative to gravel braided streams suggest that gravel bedded meanders develop under conditions of low sediment supply. Estimates of the relative input of gravel from banks versus the transport capacity indicate that gravel meanders are primarily exchanging gravel between eroding banks and downstream point bars, with little gravel supplied from upstream and little net downslope transport. Collectively our observations suggest that active gravel bedded meanders that experience periodic cutoff and regrowth are uniquely associated with low gravel sediment supply and low Shields stresses that are able to erode outer banks but cause limited net transport. Meander bends with islands (and cutoffs) experience somewhat higher Shield stresses, perhaps greater coarse sediment load, and may have lower bank strengths. The meanders without cutoffs are unexpected theoretically and maybe of diverse origins: emergence of a sinuous form without migration or cessation of migration due to changing conditions. For restoration purposes the distinction between actively migrating (to cutoff) and static form is important and field investigations are needed to understand what leads to stable meander form.

## 3.2 Introduction

It is surprising that gravel bedded rivers can have a meandering planform. In both gravel and sand bedded meanders, the deposited gravel and sand has no cohesive strength, hence upon exposure in outer bank walls the sediment should be subject to relatively rapid erosion, leading to channel widening, mid-channel bar growth and braiding [e.g., Friedkin, 1945; Federici and Paola, 2003]. Despite this, meanders are common, even when cutting through floodplain deposits of their own making, and many have suggested that they occur because deposited coarse sediment is either capped with cohesive material (from deposition of suspended sediment) or strengthened via vegetation [e.g., Friedkin, 1945; Brice, 1964; Millar, 2000; Micheli and

Kirchner, 2002; Parker et al., 2011]. Even at bankfull stage, however, gravel bedded rivers typically have Shields stresses close to threshold of transport [Parker et al., 2007; Zolezzi et al., 2009; Metivier and Barrier, 2012], possibly making meandering, which reduces the channel slope, less likely. Increases in bed load supply would tend to expand the finer surface areas of strong bedload transport [e.g., Dietrich and Whiting, 1989] and force the slope to increase and thus reduce meandering tendencies. In contrast, sand bed channels typically have Shields stresses well above their critical transport threshold [Parker et al., 2003; Wilkerson and Parker, 2011], and are able to accommodate changes in sediment supply through changes in the morphology of bedforms as well as slope [Dietrich and Whiting, 1989]. Some river classification systems therefore exclude full meandering as a planform in gravel bedded rivers [e.g., Church, 2002; Church, 2006], implying that instead that conditions capable of transporting gravel will promote alluvial channels that are predominantly braided or wandering. Gravel meanders nonetheless occur and have received some mechanistic study [Dietrich and Whiting, 1989; Clayton and Pitlick, 2007] and description of their sedimentology [e.g., McGowen and Garner, 1970; Bluck, 1971; Nanson, 1980]. They are often created for stream restoration projects [Kondolf et al., 2001; Smith and Prestegaard; 2005; Kondolf, 2006; Harrison et al., 2011] because they provide extensive habitat diversity [e.g., Trush et al., 2000] relative to other gravel bedded river planforms. Despite many years of study and restoration application, the geography and hydraulic characteristics that lead to and maintain meandering rather than braiding in gravel bed channels remain uncertain. In this paper, we compile an expanded database of gravel bedded meanders (hereafter referred to as gravel meanders) to explore where gravel bedded rivers meander in terms of both their geographic distribution and the hydraulic conditions that support their formation.

Theory suggests that the width to depth ratio (B/H) and $\tau^*$ strongly influence the form of channel bars and channel pattern [e.g., Colombini et al., 1987; Seminara and Tubino, 1989; Crosato and Mosselman, 2009]. B/H and $\tau^*$ may also control the migration and form of meandering channels [Blondeaux and Seminara, 1985; Seminara, 2005; Zolezzi et al., 2009]. Local increases in width can promote the development of mid-channel bars in gravel meanders [Luchi et al., 2010a; Luchi et al., 2010b], but they can also arise in uniform width channels due to curvature effects in short bends [Luchi et al., 2010a]. The absence of a general theory for channel width has caused most meander migration models to assume the width is constant [e.g., Ikeda et al., 1981; Johannesson and Parker, 1989; Howard, 1992; Sun et al., 1996]. Channel width can be assigned based on hydraulic geometry relationships [e.g., Ferguson, 1981; Kleinhans and van den Berg, 2010] or regime theory [e.g., Millar, 2000; Eaton et al., 2010], both of which are subject to large uncertainties. Numerical models are currently being developed that use flow and sediment transport mechanics to independently model outer bank erosion and inner bank deposition and could be used to explore what processes sustain meandering in coarse bedded rivers, but these models are in their early stages of development [e.g., Parker et al., 2011; Asahi et al., 2013].

Because of the difficulty of modeling the physics of flow and sediment transport to predict channel width and channel pattern, many studies have used correlation analyses of empirical datasets to define boundaries between meandering and braided morphology [Leopold and Wolman, 1957; Schumm, 1963; Carson, 1984; Ferguson, 1987; van den Berg, 1995; Xu, 2008; Kleinhans and van den Berg, 2010 among many others]. The Leopold and Wolman [1957]

analysis is the most widely used method to predict channel form. The threshold between braided and meandering channels in their dataset be defined by the equation:

$$S = 0.013{Q_{bf}}^{-0.44} \quad (3.1)$$

where S is the channel slope and $Q_{bf}$ is the bankfull discharge in $m^3/s$. Equation 3.1 had been adapted from the English units used in Leopold and Wolman [1957] to metric units. Meandering rivers have slopes less than predicted by the line whereas braided channels are steeper. Subsequent studies have shown that this threshold correctly identifies braided gravel channels and sand meandering channels but not gravel meanders [e.g., Carson, 1984; Ferguson, 1987]. Rivers with coarser beds tend to plot further from the threshold than rivers with finer beds [e.g., Carson, 1984; Ferguson, 1987]. Other channel pattern predictors combine channel slope and discharge into the stream power or unit stream power, where hydraulic geometry is used to predict channel width [Ferguson, 1981]. Because sinuosity is a function of channel pattern (meandering channels are sinuous while braided channels are straight) valley slope is often used rather than channel slope [van den Berg, 1993; Alabyan and Chalov, 1998; Kleinhans and van den Berg, 2010].

Compilations of field data show that relative to braided rivers of equivalent bankfull discharge meandering rivers are less steep [Leopold and Wolman, 1957; Ferguson, 1981; Beechie et al., 2006], are less steep for equivalent surface grain size [Henderson, 1966; Carson, 1984; Ferguson, 1987; van den Berg, 1995; Xu, 2008; Kleinhans and van den Berg, 2010; Eaton et al., 2010], or have stronger banks due to either vegetation [Millar, 2000; Beechie et al., 2006; Eaton et al., 2010] or cohesive sediment [Schumm, 1963]. Similar to Leopold and Wolman [1957], subsequent channel pattern discriminators successfully predict transitions from gravel braided channels to sand bed meanders, gravel meanders overlap with gravel braided rivers and sand meanders [e.g., Carson, 1984; Kleinhans and van den Berg, 2010]. Empirical and theoretical studies of river channel patterns emphasize that transitions between channel patterns are gradual rather than abrupt with many intermediate forms [e.g., Leopold and Wolman, 1957; Kellerhals et al., 1976; Parker, 1976]. Kleinhans and van den Berg [2010] discriminated channel patterns based on the median surface grain size and the "potential unit stream power', the product of valley slope and the square root of discharge. They found that the onset of gravel meanders with scroll bars occurs at lower potential unit stream power for a given surface grain size than gravel meanders with chute bars, but there is still considerable overlap between gravel meanders and gravel braided channels [Kleinhans and van den Berg, 2010].

Previous research has emphasized that in order to have sufficiently small width-depth ratios, gravel meandering rivers require relatively high bank strength [Schumm, 1985; Metivier and Barrier, 2012] and low sediment supply [Carson, 1984; Schumm, 1985; Ferguson, 1987; Metivier and Barrier, 2012], neither of which are easily quantified in correlation analysis. Field and laboratory studies of river morphology both emphasize that bank strength is a crucial component for meandering [Schumm, 1985; Ferguson, 1987; Smith, 1998; Tal and Paola 2007; Braudrick et al., 2009; Parker et al., 2011; Metivier and Barrier, 2012; van Dijk et al., 2013]. Flume experiments show that without bank strength, channels braid, and the addition of bank strength can have a profound effect on channel form [Friedkin, 1945; Smith, 1998; Tal and Paola, 2007; 2010]. Bank strength (when the bank is composed of sediment deposited by the

river) can be derived from vegetation [Hickin, 1984; ASCE Task Committee, 1998; Micheli and Kirchner, 2002] or material cohesion from silts and clays [Schumm, 1963; ASCE Task Committee, 1998; Constantine et al., 2009]. Although the bank failure mechanisms often differ, the ability to remove material deposited at the toe of eroded banks limits the migration of some rivers [e.g., ASCE Task Committee, 1998; Parker et al., 2011]. Highly vegetated channels tend to be narrower than less densely vegetated channels [Andrews, 1984; Hey and Thorne, 1986; Metivier and Barrier, 2012]. Channels with denser vegetation also have higher average Shields stresses than channels with less dense vegetation, suggesting that banks strengthened by dense vegetation can withstand higher bank stresses [Parker et al., 2007]. Vegetation not only adds strength to the banks, but can also strengthen the floodplain, limiting cutoffs and promoting higher sinuosity [Smith, 2004; Braudrick et al., 2009; Kleinhans, 2010]. Experiments suggest that strength from vegetation alone is not sufficient and that fine sediment is also required to allow bars to grow to the elevation of the floodplain, particularly downstream of the bend apex [Braudrick et al., 2009].

There are few measurements of sediment supply that can be used to directly compare the role of sediment supply in channel patterns [e.g., Metivier and Barrier, 2012; Pitlick et al., 2012], so instead the channel is assumed to be at equilibrium with the sediment supply and the Shields stress ($\tau^*$) is often used as a proxy for sediment supply [e.g., Metivier and Barrier, 2012]. The Shields stress is:

$$\tau^* = \frac{\tau_b}{(\rho_s - \rho) g D_{50}} \tag{3.2}$$

where $\tau_b$ is the boundary shear stress, $\rho$ is the density of water, $\rho_s$ is the density of sediment g is gravitational acceleration, and $D_{50}$ is the median grain size of the bed surface. $\tau^*$is higher on average for gravel braided than gravel meandering channels, but gravel meandering channels span nearly the entire $\tau^*$ range of the braided channels [Metivier and Barrier, 2012], suggesting that some gravel meanders are resilient to high sediment supply (i.e., they do not transform to a braided morphology). Bedload measurements in gravel meanders show that 30-60% of the bedload trapped in gravel meanders is sand, even though it is not present on the bed surface [Leopold, 1992; Ferguson et al., 1996; Clayton and Pitlick, 2007]. Moreover, there may be strong size-selective transport with the 85% of the load finer than the median size of the bed surface [e.g., Dietrich and Whiting, 1989; Clayton and Pitlick, 2007] and the gravel that makes up the bulk of the bed may rarely move, and when it does movement is limited to short distances [Leopold, 1992].

This paper explores the geographic distribution of meandering in gravel bedded rivers using an expanded database from the literature coupled with aerial photographic investigation of each of the sites using Google Earth. We use these data to explore the physical conditions of gravel meanders and document the geographic distribution of such channels and their floodplain characteristics. Our data compilation relies on English language literature and is, thus, biased towards countries where English is spoken. Despite this bias, the compiled data reveal important controls on the conditions where meandering occurs in gravel bedded rivers. Using Google Earth and descriptions in the literature, we were careful to only include rivers with alluvial banks and beds where the interaction with bedrock banks and terraces was less than 10% of the bank length.

We found when examining the Google Earth imagery that sites defined in the literature as "meandering" differed in important ways. We therefore subdivided gravel bedded meanders into three morphologies: meanders with cutoffs and without islands, meanders with cutoffs and islands, and meanders without cutoffs. The unanticipated category was third one in which the Google Earth imagery indicates that the channel has not swept across its floodplain. This distinction has practical considerations: some restoration projects want a dynamically shifting gravel-bedded meander and others do not. This raises the question of whether there are empirical differences between the two that are not distinguished by channel planform–potentially an important observation for stream restoration.

## 3.3 Methods

### 3.3.1 Characteristics of gravel meanders database

We have compiled 166 gravel meanders for our database (Appendix B–Table B1). Many of these were included in previous data compilations [Leopold and Wolman, 1957; Church and Rood, 1983; Andrews, 1984; Hickin and Nanson, 1984; Hey and Thorne, 1986; van den Berg, 1995; Beechie et al., 2006; Kleinhans and van den Berg, 2010; Metivier and Barrier, 2012] and we have expanded previous datasets using additional data from gravel meanders reported in the literature (see Appendix B–Table B1). We did not include obviously incised meanders, meanders with bedrock beds, or meanders with a >10% of their length abutting hillslopes or terraces rather than floodplain deposits. We also did not include rivers that were individual branches of anabranching systems (e.g., the Ovens River, Australia), regardless of their morphology because the anabranching form alters how flow and sediment are routed at during different flood stages. Where possible, we checked the original data source to verify the data, which has resulted in a few minor differences between our dataset and the same rivers in previous compilations. To facilitate comparisons with other channel types, our database includes 74 sand bed meanders and 36 gravel braided streams primarily from van den Berg [1995] and Kleinhans and van den Berg [2010] (Appendix B–Tables B2 and B3).

The data available and collection methods varied from site to site and ranged from a minimal description of the river as a gravel meander (e.g., Derry Burn) to a complete set of hydraulic variables (Appendix B–Table B1). Data include the location, bankfull discharge, drainage area, bankfull width and depth, bankfull width-depth ratio, surface median grain size, channel slope, valley slope, sinuosity, and channel migration rate (Appendix B–Table B1). We used the reported bankfull discharge from each site. Where bankfull discharge was not defined, we used the 1.5 or 2 year flow. Morphologic data were averaged over reaches of uniform slope and discharge. The data collection method for grain size varied from photogrammetric methods to pebble counts, to surface bulk samples, and likely contains some uncertainty.

For every site we defined a reach where the channel morphology was relatively constant. The reach length varied from site to site, and tended to be shortest for channels in small intra-mountain meadows and urban rivers. Using Google Earth in combination with site descriptions from the literature, we noted the presence of cutoffs and islands, the vegetation type and the dominant land use. If cutoff scars were visible on Google Earth, we categorized the channel as having cutoffs regardless of their degree of infilling. The lack cutoff scars on floodplains implies that the channel is not migrating, but because Google Earth photographs often span only a few

years it is possible that these channels are migrating very slowly or only during very large floods. We noted the presence and type of islands in each study reach. Because island visibility on aerial photographs is often function of flow stage, we examined images from multiple years where possible. If islands only occurred on one bend of a long reach, we noted their presence but categorized the channel as not having islands. Islands could be either unvegetated mid-channel bars exposed at low flow or vegetated islands. Vegetation was categorized into 4 types: grasses/shrubs (Class 1), predominantly grasses/shrubs with sparse forests (Class 2), predominantly riparian forest with grasses/shrubs (Class 3), and forested (Class 4). The portion of trees on the channel banks increases with increasing vegetation class. Land use was categorized into agricultural, urban/industrial, forested, and rangelands.

Our approach assumes that the channel patterns in aerial photographs are linked to hydraulic and sediment data collected for the sites. This may lead to a temporal disconnect between the photographs and the site characteristics given that we are using recent aerial photographs, and surveys of channel dimensions, slope, and grain size may date back as far as Leopold and Wolman's measurements published in 1957. We also assume that the current channel form is related to the calculated Shield stress, which is a surrogate for gravel sediment supply averaged over a morphologically significant time period.

### 3.3.2 Data Analysis

Where data were sufficient, we made several calculations to calculate proxies for sediment transport and assess hydraulic variables. The boundary shear stress is:

$$\tau_b = \rho g R_h S \tag{3.3}$$

where $\tau_b$ is the boundary stress, $\rho$ is the density of water (assumed to be 1000 kg/m$^3$), g is gravitational acceleration (9.81 m/s$^2$), and $R_h$ is the bankfull hydraulic radius (if not provided $R_h$ was calculated assuming a rectangular cross section).

The particle Reynolds number ($Re_p$) is:

$$Re_P = \frac{\sqrt{\frac{(\rho_S - \rho)}{\rho} g {D_{50}}^3}}{\nu} \tag{3.4}$$

where $\nu$ is the kinematic viscosity (assumed to be $10^{-6}$ m$^2$/s) and $\rho_s$ is assumed to be 2650 kg/m$^3$.

To assess the maximum size of suspended sediment we calculated the Rouse Number:

$$\frac{u^*}{kW_s} = 2.5 \;\; or \;\; u^* = W_s \tag{3.5}$$

where $W_s$ is the settling velocity of the sediment, k is von Karman's constant (equal to 0.4) and u* is the shear velocity. The settling velocity was calculated using Dietrich [1982] assuming a Corey Shape Factor of 0.7, Powers Roundness of 3.5, and a kinematic viscosity of $10^{-6}$ m$^2$/s.

u* is equal to:

$$u^* = \sqrt{\frac{\tau_b}{\rho}} \tag{3.6}$$

## 3.4 Results

From our Google Earth analysis we grouped the 166 gravel bed meanders based on the presence of cutoffs and islands. The dataset contained 40 gravel meanders with cutoffs and without islands (hereafter referred to as gravel meanders with cutoffs), 55 gravel meanders without cutoffs, and 71 gravel meanders with islands/mid channel bars and cutoffs (hereafter meanders with islands). Of the 55 gravel meanders without cutoffs, 14 had islands. Examples of each channel type are shown in Figures 3.1-3.3. Some meanders with cutoffs had well-developed point bars (Pearl River, LA, Figure 3.1b) and other had well-developed scrolls (e.g., Taieri River, New Zealand, Figure 3.1d). Cutoff scars ranged from open and still attached to the channel (Figure 3.1d) to completely filled in and vegetated (Figure 3.1a). Island meanders contained both vegetated and unvegetated islands. Eighteen of the meandering channels with islands contained only unvegetated islands, 16 contained only vegetated islands, and 33 contained a mix of vegetated and unvegetated islands. Islands were not continuously present through the reaches, but occurred as mid-channel bars in locally wide sections or in chutes along the inside of point bars (Figure 3.2). Of the 49 sand meanders with location data, 7 had islands and 47 had cutoffs (Appendix B–Table B2).

### 3.4.1 Geographic Distribution of Gravel Meanders

Gravel bed meanders in our database are concentrated in western North America and Great Britain, which together make up nearly 90% of the dataset (Figure 3.4). This reflects a bias in both the English-language literature and also likely reflects a bias in the site selection of researchers. In North America, gravel meanders are mostly found in the Rocky Mountain region in the US and Canada, in the plains adjacent to the Canadian Rockies, the Piedmont of the Eastern US, and in Puget Sound and Olympic Peninsula. The geography of gravel bed meanders provides clues to both the source of coarse sediment and also the source of bank strength. Most of the rivers in the dataset are located along mountain ranges (particularly the Rocky Mountains), in formerly glaciated landscapes (Great Britain), or periglacial landscapes (Piedmont region of the Eastern U.S.). Two US Piedmont sites on Watts Branch were influenced by mill dams (Walter and Merritts, 2008; Merritts et al., 2011), but the influence of mill dams on the 5 other Piedmont rivers is unknown. The Pearl, Amite, and Bogue Chito rivers in Louisiana derive their gravel from Plio-Pleistocene glacio-fluvial terraces [Self, 1983], suggesting that gravel meanders far from a glacial source can also be a legacy of past climates. Several rivers have no obvious nearby gravel sources, and gravel appears to be a lag deposit of particles with low breakdown rates or a previous climatic regime. In these streams (notably, the Congaree in South Carolina and the Neosho River in Kansas), gravel is mostly exposed on bars and is concentrated in a thin layer overlain by sand and silt [Levey, 1977; Juracek and Perry, 2004].

The geographic distribution of rivers in the database suggests that climate may also affect the distribution of gravel bed meanders. Nearly the entire database is located in either moderately humid regions (Britain, eastern US) or along mountain ranges with snowmelt hydrographs (western North America). There are only 2 arid gravel meandering rivers in the dataset: the Lower Jordan River between the Sea of Galilee and the Dead Sea and the Nueces River near

Uvalde, TX. The Nueces River has extreme discharge variation and occasionally runs dry at a drainage area of 5,050 $km^2$ [Gustavson, 1978]. In places, the Lower Jordan River and the Nueces River abut marly-rich terraces that supply high loads of fine material to the channel that deposits in the channel banks [Schattner, 1962; Gustavson, 1978]. In the Lower Jordan River, marly deposits provide fine-grained cohesive sediment to the river and the most sinuous reaches are associated with regions of marly bedrock [Schattner, 1962].

Gravel meanders with cutoffs occur throughout the geographic range of the dataset, nearly three-quarters are located in North America, mainly along the Rocky Mountains in the US and Canada (Figure 3.4B). These rivers are located along mountain fronts and also in high elevation inner-montane valleys. Just over one-quarter of meanders with cutoffs are at elevations greater than 1000 m, a much higher portion than sand meanders and gravel meanders without cutoffs (Figure 3.5). Elevation is likely a proxy for the type of hydrograph, with snowmelt hydrographs common in high-altitude channels. Gravel meanders with islands are common in the Rocky Mountain Front Range, Pacific Northwest, and also occur in Alaska, and New Zealand. Over 1/3 of meanders with islands are located at elevations greater than 1000 m (Figure 3.4). Nearly 70% of British rivers in the database are meanders without cutoffs (Figure 3.4). Despite only comprising about one-fourth of the gravel bed meandering dataset, British rivers comprise over half of the meanders without cutoffs. Agricultural fields surrounded nearly every British meander without cutoffs with a narrow band of large trees between the river and the farmland (Figure 3.3b for example). Four Pennsylvania rivers labeled as meanders without cutoffs are, in fact, actively migrating [Hession et al., 2003; Allmendinger et al., 2005]. These migrating rivers were recently deforested [Pizzuto, personal communication], and there has perhaps not been sufficient time for these channels to migrate to cutoff. There was no evidence of migration in the other meanders without cutoffs.

### 3.4.2 Slope, discharge, and sinuosity of gravel meanders

The channel slope and bankfull discharge of gravel bed meanders both span over 3 orders of magnitude (0.0001–0.014 and 1.8–5700 $m^3/s$, respectively) (Figure 3.6). Channel slope generally decreases with increasing bankfull discharge, with approximately an order of magnitude of scatter in channel slope for a given discharge (Figure 3.6). For a given discharge, most gravel bed meanders have intermediate channel slopes between the steeper braided channels and lower slope sand meanders (Figure 3.6, Table 3.1). One-third of the sand meanders have bankfull discharge and channel slope that fall within the range of gravel meanders (Figure 3.6). The upper panel of Figure 3.6 also shows the braided-meandering threshold relationship described by Leopold and Wolman [1957] (equation 3.1) with braided channels expected to occur at slopes greater than the threshold line and meandering channels at slopes less than the threshold. Similar to previous studies [Carson, 1984; Ferguson, 1987; Church, 2002] we found that this threshold does not accurately predict the morphology of gravel meanders. The Leopold and Wolman [1957] threshold was exceeded for 48% of the gravel bed meanders. This threshold correctly separates the gravel braided channels from the sand meanders.

The median channel slope is similar for meanders with islands and meanders with cutoffs (0.0017 and 0.0015, respectively), but meanders with islands have much higher median bankfull discharge than meanders with cutoffs (155 $m^3/s$ versus 46.5 $m^3/s$, respectively) (Table 3.2). Meanders without cutoffs are steeper with a median channel slope of 0.003 with an intermediate

median bankfull discharge (81 $m^3/s$) between meanders with cutoffs and meanders with islands (Figure 3.6). Ten of the fifteen rivers with the highest bankfull discharges in the gravel meander dataset are island meanders, including the 7 of the 8 gravel meanders with bankfull discharge exceeding 1000 $m^3/s$. The Leopold and Wolman [1957] threshold line correctly lies above 87% of the data points for meanders with cutoffs, considerably better than for the other gravel meander types. Approximately 53% of island meanders and 36% of meanders without cutoffs had channel slopes exceeding the threshold defined by Leopold and Wolman given their bankfull discharge (Figure 3.6).

The trends for valley slope relative to bankfull discharge are similar to channel slope, with increased overlap between gravel meanders and gravel braided datasets, and slightly more overlap with the different meander types. Valley slopes range from 0.0003 to 0.022 for gravel meanders. The median valley slope for meanders without cutoffs is 0.003, which is steeper than meanders with islands and meanders with cutoffs, which both have median slopes of 0.0022 (Table 2, Figure 3.6).

Sand meanders have a higher proportion of their sinuosities ≥ 2 than gravel meanders (Figure 3.7). Nearly 30% of sand meanders in the database have sinuosity ≥2, while only about 14% of the gravel bed meanders are that sinuous (ranging between 9 and 16% of each gravel meander type). Although meanders with cutoffs have a higher median sinuosity than meanders with islands and meanders without cutoffs, meanders with cutoffs have fewer rivers with sinuosity>2. Differences among channel types for sinuosities between 1.25 and 1.5 could reflect thresholds of sinuosity used by different datasets in our compilation. Approximately 25% of meanders with cutoffs have sinuosities between 1.25 and 1.5, while just over 40% of meanders with islands and half of meanders without cutoffs had sinuosities ≤1.5.

### 3.4.3 Bank vegetation and channel width-depth ratio

Because quantifying bank strength in the field is challenging, and there are little bank strength data in the gravel bed meander dataset, inferences regarding bank strength rely on a combination of vegetation category and width-depth ratio. Aerial photographic analysis is not a robust way to examine the bank strength of streams, but given the paucity of bank strength data in the dataset, it still allows us to make first-order estimates of bank strength controls. Of the 166 gravel meanders, 29 had grass/shrub vegetation on the banks (Vegetation Class 1), 53 had banks that were predominantly grass/shrub with some trees (Vegetation Class 2), 38 were predominantly trees with some grass/shrubs (Vegetation Class 3), and 46 were forested (Vegetation Class 4) (Figure 3.8). There is little difference in the vegetation class among the gravel meander planform types. The mean vegetation class is 2.5 for meanders without cutoffs, 2.6 for meanders with cutoffs, and 2.8 for meanders with island (Figure 3.8). On average, large rivers are more likely to have trees rather than grasses/shrubs dominate their banks. The median bankfull discharge is highest for Vegetation Class 3 (302 $m^3/s$) and lowest for Vegetation Class 1 (15 $m^3/s$) (Figure 3.9, Table 3). Gravel meandering rivers with bankfull discharge greater than the median (93 $m^3/s$) have a mean vegetation class of 3.0 while gravel meanders with bankfull discharge less than 93 $m^3/s$ have a mean vegetation class of 2.3. Riparian land use is predominantly agricultural for gravel meanders without cutoffs, gravel meanders with cutoffs, and sand meanders, while the floodplains of gravel meanders with islands and gravel braided channels have fewer farms and more rangelands adjacent to the channel (Figure 3.8). It is unclear

whether land use differences among the channel types represent alter the channel morphology (via artificial changes in bank strength along farmlands) or if land use reflects the channel pattern (i.e., farms are more likely to be located along laterally stable rivers).

The width-depth ratio (B/H) of the gravel meander dataset as a whole ranges from 7 to 150, with a median of 21.8 for the entire dataset (Table 1, Figure 3.10). Sand meanders have a median B/H of 16, while gravel braided rivers have a median B/H of 270 (Table 1). Over 80% the gravel meander dataset and 29 of the 33 sand meanders have B/H ≤ 40, whereas 26 of 27 gravel braided channels have B/H>40. Gravel meanders with B/H>40 typically have islands. The median B/H is 18.6 for meanders with cutoffs, 19.5 for meanders without cutoffs, and 29.2 for meanders with islands (Figure 3.10, Table 3.2). Only four of the meanders without cutoffs have B/H < 10, and bars were observed in many meanders without cutoffs. This suggests that although they are not migrating, theory [e.g., Parker, 1976] and observations suggest that they contained point bars. The median B/H ranged from 17.4-29.2 for Vegetation Class 2 and Vegetation Class 4, respectfully (Table 3.3).

### 3.4.4 Sediment supply

For a given bed material size (sand or gravel), the higher the bankfull $\tau^*$ the greater the bedload flux. This flux rises non-linearly above critical values [e.g., Meyer-Peter and Muller, 1948; Parker, 1979; and many others]. As others have done [e.g., Metivier and Barrier, 2012], we hypothesize, then, that for a given bed size, the higher the bankfull $\tau^*$, the greater the coarse sediment load to which the channel is adjusted. Figure 3.11 shows the particle Reynolds number (Equation 3.4) relative to $\tau^*$ (Equation 3.1). Because all of the parameters in the particle Reynolds number are held constant other than grain size, changes in the particle Reynolds number are solely a function of median grain size, which is shown on the upper axis. The plot has three solid lines, the lower line represents the critical Shields stress ($\tau^*_{crit}$) calculated following Parker et al. [2003]. Parker et al. [2003] fit a curve to the original Shields data by Brownlie [1981] and corrected it to match field data by dividing by that relationship by 2 so that $\tau^*_{crit}$ for gravel is equal to 0.03. Uncertainty in measurement and specifics of local conditions (e.g. particle shape, packing, abundance of finer sediment, etc.) have led to large variations in reported values of $\tau^*_{crit}$ for individual cases which range from 0.03 to 0.086 [e.g., Buffington and and Montgomery, 1997]. The Parker et al., [2003] $\tau^*_{crit}$ for gravel is therefore a lower bound. This curve can be defined by the equation:

$$\tau^*_{crit} = \frac{1}{2}\left(0.22Re_p^{-0.6} + 0.06 \cdot 10^{-7.7Re_p^{-0.6}}\right) \quad (3.7)$$

The upper curve shows the suspension threshold for the median surface grain using equation 3.5 as the suspension criteria. The straight line on the plot represents $\tau^*$ corresponding to the critical settling velocity for 2 mm sand. Rivers that plot above the suspension line transport 2 mm sand in suspension at bankfull flow.

The range of surface grain sizes for the different gravel meander morphologies is similar, with $D_{50}$ between 10 and 100 mm for most rivers in the dataset (Figure 3.11, Appendix B–Table B1). Thirty five of the 133 rivers have $D_{50} \leq 20$ mm while only one of the gravel braided channels had $D_{50} \leq 20$ mm. On average, the median surface grain size was finer for gravel

meanders with cutoffs (median $D_{50}$=23 mm) than meanders with islands (median $D_{50}$=36 mm) and meanders without cutoffs (median $D_{50}$=41 mm).

There are sufficient data to calculate $\tau^*$ at bankfull conditions for 115 of the gravel meandering rivers (27 meanders with cutoffs, 45 meanders with islands, and 44 meanders without cutoffs). Just over half of the gravel meanders had bankfull $\tau^*$ less than 0.045 (Figure 3.11). The median $\tau^*$ was over twice as high for the gravel braided dataset (0.096, n=23) than for the gravel meanders dataset (0.044, n=115) and bankfull $\tau^*$ for sand meanders were typically an order of magnitude greater than the critical threshold at bankfull flow (Figure 3.11, Table 3.1). In general, meanders without cutoffs and meanders with islands have similar $\tau^*$, which are generally greater than meanders with cutoffs (Figure 3.11, Table 3.2). The proportion of rivers with $\tau^*$ less than the critical threshold is slightly higher for meanders with cutoffs (6 of 26 rivers) than meanders with islands (8 of 45 rivers) and meanders without cutoffs (6 of 44 rivers).

Gravel meanders with fine median grain sizes have transitional $\tau^*$ between the relatively low $\tau^*$ coarser gravel meanders and the high $\tau*$ sand bedded meanders (Figure 3.11). The threshold of this transition is uncertain, but occurs somewhere between 14 and 6 mm. Gravel meanders with cutoffs with $D_{50}\leq$8 mm had $\tau^*$ that were at least double the $\tau^*$ of coarser rivers of the same channel type (Figure 3.11). If we analyze coarse ($D_{50}>$ 8 mm) rivers independently, gravel meanders with cutoffs with $D_{50}>$ 8 mm plot in a narrow range of $\tau^*$ with a median value of 0.037 (Table 3.4), and ¼ of the data had $\tau^* < 0.03$. All but two (90%) of the gravel meanders with cutoffs and $D_{50}>$8 mm had $\tau^*< 0.047$. In contrast, 45% of island meanders and 50% of meanders without cutoffs with $D_{50} >$ 8 mm had $\tau^*> 0.047$. For rivers with $D_{50} >$ 8 mm, island meanders and meanders without cutoffs had a median bankfull $\tau^*$ of 0.044 and 0.045, respectively, but meanders without cutoffs were more likely to have $\tau^*$ exceeding 0.05. Nearly all gravel meanders ($D_{50}>$8 mm) have $\tau^*< 0.063$ (2.1 times the critical stress), suggesting that they undergo size-selective transport [e.g., Wilcock and McArdell, 1997].

Calculations suggest that bedload transport of 2 mm sand occurs during bankfull flow in nearly 3/4 of gravel meanders and only 1/4 of gravel braided streams (Figure 3.11). Sand meanders typically exceeded the suspension threshold for their median bed particle size at bankfull flow, but the form drag on bedforms will greatly reduce the shear stress available for transport. Nearly all (92%) of the gravel meanders with cutoffs and 73% of meanders with islands and 66% of meanders without cutoffs transport 2 mm sand as bedload rather than suspended load (Figure 3.11).

Figure 3.12 shows the geographic distribution of $\tau^*$ for channels with surface $D_{50}>$8 mm in North America, Britain, and New Zealand. These three panels show the entire distribution of $D_{50}>$8mm that have sufficient data to calculate $\tau^*$. 13 rivers had $D_{50}\leq$8mm and are not shown in Figure 3.12 for clarity. Rivers without grain size data are indicated by gray symbols, with red and yellow symbols indicating $\tau^*<0.05$, and green and blue symbols indicating $\tau^*>0.05$. Low $\tau^*$ rivers are primarily located along the Rocky Mountains, with only 1 river having a $\tau^*$ greater than 0.05 (The Sheep River at Okotos a gravel meander with islands with a $\tau^*$ of 0.076). All seven Alaskan rivers from the Emmett [1972] dataset have $\tau^*$ above 0.055, 4 of the 7 had $\tau^*$above 0.1. Two of the rivers had median diameters between 8 and 9 mm. These rivers are all

north of 61degrees latitude, and although the presence of permafrost at the study sites was not noted by Emmett, several of the rivers have permafrost banks [Viereck et al., 1970; Kreig, 1977]. Rivers of similar latitude from the Yukon Territory, which presumably also have permafrost banks have $\tau^* \leq 0.037$, suggesting that permafrost alone does not explain the high $\tau^*$ of the Emmett [1972] dataset. $\tau^*$ is only available for 1 of the 10 rivers in Puget Sound, and this one channel (the Green River) has a relatively high $\tau^*$. Gravel meanders in New Zealand have a wide range of $\tau^*$ from 0.027 to 0.1, but $\tau^*$ exceed 0.05 for 4 of the 7 New Zealand Rivers. The Selwyn River in New Zealand [Carson, 1984] has a $\tau^*$ exceeding 0.1 despite a relatively coarse bed. The Selwyn River, however, transforms to a braided morphology following floods [Carson, 1984], and braided channel scars are visible on the floodplain. Rivers with cutoffs in Britain have intermediate stresses with only two of the meanders with islands exceeding a bankfull $\tau^*$ of 0.05, and meanders with cutoffs have $\tau^* < 0.05$. From our Google Earth analysis and review of the site descriptions in the literature, this difference is not due to increased roughness from large wood in the channel or on the banks.

The regional bias is particularly evident in the $\tau^*$ data, because not only are data on gravel bed meanders absent from much of the globe (Figure 3.4), of the locations where we have data, grain size is measured in some regions (e.g., Rocky Mountains, Britain) and not measured in others (e.g., Puget Sound and British Columbia). Coarse gravel meanders with islands generally have $\tau^* < 0.05$, but stresses are higher in New Zealand and Alaska, two locations with relatively high gravel supply.

Our analysis of $\tau^*$ does not take into account stress extracted by bedforms such as channel bars and dunes [see Nelson and Smith, 1989; Garcia, 2008] and large wood [e.g., Manga and Kirchner, 2000], and the boundary stress available for sediment transport at bankfull flow is likely lower than our calculation. Examination of Google Earth did not reveal a correlation between high $\tau^*$ sites and abundant large wood in the channel. Additionally, $\tau^*$ was not systematically higher for forested channels than grassy channels (Figure 3.13). This suggests that resistance imposed by exposed roots on the banks is not responsible for gravel bedded meanders with high $\tau^*$, provided that roots exposure is solely a function of vegetation class. Field studies show that for gravel meandering rivers, the stress does not increase appreciably during overbank flows where the valley width is large relative to the channel width [e.g., Clayton and Pitlick, 2007; McKean and Tonina, 2013]. In these channels the large floodplain width limits stage increases above bankfull and may alter the water surface slope [McKean and Tonina, 2013].

Differences in bankfull $\tau^*$ could reflect differences in $\tau^*_{crit}$ rather than differences in sediment supply. $\tau^*_{crit}$ varies due to particle shape, particle packing, the grain size distribution of the supply [Buffington and Montgomery, 1997; Mueller et al., 2005], channel slope [Mueller et al., 2005; Parker et al., 2007; Lamb et al., 2008;], and the presence of sand on gravel beds [Ikeda and Iseya, 1988; Wilcock, 1998]. Assuming a single $\tau^*_{crit}$ for gravel bed meanders across the globe is likely an oversimplification. Because most meanders with cutoffs are in the Rocky Mountain Region and most meanders without cutoffs are located in Britain, there could be regional effects that influence the grain size distribution, particle shapes, or particle packing.

## 3.5 Discussion

### 3.5.1 Spatial bias in river databases

The gravel meander dataset is strongly biased toward North America and Britain, and only includes one river from South America (the Sinu River, Columbia), one from Asia (the Nuporomaporo River, Hokkaido, Japan), and one from Papua New Guinea (the Strickland River). This is at least partially due to the English language focus of the literature reviewed and likely also reflects a bias in the location of geomorphic studies. The North American bias is much stronger for gravel meanders than for the smaller sand meander database. The sand meander database was assembled from the same literature and includes rivers from South America, Australia, Africa, and India, with 22 of the 72 sand bed rivers from outside of North America, Britain, and New Zealand. Both the sand meander database and the gravel meander database lack data in China, and much of India. Perusal of Google Earth shows that meandering rivers occur in these regions, but hydraulic and grain size data have not been published in the literature. Xu [2004] used 61 sand bedded meandering and braided rivers from China, but the data were not included in the publication. Expansion of field observations to rivers systems where meanders are observed near active mountain ranges, such as the Andes, will help to determine whether the correlation between low sediment supply and meandering in gravel bed rivers is a function of supply or the geographic distribution of the existing dataset.

The geographical extent of data compilations may limit their implications. Using similar datasets both Parker et al. [2007] and Zolezzi et al. [2009] showed that British rivers (primarily from Hey and Thorne, [1986]) differed from other rivers in their database. Our analysis shows that much of this difference may be due to the large number of rivers without cutoffs in their data. Only two of the rivers in Hey and Thorne [1986] are actively migrating. For UK rivers with D50>8 mm, just 8 of 29 are actively migrating.

### 3.5.2 Sediment supply and channel migration

Several studies have suggested that for gravel bedded meanders with low sediment supply, sediment derived from bank erosion may dominate the bedload flux [e.g., Blacknell, 1982; Hickin and Nanson, 1984; Neill, 1984; Hooke, 2003; McKean and Tonina, 2013], although this is generally inferred rather than measured or calculated. These observations are supported by flume experiments which show that for low transport rates bedload is laterally exchanged between bars in actively migrating meandering rivers [Braudrick et al., 2009]. We can use this dataset to assess the importance of bank erosion to the bedload conveyed by a gravel bedded meander. Because there are only four rivers in the gravel meander dataset with bankfull bedload transport measurements, we instead need to calculate the sediment transport rate. Here we use Parker [1979], because it was developed for use in gravel bedded rivers, and the critical $\tau^*_{crit}$ of 0.03 is typical for gravel bedded rivers in the field [Buffington and Montgomery, 1997; Parker et al., 2003]. The dimensionless transport capacity (q*) from Parker [1979] is:

$$q^* = \frac{q_{gc}}{\sqrt{\frac{(\rho_S-\rho)}{\rho} g {D_{50}}^3}} = 11.2 \frac{(\tau^*-0.03)^{4.5}}{{\tau^*}^3} \quad (3.8)$$

where $q_{gc}$ is the gravel transport capacity in $m^2/s$. Equation 3.8 may underestimate sediment transport rates if sand is also located on the bed [e.g., Wilcock, 1998; Wilcock and Kenworthy,

2002], but incorporating the effects of sand requires knowing the portion of the bed covered with sand at bankfull discharge, which depends both on the Rouse Number (equation 3.5) and on the local supply of sand. The local supply of sand is unknown for nearly all of our dataset and varies significantly based on local conditions of the banks, bed, and tributaries [e.g., Knighton, 1998].

Equation 3.8 only applies to rivers with $\tau^*>0.03$, for rivers with $\tau^*\leq 0.03$, we set the transport rate equal to the reference transport rate defined by Parker and Klingeman [1982] as:

$$W^*_{ref} = 0.002 = \frac{q_{gc}\frac{(\rho_S-\rho)}{\rho}g}{u^{*3}} \tag{3.9}$$

where $W^*_{ref}$ is the dimensionless reference transport rate equal to 0.002. For low $\tau^*$, this provides non-zero values for $q_{gc}$, and recognizes that below the threshold of motion, a very small amount of particle movement occurs.

The volumetric gravel transport capacity is:

$$Q_{gc} = q_{gc}B \tag{3.10}$$

The coarse sediment supply due to bank erosion for an individual bend ($Q_{gbank}$) is:

$$Q_{gbank} = \dot{E}_{bank}H_{bank}F_{gbank}L_{bank}(1-\phi_{bank}) \tag{3.11}$$

where $\dot{E}_{bank}$ is the bank erosion rate in m/yr, $H_{bank}$ is the average bank height, $F_{gbank}$ is the fraction of gravel in the bank, $L_{bank}$ is the length of the eroding bank, and $\phi_{bank}$ is the bank porosity, assumed to be 0.4 (Figure 3.14). Site-specific sediment fluxes through time would be more accurately calculated using Lauer and Parker [2008], who include the effect of curvature on the length of the eroding bank rather than the centerline, and include the effect of unequal bank heights, but this analysis requires more data than are available for our dataset. There are few data on $F_{gbank}$ for gravel bed meanders. Stratigraphic studies of point bars and eroding banks in gravel bed meanders range varies based on bar position [e.g., Bluck 1971; Jackson, 1976]. Gravel can be nearly absent from the channel banks [Leopold and Wolman, 1960; Nanson 1980] to nearly 80% of the channel bank as shown in for Bear Valley Creek in Figure 3.15. For channels that maintain a constant channel width during migration, the bank erosion rate is equal to the channel migration rate. We assume that the average $L_{bank}$ is:

$$L_{bank} = \frac{1}{2}\lambda P \tag{3.12}$$

where $\lambda$ is the bend wavelength and P is the sinuosity. Bend wavelength was measured from Google Earth for the rivers with migration data and is given in Appendix B–Table B1 and shown in Figure 3.16. The best-fit line to the data was $B=11.1\lambda$ (Figure 3.16), very close to the relationship found by Leopold and Wolman [1960] for wavelength–$B=10.9\lambda^{1.01}$. There is considerable variability in the data set, with $B/\lambda$ ranging from 6.8 to 26. To compare the calculated gravel transport capacity with the supply from bank erosion, we converted the transport capacity from $m^3/s$ to $m^3/yr$. To do this, we assumed that bankfull flow occurs 8 days per year, on average, following Braudrick et al. [2009] based on field measurements from Dunne

and Leopold [1979] and Andrews and Nankervis [1995]. This is an upper bound for other estimates of bankfull frequency in the Rocky Mountains [Torizzo and Pitlick, 2004; Mueller and Pitlick, 2013]. This estimate is likely inaccurate over short time scales, but might be reasonable given the long time scales of measurements of bank migration (often several decades). Migration rates were available for only 19 of the 155 gravel bed meanders in the dataset, and only 17 of the rivers had sufficient data to calculate the sediment flux (Figure 3.17, Appendix B–Table B1). The migration rates of the 4 gravel meanders were from short reaches ranging from 1-2 bends in length. Their migration rates were calculated by dating the age of floodplain (1-2 decades) since migration began [Allmendinger et al., 2005]. Migration rates ranged from 0.0075 to 0.098 channel widths/yr with a median migration rate of 0.022 channel widths/yr (Figure 3.17).

Figure 3.18 shows how the ratio of the gravel transport capacity (equation 3.10) to the calculated gravel input from bank erosion (equation 3.11) varies with $\tau^*$ for the 17 rivers where we have both channel migration rates and sufficient data to calculate the transport capacity. $F_{gbank}$ was set equal to 0.5, with the upper and lower error bars calculated using $F_{gbank}$=0.8 and 0.1, respectively. The horizontal line at $Q_{gc}/Qg_{bank}$=1 defines when the flux from bank erosion is equal to the transport capacity. The supply of sediment from the banks exceeded the transport capacity in 15 of the 17 reaches, regardless of the value of $F_{gbank}$. All 13 of the rivers with $\tau^*$<0.47 and 2 of the 4 rivers with $\tau^*$>0.05 had $Q_{gc}/Q_{gbank}$<1. The transport capacity exceeded the bank erosion rate in two reaches: Towamencin Creek, Pennsylvania [Hession et al., 2003; Allmendinger et al., 2005] and The Kern River [Micheli and Kirchner, 2002] with $\tau^*$ =0.055 and 0.14, respectively. Similar to the other rivers in Hession et al., [2003] and Allmendinger et al., [2005] Towamencin Creek is actively migrating, but has not cutoff. The Kern River had a fine bed ($D_{50}$=4 mm) and had a correspondingly high $\tau*$ (0.14), and the portion of the basal stress accommodated by bedforms in the Kern River is unknown. The Kern River is also incising in some reaches [Micheli and Kirchner, 2002].

This analysis in based on only 17 data points and the single-grain size transport capacity measurement using equation 3.8 is likely an underestimate of the transport rate particularly for rivers close to the critical movement threshold. Bedload transport measurements for rivers with reach average $\tau^*$ <0.03 show that bankfull transport rates can be near zero [McKean and Tonina, 2013] or much higher than predicted by equation 3.8, particularly if the river is transporting mostly sand as bedload [Clayton and Pitlick, 2007].

Although based on limited data, the implication of Figure 3.18 is that in gravel bedded meanders much of the bedload transport simply results in the transfer of sediment eroded from the bank to the next downstream bar where it is eventually incorporated into the floodplain as the channel laterally shifts, with very little net flux of sediment downstream. This places such rivers in environments where upstream coarse sediment supply is low, and implies that if the river is maintaining a quasi-steady width over time, that bank erosion of successive bends may be linked through deposition of sediment on the point bar. Lateral exchange of sediment may therefore act as a buffer, accommodating spatial and temporal variations in sediment supply.

### 3.5.3 Channel planform, width to depth ratio, and bankfull $\tau^*$

Our analysis, which combines various datasets and adds new observations, shows that braided gravel bedded channels, meandering gravel bedded channels, and sand bedded channels

differ markedly in their: 1) slopes for a given bankfull discharge (e.g., Figure 3.6), 2) in their bankfull $\tau^*$ for a given median grain size (e.g. Figure 3.11), and 3) in their width to depth ratio for a given bankfull discharge (e.g. Figure 3.9). These findings match and expand upon previous analyses [e.g., Kleinhans and van den Berg, 2010; Metivier and Barrier, 2012]. But our analysis also suggests that it is useful to distinguish three gravel bedded meanders types: meanders with cutoffs (but no islands), meanders with islands (and cutoffs), and meanders without cutoffs. This classification requires us to consider only truly alluvial meanders, primarily cutting against their own earlier floodplain deposits, and lying in a sufficiently wide floodplain that cutoffs can occur unimpeded by resistant bounding hillslopes. Furthermore, we noticed for bed sizes approximately smaller than 8 mm, much of the bed is sand, which leads to different morphology and hydraulic relationships.

The data on these three types of gravel bedded meanders straddle the Leopold and Wolman planform threshold line (Figure 3.6), with the meanders with cutoffs lying below the line (i.e. have lower slopes) and the other two lying on either side of the hypothetical threshold. Consistent with this observation, the meanders with cutoffs tends to have a lower bankfull $\tau^*$, except where the $D_{50}$ fines significantly. The meanders with cutoffs also tend to have a lower upper range of width to depth ratios for a given discharge.

Little distinguishes meanders with island bars (and cutoffs) from the gravel bedded meanders without cutoffs, despite there striking difference morphologically. Most of the island bar meanders have higher width to depth ratios than for meanders without cutoffs, but otherwise there is considerable overlap in $\tau^*$ and channel slope. Despite these similarities, the two channel types express very different behaviors: island bar formation, active channel migration and cutoff versus no island bars and essentially no lateral migration. We hypothesize these differences may be linked to bank strength and sediment supply characteristics. Both channel types tend to support higher $\tau^*$ than the gravel bedded meanders with cutoffs. For the same $\tau^*$, island bar formation may arise where lower bank strength leads to relatively channel widening (B/H) or where fine sediment load is low, such that back channel areas are not infilled with suspended sediment [e.g. Braudrick et al., 2009].

The meandering channels without cutoffs (and lacking scroll bar complexes) are most puzzling. They may be sinuous channels that never progressively migrated, or, more unexpected, meandering channels in which at some degree of sinuosity cease migration. These channels have comparable $\tau^*$ to the island meanders and higher values than meanders with cutoffs. These could be channels with exceptionally high bank strength (effective slowing migration rates), or high $\tau^*_{crit}$ such that little transport occurs at bankfull stage. Migration has been observed to cease on formerly actively migrating channels [e.g., Dietrich et al., 1999] but such channels retain scroll bars and cutoffs from prior migration activity. Field investigations are now required to understand how these meanders developed.

## 3.6 Conclusions

Previous studies have suggested that meandering in gravel bedded rivers requires additional bank strength from either vegetation or cohesive sediment, and low sediment supply. Previously published predictions of channel patterns did a reasonable job of identifying sand

bedded meanders and gravel braided channels, but struggled to identify gravel bedded meanders. Comparison of our compilation of 166 gravel bedded meanders from the literature with previously published compilations of 74 sand bedded meanders and 36 gravel braided channels shows that for a given discharge, gravel meanders occur at intermediate channel slopes relative to gravel braided rivers and sand bedded meanders. Similar to previous studies, we found that gravel bedded meanders have relatively low bankfull Shields stress suggesting a low sediment supply.

Gravel meanders were primarily located in either formerly glaciated landscapes (Britain) or along mountain ranges, particularly the Rocky Mountains in the US and Canada. Gravel meanders in unglaciated landscapes far from mountain ranges mostly derived their sediment from Pleistocene gravel deposits. Inspection of the sites in Google Earth revealed that gravel bedded meanders occurred in three morphologies: gravel meanders with cutoffs and without islands, gravel meanders without cutoffs, gravel meanders with islands and cutoffs. Four of the gravel meanders without cutoffs located in the Piedmont of the eastern US were actively migrating, but the remainder showed no evidence of migration. The four actively migrating channels had recently been deforested and they had perhaps not had time to migrate to cutoff. There is considerable overlap in the either the channel and valley slopes for a given discharge between the gravel meander types, but the range meanders without cutoffs and with islands extend to higher slopes than meanders with cutoffs. More than half of the meanders without cutoffs in the database were located in Britain.

We used width-depth ratios and vegetation type as proxies for bank strength. Gravel meanders with cutoffs and gravel meanders without cutoffs had similar width-depth ratios to sand bedded meanders. Gravel meanders with width-depth ratios > 40 typically had islands. There was little difference in vegetation class (grassy versus forested) between gravel bedded meanders, gravel braided channels, and sand bedded meanders.

To explore the role of sediment supply on gravel bedded meanders we calculated the bankfull Shields stress of the rivers in our data compilation. Gravel bedded meanders with median surface grain sizes > 8 mm have lower Shields stresses than gravel braided rivers and sand bedded meanders, suggesting that they have lower bedload supply. The Shields stress increases for gravel bedded meanders finer with median surface grain sizes < 8 mm. Descriptions of the sedimentology of fine grained gravel bedded meanders shows that they have abundant sand on their surfaces, and their bedforms are extracting stress from the flow.

For rivers with migration data, we calculated the gravel supply from bank erosion and compared this with the annual transport of gravel using a single-grain size approach. For 17 of the 19 rivers with bank erosion data, the gravel supplied from bank erosion exceeded the transport capacity, suggesting that gravel meanders are primarily exchanging sediment laterally between eroded banks and the next bar downstream, as observed in flume experiments.

Future research is required to explore the conditions that create meandering rivers but cause migration to cease as observed in the meanders without cutoffs in the database. Additionally, coupled studies of gravel supply relative to the supply of gravel from bank erosion to better quantify the relative lateral and downstream flux of sediment.

## 3.7 Acknowledgements

This research was funded by the CALFED Ecosystem Restoration Program (Grant No. ERP-02D-P55), the STC program of the National Science Foundation (NSF) via the National Center for Earth Surface Dynamics (NCED) under agreement EAR-0120914, the Donors of the American Chemical Society Petroleum Research Fund, and an American Geophysical Union Horton Research Grant to Braudrick. Tim Beechie provided data from Washington state rivers. Gary Parker provided insightful feedback on early versions of the data presented here.

## 3.8 Tables

Table 3.1. Summary statistics for sand meanders, gravel braided, and gravel bed meanders.

| | Sand Meanders | | Gravel braided | | Gravel meanders | |
|---|---|---|---|---|---|---|
| | Median (25th-75th percentile) | n | Median (25th-75th percentile) | n | Median (25th-75th percentile) | n |
| Bankfull discharge ($m^3/s$) | 566 (133-3010) | 43 | 385 (233-1140) | 31 | 101 (22.7-340) | 138 |
| Channel slope | 0.00025 (0.0001-0.00053) | 71 | 0.0062 (0.0046-0.01) | 28 | 0.0018 (0.00095-0.0036) | 159 |
| Valley slope | 0.00048 (0.00019-0.00088) | 67 | 0.0066 (0.004-0.009) | 34 | 0.0028 (0.0015-0.0051) | 114 |
| Sinuosity | 1.8 (1.6-2) | 67 | 1.07 (1.04-1.1) | 28 | 1.54 (1.41-1.8) | 120 |
| Width depth ratio | 16.1 (9.85-20.4) | 33 | 271 (90.5-508) | 27 | 21.8 (16-32.6) | 126 |
| $D_{50}$ (mm) | 0.4 (0.3-0.6) | 68 | 37 (30-67) | 34 | 36 (18-53) | 134 |
| Shields stress | 1.1 (0.74-2.1) | 30 | 0.096 (0.063-0.13) | 23 | 0.044 (0.033-0.062) | 115 |

Table 3.2. Summary statistics for gravel bed meandering rivers for all grain sizes.

| | Meanders with cutoffs | | Meanders with islands | | Meanders without cutoffs | |
|---|---|---|---|---|---|---|
| | Median (25th-75th percentile) | n | Median (25th-75th percentile) | n | Median (25th-75th percentile) | n |
| Bankfull discharge ($m^3/s$) | 46.5 (12.2-222) | 30 | 155 (27.4-502) | 61 | 81 (19.1-271) | 47 |
| Channel slope | 0.0015 (0.00063-0.002) | 37 | 0.0017 (0.00073-0.0035) | 67 | 0.003 (0.0014-0.0048) | 55 |
| Valley slope | 0.0021 (0.00066-0.0038) | 29 | 0.0022 (0.0014-0.005) | 45 | 0.0033 (0.0022-0.0075) | 40 |
| Sinuosity | 1.7 (1.5-1.79) | 29 | 1.53 (1.41-1.87) | 48 | 1.5 (1.33-1.67) | 43 |
| Width depth ratio | 18.6 (15.4-22.3) | 30 | 29.2 (20.1-45.2) | 51 | 19.5 (13.9-25.6) | 45 |
| $D_{50}$ (mm) | 23 (12-45) | 29 | 36 (18-52) | 54 | 41 (23-58) | 51 |
| Shields stress | 0.038 (0.032-0.065) | 26 | 0.047 (0.033-0.06) | 45 | 0.045 (0.034-0.06) | 44 |

Table 3.3. Summary statistics of bankfull discharge width depth ratio for each vegetation type.

| Vegetation Class | Bankfull Discharge ($m^3/s$) | | Width Depth Ratio | |
|---|---|---|---|---|
| | Median (25th-75th percentile) | n | Median (25th-75th percentile) | n |
| 1 | 15 (9.3-65.8) | 21 | 21.5 (16.8-29.1) | 21 |
| 2 | 40.7 (14.5-119) | 47 | 17.4 (13.5-24.3) | 45 |
| 3 | 302 (121-457) | 29 | 24.1 (17.1-35.2) | 27 |
| 4 | 222 (64-710) | 41 | 29.2 (18.7-54) | 33 |

Table 3.4. Summary statistics for gravel bed meandering rivers coarser than 8 mm.

| | Meanders with cutoffs | | Meanders with islands | | Meanders without cutoffs | |
|---|---|---|---|---|---|---|
| | Median (25th-75th percentile) | n | Median (25th-75th percentile) | n | Median (25th-75th percentile) | n |
| Bankfull discharge ($m^3/s$) | 30 (12.1-76.1) | 21 | 101 (22.7-347) | 45 | 66 (19.4-253) | 41 |
| Channel slope | 0.0019 (0.0011-0.0022) | 24 | 0.0023 (0.001-0.0041) | 47 | 0.0031 (0.0015-0.0059) | 48 |
| Valley slope | 0.0031 (0.0015-0.0039) | 18 | 0.0028 (0.0015-0.0052) | 36 | 0.0035 (0.0022-0.0075) | 38 |
| Sinuosity | 1.73 (1.6-1.89) | 21 | 1.5 (1.4-1.8) | 37 | 1.5 (1.3-1.6) | 41 |
| Width depth ratio | 17.4 (14.5-28.7) | 21 | 31.2 (20.4-52.5) | 39 | 19.7 (14.2-25.2) | 42 |
| $D_{50}$ (mm) | 28 (16-46) | 24 | 40 (21-54) | 49 | 42 (23-0.059) | 48 |
| Shields stress | 0.037 (0.029-0.04) | 21 | 0.044 (0.032-0.05) | 39 | 0.045 (0.034-0.056) | 42 |

## 3.9 Figures

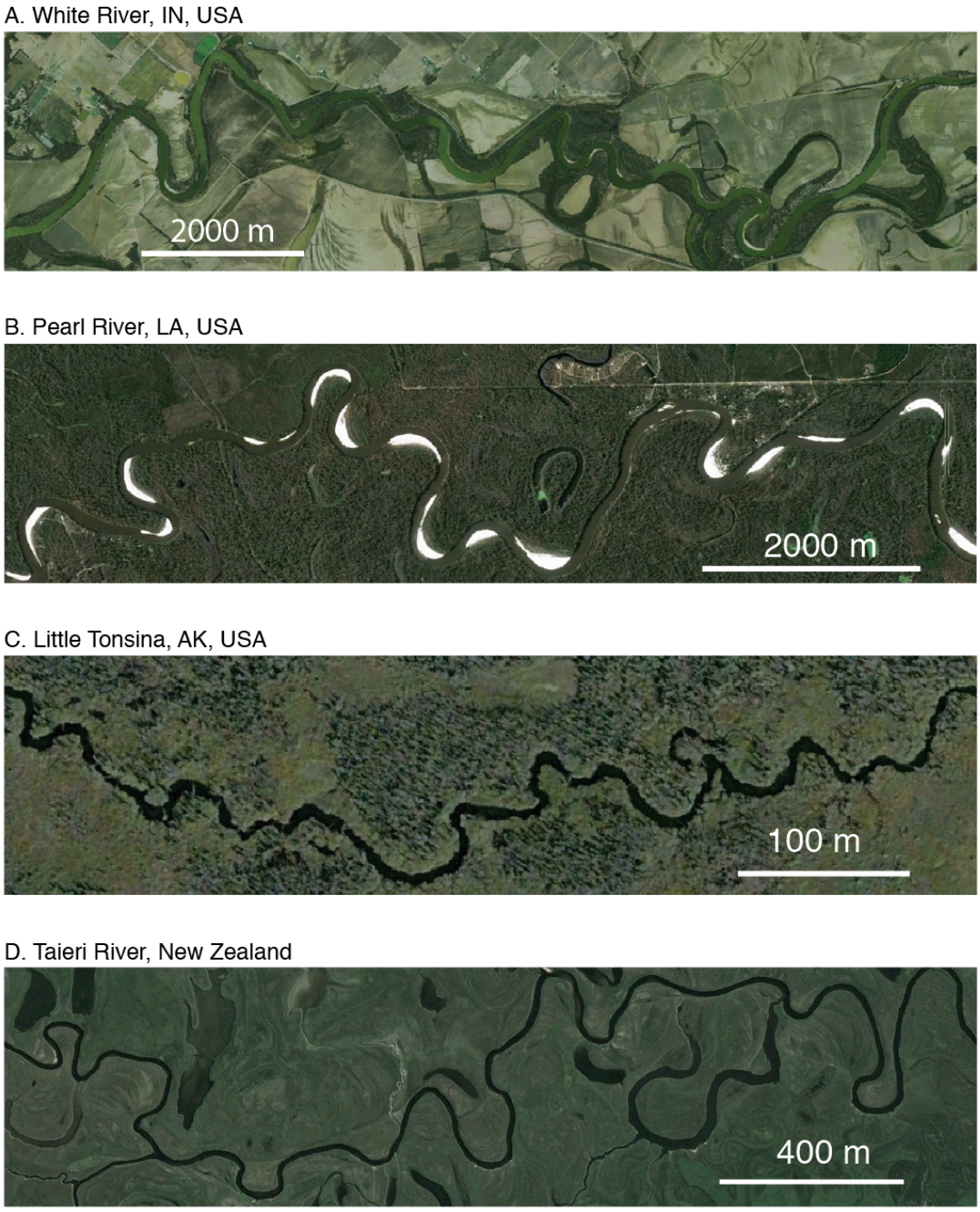


Figure 3.1. Google Earth aerial photographs of meanders with cutoffs and without islands.

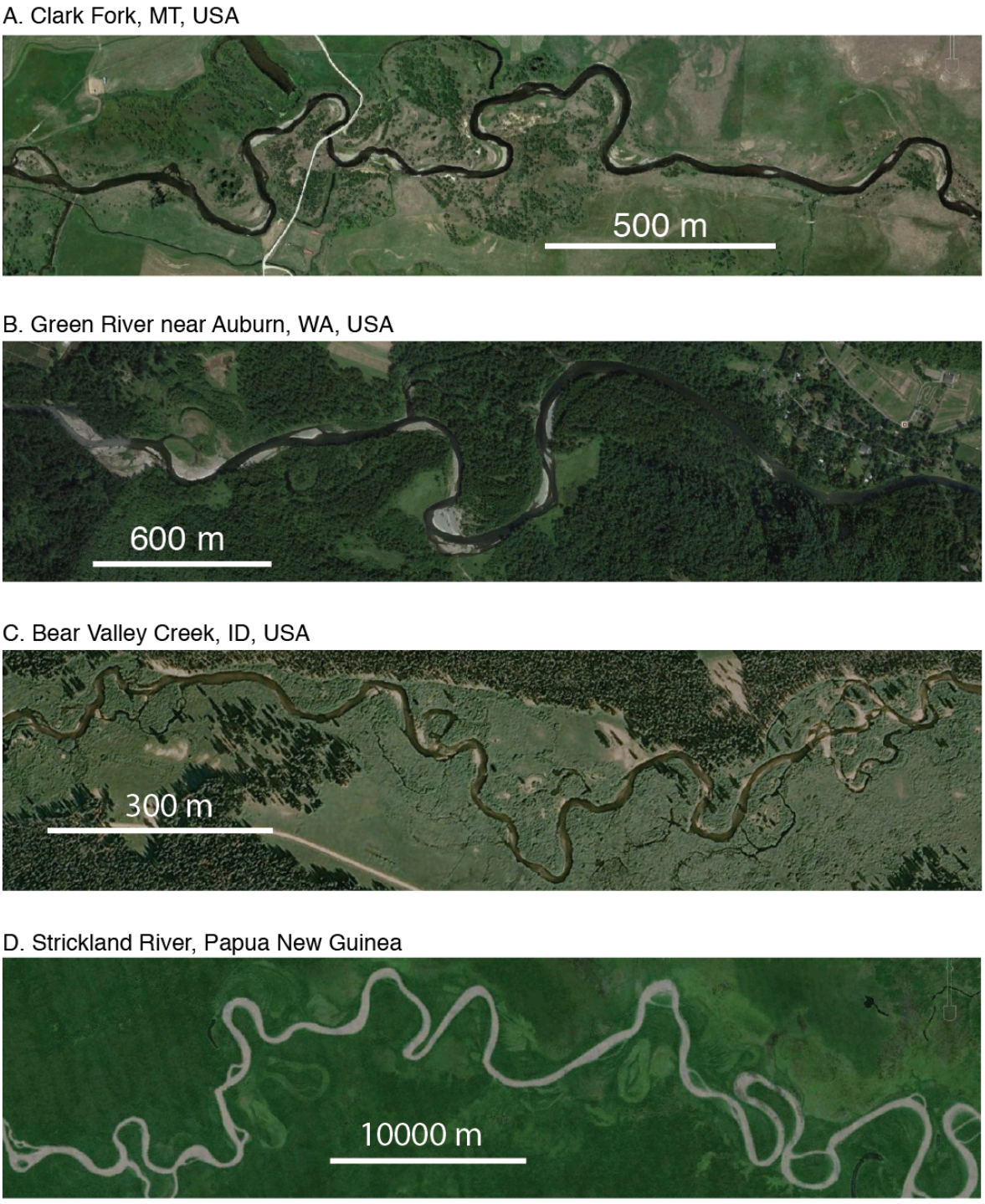


Figure 3.2. Google Earth aerial photographs of meanders with cutoffs and islands.

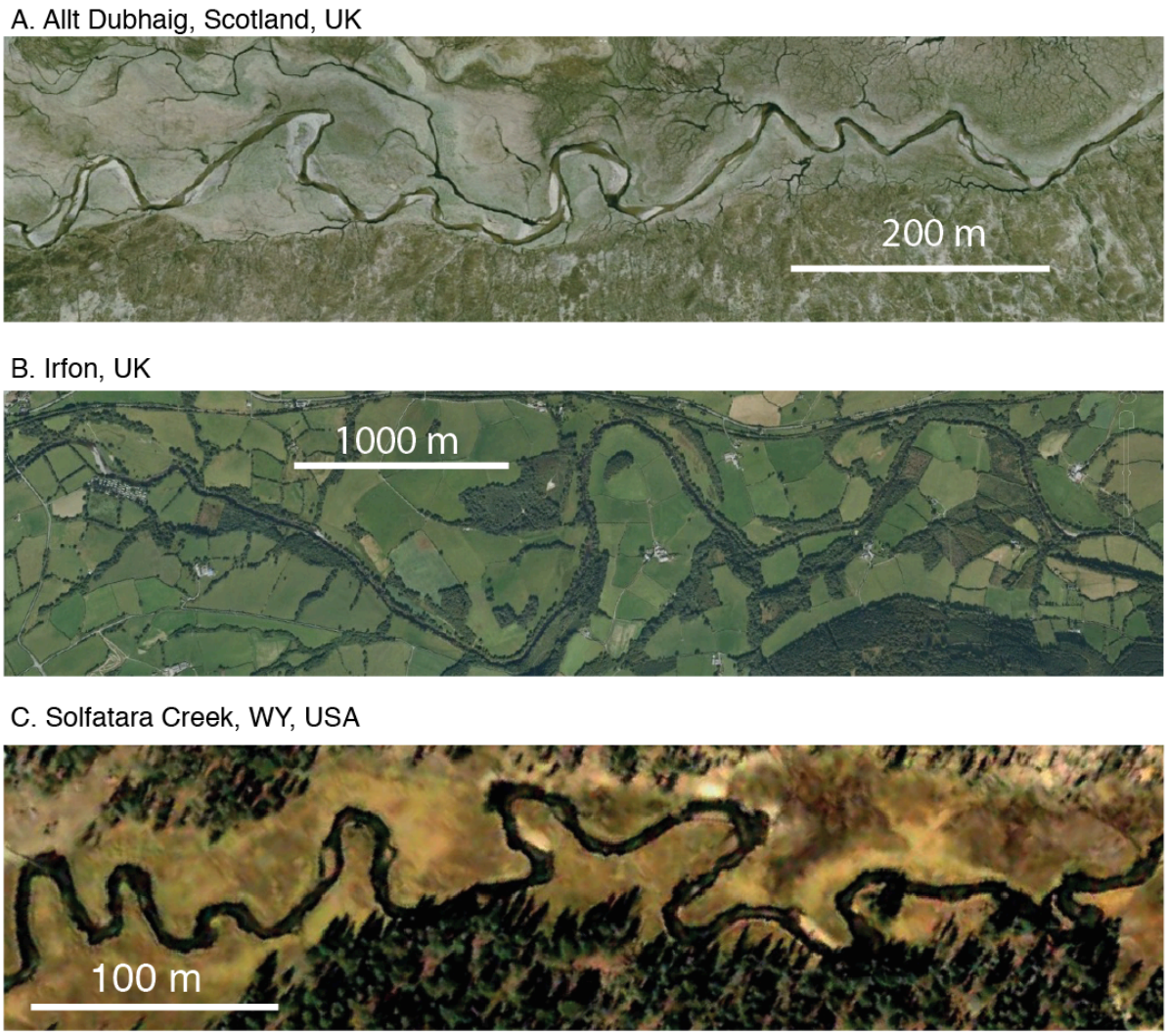


Figure 3.3. Google Earth aerial photographs of meanders without cutoffs.

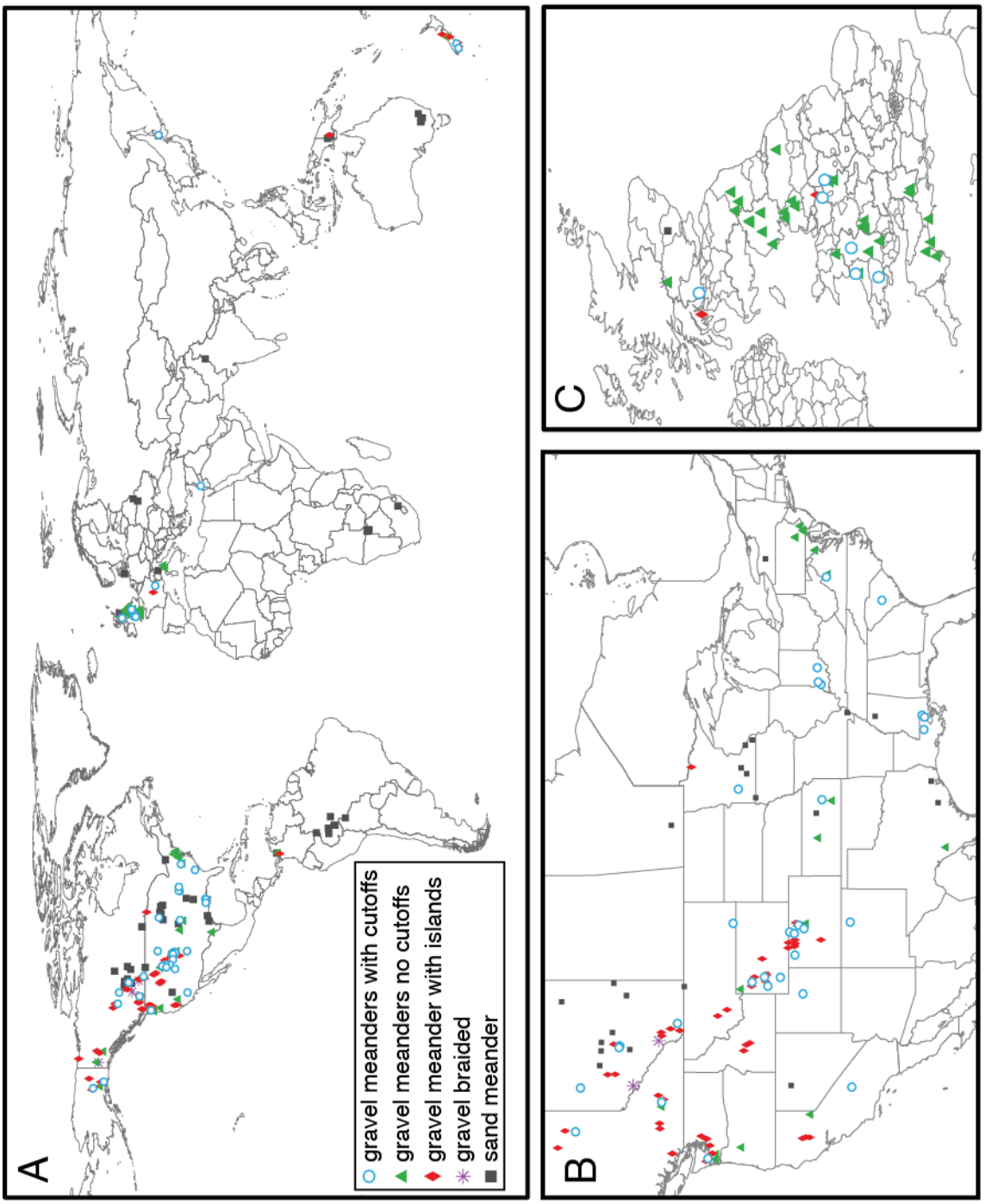


Figure 3.4. A. Location and morphology of rivers in the gravel meander database. Sand meanders and gravel braided channels are also shown for context. Panels B and C show the distribution of gravel meanders in North America and the United Kingdom.

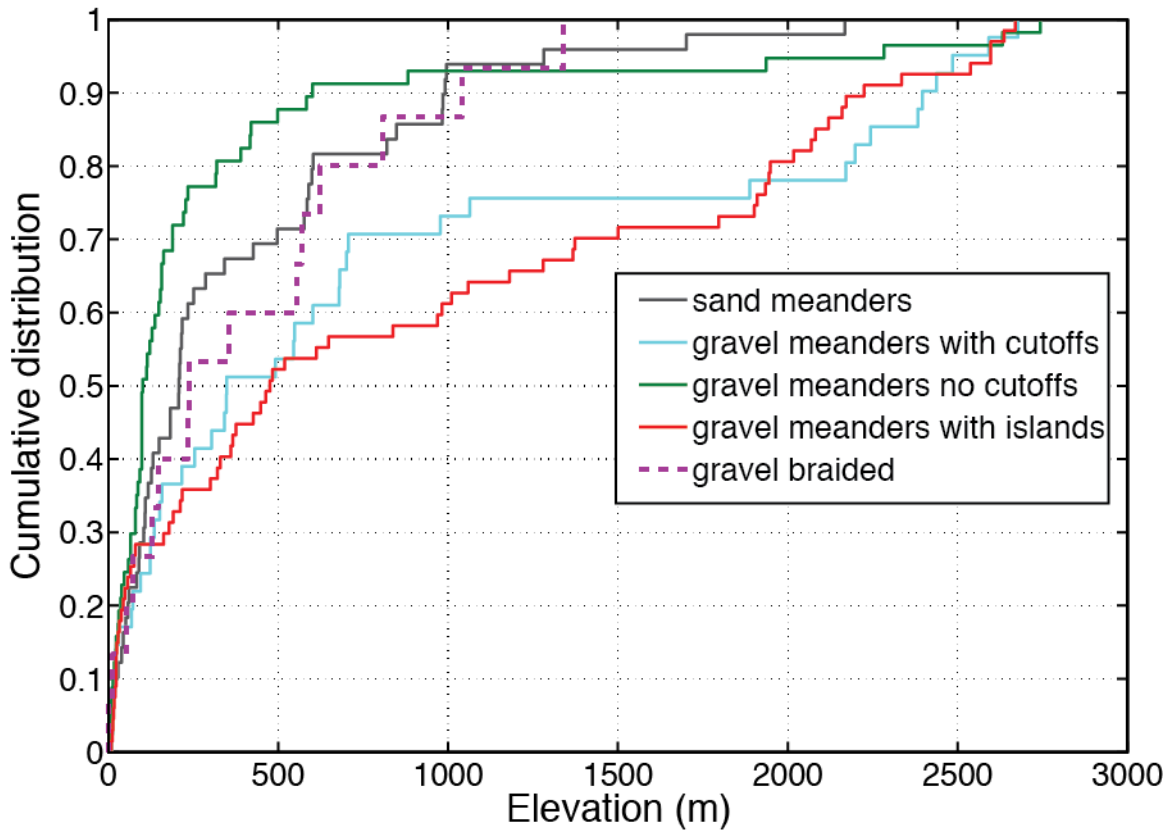


Figure 3.5. Cumulative distribution function of elevation for each river morphology. Meanders with islands and meanders with cutoffs are more frequently in higher elevation valleys than the other channel types, reflecting the large number of sites in the Rocky Mountains region in North America.

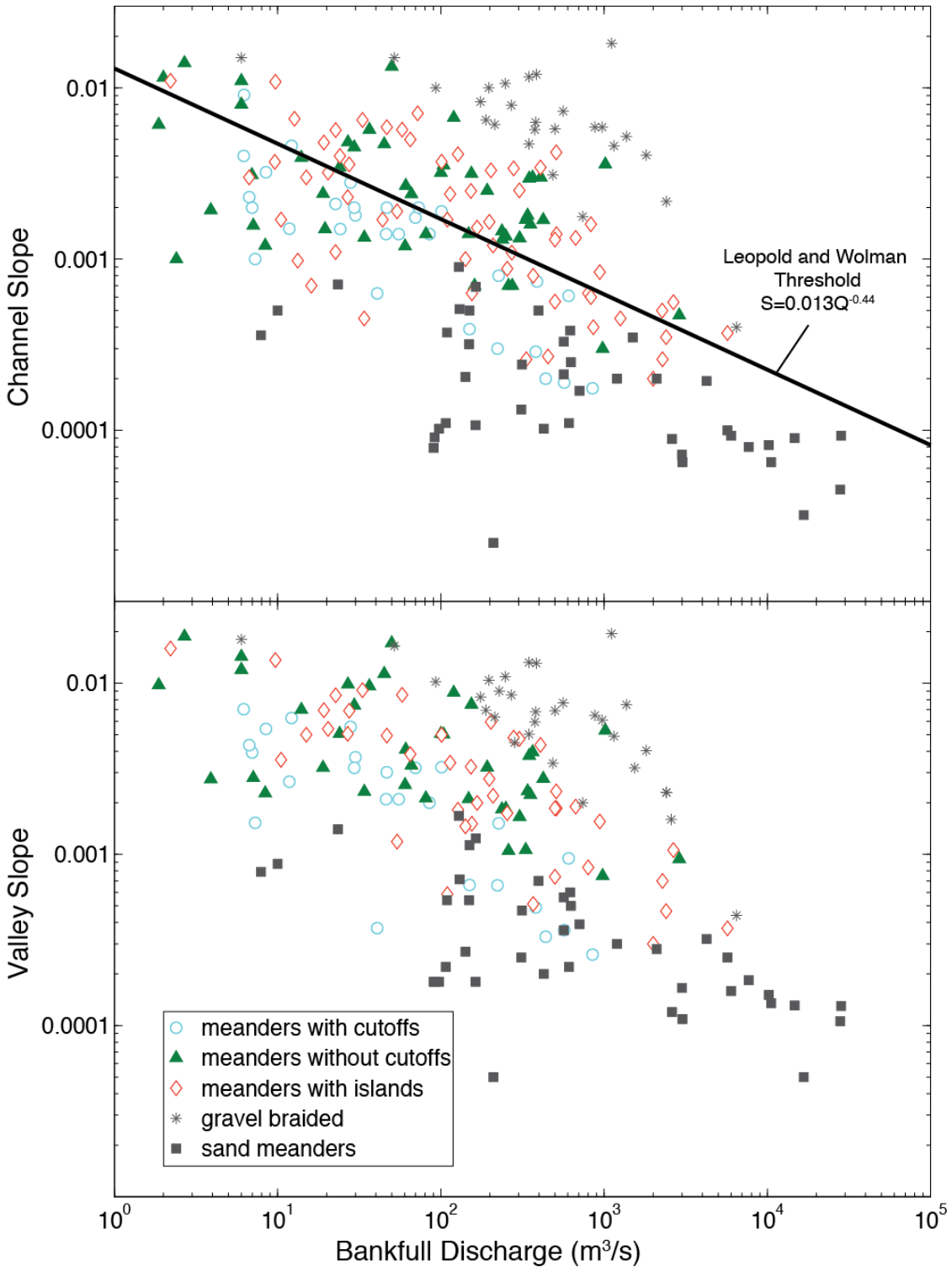


Figure 3.6. Plot of bankfull discharge versus channel slope and valley slope for different channel morphologies. The braided meandering threshold from Leopold and Wolman [1957] is shown in the upper panel.

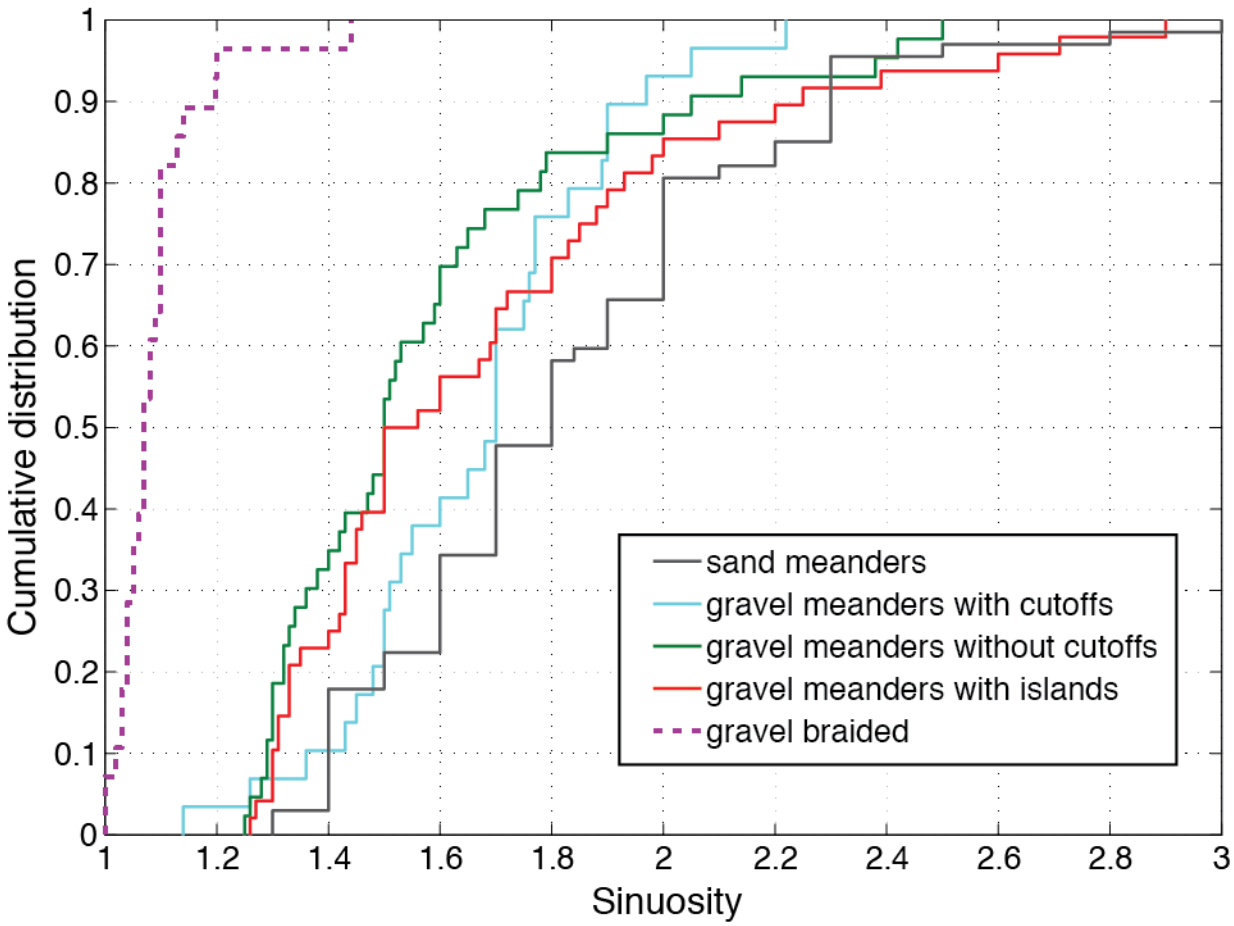


Figure 3.7. Cumulative density function of sinuosity for each channel morphology.

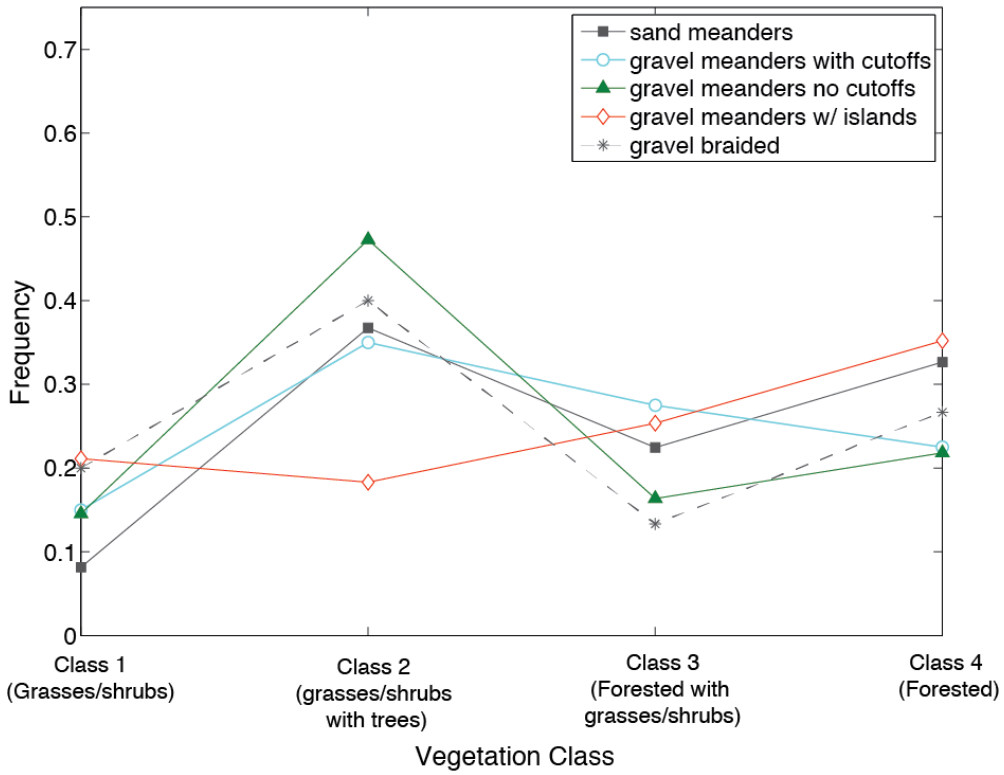


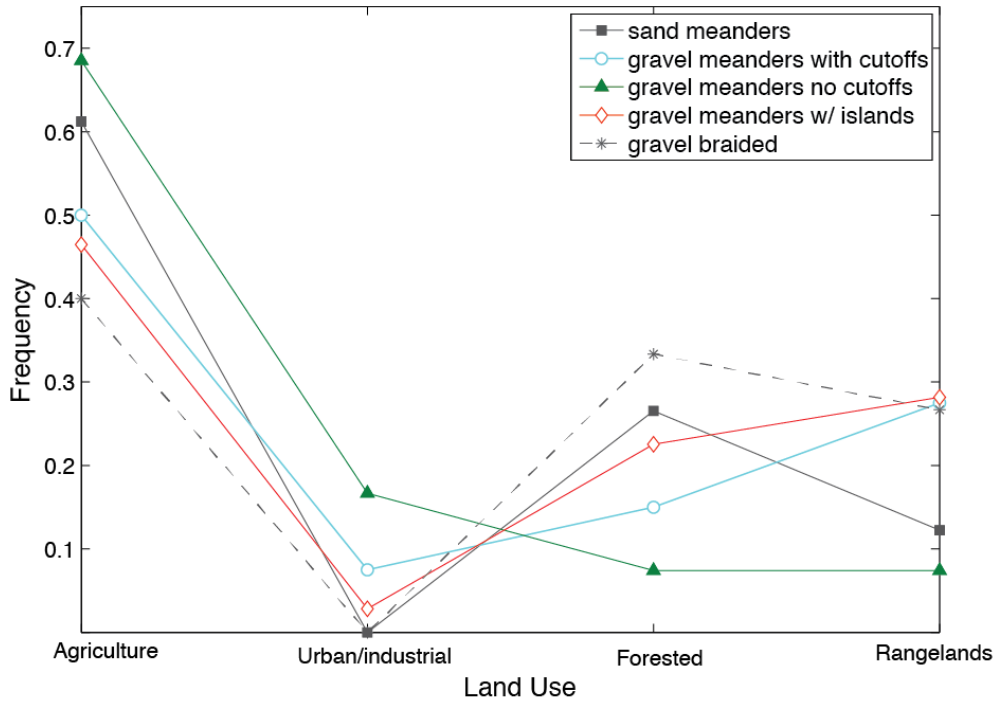


Figure 3.8. A. Distribution of vegetation classes by channel morphology. B. Distribution of land use classes by channel morphology.

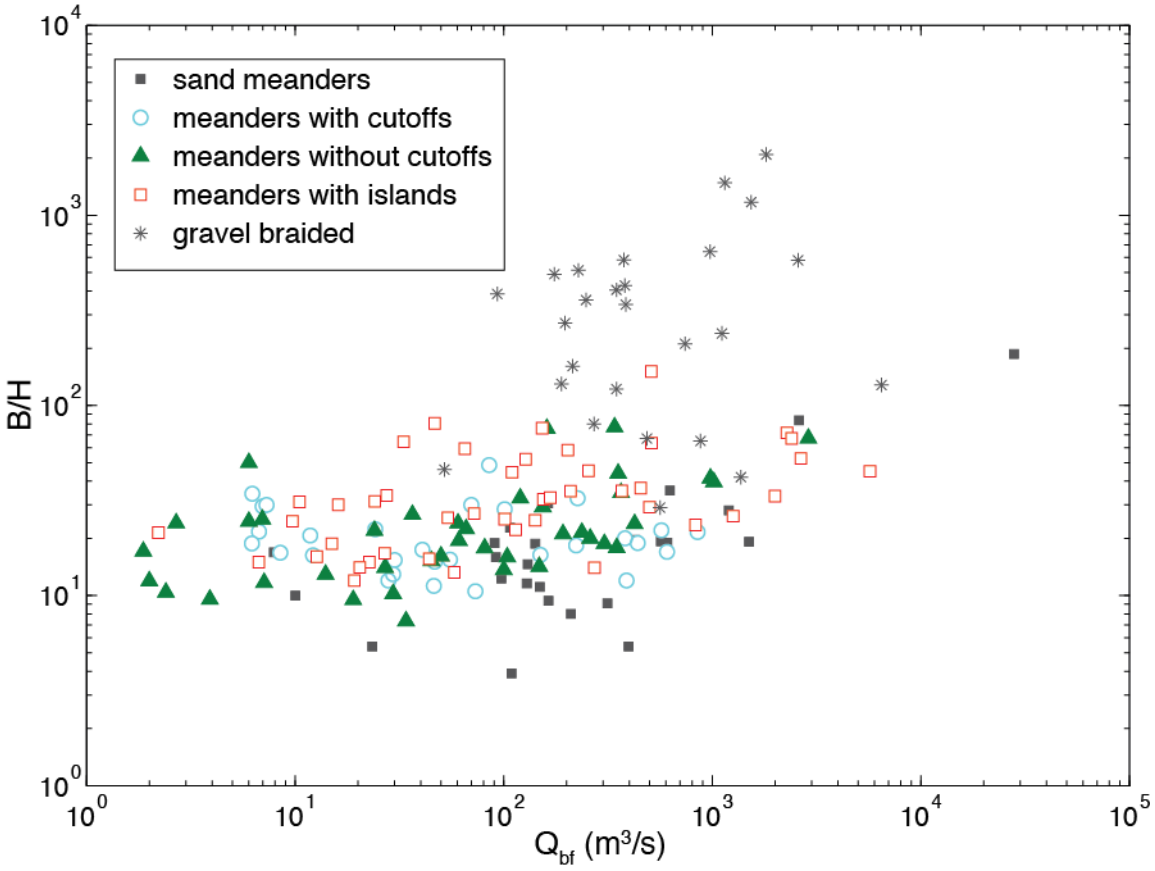


Figure 3.9. Bankfull discharge and width-depth ratio of the river datasets.

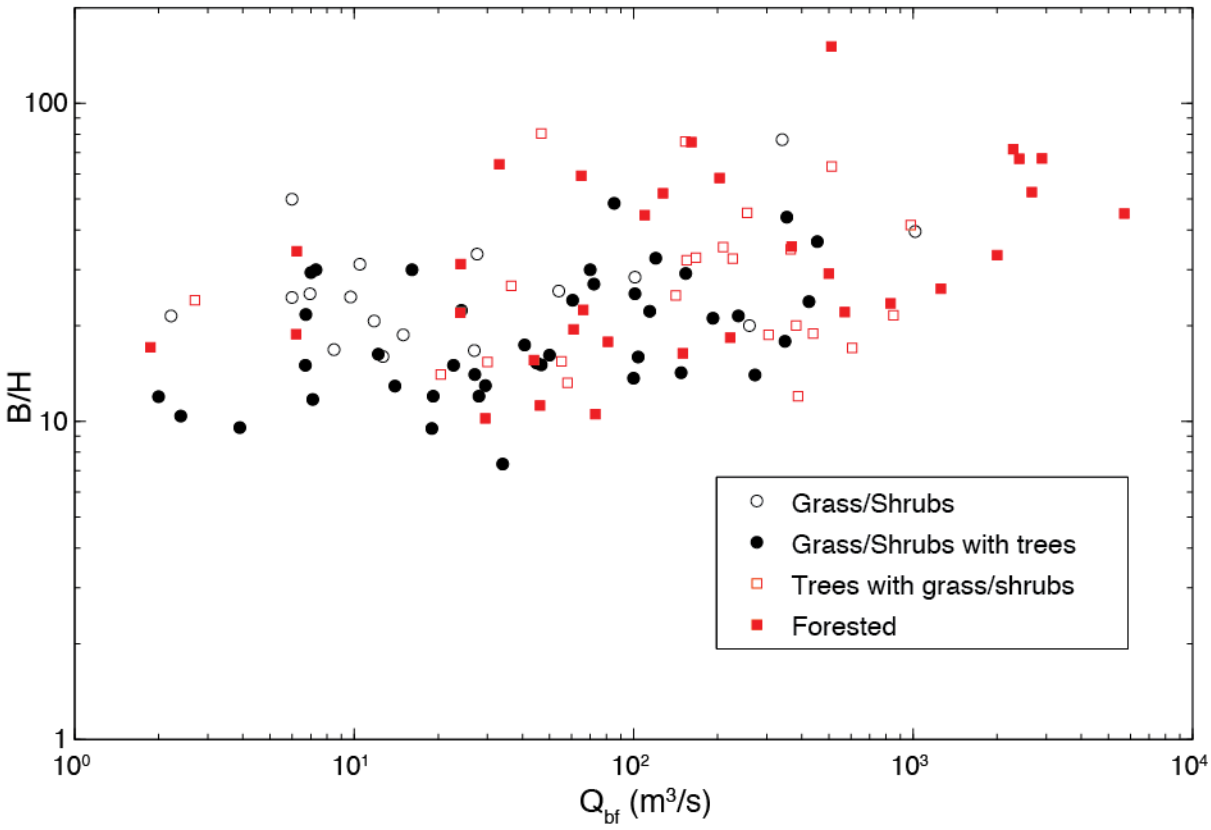


Figure 3.10. Bankfull discharge and width depth ratio by vegetation class for gravel bed meanders of all morphologies. Red symbols are dominantly trees while black symbols are dominantly grasses/shrubs.

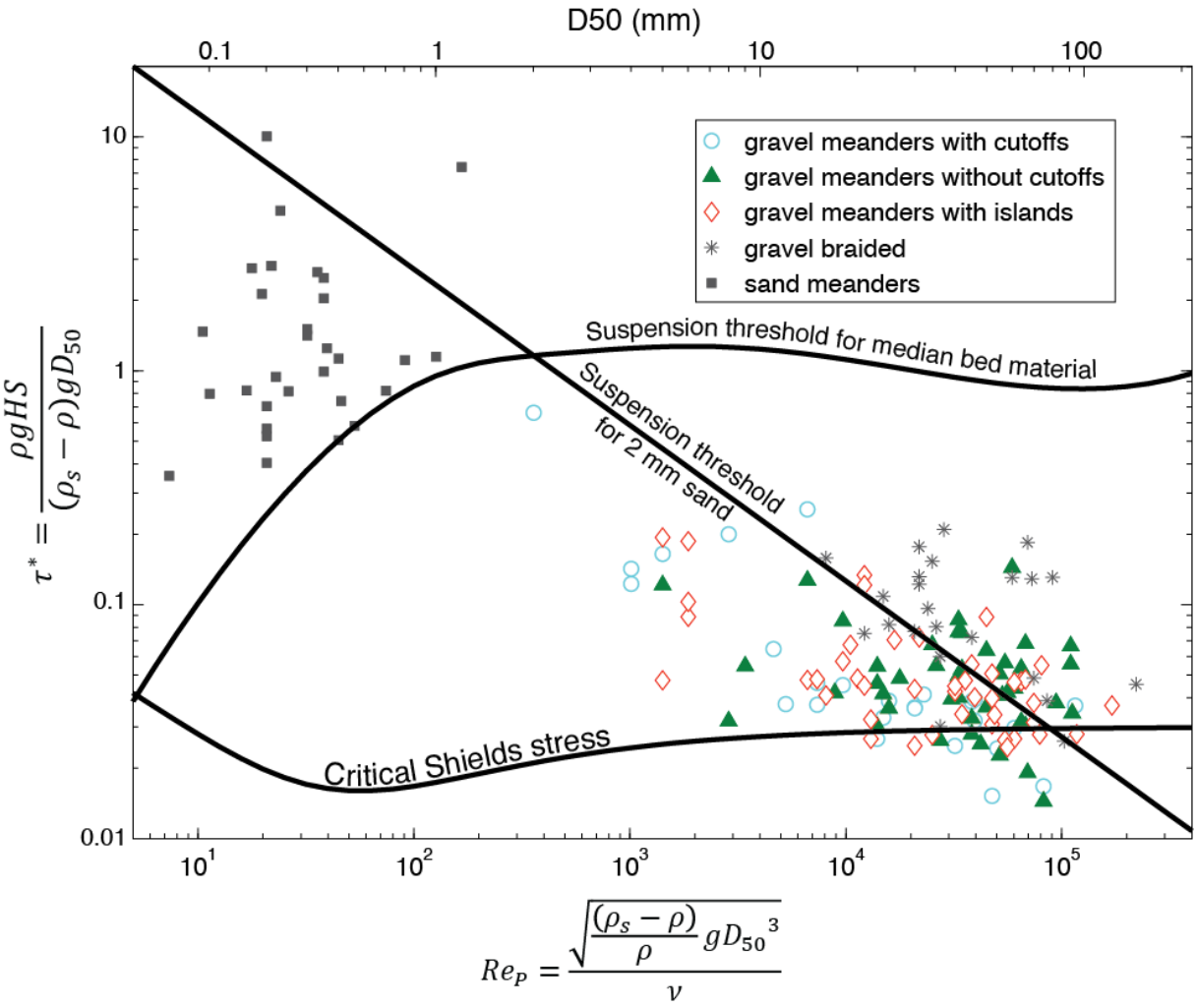


Figure 3.11. Particle Reynolds number and Shields stress for rivers in the dataset. The median grain size corresponding to the particle Reynolds number is shown on the upper axis. The three lines delineate the critical Shields stress, the suspension threshold for 2 mm sand, and the suspension threshold for the median bed material.

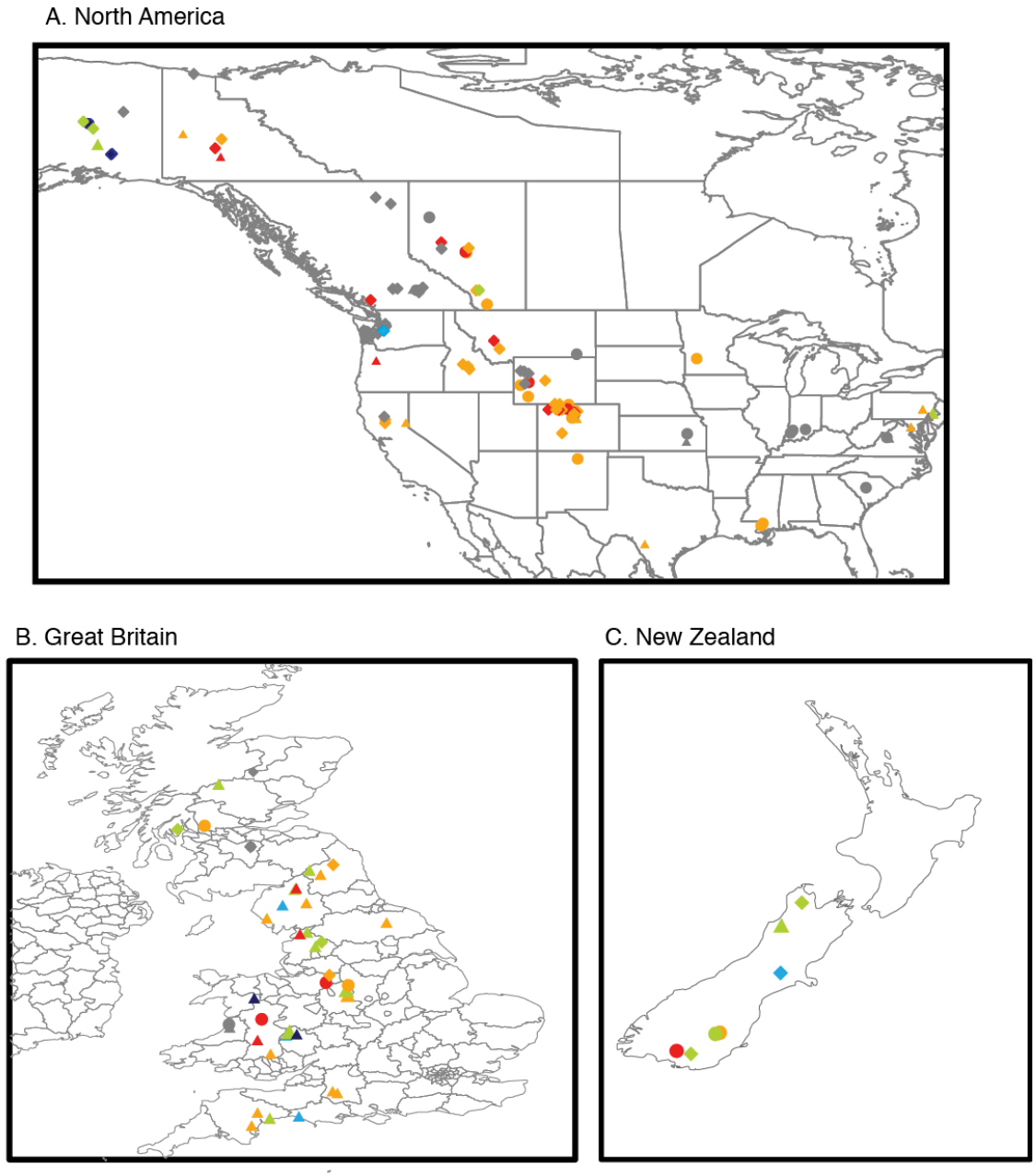


Figure 3.12. Map of Shields stress for rivers with D50>8mm in North America, Great Britain, and New Zealand.

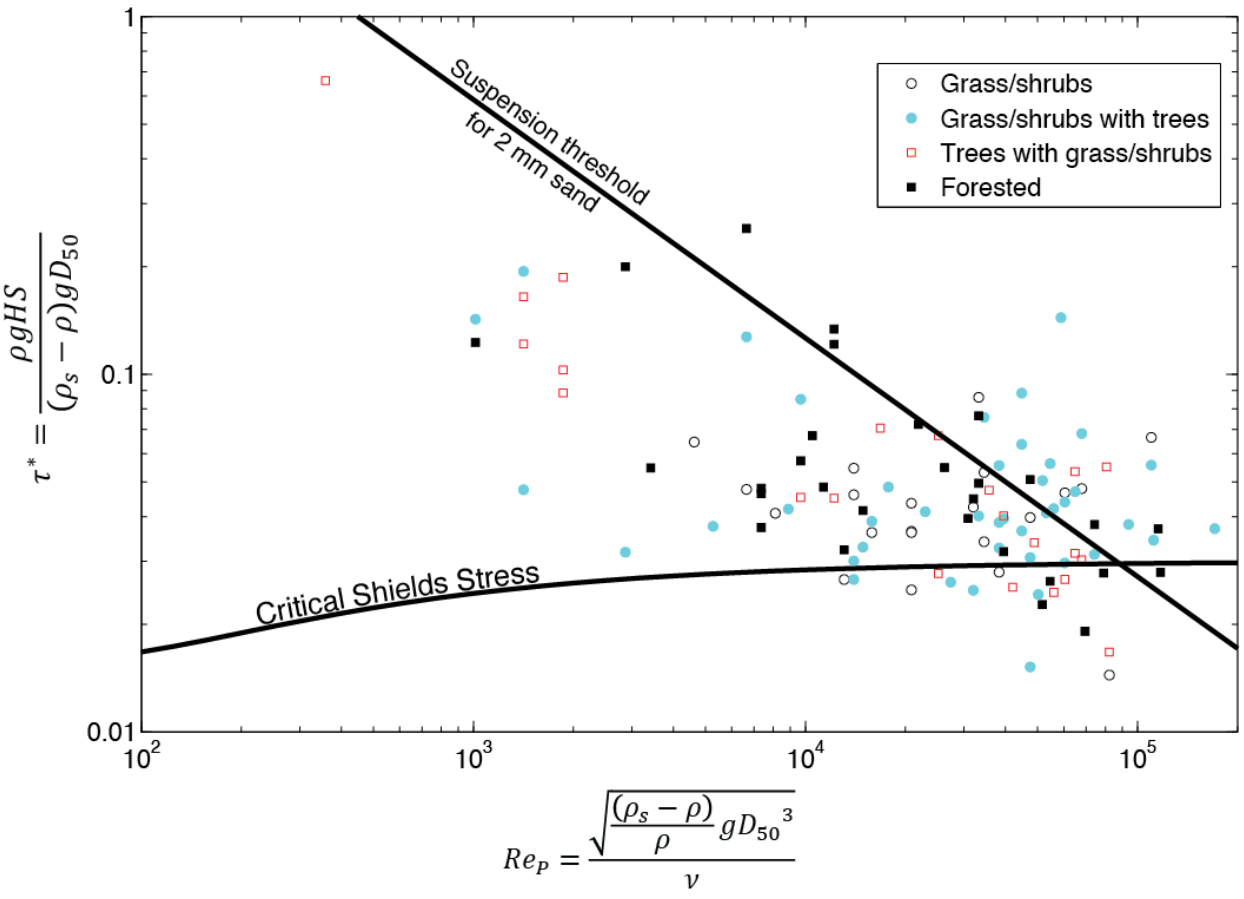


Figure 3.13. Particle Reynolds number versus Shields stress for gravel bedded meanders in the database grouped by vegetation class.

A. Parameters used to calculate sediment flux from bank erosion

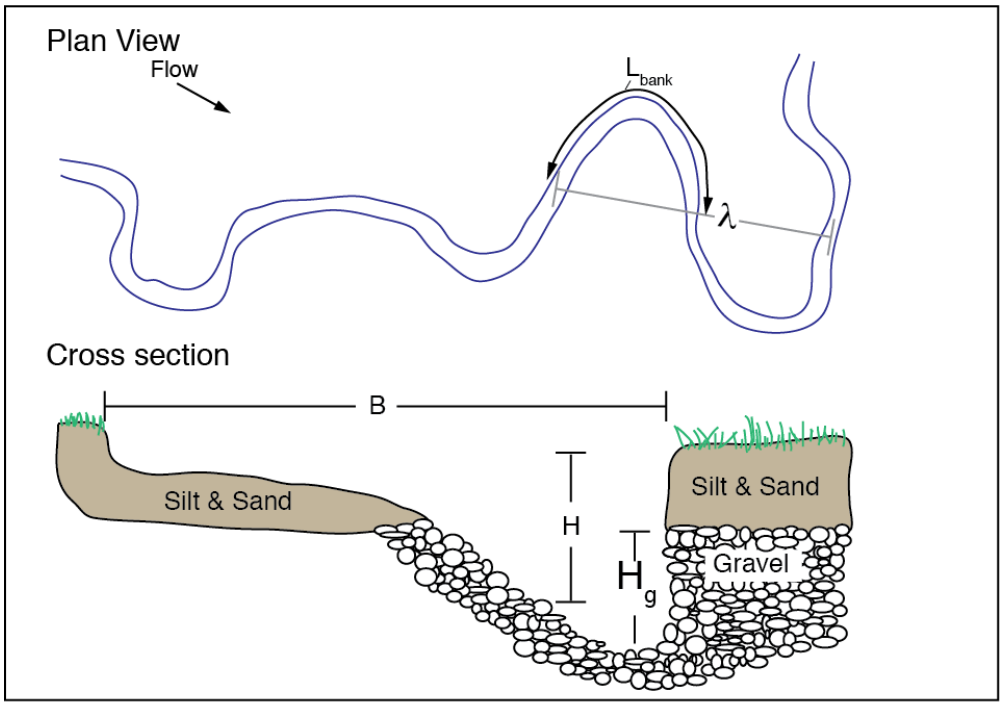


B. Bank erosion and bar deposition during channel migration

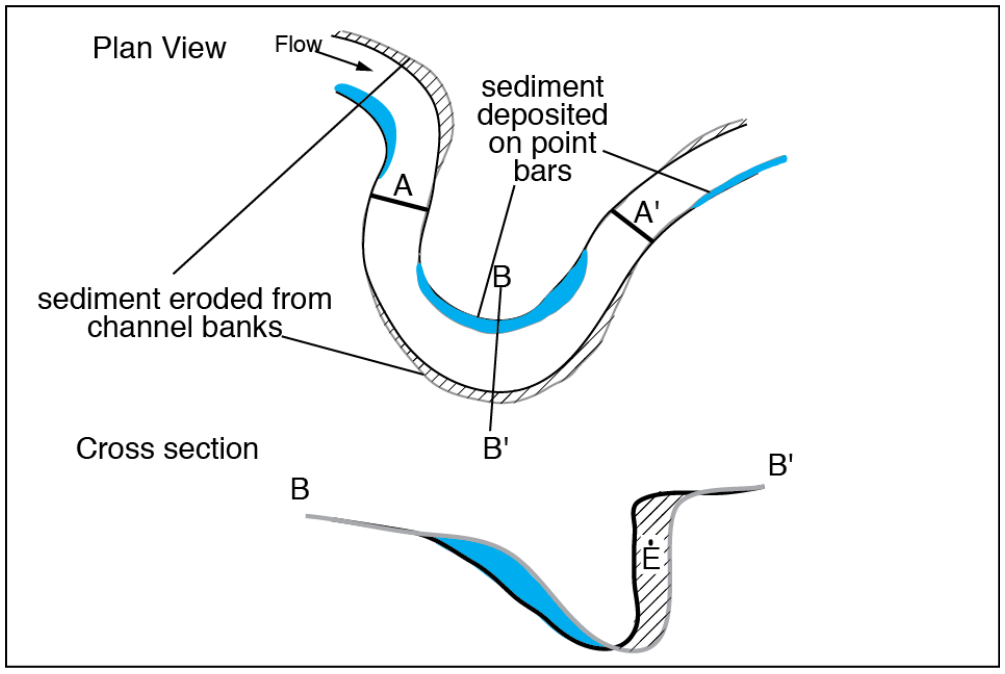


Figure 3.14. Schematic illustration of bank erosion parameters and areas of deposition and erosion during migration. The reach-average parameters are shown for a specific location for clarity.

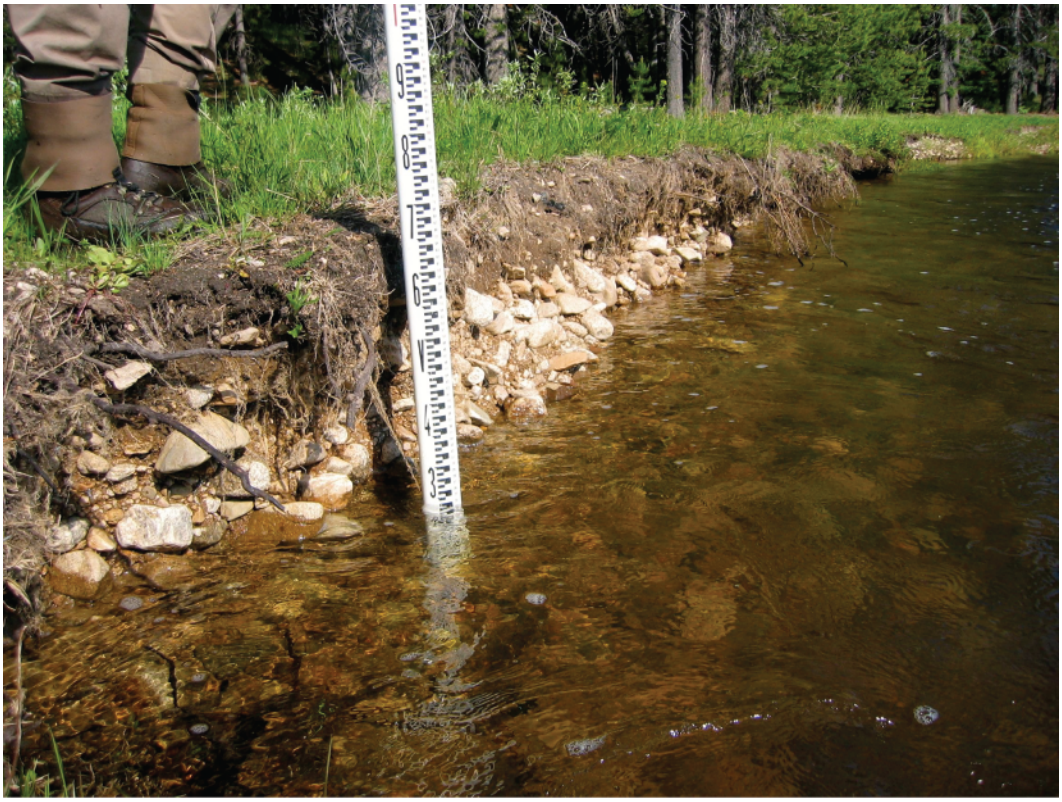

Figure 3.15. Photograph of channel bank in Bear Valley Creek, ID where the bank grades from gravel to gravelly sand to a thin layer (< 10 cm) of fines at the top of the bank. The predominantly gravel facies makes up about 80% of the total bank height.

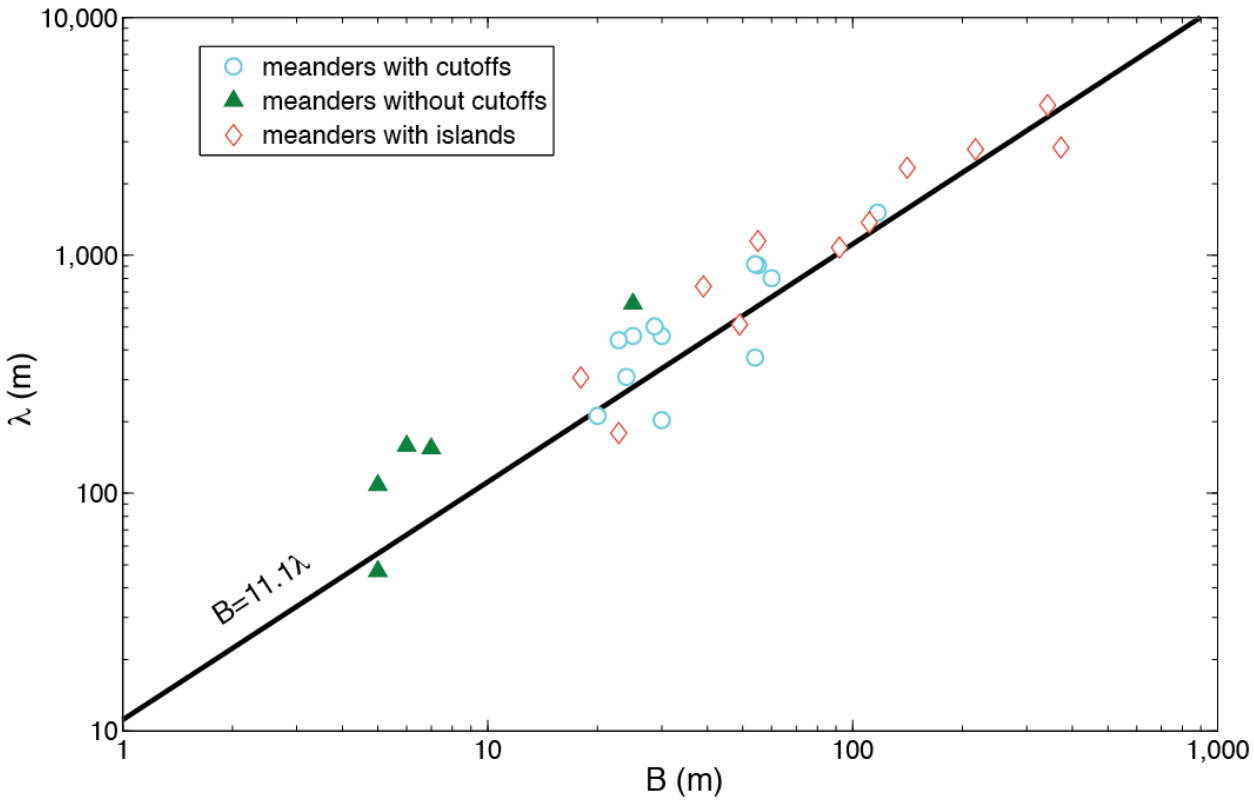


Figure 3.16. Bankfull width and bend wavelength for rivers with measured migration rates in the gravel meander database. The best-fit line assumes that the line passes through the origin.

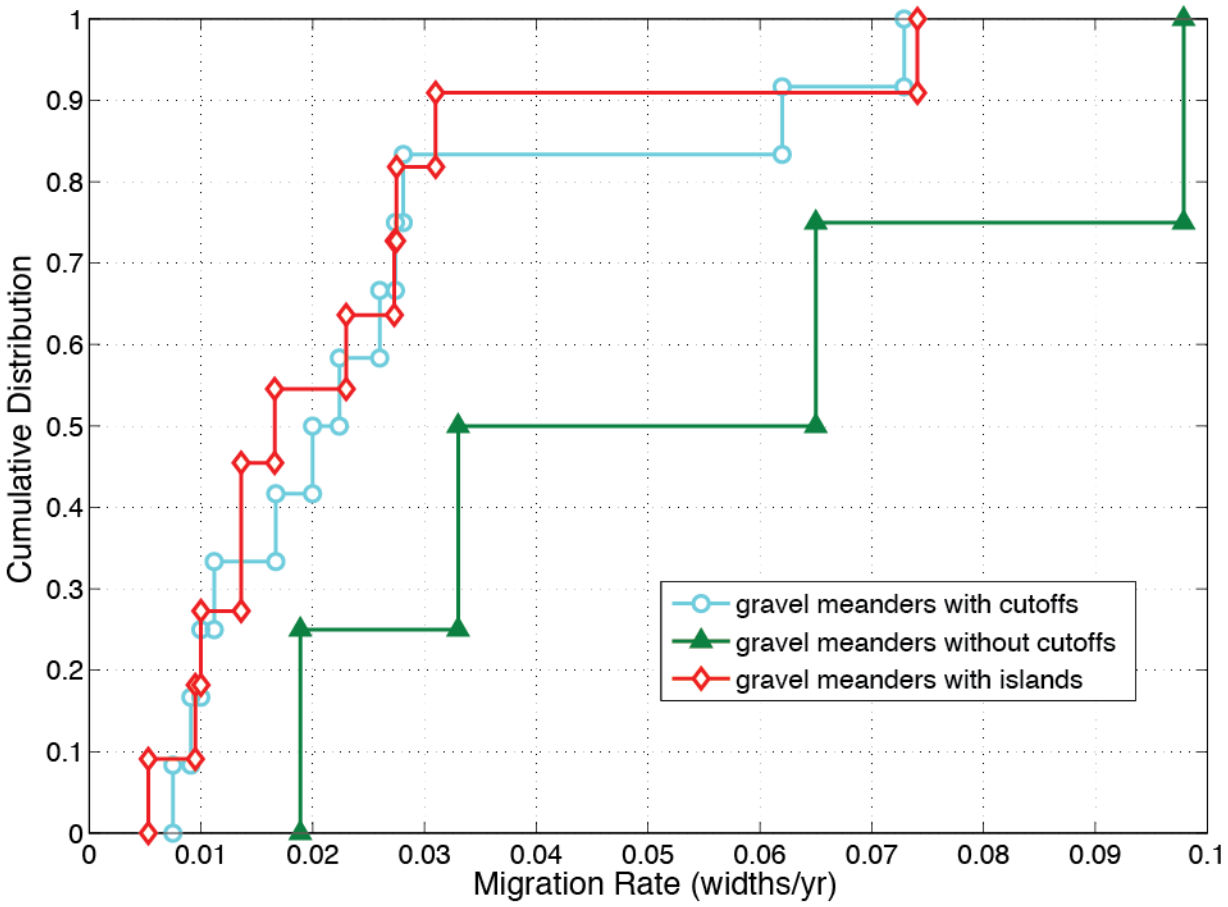


Figure 3.17. Rates of channel migration in the gravel meandering database. The migrating channels without cutoffs are from recently deforested stream reaches in Pennsylvania.

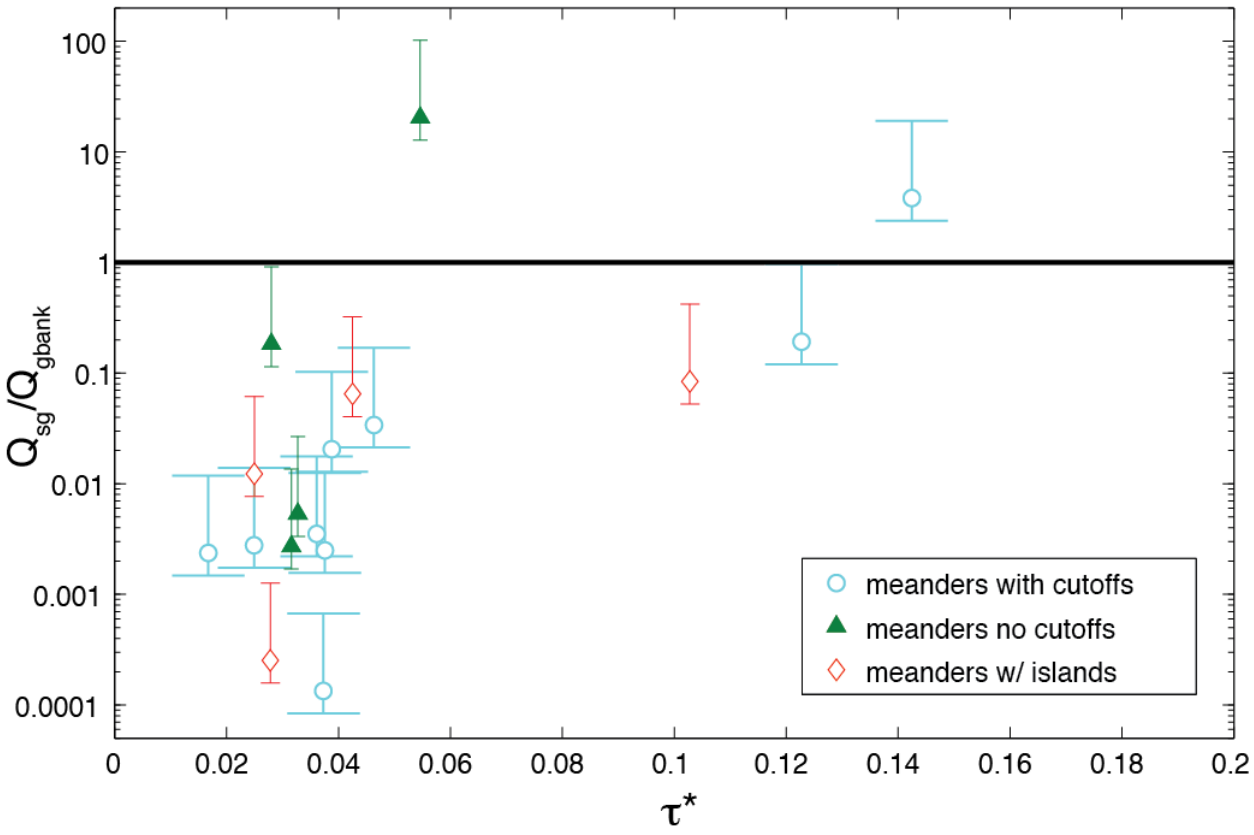


Figure 3.18. Shields stress versus relative supply of sediment from bank erosion. The points assume that 50% of the eroding bank is gravel, while the upper and lower error bars assume the banks are 80% and 10% gravel, respectively.

# 4 The response of fixed-wall meandering channel to increased sediment supply

## 4.1 Abstract

Sediment supply to meandering rivers constantly varies as migrating channels shift and reduce their slope and cutoffs bring in large increases in supply. Larger scale and longer duration sediment supply dynamics arise from watershed scale changes in climate, landuse and tectonics. To examine how sinuous channels respond to increased sediment supply, we conducted a flume experiment in a 0.45 m wide and 22.5 m long sinuous channel with an average flow depth of approximately 2.8 cm. The channel had 9 bends of varying curvature that were fixed in place. We ran a constant feed rate of 6 kg/hr for approximately 60 hours. During this time, the water surface slope equilibrated at 0.0048, and the bed was strongly sorted with coarse patches in the pools and upstream end of bars tops and fine patches in the remainder of the flume. Flat-topped bars developed in 7 of the 9 bends. Pools ranged in depth from 5 to 10 cm, and bars occupied about 80% of the channel width. Doubling the sediment feed to 12 kg/hr caused the channel to steepen by nearly 33% to a slope of 0.0064, which coupled with a 14% decrease in mean depth increased the boundary shear stress by about 20%. These changes alone were not enough to accommodate the increased load, so it is likely a combination of changes in the surface grain size field and the corresponding boundary shear stress field led to the new equilibrium flux state. The morphology of two of the 5 bends remained constant, and a third bend had only minor adjustments. The pools in the two bends with larger topographic adjustments shoaled due to deposition of coarse sediment. Both responsive bends had intermediate curvature, backwater associated with the fixed wall, and long straight reaches upstream. This experiment suggests that where channel slope can be adjusted, slope adjustments likely dominate response to increased supply, with muted response in bars and pools. Subsequent removal of the fixed wall allows aggradation to cause overbank flooding which lead to channel cutoff and then avulsion. This suggests that there may be a fairly narrow range of long duration sediment load increase that will not lead to major morphodynamic change.

## 4.2 Introduction

As they migrate across their floodplains, meandering rivers are constantly adjusting to local bedload perturbations as they erode their banks, reduce their slopes, and temporarily store and release sediment during bend expansion and cut-off [e.g., Zinger et al., 2011]. Perturbations to supply can also arise naturally from landslides and tributary inputs. It is generally assumed that although supply is never constant in rivers, rivers tend to damp out small perturbations such that we can define some statistically average channel characteristics, which are a function of a statistically average supply leading to the concept of a graded river [e.g., Mackin 1948]. Longer timescale changes in sediment supply due to climate change [e.g., Schumm, 1968; Blum and Törnqvist, 2000], tectonism, and changes to upstream watershed area via stream capture [e.g., Fisk, 1944], will force the channel to adjust to its new supply regime.

For a gravel bedded meandering channel at equilibrium with upstream sediment supply the channel can potentially adjust to the increases in supply in six ways, which may occur individually or in combination. (1) Either by increasing the extent of finer patches or by the

average bed surface becoming less coarse, leading to greater sediment transport for a given boundary shear stress [Dietrich et al., 1989; Pryor et al., 2011; Podolak and Wilcock, 2013]. (2) Pool depths may shallow [Lisle 1982; Lisle and Hilton, 1992; Major et al., 2012; Podolak and Wilcock, 2013] reducing the form drag. (3) Bars may grow into pools [Doyle et al., 2003; Constantine, 2006], perhaps increasing cross-stream relief [Miwa et al., 2005] and creating zones of heightened shear stress [Legleiter et al., 2011], and thus increasing the overall flux. (4) The channel differentially aggrades, steepening the water surface slope and increasing the boundary shear stress [Gilbert, 1917; Schumm, 1968; Madej, 1978; Madej and Ozaki, 1996; Wathen and Hoey, 1998; Hoffman and Gabet, 2007; Pryor et al., 2011; Major et al., 2012]. (5) The channel straightens through cutoff or avulsion, thus steepening the slope. (6) The active channel bed widens at a rate faster than the corresponding flow depths declines. One might expect pool depth and surface grain size adjustments to occur first, as they require the least amount of sediment deposition, but the response may also vary along a river depending on the shape of meander bends and the proximity of the bends to sediment sources.

Channel steepening can occur in a fixed-wall flume or channel bounded by bedrock, because the walls can contain the aggraded bed. In natural channels, however, bed aggradation may lead to avulsion [e.g., Smith et al., 1989] or successive cutoff and braiding [Madej and Ozaki, 1996; Hoffman and Gabet, 2007]. Over the long term, persistent high sediment supply may cause the aggradation of the channel and floodplain allowing channel morphology to adjust fully to the higher load, while the response to short-term changes in supply may be only temporary [e.g., Wathen and Hoey, 1998].

Field studies also suggest that supply increases may increase the channel migration rate [Dunne et al., 1981; Dietrich et al., 1999; Constantine, 2006]. Increased migration has been observed in reaches of decreasing boundary shear stress and deposition [Dunne, et al., 1981], and where tributaries increase bedload supply [Dietrich et al., 1999; Constantine, 2006]. Dunne et al., [2010] proposed bar aggradation can increase the convective accelerations of flow around bars leading to higher bank shear stress and erosion. Using Fluvial-12 [Chang, 2006], Dunne et al. [2010] showed that increased sediment supply could increase the bank erosion rate, even though Fluvial-12 does not explicitly account for convective accelerations associated with flow around bars. Although observation suggest that supply increases increase channel migration, the mechanisms by which increased supply alters the migration rate remains uncertain.

One-dimensional numerical models have been widely used to predict the effects of changes to sediment supply on the channel slope and surface grain size in field and laboratory channels [Cui and Parker, 2005; Dietrich et al., 2006; Cui and Wilcox, 2008; Pickup and Cui, 2008], but these models do not include adjustments to bar-pool morphology. A crucial component in linking channel migration and sediment supply is to observe the mechanisms by which sediment supply alters bar morphology in sinuous streams [Harrison et al., 2011]. Meander river evolution has been explored using morphodynamic models predict eroding the outer banks and assume inner banks follow [e.g., Ikeda et al., 1981; Blondeaux and Seminara, 1985; Johannesson and Parker, 1989; Howard, 1992; Sun et al., 1996]. In some of these models the point bar deposit along the inner bank may alter flow field and the resulting stress on the outer bank-- which changes with curvature and excess Shields stress [Seminara, 2005]. Recently proposed models can assess changes to outer banks and point bars independently [Parker et al.,

2011; Asahi et al., 2013], but these models are in their developmental stages and have yet to explore the role of sediment supply on meandering channel morphodynamics.

Existing theory and experimental data suggest that in straight channels, bar amplitude is a function of the width-depth ratio, the particle size relative to the flow depth, and the excess Shields stress [Colombini et al., 1987; Garcia and Nino, 1993], with bar height increasing with increasing width-depth ratio [Colombini et al., 1987]. In sinuous channels, bar morphology is also a function of the local channel curvature [Johannesson and Parker, 1989; Garcia and Nino, 1993] and the degree to which the upstream and downstream bends influence bar morphology depends on the resonance [e.g., Zolezzi and Seminara, 2001]. Gravel meanders tend to be super-resonant, where both upstream and downstream bends influence channel morphology [Zolezzi et al., 2009]. Experiments show that in straight channels with alternate bars, graded sediments tend to suppress bar amplitude and wavelength relative to uniform sediment [Lanzoni, 2000a]. Numerical models of flow and sediment transport in straight channels with alternate bars suggest that due to the non-linearity in sediment transport sediment flux can increase relative to plane bed channels when the flow drops below bankfull [Francalanci et al., 2012], but to our knowledge the effects of supply on bar-pool morphology has not been explored using morphodynamic theory.

The mechanisms by which sediment supply alters channel morphology has been investigated in straight laboratory flumes with plane beds [Dietrich et al., 1989; Cui et al., 2003; Venditti et al., 2010] and alternate bars [Lisle et al., 1993; Miwa et al., 2005; Madej et al., 2009; Pryor et al., 2011; Venditti et al., 2012; Podolak and Wilcock, 2013]. Reduced sediment supply in plane bed flumes causes the water surface slope to decrease, the bed to coarsen, and the width of active sediment transport to decrease [Dietrich et al., 1989; Venditti et al., 2010]. The decreased supply was also associated with a decreased wavelength of bedload sheets [Nelson et al., 2009]. In channels with alternate bars, decreasing supply caused the bars to wash out [Miwa et al., 2005; Venditti et al., 2012], translate down the flume and not reappear [Venditti et al., 2012], or to be left behind as abandoned terraces as the channel incises into the pools [Lisle et al., 1993]. Presumably channel response of these kinds is symmetric, i.e. increasing sediment supply induces response an opposite response to that caused by reduction. Incision into pools may occur in channels with low excess stress, while washing out may occur in channels with higher stress [Venditti et al., 2012]. Experimental suggest that increasing supply in straight flumes with alternate bars may cause pools to shoal and decreasing cross stream relief [Podolak and Wilcock, 2013], or that cross stream relief increases particularly in reaches where aggradation is greatest [Miwa et al., 2005]. Increased supply causes the bed surface to fine during aggradation [Pryor et al., 2011; Podolak and Wilcock, 2013] and transient short-wavelength bedforms can arise on the bed either replacing or superimposed on alternate bars [Podolak and Wilcock, 2013].

To our knowledge, there have been only two expeirments that investigated the role of supply in sinuous non-migrating channels. Eaton and Church [2009] found that bar-pool morphology was similar for runs with equivalent discharge and sediment supply that varied by nearly a factor of two in a moderately sinuous channel (sinuosity = 1.2) with fixed walls. These experiments had identical initial plane-bed conditions, so the effects of supply changes on bar-

pool morphology were not investigated directly, but their results suggest that in non-migrating gravel bed rivers, bar-pool morphology might be similar regardless of sediment supply.

A second experiment was conducted at the Outdoor Stream Lab (OSL), a sinuous, nearly field-scale flume at the University of Minnesota [Erwin, 2012; Erwin et al., in preparation]. In the OSL experiments the sediment supply was increased by a factor of five and Erwin [2012] focused on the growth of a sand bar in response to the supply change. Erwin [2012] found that in response to the increased supply, the bar elongated, widened, and the pool shoaled by about 2/3 of the mean channel depth (Figure 4.1). The OSL, however, has several characteristics that make it difficult to assess. In particular, cobble riffles at the upstream and downstream ends of the bend control water surface elevations and may alter the path of sand. The experiments by Erwin [2012] suggest that supply has a profound effect on bar morphology, while Eaton and Church [2009] found that steady state bar morphology is similar in non-migrating sinuous bends. Further experiments are needed to resolve this conflict, and also to explore the change in morphology during channel adjustment to the new supply regime.

To address uncertainty in how meandering channels respond to changes in sediment supply, we conducted an experiment at the Richmond Field Station (RFS) using sand to model a scaled-down gravel meander in a 45 cm wide and 23 m long sinuous flume. The channel was fixed in place to maintain temporally constant curvature and limit the cross-stream topographic response to bar and pool topography. After running the flume at equilibrium conditions, we doubled the sediment supply while holding all other variables constant. We hypothesized that a doubling of supply would be large enough to observe morphologic changes without requiring a very long experiment to reach equilibrium. We measured the sediment flux at the flume outlet, the evolution of bed topography, the water surface slope, and surface grain size. We noted the mechanisms by which the channel adjusted to the supply increase. These results were used to infer how supply might alter morphology in freely migrating channels.

## 4.3 Methods

This experiment was conducted in the large basin at the Richmond Field Station (RFS), the same basin used by Braudrick et al., [2009]. Following a freely migrating experiment, we fixed the channel boundary in place using 30 cm wide strips of sheet metal (Figure 4.2). There are some differences between the freely migrating channel and the fixed channel where the channel boundary had been disturbed during repairs to the channel outlet and the movable cart, and also bends with two locations points of maximum curvature were adjusted to have only one curvature maximum. Because it takes some distance for water and sediment to move in phase in flume experiments, a bend was added to the upstream end of the flume to disconnect the downstream channel from the upstream boundary more readily. Sand with the same size distribution as the feed was attached to the sheet metal by mixing it with sheet metal paint. The deepest portion of the pools exposed the lower half of the sheet metal because the channel incised in the beginning of the experiment and the bends were deeper than in previous experiments. The channel had 9 bends with a total sinuosity of 1.5 (Figure 4.2). Similar to Braudrick et al., [2009], these experiments were designed as a 1/50 or 1/100 scaled-down gravel bed river.

Water and sediment were fed at the upstream end of the flume. The graded sediment feed was identical to the sediment in the channel with a median grain size of 0.75 mm (Figure 4.3). The discharge was set to 2.6 l/s and measured using a V-notch weir upstream of the flume inlet. Flows were subcritical and turbulent (Table 4.1). At the conclusion of each day's run, a water tap was turned on at the downstream end of the flume to create a backwater through the flume to reduced adjustments to bar topography that occurred if the water surface dropped quickly. It took approximately 20 minutes for the backwater to extend up to the top of the flume. The backwater was then slowly drained overnight with a siphon. In early runs prior to backfilling the flume with water, we observed that as the water surface dropped, flow acceleration over the bar tops caused the bars to erode and deposit their sediment in the pools thereby decreasing pool depth. Starting the flume with a backwater was not possible, but care was taken to reduce transport due to unsteady flows, but some minor adjustments undoubtedly occurred at the beginning of each day.

Bed topography was measured using two oblique cameras and vertical laser sheet attached to a movable cart that spanned the basin. The images were processed in Matlab. Pixel size was approximately 1 mm in the x and y directions, with cross sections measured every 5 cm down the length of the flume. Water surface topography was measured using a point gauge attached to the movable cart. Typically, points were spaced 0.5-0.75 m apart and were centered with respect to the zone of active sediment transport normal to the flow. Because we were unable to measure sediment transport in the flume without disturbing the bed, the boundaries of the active transport zone were noted by eye, and measured using a ruler normal to flow. Channel topography and water surface elevation were used to calculate channel depth. The centerline was defined in ARC-GIS using the planform statistics toolbox using the x-y coordinates of the channel walls. The s-coordinates of the channel centerline are shown in Figure 4.2c. To calculate depth we converted the water surface elevations and depth measurements into streamwise-normal-elevation (snz) coordinates following the methods described in Legleiter and Kyriakidis, [2006]. Water surface elevations were interpolated every 5 cm. We then subtracted the bed elevation from the centerline water surface elevation in 5 cm s-coordinate bins, assuming the centerline water surface elevation represented the water surface elevation across the entire cross section. The difference in cross-channel water surface elevation at bends was generally less than 1-1.5 mm (up to 5% of the average depth).

Detailed maps of water surface through the flume were measured between -9 and -3 hours, and 73-80 hours. We measured the water surface elevation using a point gauge every 5-10 cm across the flume and every 10-20 cm downstream, with the survey density adjusted depending on the orientation of the channel relative to the flume.

The surface grain size distribution of the bed was mapped into 4 grain size classes: fine (less than 1 mm), mixed fine (greater than 50% fine sediment, with more than 20 percent coarse), mixed coarse (greater than 50% coarse sediment, with more than 20 percent fine), and coarse (>1 mm). Emergent surfaces were also mapped onto facies maps. The facies mapping was verified using digital photography following the methods outlined in Barnard et al., [2007] and Rubin [2004]. A camera was mounted to the cart and placed 18 cm from the bed. Each photograph covered approximately 1.6 cm by 2.3 cm area of the bed and 5 photographs were taken at each facies patch. To maintain constant lighting and contrast in the photographs, the bed was sprayed with water to adjust for differences in bed moisture due to grain size and a light was mounted

near the camera. The grain size distribution of each photograph was calculated using Barnard et al., [2007]. The bed photographs worked well for delimiting facies, but underestimated the distribution of sediment between 0.5 and 1 mm. Although making up 30% of the feed, sediment with diameter from 0.5-1 mm sediment made up only a small fraction of the grain size distribution measured with digital photographs. This is likely due to the condition of the fine facies in the flume. The fine facies stayed wet for several days after each run and photographs therefore had to be taken when the fine facies was still wet, and densely packed. This reduced the contrast between finer grain sizes and the photographic analysis found very little sediment between 0.5-1 mm, which makes up 25% of the feed. Hence, although we can consistently delineate the four facies, we cannot calculate an average bed surface grain size accurately.

At the downstream end of the channel water and sediment spilled into a small stilling basin where a free spill condition at the downstream end of the flume led to an eductor which transferred water and sediment to a stilling basket attached to a load cell. The load cell measured the mass of the submerged sediment basket every 0.2 seconds. These data were then smoothed twice using a 15-minute running-average filter.

The experiment was conducted in two phases. The first phase had a sediment feed rate of 6 kg/hr. The intitial feed rate was chosen to match the sediment flux at the bottom of the flume during preliminary experiments. After 60 hours, the sediment feed was doubled to 12 kg/hr with all other variables held constant. In this paper, we present the results from the final 27.5 hours of the 6 kg/hr feed rate when channel had equilibrated and the measurement techniques were constant. All times are reported with zero hours at the beginning of the increased feed, with negative time indicating the lower feed rate and positive time indicating time since the feed increase. Experimental conditions are summarized in Table 4.1.

During the experiment we will document six responses: 1) the sediment flux at the downstream end of the flume, 2) the spatial patterns of sediment facies, 3) the width of active sediment transport, 4) the bed topography, 5) the water surface slope, and 6) the mean depth. Response variables 2-6 will assess changes for the flume as a whole and for individual bends. We will use all six response variables to assess the time it takes for the channel to reach a new equilibrium.

## 4.4 Results

### 4.4.1 Low (6 kg/hr) feed rate (-27.5 to 0 hrs)

During the low feed rate the channel developed bar pool topography at 7 of the 9 bends in the channel (Figure 4.4a). The bends are labeled on Figure 4.4 for clarity. Bars did not develop in Bends 6 and 7, and the pool in Bend 7 was along the left (inner) bank (Figure 4.4a). Whiting and Dietrich [1993b] defined theoretically the conditions where the pool may not be on the outside of the bend where:

$$\frac{M}{B} < \frac{1}{\cos\omega \sin\omega} + 2 \qquad (4.1)$$

where M is the bend wavelength, B is the channel width, and ω is the angle of the bend with respect to the downstream flow direction. For Bends 6-7, the right hand side of Equation 4.1 was

12.6 and 54 while the left hand side is 4.42 and 4.13, thus the absence of point bars is consistent with the model. The Whiting and Dietrich [1993b] relationship would predict that bars would migrate through bends 6 and 7, but in our experiments the bars seemed fixed.

The ratio of the minimum radius of curvature to channel width ($R_c/B$) for the bends with point bars ranged from 0.86-1.7 and the sinuosity ranged from 1.2-2.2 for the bends that developed bars (Table 4.2). On average, the slope break from bars to pool occurred at depth of 1.5 cm. If bars are defined as areas shallower than 1.5 cm, the wide flat-topped bars generally covered about 80% of the channel width. Maximum pool depth relative to mean depth ($H/H_{max}$) ranged from 2.8 to 3.8 prior to the feed increase (Figure 4.5). Maximum pool depth was greatest for Bends 4 and 8, which had an intermediate $R_c/B$ of 1.1 between the higher curvature Bends 5 and 9 and the lower curvature Bend 3. The maximum depth downstream of the apex of Bend 4 is underestimated because the pool at s=11 m was partially obscured by the walls in our survey.

Prior to increasing the feed, both the water surface slope and the sediment flux at the flume outlet had equilibrated. The water surface slope was stable at 0.0046 with minor changes due to local topographic adjustment (Figure 4.6). The sediment flux at the downstream end of the flume was quasi-steady around the 6 kg/hr feed rate (Figure 4.7). The mean flow depth was 2.8 cm and the mean active channel width was 28 cm (Table 4.1).

During the low feed rate the area and distribution of sediment facies remained relatively constant, with minor variations at bar crossovers where the paths of coarse and fine sediment intersected. The bed had very strong sorting, with coarse sediment on the outside of bends and fine sediment making up most of the bed (Figure 4.4b). Dunes, 1.5 to 2 cm high, spaced about 10 cm apart were present in the fine facies, particularly downstream of deep bends (Figure 4.4b). Prior to the feed increase, fine facies with dunes made up about 20% of the total bed area. Dunes were not present in Braudrick et al., [2009] or any experiments with migrating banks likely because the pools were shallower and sediment was supplied primarily through erosion of the poorly sorted bank sediment. Mixed sediment facies were limited to the upstream end of bars, where the paths of coarse and fine sediment crossed as described in Dietrich and Smith [1984]. Emergent areas were a remnant of the channel adjustment at the beginning of the experiment, when bars and pools developed while the slope adjusted from the initial bed.

Detailed water surface profile measurements prior to the feed increase show that the water surface was elevated on the outside of bends, and that the water surface topography was steeper in the bends and gentler in crossovers, with still water on the inside of Bends 4 and 8 downstream of the bend apex (Figure 4.8). There are strong gradients in cross-stream gradients in water surface topography in bends, reflecting zones of high cross-stream velocity.

### 4.4.2 Increased supply

*Sediment flux and sediment facies*

After the sediment supply was increased at the upstream end of the flume, the sediment transport rate at the flume outlet remained constant at about 6 kg/hr for approximately 20 hours (Figure 4.7). For the next 15 hours (20-35 hours), the sediment transport rate at the outlet increased to just below 8 kg/hr. The transport rate at the outlet then gradually increased to just under 12 kg/hr and varied around that value from 55-66 hours. From 66-75 hours, the flux

dropped ranging between 9-12 kg/hr with an average of about 11 kg/hr. For the last 25 hours of the experiment (75-100 hours) the flux varied around 12 kg/hr (Figure 4.7).

Following the feed increase, the extent of coarse, fine, and emergent facies declined while the extent of mixed coarse and mixed fine facies increased (Figures 4.9 and 4.10), resulting in an overall fining of the flume surface. By 38 hours after the feed increase, coarse patches had begun to fine throughout the flume length as the mixed fine facies increased in area and the coarse facies in Bend 7 fined (Figures 4.9 and 4.10). Coarse patches expanded in pools as pools filled in Bend 4 at 11.8 hrs and also at Bend 8 at 80 hrs (Figures 4.9 and 4.11). As the pools filled in with coarse sediment, and the zone of active sediment transport moved toward the inner bank causing the fine facies over the bar to coarsen (Figure 4.9). Emergent areas on the inside of the point bar near the bend apex of each bend at 0 and -9 hours in Figure 4.9 became submerged as aggradation proceeded downstream starting at 11.8 hrs after the feed increase. The inundation of these submerged features occurred as the channel aggraded and first occurred in the upstream reaches (Figure 4.11). After 20 hours, the emergent patches were no longer present in the flume (Figures 4.9-4.11). The inundated emergent areas became patches of fine sediment, and were generally in areas of low velocity. A coherent patch of mixed fine sediment similar to a bedload sheet propagated downstream and is visible in Bends 6 and 7 at 38 and 55 hours and Bend 8 at 80 and 100 hours (Figures 4.9 and 4.11). Bend 4 also fined at 55 hours, prior to the pool deepening. The areal extent of coarse sediment decreased in Bends 1-3 as zones of mixed coarse and mixed fine sediment expanded (Figures 4.9 and 4.11). There was little change to sediment facies in Bends 5 and 9 (Figure 4.11).

*Hydraulic adjustments to the supply increase*

After the feed increase, the water surface elevation increased as sediment was differentially deposited at the upstream end of the flume (Figures 4.6 and 4.12). The water surface slope increased rapidly for the first 20 hours after the feed increase, then slowed down. At 55 hours when the sediment flux was just under 12 kg/hr, the mean water surface slope for the flume was 0.0062. The water surface slope stabilized at an average slope of 0.0064, 72.5 hours after the feed increase (Figure 4.12). This represents a 33% increase in water surface slope from the initial slope of 0.0048.

After the feed increase, the water surface topography was steeper, but was otherwise similar to that before the feed increase (compare the upper and lower panels of Figure 4.8). The water surface topography adjusted in Bend 4 as the area of still water moved upstream. Steep sections of water surface topography were located in similar reaches (i.e., downstream of bars) before and after the feed increase (Figure 4.8).

Total aggradation was about 4 cm at the upstream end of the flume and decreased downstream. Aggradation was about 2 cm in Bend 5 and less than 1 cm in Bends 8 and 9 (Figure 4.13). Aggradation at Bends 1-5 was apparent after the first survey following the feed increase (11.8 hours). Downstream aggradation at Bends 6-9 was first visible about 20 hours after the feed increase. The average bed elevation stabilized at 80 hours, but aggradation was limited to a few mm after 55 hours (Figure 4.13).

During the experiment the average depth decreased from 2.8 cm at 0 hours to 2.6 cm at 55 hours and finally to 2.4-2.5 cm from 80-100 hours when the water surface slope was stable (Figure 4.12). Conservation of mass dictates that the decrease in average water depth must accompany an increase in slope (and hence velocity) if the bed roughness and channel width are constant. The average active channel width was increased from 28-31 cm prior to the feed increase to 31-32 cm following the feed increase (Figure 4.12).

Using the reach average water surface slope and average depth, we calculated the reach average boundary shear stress ($\tau_b$) through time using:

$$\tau_b = \rho g H S \tag{4.2}$$

where ρ is the water density (assumed to be 1000 kg/m$^3$), g is gravitational acceleration (9.81 m/s$^2$), H is the average water depth, and S is the water surface slope. $\tau_b$ ranged 1.2-1.3 Pa prior to the feed increase (Figure 4.14). After the feed increase, $\tau_b$ increased to 1.64 Pa by 71 hours (an increase of 26%), before decreasing to 1.5 Pa at 80 hours as the mean flow depth decreased. $\tau_b$ remained between 1.5 and 1.6 Pa for the remainder of the experiment, an increase of 15-23% relative to 0 hours (Figure 4.14).

*Spatial changes in channel hydraulics*

The streamwise changes in average flow depth shown in Figure 4.15 (top panel) reflect differences in data density with more uncertainty where the fixed walls partially obscured the bed or where the fixed-wall channel was oblique to the survey cart, which was oriented perpendicular to the x coordinate shown in Figure 4.4. Temporal changes in mean flow depth in Figure 4.15 are not an artifact of surveys (which did not change location or methods), but represent real changes in depth. The mean flow depth decreased throughout the length of the flume between 0 and 100 hours. The decreases in depth were greatest in Bends 4 and 5 reflecting a decrease in backwater they induced upstream of their apex as the channel steepened. Otherwise the decrease in depth was relatively uniform.

The local water surface slope varied from -0.007 to 0.016 prior to the feed increase (Figure 4.15, middle panel). The negative slope occurred in a backwater in Bend 4. At 100 hours, the local water surface slope had steepened relative to 0 hours in most reaches (Figure 4.15). Local water surface slopes fluctuated through time as the channel adjusted to the new supply (Figure 4.15). Short-term slope increases were highest at the upstream end of the flume and Bends 5 and 9. In Bend 5 the local slope doubled to 0.018 at 80 hours before decreasing to 0.013 at 100 hours. The local slope increase in Bend 9 was associated with a decrease in slope just upstream. Otherwise, the water surface slope fluctuations were within the range of the water surface slopes measured at 0 and 100 hours (Figure 4.15).

The active width varied spatially and temporally before and after the feed increase (Figure 4.15, lower panel). The active width temporarily increased by nearly 80% in the downstream portion of Bends 4 and Bend 5 (shown by the grey lines) as the morphology of Bend 4 changed and the emergent areas of the flume were inundated (Figure 4.15). By 100 hours the active width in this reach was similar to the active width at 0 hours. For the entire 100 hours after the feed increase, the active width in the upper portion of Bend 4 decreased relative to 0 hours.

Between bends 8 and 9 the active width was volatile and ranged between 20 and 28 cm, although the width at 0 and 100 hours were similar. This volatility occurred prior to the feed increase (see the black line from -9 hours at s=18-20 m in Figure 4.15).

*Changes in bed topography*

Figures 4.16 and 4.17 show the distribution of depth through time and the change in depth relative to 0 hrs, respectively. These figures show that cross-stream topographic change occurred first in the upstream bends and propagated downstream. For the most part, bar morphology was relatively stable. We saw only limited evidence of bars advancing into pools (Bend 3 at 11.8 hours), and the bar associated with Bend 4 extended upstream at 11.8-20 hours. All of the pools shoaled during the experiment, but $H_{max}/H$ was similar through time, with short-term increases in $H_{max}/H < 15\%$ for Bends 5 and 9 as the channel aggraded. By 100 hours, $H_{max}/H$ decreased by about 5% in Bend 3, 10% in Bend 8, and 22% in Bend 4 (Figures 4.5 and 4.18). At 20 hours, $H_{max}/H$ decreased by 15% relative to 0 hours in Bend 4 as the pool filled with coarse sediment. The location of the maximum pool depth shifted upstream 0.9 m in Bend 4 and moved downstream 0.2 m in Bend 3 but otherwise they remained in place. The upstream shift in $H_{max}/H$ for Bend 4 was associated with the upstream growth of the point bar (Figure 4.17).

The most visible topographic response to the increased supply was the shoaling of the pools in Bends 4 and 8 at 11.8-20 and 80 hours, respectively (Figure 4.19). The changes in topography coincided with a coarsening of the bed as the pool filled with coarse sediment. Visual observations of sediment transport patterns showed that as the pools filled in in Bends 4 and 8, the sediment transport moved toward the middle of the channel and away from the outer bank. As the pool filled in at Bend 4, the bar extended 1 m upstream (Label A in Figure 4.19), whereas the pool filling at Bend 8 was not associated with upstream growth of the bar (Figure 4.19). In Bend 4, the pool aggraded by up to 6 cm near the former location of maximum depth, effectively flattening the cross section (Figure 4.19). The topographic changes in Bend 4 began soon after the feed increase. There was little change in cross-stream topography at Bend 4 from 20-71 hours even though the average bed elevation increased by over 2 cm (75% of the channel depth) in that time. Bend 4 transformed from a bend with a single point bar and pool to a bend with shingle bars and 2 pools (Figure 4.18), which consist of successive bars and pools on the same side of the channel separated by a relatively uniform cross section (e.g., Whiting and Dietrich, 1993a). The shingle bars at Bend 4 persisted until 71 hours, the morphology in this bend became unstable, and oscillated between a shorter bar and single deeper pool similar to that before the feed increase, and the shingle bars present after 20 hours (not visible in Figure 4.19).

## 4.5 Discussion

### 4.5.1 Topographic change in response to increased supply

Our experiments found that the bed steepened following the doubling of sediment feed, but otherwise changes to bed morphology were limited to Bends 4 and 8, despite aggradation of over one channel depth in the upstream half of the flume. Small, short-lived changes to bed morphology included both a slight (~12 %) deepening of the pool in Bend 5 and pool shoaling in Bends 4 and 8. The shoaling of the pool in Bend 4 persisted, while the pool depth increased in Bend 8 between 80 and 100 hours. The topographic changes were associated with coarsening of the bed surface in Bends 4 and 8. In both Bends 4 and 8 the extent of coarse facies increased as

the pools filled, while the extent of fine facies remained quasi-steady (Figure 4.11). In Bend 5, however, the extent of fine facies increased slightly (Figure 4.11) while the extent of coarse facies decreased, causing an overall fining of the bed. Changes to the sediment facies in Bend 9 were very small.

Bends 4 and 8 had intermediate curvature between Bend 3 (where the bar and pool moved downstream) and Bends 5 and 9 (where changes in bar and pool morphology was small). Bends 4 and 8 also have stronger backwater effects on water surface topography than Bends 5 and 9 (indicated by the lower local slopes in Figure 4.15, middle panel and the decreased gradient near the bends in Figure 4.8). These backwater effects upstream of sharp bends may have increased deposition as the supply increased. Additionally, the long straight reaches upstream of Bends 4 and 8 (that are absent from Bends 5 and 9) likely play a role in their response to the increased feed. The filling of the pool in Bend 8 occurred when a fine-grained bedload sheet mobilized a patch of coarse sediment in the reach upstream. The temporary increase in coarse sediment supply overwhelmed the transport capacity of the bend and the pool filled, and this sediment was slowly delivered to Bend 9 downstream. Numerical modeling of flow and sediment transport of these flume experiments may determine if the subtle changes to Shields stress was sufficient to cause this reach of channel to transmit the increased sediment supply.

### 4.5.2 Slope and depth changes to the sediment transport rate

Figure 4.14 shows that between 80-100 hours, the average boundary shear stress increased between 15-26% relative to 0 hours. To explore whether this is sufficient to accommodate the doubling of sediment supply I used a simple sediment transport model. Models to predict sediment transport (e.g., Meyer-Peter and Muller, 1948) often have the form:

$$q^* = k(\tau^* - \tau^*_{crit})^n \tag{4.3}$$

where q* is the dimensionless sediment transport rate per unit channel width, k and n are empirically measured. The exponent n is typically 1.5 [see Garcia, 2008 for a compilation of sediment transport formulae]. My visual observations suggest that $\tau^*_{crit}$, the critical Shields stress at which particle motion begins is about 0.03 in our flume. q* is

$$q^* = \frac{q_c}{\sqrt{\frac{\rho_s - \rho}{\rho} g {D_{50}}^3}} \tag{4.4}$$

where $q_c$ is the volumetric transport capacity per unit width, $\rho_s$ is the density of sediment and $D_{50}$ is the median particle size of the bed. $\tau^*$ is the Shields stress defined as:

$$\tau^* = \frac{\tau_b}{(\rho_s - \rho) g D_{50}} \tag{4.5}$$

Because our digital grain size calculation did not accurately assess the particle sizes between 0.5 and 1 mm, we cannot use it to calculate $D_{50}$ of the bed. We can make a preliminary estimate of $\tau^*$ by assuming that $D_{50}$ is constant and equal to the $D_{50}$ of the feed (we did not observe obvious armoring of the bed, so this is a reasonable first approximation). Using this approximation for $D_{50}$, the calculated 20% increase in $\tau_b$ (and hence $\tau^*$) would lead to a 55%

increase in q*, and $q_c$. This is not sufficient to accommodate the doubling of sediment supply, suggesting that the bed either did fine (reducing $D_{50}$) to accommodate the doubling of supply, or changes to the bed morphology may increase transport rates in part of the bed. Had the initial bed been 50% coarser than the feed (i.e., D50=1.1 mm), a fining of the bed to 0.75 mm coupled with the observed increase in stress would have been sufficient to accommodate the doubling of supply. Given that the changes to bar morphology were limited to only 3 bends, it seems unlikely that bed topography alone will alter the sediment transport rate in the flume . It is hoped that further work with the photographic record will enable a quantitative assessment of surface grain size changes, perhaps using a different methodology [e.g., Bellugi, 2012]. Additionally we can use a 2-dimensional hydraulic model to assess the spatial variation of shear stress in the flume. The decrease in the extent of the coarse and fine facies in the flume suggests that changes to the average $D_{50}$ of the flume surface are possible.

### 4.5.3 Comparison with previous experiments

Although the OSL experiment had a much larger increase in sediment supply than the RFS experiment, the OSL experiment adjusted to the higher feed rate through aggradation of the bar and pool, while the experiments reported here mostly accommodated the increased supply through steepening and fining of the bed. Prior to the feed increase, the OSL bar was relatively small (Figure 4.1), not created by pre-existing equilibrium flow and sediment transport conditions, with a large recirculating eddy on the inner bank. Increasing the feed caused the bar to enlarge laterally and the pool to fill, but the bar took up only about 55% of the channel width, and did not have the wide, flat bar top seen in all bars in the RFS experiment (compare Figures 4.1 and 4.4). In the RFS experiment, the bar covered about 80% of the channel width.

The difference in bar morphology likely lies with a difference in the origin of the bars. The OSL channel at the study bend has a width-depth ratio of approximately 9, within the range of 8-10 that is transitional between channels that support alternate bars and channels with plane beds [Parker, 1979]. Using the thresholds for alternate bars defined by Colombini et al. [1987], the width-depth ratio of the OSL is well below the threshold for alternate bars given the median grain diameter of the sediment feed. The morphology of the OSL channel therefore likely supports forced rather than fixed bars. Fixed bars are fixed in place by curvature, but if the channel were straight would be present as alternate bars, whereas forced bars occur due to curvature, but in the absence of the bend the channel bed would be flat because the width-depth ratio is small [Ikeda, 1989]. Sand bars are not present in areas of the OSL flume without bends. These results suggest that forced bars may more readily respond to changes in sediment supply than fixed bars, because the top of fixed bars often control the water surface slope, while forced bars may be a function of water surface elevation.

For the two of the bends (Bends 5 and 9), the equilibrium bar response observed in the present experiments is similar to those observed by Eaton and Church [2009], in that the bar and pool morphology was relatively consistent for regardless of supply. The degree to which pool filling in Bends 4 and 8 was a function of the grain size distribution and the dynamics of grain interactions is unknown, but given the strong sorting of the bed and the very strong sorting of the sediment a uniform grain size distribution may have had a very different response.

The experiments presented here as well as the experiments of Eaton and Church [2009] and Erwin [2012] investigate bar unit response to sediment supply for channels with fixed banks. Results likely differ if the outer bank is actively eroding. In the actively eroding case, changes in bar morphology could be associated with adjustments to channel width, accelerated channel shifting and corresponding changes in the boundary shear stress field. Such a response could be investigated by conducting flume experiments with erodible banks and also recently developed numerical models that allow the channel width to evolve [Parker et al., 2011; Asahi et al., 2013]. As discussed above, freely migrating channels derive large amounts of sediment from bank erosion and this may influence the degree of bed surface sorting relative to fixed-wall experiments. $H_{max}/H$ in experiments using alfalfa at the Richmond Field Station (e.g., Chapters 2 and 5) is typically around 2, much lower than the pools in the fixed-wall channel, suggesting that bar-pool morphology is tied to the strength of the banks and channels with lower bank strength may respond differently to supply changes. The flat bar tops observed in the fixed-wall channel, however, would be colonized by alfalfa in our experiments, effectively narrowing the channel and contributing to lateral shifting.

### 4.5.4 Bank erosion and sediment supply

For the upper 2 bends, the total change in mean bed elevation was greater than mean channel depth, and the total aggradation was over half the mean depth in 7 of the 9 bends. This level of aggradation is not possible in meandering rivers without the channel cutting off or avulsing. We observed such a change for an experiment shown in Figure 4.20. This experiment was conducted immediately after the fixed-wall experiments after the walls were removed. Following Braudrick et al., [2009], we added alfalfa to the floodplain to provide bank strength. The steady bankfull discharge was 2.2 l/s (slightly lower than the fixed-wall experiments), with a much higher alfalfa density and hence bank strength than Braudrick et al., [2009]. The initial coarse sediment feed rate of 3.2 kg/hr was adjusted throughout the experiment in an attempt to limit the aggradation, with an average coarse sediment feed of 0.85 kg/hr. The average fine (plastic) sediment feed was 4 kg/hr.

The feed rate exceeded the transport capacity and the channel aggraded, primarily at its upstream end. Unlike the RFS experiments with fixed walls, the aggradation led to increased flow overbank further reducing the ability of the channel to transport sediment. This eventually caused the cutoff and avulsion shown in Figure 4.17 at 33 hours effectively ending the experiment. We would expect a similar response to very large supply increases for meandering channels in the field, particularly if supply increases are not associated with large floods able to erode the banks and widen the channel.

## 4.6 Conclusions

We explored the response of a gravel bedded meander whose banks had been fixed to a doubling of sediment supply. The flume was 22.5 m long, 45 cm wide and 2.8 cm deep with a steady bankfull discharge of 2.6 l/s. We initially ran the flume at a constant discharge and sediment supply for approximately 60 hours. The channel slope stabilized at 0.0048 and bar pool topography developed for 7 of the 9 bends in the channel. The bars were flat-topped and created strong sorting with coarser facies located in the pools and the upstream end of bars. Upon doubling the sediment supply, the channel adjusted by increasing the water surface slope from

0.0048 to 0.0064 and fining coarser patches of sediment and increasing the extent of mixed coarse and mixed fine facies. The changes to the surface size distribution of the bed were not adequately quantified due to a methodological problem with the photographic surveys used to record grain size patterns. The slope changes caused a decrease in the average water depth from 2.8 to 2.4 cm. Aggradation ranged from just under 1 cm to 4 cm, with decreasing aggradation amount downstream. Bar-pool morphology changed little. The maximum pool depth relative to the mean depth decreased for only one of the bends in the flume, but two of the bends had extensive shoaling as they infilled with coarse sediment. Because the changes to bed topography were subtle and limited to two bends, it is unlikely that these changes altered the transport rate appreciably. Assuming the bed surface size was constant, a simple sediment transport calculation showed that the observed increase in slope coupled with the observed decrease in depth were not sufficient to accommodate a doubling of sediment supply, suggesting that a combination of local fining and changes in the corresponding local boundary shear stress field probably led to supply accommodation.

Our results differed from experiments by Erwin [2012] in which a 5-fold increase in sediment supply was fed to a single bend at the Outdoor Stream Lab. Their low width-depth ratio created a forced rather than fixed bar whose size was probably a function of the supply. Slope changes at the OSL were also limited by the grade control provided by the gravel riffles at either end of the bend. Upon completion of the fixed-wall run, we remove the walls and found that the channel aggradation at the upstream reach caused discharge to spill onto the floodplain and induce a channel avulsion. This suggests a fairly modest range of bedload sediment supply increase can be passed downstream into bends without aggradation leading to large scale channel shifting.

## 4.7 Acknowledgements

This research was funded by the CALFED Ecosystem Restoration Program (Grant No. ERP-02D-P55), the STC program of the National Science Foundation (NSF) via the National Center for Earth Surface Dynamics (NCED) under agreement EAR-0120914, the Donors of the American Chemical Society Petroleum Research Fund, and an American Geophysical Union Horton Research Grant to Braudrick. We would like to thank Stuart Foster for his tireless work to keep the Richmond Field Station flume running. Russell McArthur and Sumner Collins helped process sediment samples. Carl Legleiter provided the Matlab code used to transfer the data from xyz to snz coordinates. Thanks to Susannah Erwin and Peter Wilcock for the Outdoor Stream Lab data.

## 4.8 Tables

Table 4.1. Experimental conditions for the initial sediment feed

| Parameter | Initial value (0 hours) | Final value (100 hours) |
|---|---|---|
| Discharge (l/s) | 2.6 | 2.6 |
| Feed Rate (kg/hr) | 6 | 12 |
| Average Width (cm) | 45 | 45 |
| Average Depth (cm) | 2.8 | 2.4 |
| Width-depth ratio | 16.6 | 18.8 |
| Active width (cm) | 28 | 30 |
| Water surface slope | 0.0046 | 0.0064 |
| Froude number | 0.39 | 0.50 |
| Reynolds Number | 5800 | 5800 |

Table 4.2. Length and minimum radius of curvature relative to width ($R_c/B$) of experimental bends with point bars. The bends are labeled in Figure 4.4a.

| Bend | Bend length (m) | Sinuosity | $R_c/B$ |
|---|---|---|---|
| Bend 3 | 4 | 1.24 | 1.7 |
| Bend 4 | 4 | 2.18 | 1.1 |
| Bend 5 | 2 | 1.36 | 0.86 |
| Bend 8 | 2.5 | 1.33 | 1.1 |
| Bend 9 | 1.7 | 1.08 | 0.97 |

## 4.9 Figures

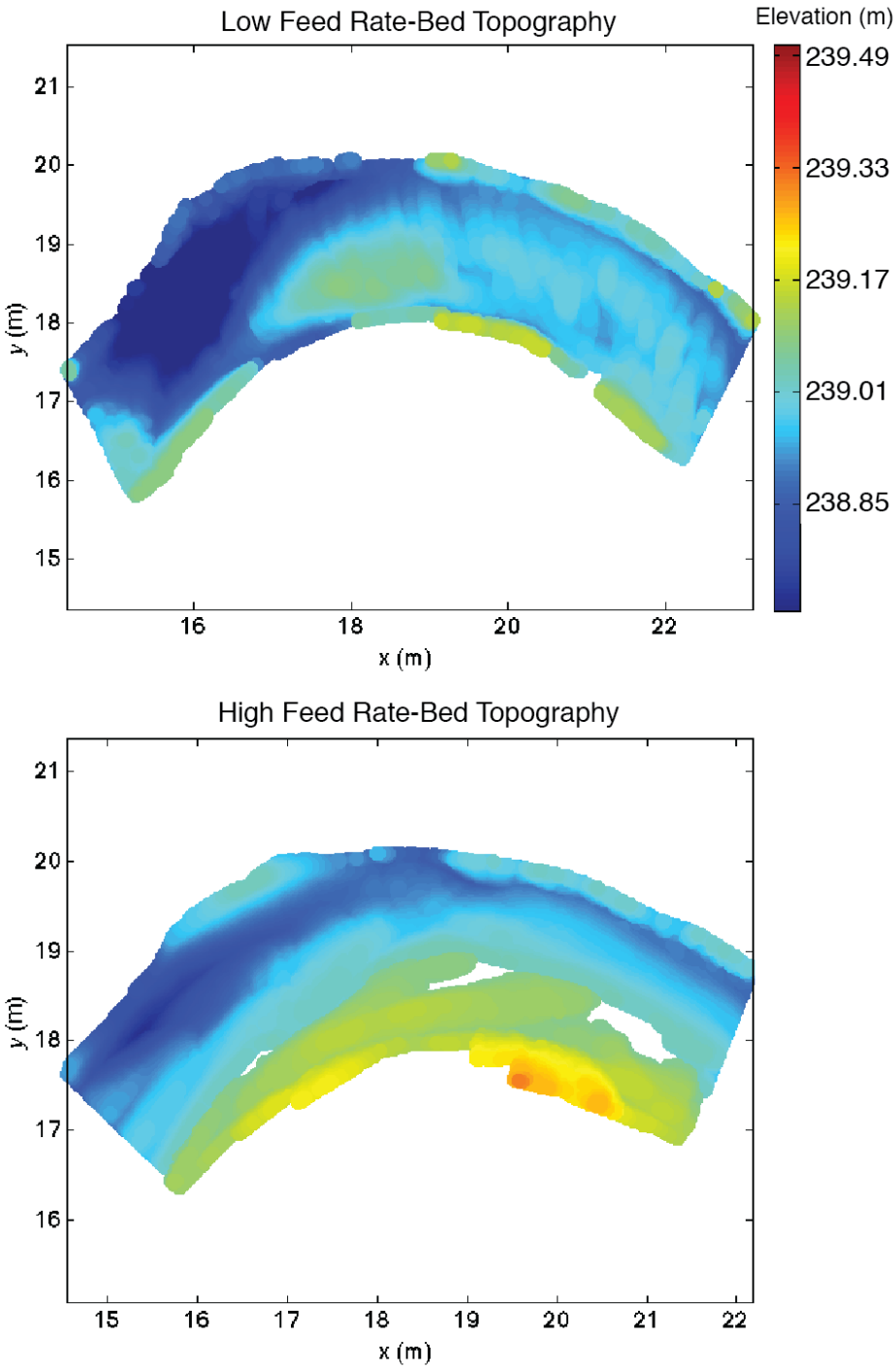


Figure 4.1. Bed topography comparing low and high sediment feeds for the Outdoor Stream Lab experiments from Erwin [2012]. Flow is from right to left. The color scale is identical for the two figures.

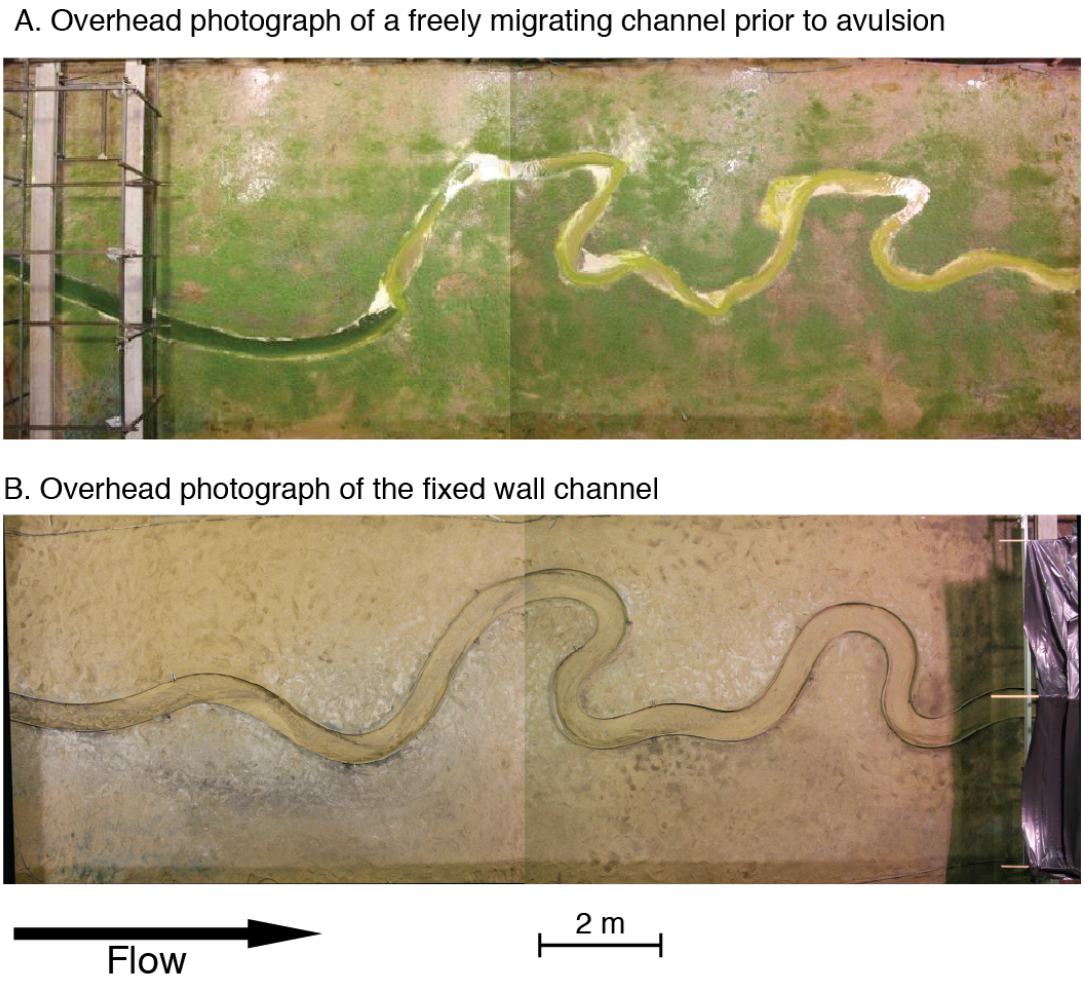


Figure 4.2. Overhead images of A. the self-formed channel using alfalfa to provide bank strength similar to Braudrick et al. [2009] prior to channel infilling due to a feeder malfunction and B. The fixed-wall channel used in the RFS experiments. An extra bend was added upstream to limit the downstream impact of the inlet condition and the walls in the two lowermost bends are slightly different as the bed was disturbed to make repairs to the flume and cart.

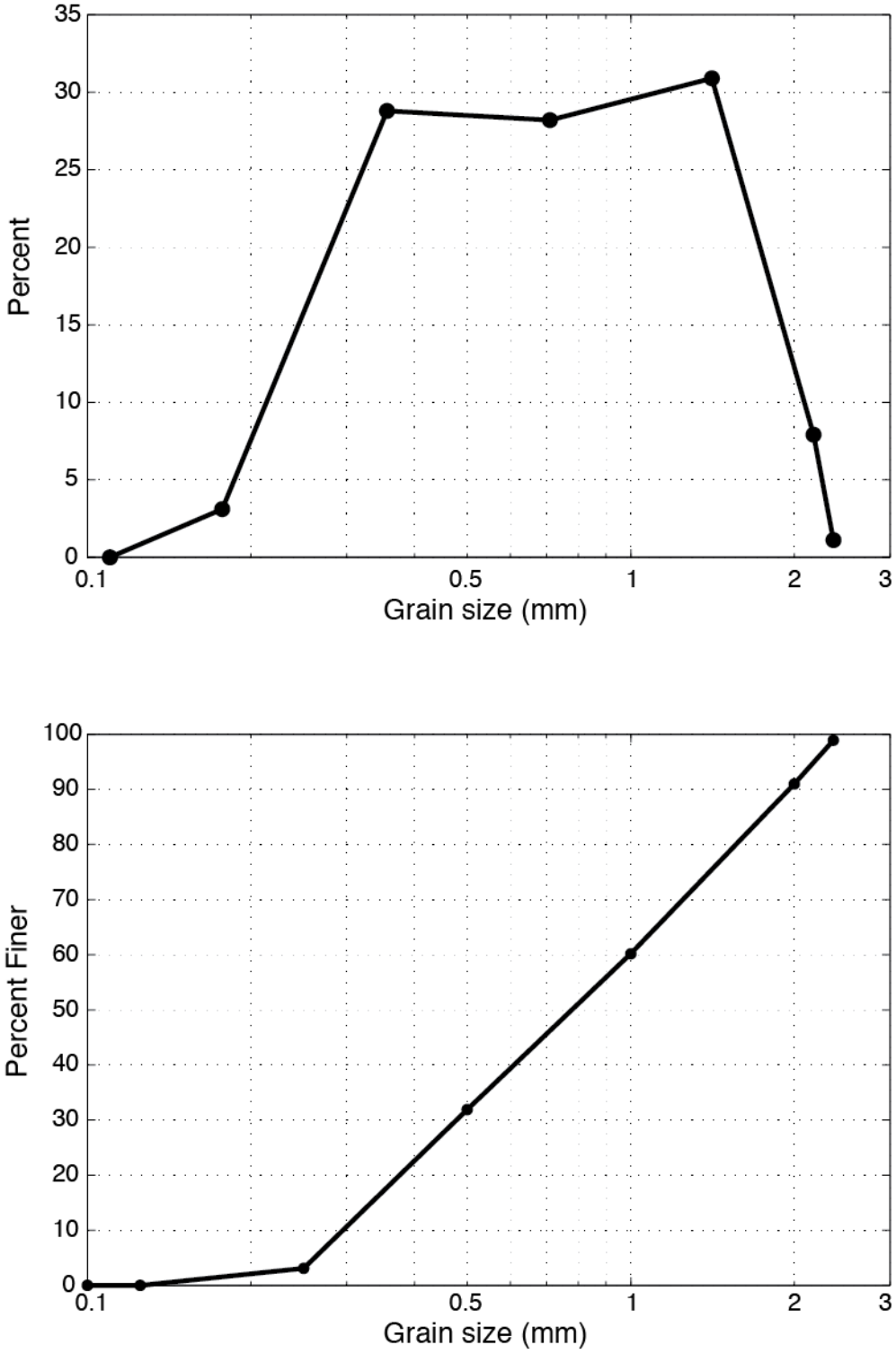


Figure 4.3. Grain size distribution of the sediment feed.

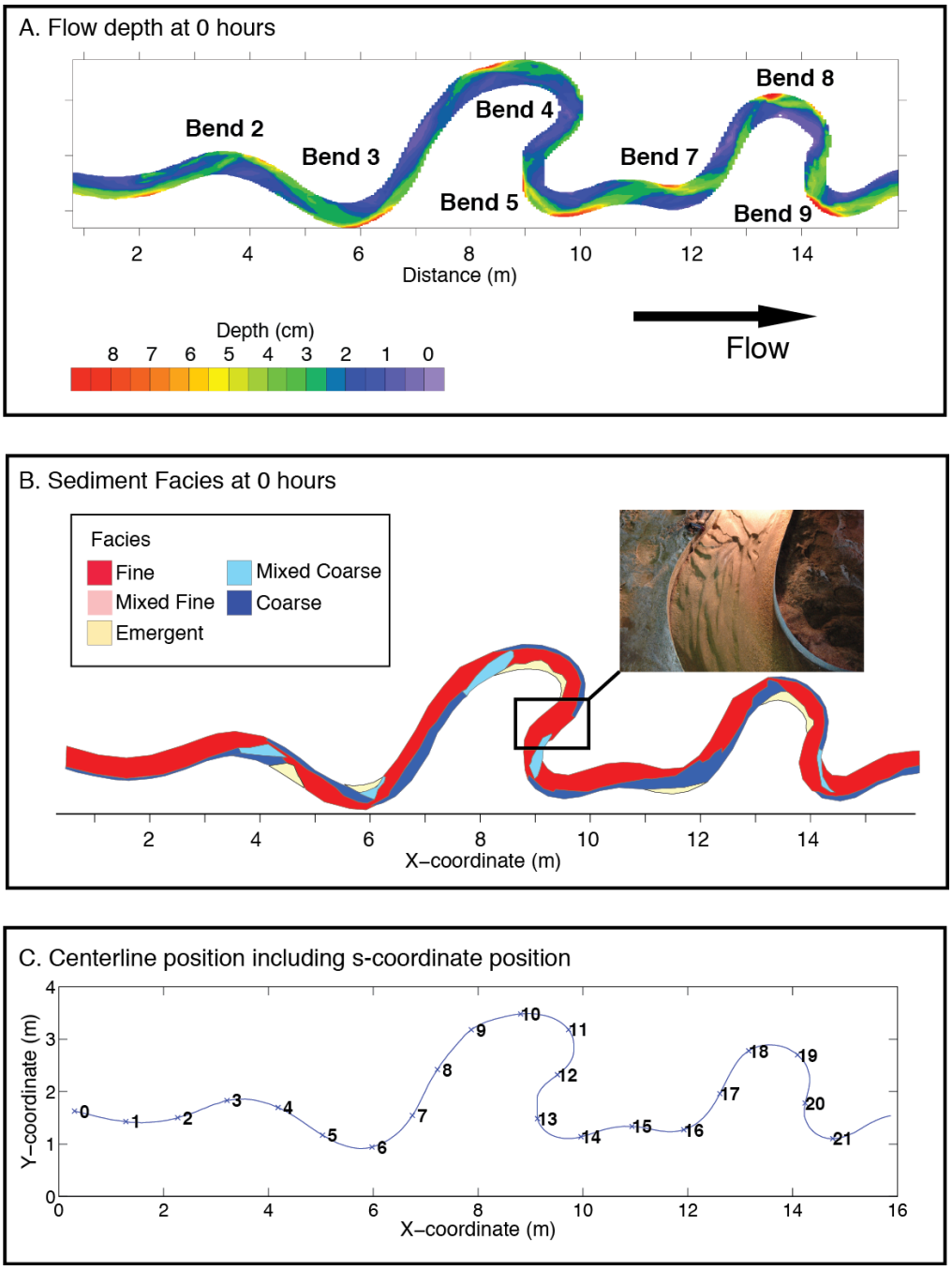


Figure 4.4. A. Channel depth at 0 hrs immediately proceeding the feed increase. Bend numbers are indicated on the Figure 4.and are numbered from upstream to downstream. The pool associated with the downstream apex in Bend 4 was not obscured by the channel walls and is not visible in this map. B. Sediment facies at 0 hrs with the inset image showing dunes present in the fine facies at the downstream end of bends. The photograph is looking upstream between bends 4 and 5. C. Channel centerline coordinates for the experiments.

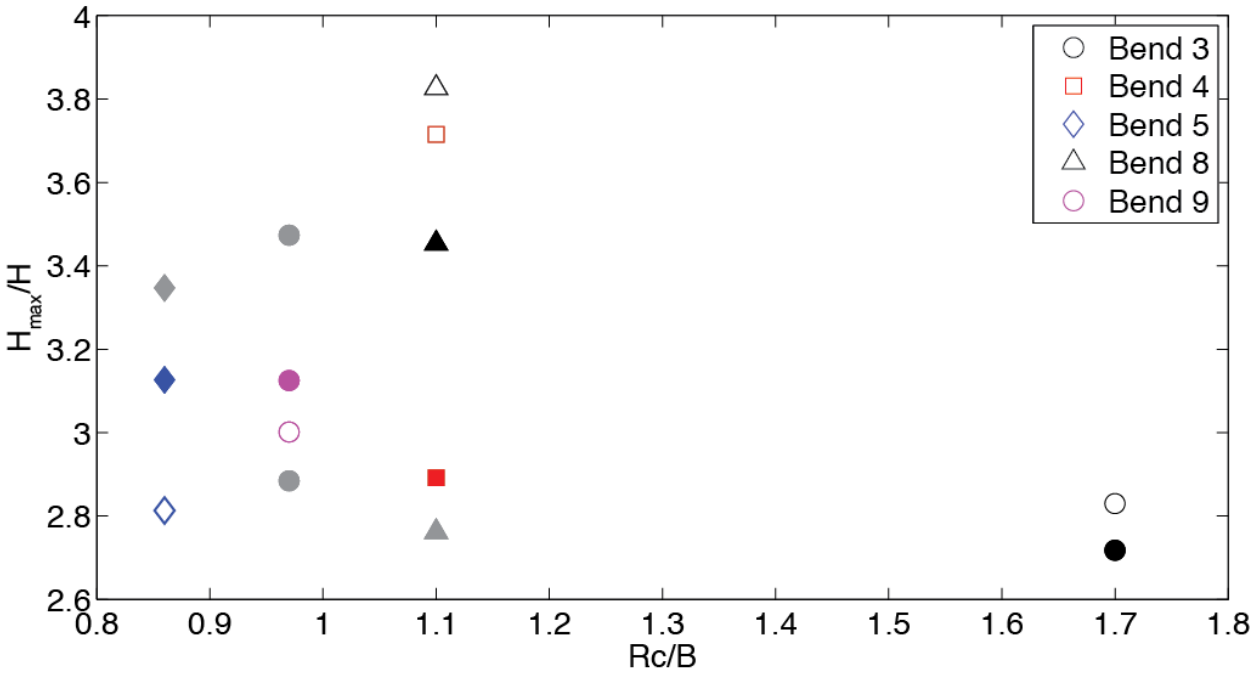


Figure 4.5. The minimum radius of curvature for a bend scaled by the flume width (45 cm) ($R_c$/B) relative to the maximum pool depth in the bend f scaled by the average depth for the flume for a given time step ($H_{max}$/H) . Hollow symbols represent 0 hours, filled color symbols represent 100 hours, and filled grey symbols represent the maximum and minimum $H_{max}$/H for each bend if they differ from 0 and 100 hours. Bends 1, 2, 6, and 7 are not shown for clarity. Bends 1 and 2 are strongly influenced by the flume inlet, and Bends 6 and 7 did not develop point bars.

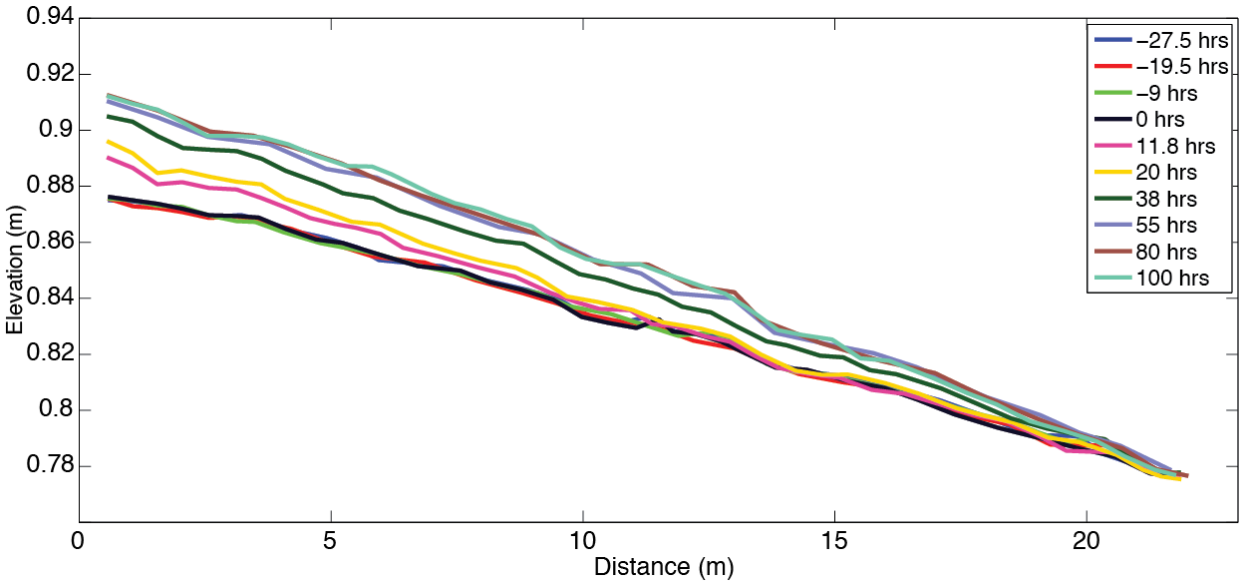


Figure 4.6. Water surface profile measurements through time. The water surface is stable between -27.5 hrs and 0 hrs and increases from 0 hrs to 55 hrs when the transport rate at the bottom of the flume stabilizes.

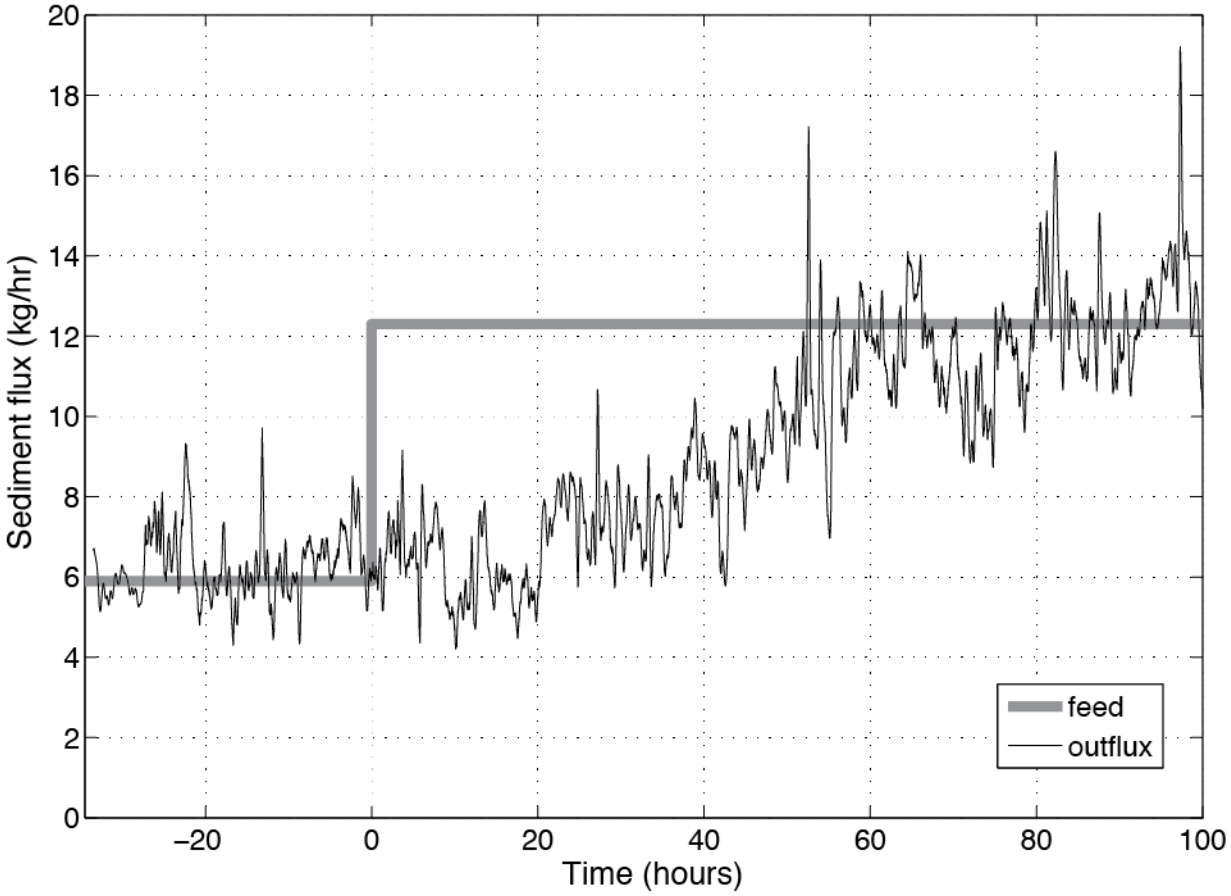


Figure 4.7. Sediment flux measured at the flume outlet. The sediment transport rate is measured at the flume outlet and is filtered twice using a 15-minute running average.

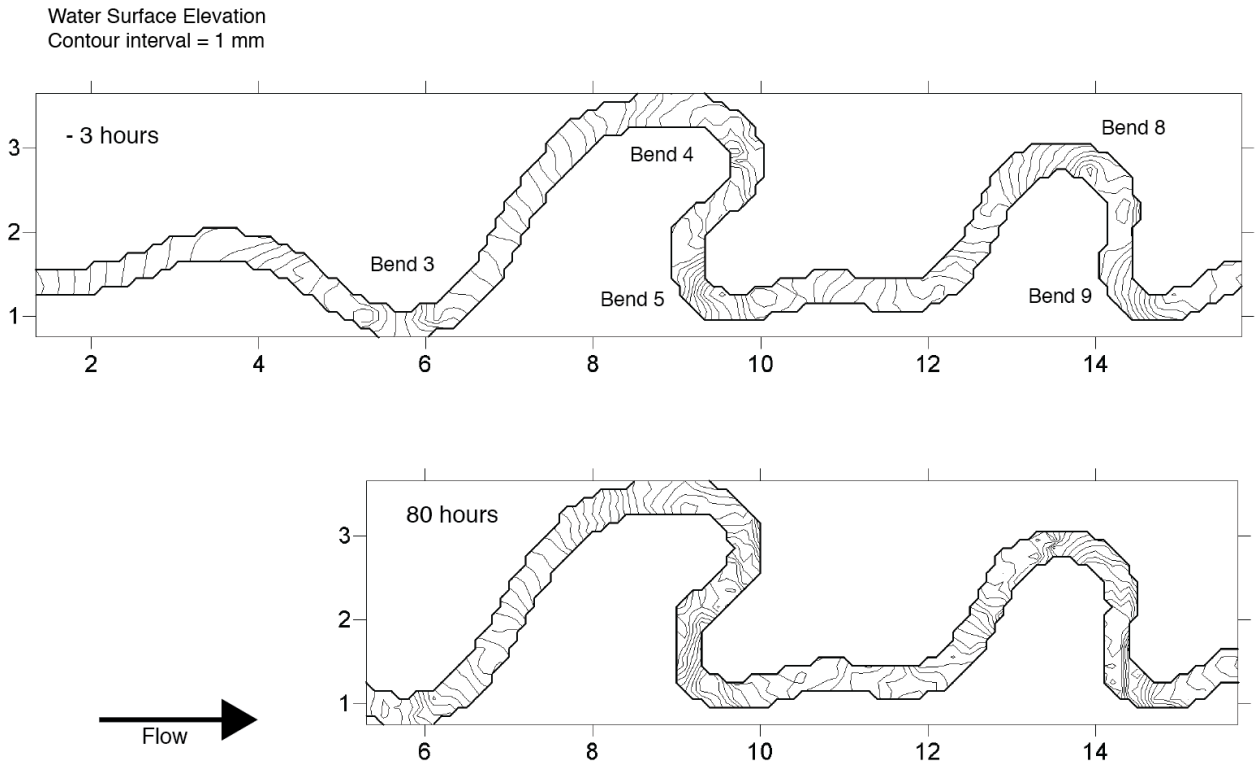


Figure 4.8. Water surface elevation maps for -3 and 80 hours. The contour interval is 1 mm in both maps. The jagged edge of the channel is a function of the coarse grid used relative to the topographic surveys.

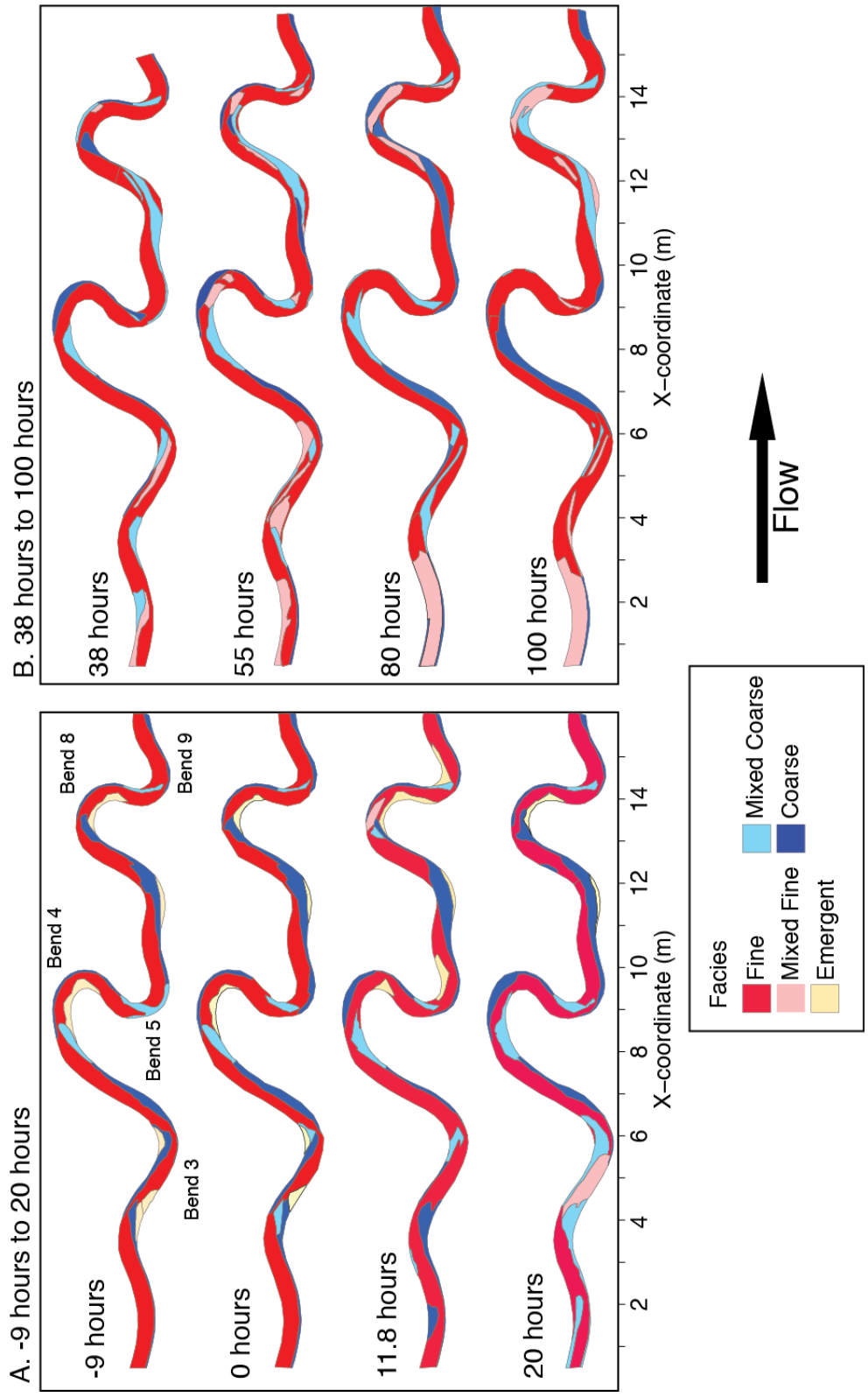


Figure 4.9. Map of sediment facies through time.

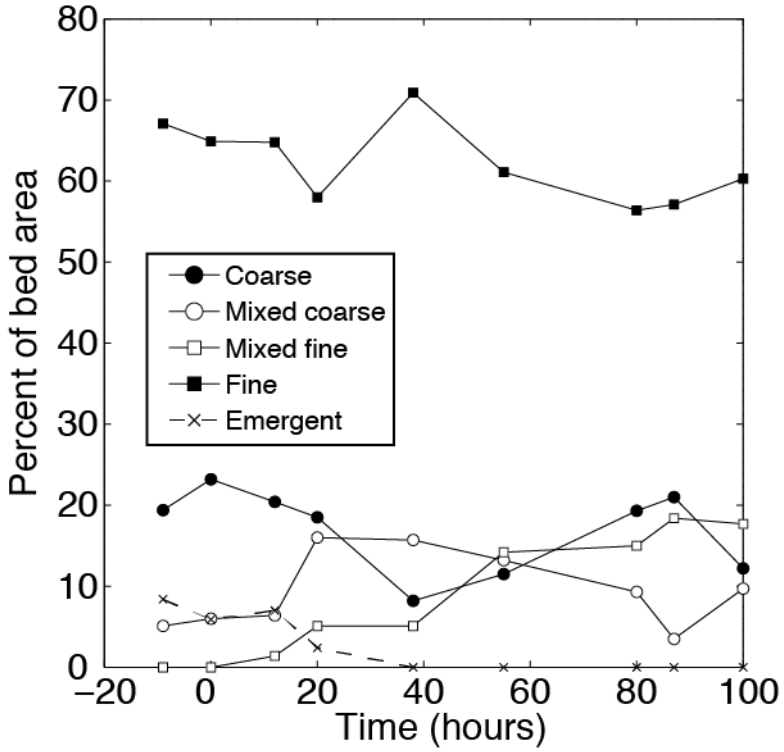


Figure 4.10. Percent of the bed area occupied by each of the sediment facies through time.

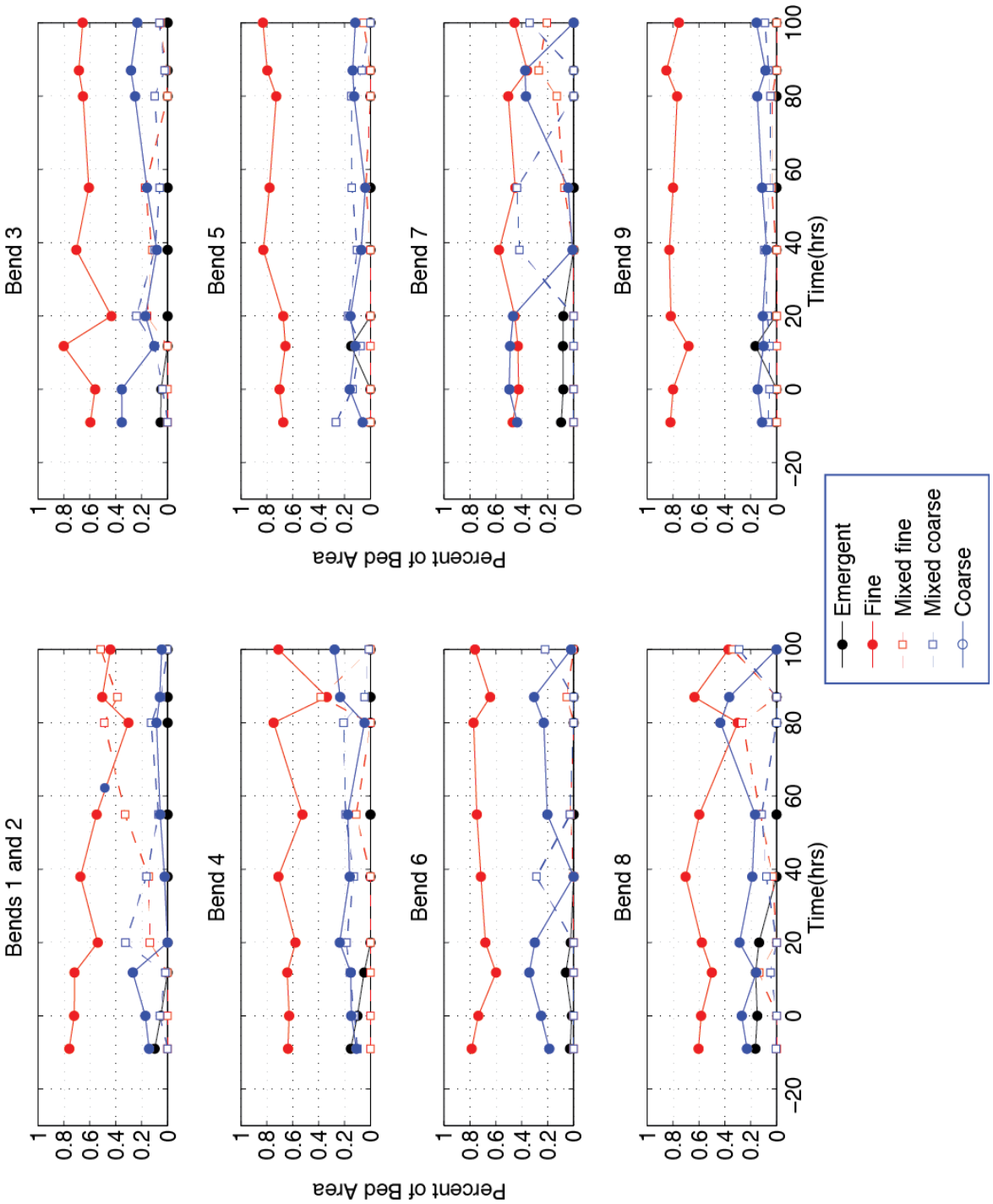


Figure 4.11. Changes in the extent of each facies by bend

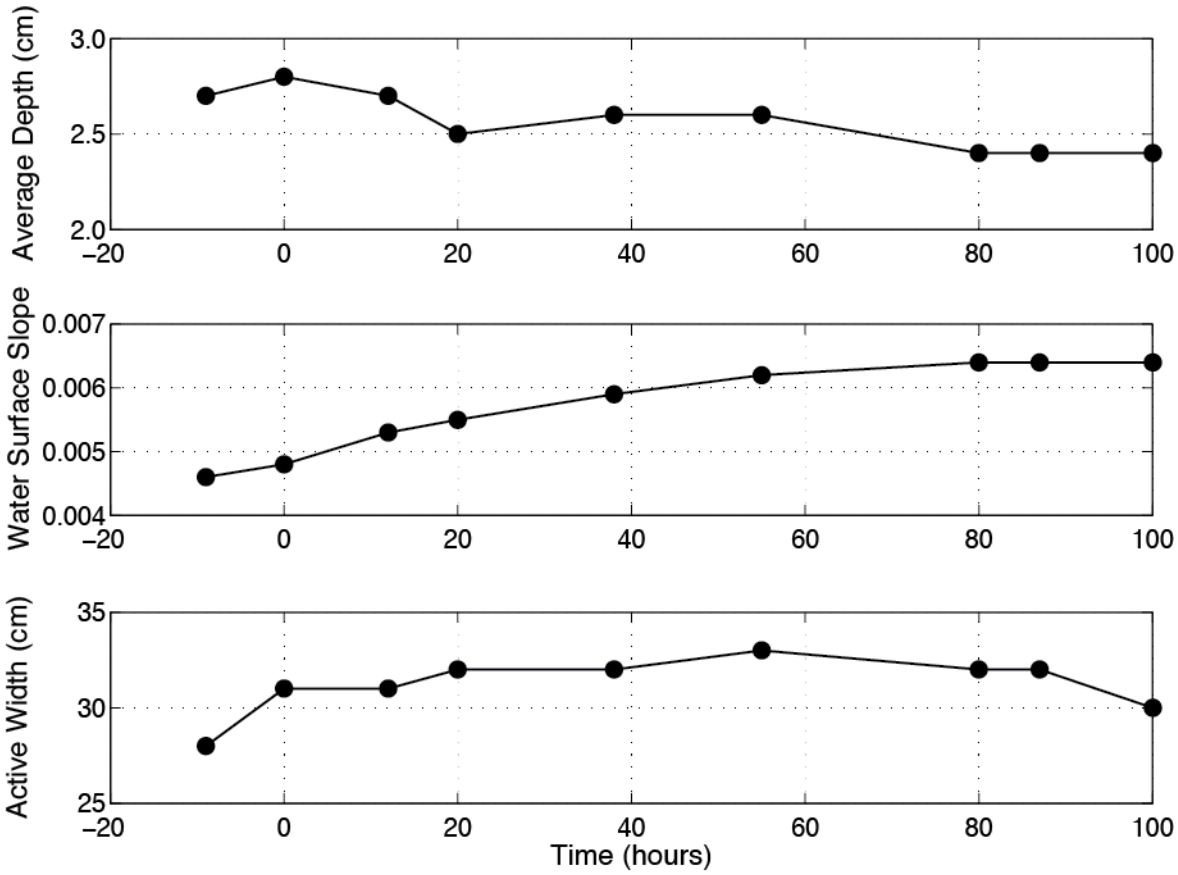


Figure 4.12. Change in hydraulic variables used to calculate the transport capacity for the RFS experiment through time.

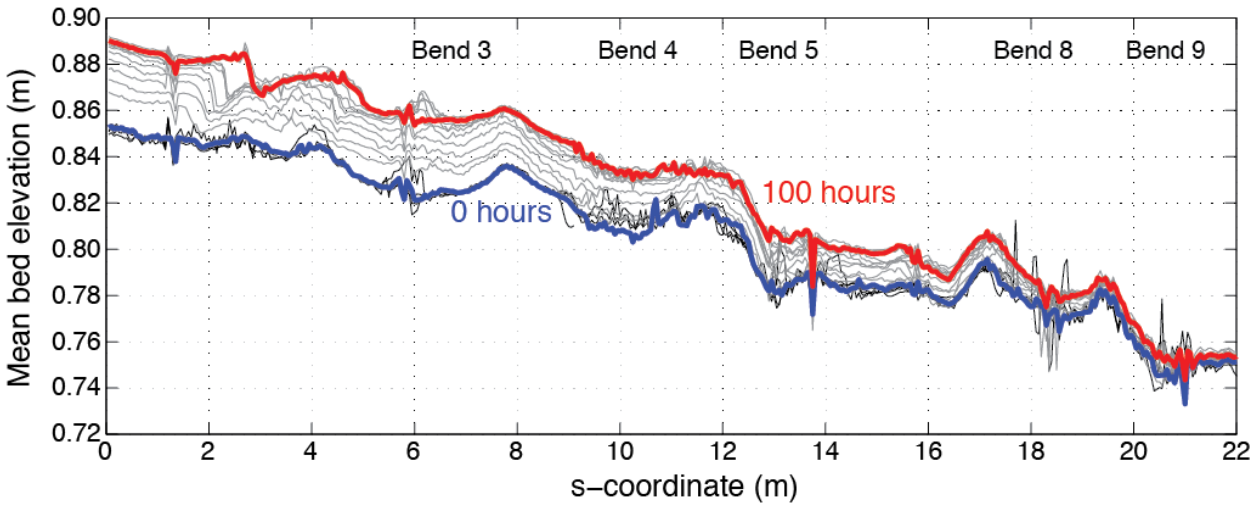


Figure 4.13. Mean bed elevation through time. The mean bed elevation is the mean of elevation data binned every 5 cm along the streamwise coordinate. The dark blue line indicates 0 hours, the dark red line indicates 100 hours, the gray lines are for time steps between 0 and 100 hours, and the black lines are for time steps prior to zero hours.

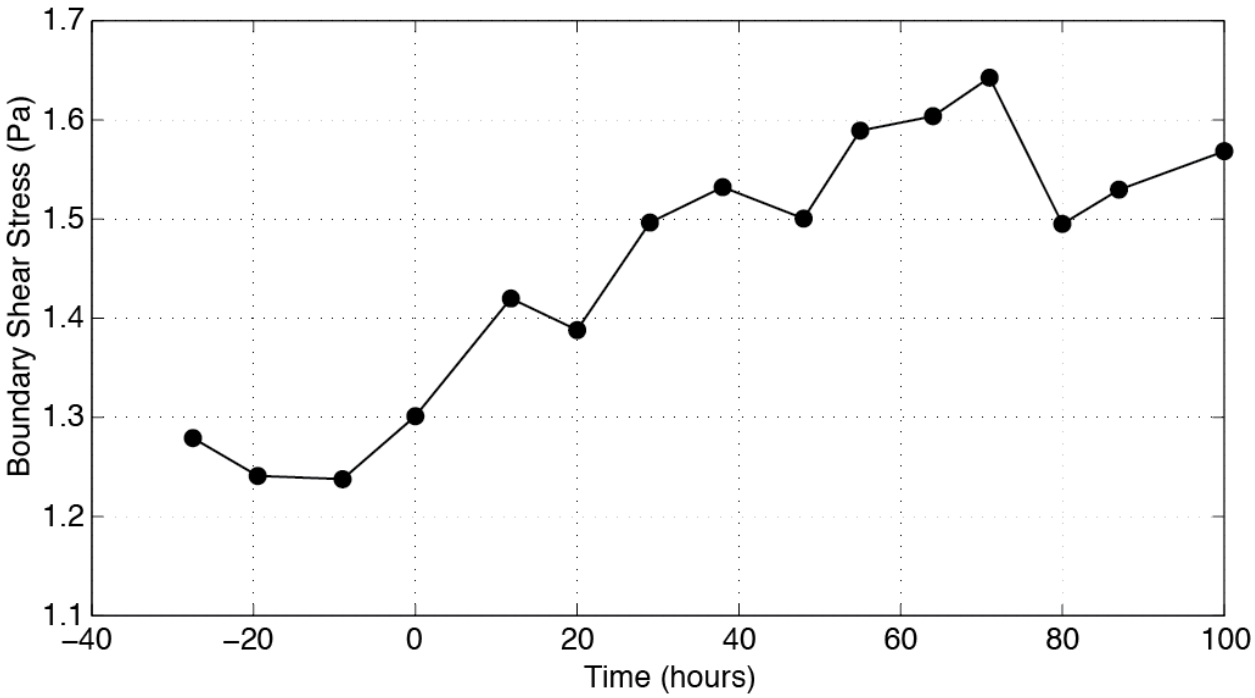


Figure 4.14 Average boundary shear stress for the entire flume length calculated using equation 4.2.

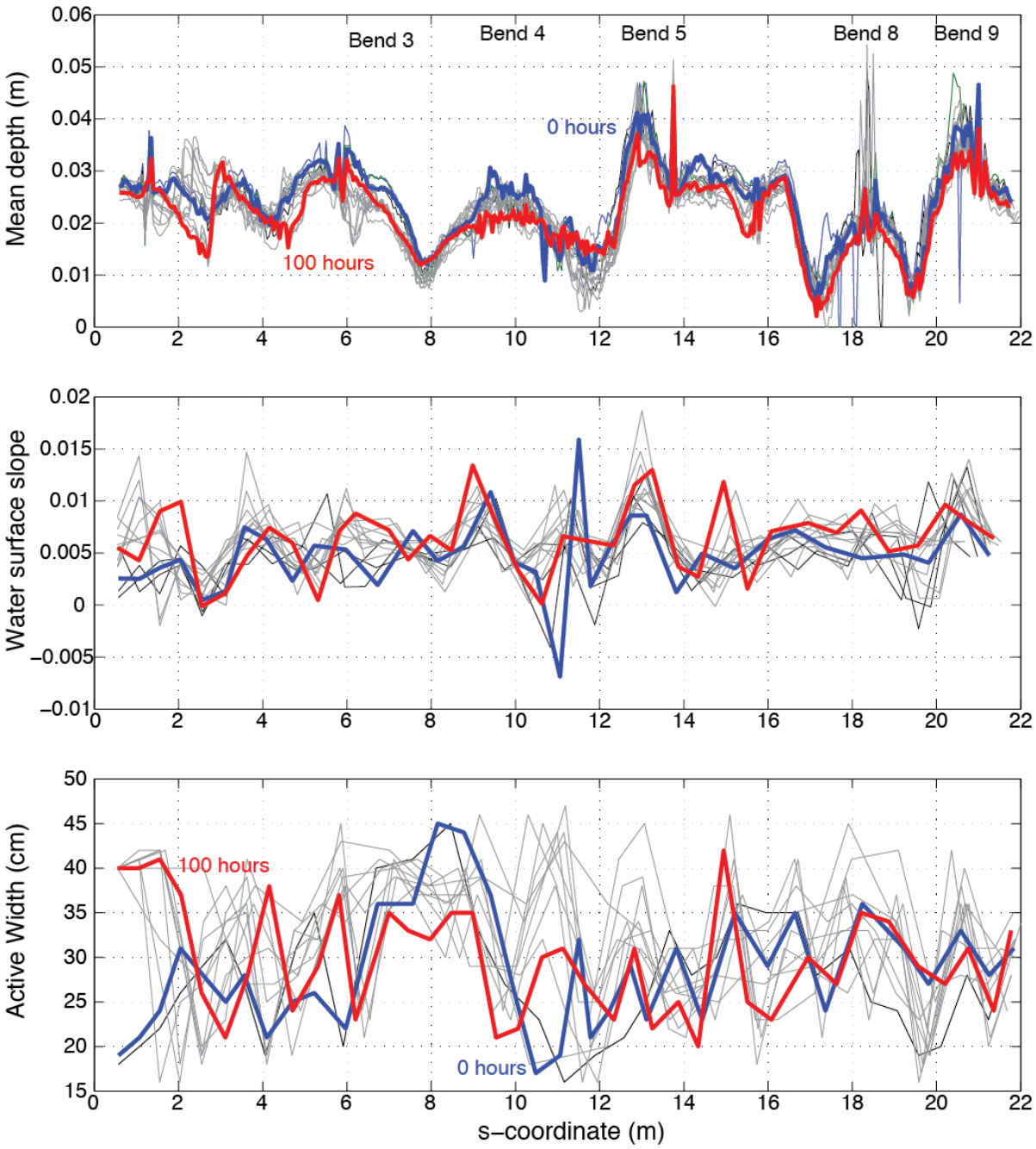


Figure 4.15. Variation in mean depth, water surface slope, and active width in the flume. The dark blue line indicates 0 hours, the dark red line indicates 100 hours, the gray lines are for time steps between 0 and 100 hours, and the black lines are for time steps prior to zero hours. The mean depth is the mean of depth data binned every 5 cm along the streamwise coordinate. Large spatial variations in mean depth occur due to sampling density changes where the orientation of the flume angle changes relative to the orientation of the bed surveys, this does not influence the temporal variations in depth. Water surface slopes are calculated as the downstream elevation change between two survey points, and negative values reflect backwaters associated with bends.

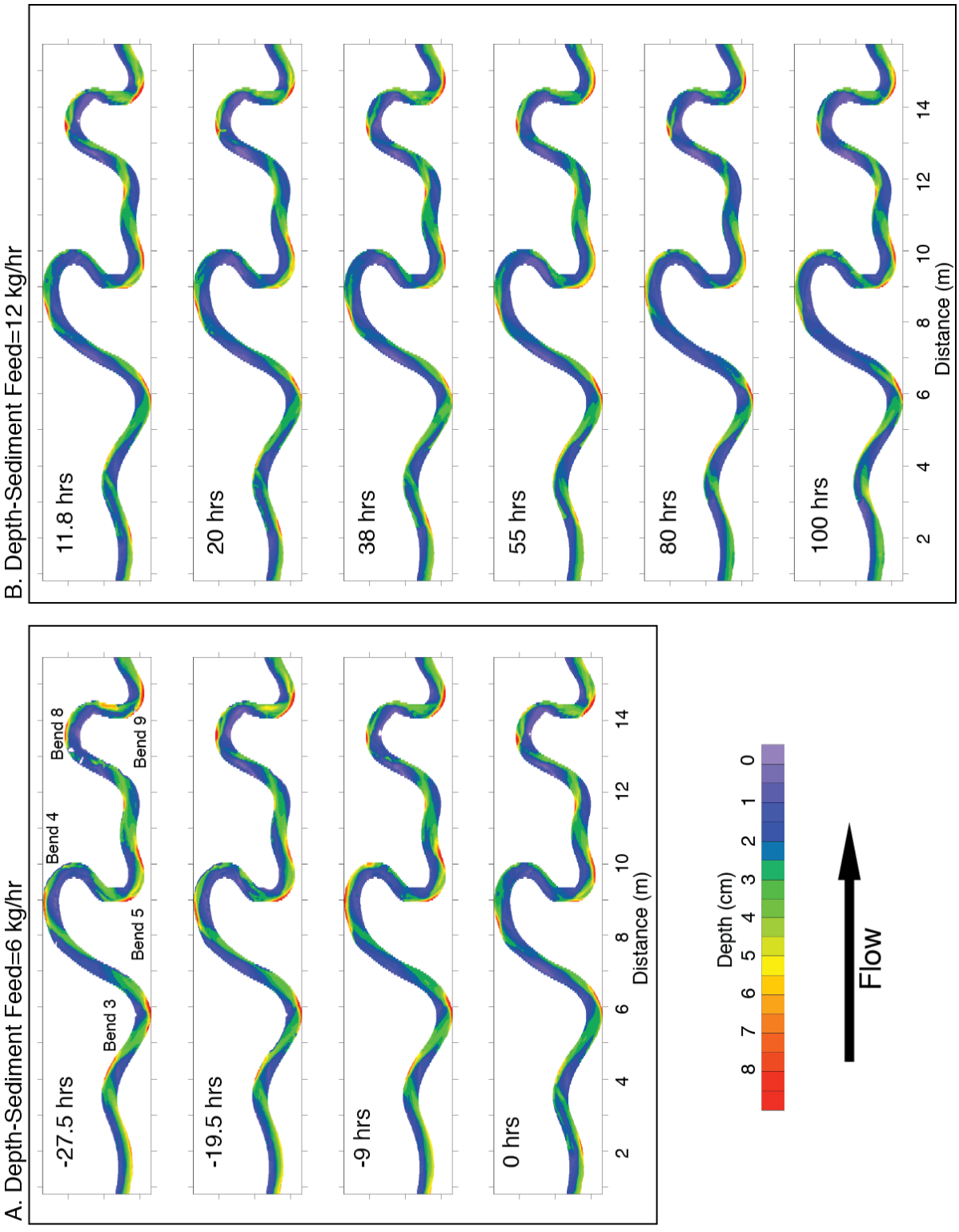


Figure 4.16. Maps of flow depth through time. Larger versions of these maps are available in Appendix C.

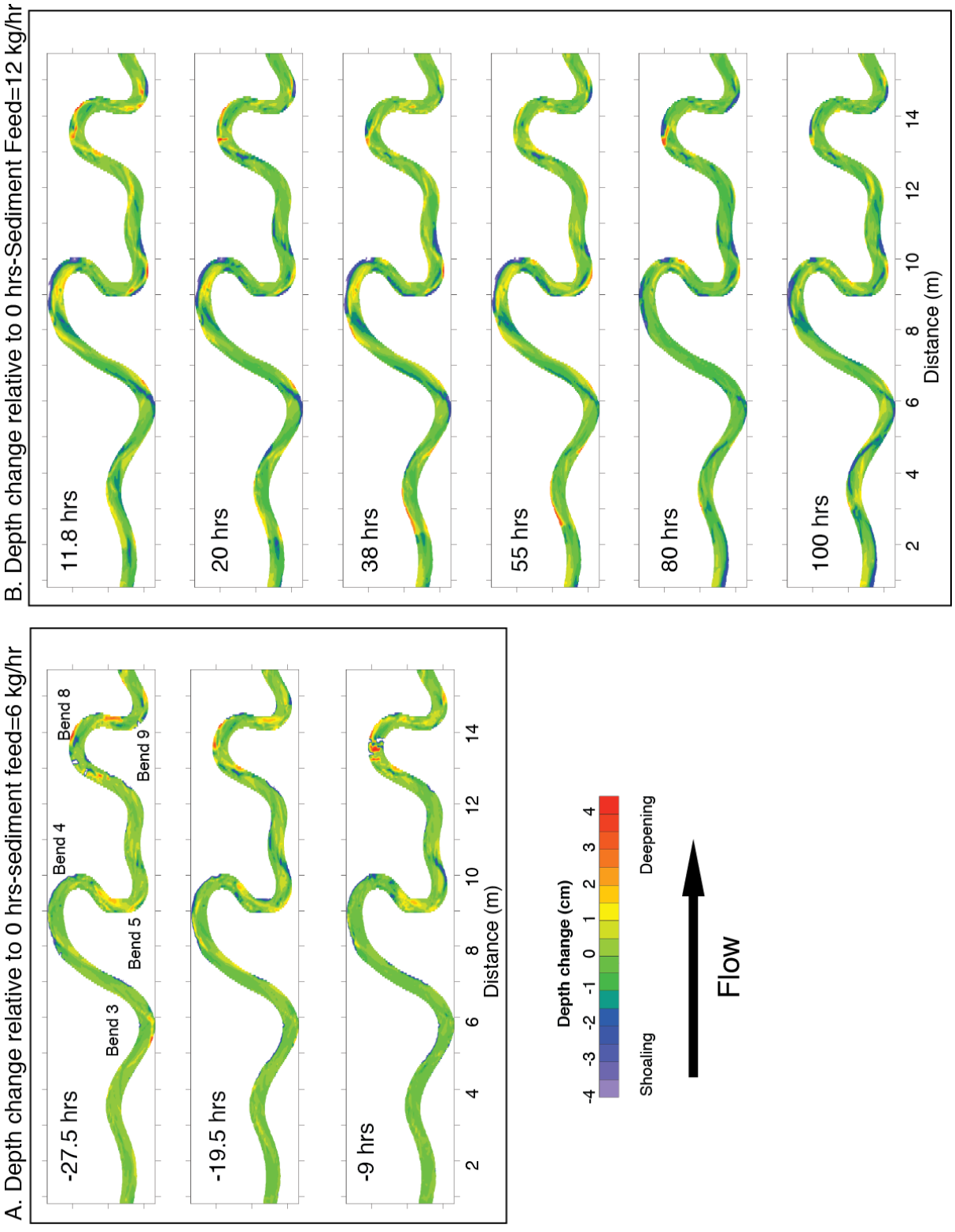


Figure 4.17. Maps of flow depth changes through time.

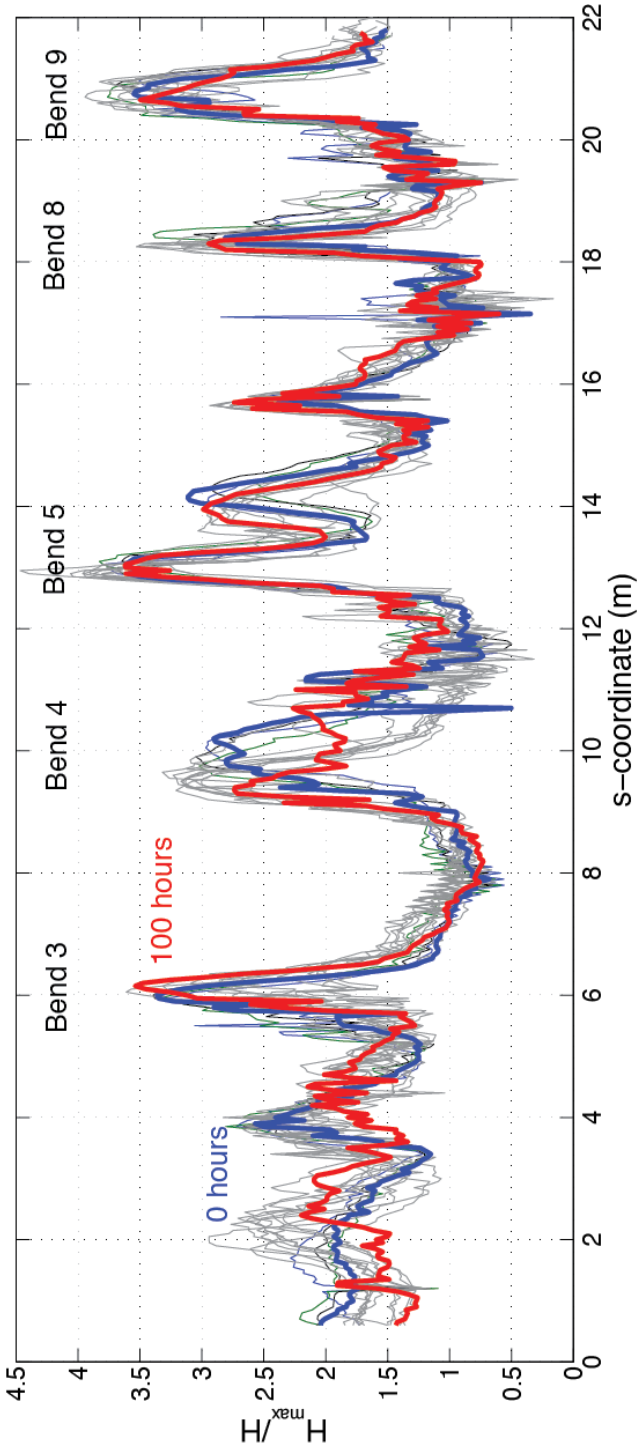


Figure 4.18. Maximum depth ($H_{max}$) divided by the mean depth (H). The mean depth is the mean depth of the entire flume at each survey time. The maximum depth is calculated for 5-cm streamwise bins. The dark blue line indicates 0 hours, the dark red line indicates 100 hours, the gray lines are for time steps between 0 and 100 hours, and the black lines are for time steps prior to zero hours.

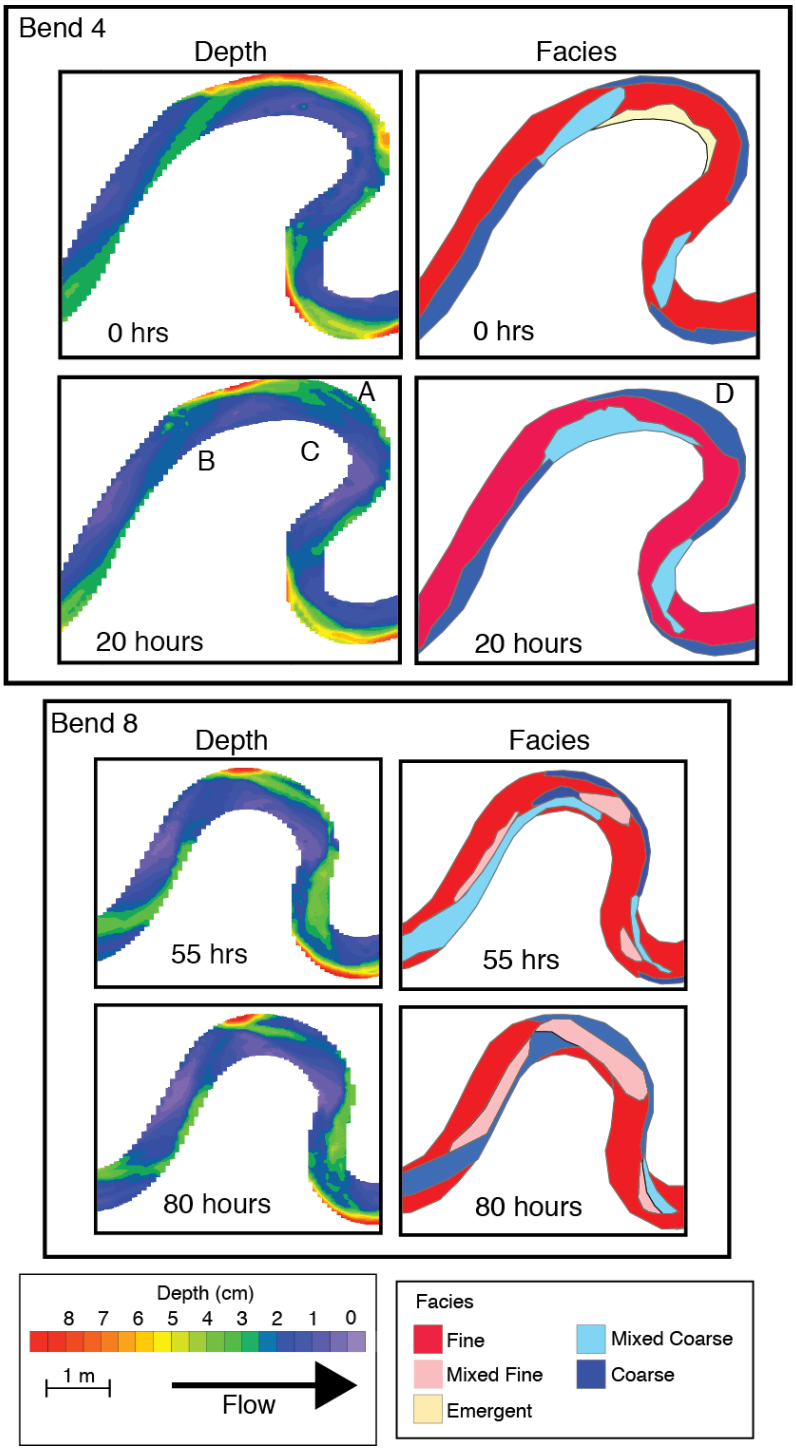


Figure 4.19. Depth and facies maps of Bend 4 at 0 and 20 hours and Bend 8 at 55 and 80 hrs. Location A denotes pool filling at 20 hours, B shows bar shoaling upstream, C represents flow deepening over the point bar, and D shows where the pool filled with coarse sediment.

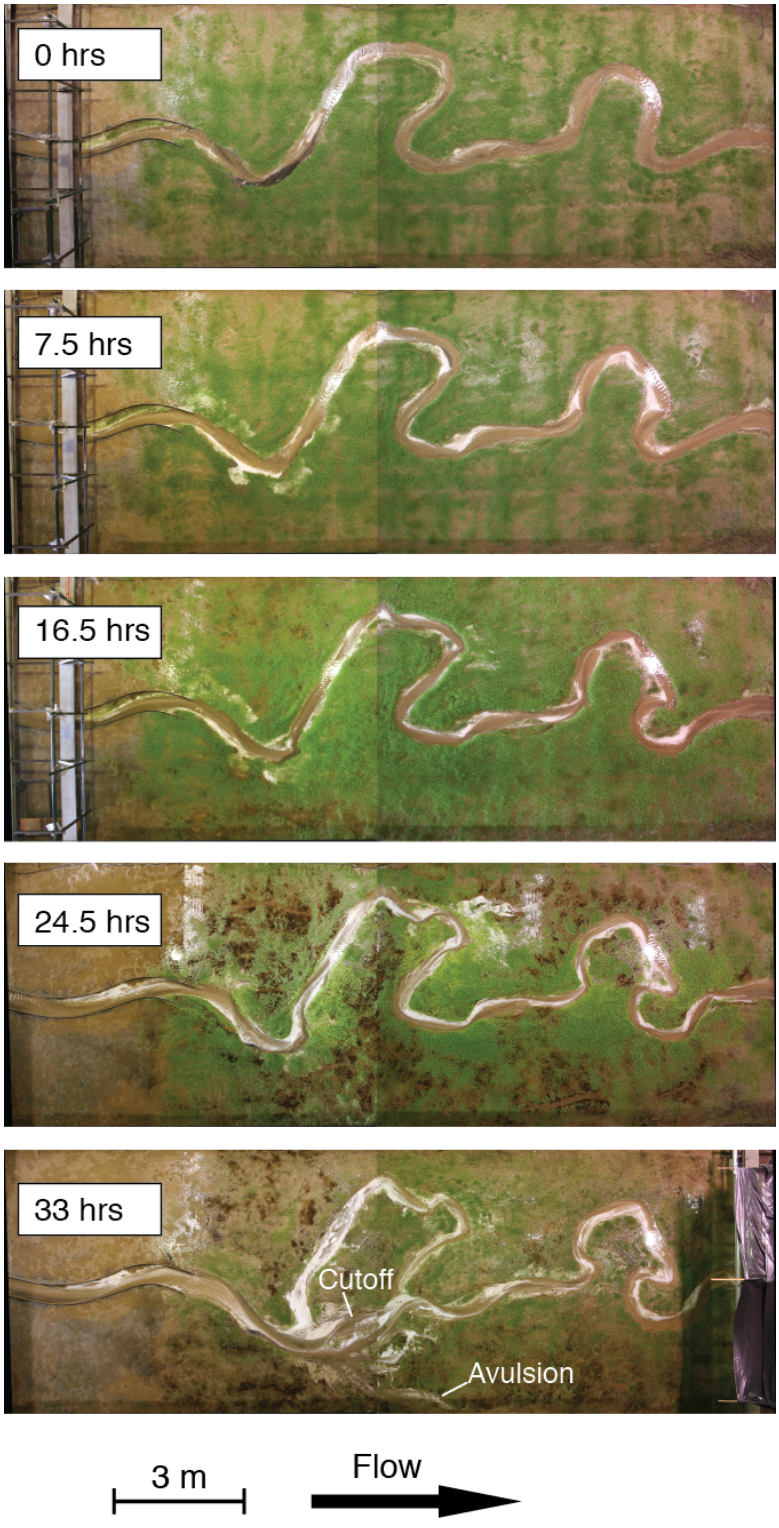


Figure 4.20. Overhead time series of experiments conducted immediately after the RFS experiments using alfalfa to provide bank strength, sand as model gravel and a lightweight sediment as model sand.

# 5 Meandering river dynamics under constant boundary conditions

## 5.1 Introduction

Meandering rivers migrate across their floodplains, eroding material on their outer banks and creating new floodplain deposits on their inner banks through growth of point bars and settling of overbank sediments. As the channel migrates and cuts the change in sinuosity leads to a reduced water surface slope. Although convective accelerations are significant in meandering channels with point bars, the offsetting forces that arise tend to leave the pressure gradient term as approximately equal to the local boundary shear stress [Dietrich and Smith, 1984]. Hence the boundary shear stress can be estimate from the local product of flow depth and water surface slope [Dietrich, 1987]. As meandering rivers slowly migrate, the water surface slope gradually decreases until cutoff resteepens the reach. For the River Bollin in the UK, the sinuosity varied from 1.5 to nearly 3 over 140 years before decreasing to 1.4 within 25 years following a series of cutoffs [Hooke, 2004]. Although there aren't water surface slope measurements for the Bollin, migration should have decreased the water surface slope by a factor of two, significantly decreasing the ability of the river to transport sediment over that period. Field measurements and numerical experiments show that if stress decreases through a decrease in flow depth as the discharge decreases, the decline in sediment transport rates may be mitigated by topographically-induced increases in local boundary shear stress [Dietrich et al., 1984; Francalanci et al., 2012]. Similar changes may also occur as boundary shear stress decreases with increases in sinuosity. In gravel-bed rivers, however, sorting effects may cause a significant offset between maximum boundary shear stress and the maximum bedload transport [Dietrich and Whiting, 1989]. The offsetting effects in gravel-bed rivers marginally above threshold Shield stresses that leads to continued net bedload transport as bends grow are not well established.

Self- maintaining, actively shifting meandering channels in the laboratory have only recently been developed [Braudrick et al., 2009 (Chapter 2); Van Dijk et al., 2012]. In Chapter 2, Braudrick et al. [2009] (hereafter the 2009 experiment) found that laboratory meanders require bank strength, fine sediment (a model sand), and surprisingly did not require overbank flooding. As described in Chapter 2, the 2009 experiment used alfalfa sprouts as model vegetation to supply bank strength and roughen and strengthen the floodplain. Additionally, these experiments used sand as a model gravel and a lightweight plastic as a model sand. The lightweight plastic traveled in suspension in high velocity zones and moved as bedload where velocities were low, but critically, because the plastic was relatively large and coarse, and was non-cohesive, it could be re-entrained once it was deposited. The lightweight plastic behaved like sand in gravel meanders, depositing in the low velocity zones in chute channels that develop between the floodplain and the point bar, and depositing downstream of the bend apex and higher elevation surfaces. The deposited plastic sediment was readily entrained when exposed in subsequent channel bank erosion. The blocking of chute channels was particularly crucial for developing sinuosity and limiting chute cutoffs [Braudrick et al., 2009]. The 2009 experiment required frequent adjustment of the coarse sediment feed to prevent aggradation at the upstream end of the flume, and for the latter half of the experiment the coarse feed was often turned off. The 2009 experiment showed that the fed sediment was not transported downstream through the flume, but rather sediment was exchanged between depositing point bars and eroding outer banks.

Subsequently, van Dijk et al. [2012] created a scaled gravel meander in a 6 m wide by 11 m long basin with slightly lower discharge (1 l/s versus 1.8 l/s) and a finer bed ($D_{50}$=0.51 mm versus 0.78 mm) than used by Braudrick et al. [2009]. Van Dijk et al. [2012] incorporated a small amount of mildly cohesive silica flour in their sediment feed to provide bank cohesion rather than using vegetation. Their coarse sediment feed was slightly higher than the coarse feed rate in Braudrick et al. [2009] (0.75 kg/hr), while the feed rates of the fine silica (0.25 kg/hr) was much lower than Braudrick et al. [2009], even accounting for the density differences. Their fine sediment diameter (0.05 mm) and feed rate were designed to optimize bank strength [Van Dijk et al., 2013]. They introduced a laterally shifting entrance condition to direct a current into a channel with low-amplitude bends formed before the entrance condition shifted.

Their channel migrated across the flume creating very complex floodplain topography with multiple floodplain channels formed on the inside of each bank. These channels form as chutes on the inside of bends after periods of rapid migration or as abandoned channels following cutoffs. The chutes were similar to those observed by Braudrick et al. [2009], but there were more of them on each bend. The more common chute channels likely occurred and persisted due to a combination of the low fine feed rate and because there was no vegetation to promote the deposition of fines in the channels. The complex floodplain topography led to more persistent islands and more frequent cutoffs as their experiments progressed.

Van Dijk et al. [2012] argued that dynamic upstream perturbation was necessary for meander instability to persist. Short laboratory flumes do suffer from stationary fixed inlets which damp or delay bar development and meandering and the use of a laterally shifting entrance condition is a clever strategy to address this. In straight experiments with free alternate bars, bars do not develop immediately at the entrance, but rather some distance downstream where the influence of the boundary conditions of flow and sediment transport diminish [e.g., Ikeda, 1983; Lanzoni, 2000b], which is problematic for the relatively short flumes used in many experiments. Our strategy in Braudrick et al. [2009] and the experiments presented in this chapter was to use a longer flume (17m versus 11 m in the van Dijk case), enabling the internal dynamics to develop and advance with fewer upstream boundary conditions effects and without the immediate upstream forcing done by van Dijk et al. [2012]. Upstream perturbations due to the bed and banks therefore have enough space to generate a meandering form, and persist after cutoff. This approach allows exploration of bank erosion, point bar development, channel bed morphodynamics without imposing a migration rate at the upstream end of the flume.

The goal of this final experiment was to confirm that we had identified the necessary conditions for successful formation of a self-formed laterally migrating channel with cutoffs by repeating the 2009 experiment. I made three major modifications relative to the 2009 experiment. First, I increased the bank strength through increased alfalfa density to decrease the migration rate and promote a higher sinuosity. Secondly, the sediment supply and discharge were constant, rather than variable as in the 2009 experiments. There were some unintentional differences as well. Due to settling of sand in the basin, the slope at the lower end of the flume was steeper than in the 2009 experiment.

In this chapter I show that: 1) the experiment is repeatable: a self- maintain cutoff system develops, although you can see downslope extending upper boundary condition of fixed bends

that over time reduced the extend of active meandering , 2) although the alfalfa density was higher, patches of reduced growth due to elevated water levels during irrigation flows and channel aggradation led to pathways for flood flow to concentrate and promote chute cutoff, 3) the bend growth led to increased sinuosity and reduced slope which lead to aggradation in the upslope reaches of the bends which induced the floodplain flows that led to bend cutoff, and 4) local very sharp curved banks formed as the rest of the bends ceased laterally migrating as the shear stress dropped, presumably below a critical shear stress for bank erosion. Collectively the two experiments (2009 and 2012) suggest that sinuosity induced slope reduction can lead to aggradation and contribute to channel avulsion or chute cutoff limiting channel sinuosity. The importance of reach scale aggradation associated with bend growth in natural channels is poorly known. These experiments point to the need for field and numerical modeling studies to explore these processes further.

## 5.2 Methods

This experiment was conducted in a 6.3 m wide and 17 m long basin at UC Berkeley's Richmond Field Station (Figure 1), the same basin used in the 2009 experiment. The basin has a slope of 0.0055, and with a fixed downstream outlet elevation. Similar to Braudrick et al. [2009], I did not attempt to directly scale a specific channel from the field, but rather to replicate conditions that scaled to gravel bed meanders in general. The laboratory model represents a 0.01-0.04 scale model of a gravel bed meander from the field. The scaling between the flume and field is discussed in section 5.4.2. This experiment followed a previous (unreported) experiment using a higher discharge (2.6 l/s-the same discharge used in the fixed-wall experiments in Chapter 4) that resulted in avulsion after 38 hours. In all cases the dense alfalfa limited bank erosion, but the channel could not transmit its load. Three other experiments with a higher discharge of 2.2 l/s avulsed (e.g., Figure 4.20). The large-scale bends from the avulsed channel were filled in and the original channel was deepened by hand. This resulted in 29-cm wide initial channel with a sinuosity of 1.1 due to 6 small amplitude bends within the basin (Figure 5.1). The uppermost 4 m of the flume are fixed in place using roughened slats of sheet metal to provide an initial bend in the channel and limit the effects of aggradation at the inlet (Figure 5.1). Due to settling differences in the bed that occurred prior to the experiment, the downstream portion of the flume was steeper than the 2009 experiment (Figure 5.2), with a mean basin slope of 0.0054 between the end of the fixed wall inlet (at 5.5 m) and 10.5 m. The lower from10.5-15.9 m, the basin had a slope of 0.0075 (Figure 5.2).

As with the 2009 experiment, we used alfalfa to provide bank and floodplain strength. Alfalfa was seeded in the flume by hand while a low flow ran through the channel. The low flow irrigated the alfalfa and prevented alfalfa establishment in the channel. This irrigation flow was not sufficient to transport sediment. Every 8-20 hrs, alfalfa was replanted on exposed bar surfaces and to fill in gaps where alfalfa had rotted. The alfalfa was allowed to grow for 1 week before the next experiment. During the growth period the water surface at the outlet of the flume was held constant to maintain a high water table in the floodplain and keep the seeds moist. Six 1000-watt grow lights were suspended over the flume and turned on for approximately 16 hours/day after the seeds germinated. Occasionally the entire crop of alfalfa was reseeded, as some alfalfa started to grow too large, which caused a change in both the above ground morphology and also dramatically changed the root structure from a single tap root to a more

extensive root network that was very difficult to erode. Three times as many alfalfa seeds (measured by weight) were used in the 2012 experiments than Braudrick et al. [2009]. Similar to Braudrick et al. [2009] eroded alfalfa that deposited on the channel bed during the experiment was removed by hand.

Water and sediment input rates were held constant during the experiments. Discharge was measured using a V-notch weir at the upstream end of the flume and kept constant at 1.8 l/s, the same discharge used as bankfull discharge in Chapter 2. Similar to Chapter 2, the sediment feed consisted of sand (model gravel) and a lightweight plastic sediment (model sand). The sorted sand had a median size ($D_{50}$) of 0.75 mm (Figure 5.3). The sand was identical to the sediment that initially filled the basin before the onset of the experiments. Rather than remove deposited sediment from previous experiments, this sediment was left in the basin. This provided a limited in-stream source of plastic sediment and provided some variability in the materials making up the banks at the outset of the experiments. The fine sediment was a 2:1 mix by volume of Clear Cut (specific gravity = 1.3) and Type II Urea (specific gravity = 1.5). The specific gravity of the combined plastic sediment was 1.36. Both types of plastic were somewhat disk-shaped, with a b-axis diameter that ranged between 0.25-0.42 mm , had angular edges, and were not cohesive. The coarse and fine sediment were fed independently by Accufeed Vibrascrew feeders at the upstream end of the flume at rates of 1.4 and 5 kg/hr, respectively. The feed rate of the coarse sediment was set as low as possible while still maintaining a steady feed. The fine feed rate was identical to the fine feed rate in the later half of Braudrick et al. [2009]. The fine sediment behaved like sand in gravel bedded streams, moving both as bedload and suspended load. The lightweight plastic was crucial for allowing this behavior by combining a low settling velocity (allowing for sediment to move in suspension), while reducing the critical stress relative to natural sediment with an equivalent settling velocity (e.g. silt).

Water and sediment were removed from the downstream end of the flume using an eductor that delivered them into a submerged large nylon mesh basket attached to a load cell. Water was then recirculated while sediment remained in the load cell. All of the sediment from 8-12 hour run was removed from the load cell basket and dried. We calculated the density of the sediment transported out of the flume by weighing the dried sediment and dividing by the volume. The volume of sediment collected at the flume outlet was calculated by measuring the change in water elevation in a tank of known dimensions as the sediment was submerged. The fraction of fine and coarse sediment was calculated by solving:

$$\rho_s = \rho_c F_c + \rho_p F_p \tag{5.1}$$

$$F_c + F_p = 1 \tag{5.2}$$

where $\rho_s$ is the measured density of the sediment collected in the load cell, $\rho_c$ is the density of the coarse material (2650 kg/m$^3$), $F_c$ is the fraction of the coarse sediment, and $\rho_p$ is the density of the plastic (fine) sediment (1360 kg/m$^3$) and $F_p$ is the fraction of plastic sediment. This calculation assumes that both components of the fine sediment are transported out of the flume at the same rate, and there is not differential deposition of the denser plastic. The two plastics are slightly different colors, and we did not observe obvious differences between the feed and the plastic transported out of the flume.

Bed topography was measured using three oblique cameras and vertical laser sheet attached to a movable cart that spanned the basin. The bed topography was measured when the flume bed was drained. The images were processed in Matlab. Pixel size was approximately 1 mm in the x and y directions, with cross sections measured every 5 cm down the length of the flume. There were 18 topographic surveys during the 120-hour experiment. Water surface centerlines were measured using a point gauge attached to the movable cart. Typically, points were spaced 0.5-0.75 m apart and were centered by eye in the channel. Overhead images of the experimental channel were taken every 10 minutes by two cameras mounted above the flume. These images were corrected for distortion and stitched together using Matlab.

Channel topography and water surface elevation were used to calculate channel depth. The centerline was defined in ARC-GIS using the NCED planform statistics toolbox developed by Wes Lauer. To calculate depth we converted the water surface elevations and depth measurements into streamwise-normal-elevation (snz) coordinates following the methods described in Legleiter and Kyriakidis, [2006]. Water surface elevations were interpolated every 5 cm. Centerline water surface elevations were interpolated every 5 cm down the length of the flume. We then subtracted the bed elevation from the interpolated water surface elevation at the centerline in 5 cm s-coordinate bins, assuming the centerline water surface elevation represented the water surface elevation across the entire cross section. The difference in cross-channel water surface elevation at bends was generally less than 1-1.5 mm. Because the banks of the upper portion of the channel are fixed in place, all reported statistics are only for the 9.9 m-long reach from X=6 m-the downstream of the flume inlet to the downstream end of the surveyed reach at X=15.9 m (approximately 1.1 m upstream of the flume outlet). X=6 m is the approximate boundary between the bend created by fixed walls and the first free bend downstream.

The channel banks were defined by hand in ARC-GIS using the topographic maps. Because the width varied, we calculated the erosion and deposition rates (in cm/hr) for each bend independently. For the 18 surveys, we calculated the offset of each bank every 5 cm normal to the previous bank location, and used the average offset as the erosion or deposition rate. When a bend cut off between surveys, we did not calculate its erosion or deposition during that time step.

### 5.2.1 Differences with the previous experiment

The experimental methodology differed from the 2009 experiment in several important ways (Table 5.1). As discussed above, the alfalfa was 3 times denser in the current experiments (2012) than the 2009 experiment, and the inlet walls were extended slightly downstream. The 2012 discharge was constant, was as the hydrograph during the first 71 hours of the 2009 experiment consisted of a bankfull discharge of 1.8 l/s and periodic overbank flows that were typically 2.7 l/s but up to 4.4 l/s. The sediment feed characteristics also differed. The coarse and fine feed rates in the 2012 experiment were held constant at 1.4 kg/hr and 5 kg/hr, respectively. The 2009 experiment varied the coarse sediment feed, turning it off for long periods to prevent aggradation at the upstream end of the flume. The overall coarse feed rate in the 2009 experiment was 0.75 kg/hr. The fine feed rate also varied in the 2009 experiment, but to a lesser degree with an average fine feed rate of 3.4 kg/hr. The composition of the fine feed differed as well. The plastic feed in the 2009 experiment was Urea (specific gravity=1.5) for the first 65 hours and Clear Cut (specific gravity = 1.3) for the final 65 hours of the experiment, whereas the 2012 experiment had a constant mix of the two (bulk specific gravity =1.36). The 2012

experimental channel was much narrower initially (29 cm versus 40 cm) and deeper (2.7 cm initial depth versus 1.9 cm). The narrower initial channel records the effects of increased bank strength on the experiments that immediately preceded those shown here.

## 5.3 Results

The evolution of channel morphology through time is shown in Figures 5.4-5.6. Higher frequency overhead (every hour) and topographic maps (every 6-8 hours) are provided in Supplemental Videos 2 and 3 and Appendix D. For clarity we numbered the bends from upstream to downstream with Bend 1 being the first bend downstream of the fixed walls. The bend numbers are shown on Figure 5.7.

### 5.3.1 Description of bar growth and bank erosion

Banks failed not as a mass, but through the erosion of individual sand grains at the base of the bank. The alfalfa roots provided some cohesion to the banks, but also helped to roughen the near bank area, limiting bank erosion. Alfalfa also limited floodplain erosion during overbank flows. Similar to the 2009 experiment, chute channels developed between point bars and floodplains (Figure 5.7). In some areas, a thin soil-like layer developed where old alfalfa had died, provided additional bank strength. This layer failed once it was undercut, similar to failures of composite banks described by Thorne and Lewin (1979), but once the layer failed, the chunks were rapidly broken up and transported out of the flume.

Point bars were built by deposition of coarse sediment at their upstream end and fine sediment downstream of the apex. Fine sediment also deposited on the top of point bars and on floodplains when the channel capacity changed and the floodplain was submerged. Fine sediment also rapidly plugged cutoff channels. Downstream of the first bend, the coarse sediment that built point bars was primarily derived from bank erosion of the adjacent upstream bend or from upstream cutoffs rather than the sediment feed. The coarse fraction of the point bar was not sorted into the distinct patches in the fixed wall experiments detailed in Chapter 4.

Each point bar was partially separated from the floodplain by a chute channel. The chutes in Bends 3 and 4 are oxbow lakes formed following channel cutoffs (see Supplemental Video 2). The chute in Bends 1 and 2 formed during rapid downstream migration of the bend (e.g., Figures 5.7 and 5.8), similar to the chute formation processes observed in the 2009 experiment. The chutes were plugged at their upstream end and open at their downstream end (Figures 5.4, 5.5, 5.7 and Appendix D), but were a smaller portion of the bend length than the chutes observed in the 2009 experiment.

Downstream migration of bends caused rapid and extensive fine sediment deposition downstream of the bend apex along the inner bank. This happened because the downstream migration of the bend apex redirected flow away from the downstream end of the point bar, and fine sediment was deposited in relatively still water. Downstream migration occurred when bends were lengthening either in the early stages of the experiment (as in Figure 5.8) or following cutoffs (see Supplemental Video 2).

### 5.3.2 Morphologic evolution

Figures 5.4-5.6 show that channel morphology evolved in three phases during the 120-hour experiment. Their morphological evolution is described below.

*Phase 1-Bend Growth (0-35 hours)*

During the Bend Growth phase, the channel went from a relatively straight morphology to developing a series of bends both through lateral and downstream expansion of the bends. Nearly the entire channel length was migrating. This occurred over about the first 40 hours of the experiment as the sinuosity increased from 1.08 to about 1.2 and included two cutoffs (Figures 5.4-5.6). Five bends developed during the first 40 hours and there were 2 cutoffs--Bend 5 at 12.5 hours and Bend 4 at 31 hours. The cutoff at 12.5 hours occurred within 30 minutes of increasing the flow from the irrigation flow to a flood flow after the alfalfa was reseeded and allowed to grow for a week. The alfalfa grew on the bar surface but not in the chute providing a weakly vegetated path for the cutoff. The cutoff at 31 hours occurred on a sinuous bend, and was the only cutoff during the experiment where aggradation did not lead to a zone of weak alfalfa growth as discussed above (Supplemental Video 2). The cutoff at 31 hours occurred through a very small chute (<10 cm wide) that was elevated relative to the channel bed, but where alfalfa density was lower than the surrounding bar and floodplain.

The fifth bend rapidly moved downstream of the topographic surveys at the start of the experiment and is not included in our analysis. Bend 1 had a longer wavelength than Bends 2-4 (Figures 5.4-5.6), likely due to its proximity to the flume inlet. Aggradation occurred upstream of the apex of Bends 2 and 3 at the end of the Bend Growth period (visible in Appendix D). The Bend Growth phase ended at about 35 hours in Bends 2 and 3 and at about 50 hours in Bend 4.

*Phase 2 Bend skewing and aggradation (35-77 hours)*

At 35 hours in Bends 2 and 3 and 50 hours in Bend 4, the pattern of migration changed as erosion focused on the areas just downstream of their apexes, creating bends skewed downstream (Figures 5.4-5.6, Appendix D, Supplemental Videos 2 and 3). Downstream skewness increased with time and caused the sinuosity to increase from about 1.2 to 1.6 (Figure 5.9). As the bends became skewed between 35 and 77 hours, Bends 3-5 developed a second point bar between the upstream crossover with the previous bend at the point bar at the bend apex (e.g., PB2 on Figure 5.10). The two point bars were separated by a relatively straight reach that did not migrate (Figure 5.10C). There was a small amount of upstream migration associated with the upstream point bar in Bend 2 (compare panels C and D on Figure 5.10). As the channel migration slowed, the channel began to aggrade upstream of the apex of bends (Figures 5.5 and 5.10).

*Phase 3 Cutoffs and channel steepening (77-120 hours)*

During the final phase of the experiment, the channel responded to aggradation during the bend skewing phase by cutting off the three downstream bends--Bend 3 at 77 hours, Bend 2 at 87 hours, and Bend 4 at 102 hours (Figure 5.5, Table 5.2). For all three cutoffs, by raising the stream bed relative to the floodplain, aggradation upstream of the bend apex increased overbank flows on the floodplain. Aggradation was sufficient to cause ponding of water in low spots on the floodplain during the irrigation flow. Water was mostly supplied to the ponded areas via groundwater flow as the stream bed elevation approached the elevation of the floodplain upstream of the bend apex (Figure 5.5). This ponding limited alfalfa growth, creating a weak

area for the overbank flow to erode once the high flow was turned back on. For the cutoff of Bends 2 and 4, the irrigation flow established flow paths through the floodplain where alfalfa growth was limited. These flow paths were exploited and enlarged once the flood flow was turned on. The cutoff at 77 hours had little effect on downstream morphology because the newly cut channel was relatively narrow and not transmitting much water or sediment.

The cutoff of Bend 2 at 87 hours steepened the channel both by shortening the channel path, but also by cutting off the aggraded sections of Bend 2, which were increasing the upstream backwater (see Supplemental Video 2). After the cutoff, the water surface elevation dropped in the reach upstream of Bend 2, and the channel incised by up to 5 mm. Downstream of the cutoff, migration was reinvigorated as water and sediment connectivity were reestablished (see Supplemental Video 2 and Appendix D). Following the final cutoff at 101 hours, a series of island bars developed in the downstream portion of the flume (Figures 5.4 and 5.5, Appendix D) as the local sediment transport rates increased by nearly a factor of four (discussed in the next section). Periodic increases in the portion of flow carried through the secondary channel of the island bar would sweep out deposited fine sediment, preventing the blocking or filling of the secondary channel required to transform it into a point bar. The three cutoffs during the last third of the experiment shortened the local streamwise channel distance (and increased the local slope) from 50 to 70% (Table 5.2).

### 5.3.3 Sediment Flux

The sediment transport rate exceeded the feed rate from about 12 hours until 48 hours after the beginning of the experiment (Figure 5.11). Because we use a mix of lightweight plastic sediment and sand, the submerged mass of sediment measured at the flume outlet is a function of the volume of sediment transported through the flume as well as the relative proportion of sand and plastic sediment. The highest transport rates were measured between 16 and 18 hours at an average rate of about 6.5 kg/hr and gradually declined to 2 kg/hr until 30 hours, before increasing again after a cutoff of Bend 4 to about 4.5 kg/hr and gradually declining to 1.1 kg/hr at 60 hours. The transport rate stayed below 1.3 kg/hr for the next 40 hours when Bend 4 was cut off and the transport rate increased in two pulses of up to 5 kg/hr (Figure 5.11). By 100 hours the cumulative mass of sediment transported out of the flume was equal to the cumulative mass of fed sediment, and by the end of the experiment, the cumulative flux out was within 2% of the cumulative feed.

The density of the sediment collected at the outlet was relatively steady at about 1960 $kg/m^3$ for the first 45 hours (Figure 5.12). This is approximately 20% higher than the density of the feed, indicating that fine sediment was deposited in the flume and that the discharged sediment was differentially the coarse fraction derived from bank erosion upstream of the outlet. The plastic fraction prior to 45 hours was about 0.54 (Figure 5.12). As the sediment flux declined after 45 hours, the density of sediment measured at the outlet decreased and the plastic fraction increased to 0.9 (Figure 5.12), as nearly all of the sediment transported to the flume outlet was lightweight plastic. The density of the sediment collected at the flume out increased to 1730 $kg/m^3$ after Bend 4 cut off at 102 hours as the plastic fraction decreased to 0.72 (Figure 5.12). Coupling the sediment density measurements with the submerged flux measurements indicates that the flux of plastic sediment is always below the feed rate of plastic as material is lost to the bars and floodplains. The high peaks in sediment flux are periods where the coarse flux out of the flume was higher than the coarse feed rate.

### 5.3.4 Water surface slope and sinuosity

The average water surface slope downstream of 6 m had a sawtooth pattern, with three relatively large increases in slope, due to cutoffs at 12.5, 77, and 102 hours followed by decreases in slope associated with migration (Figure 5.9). The two other cutoffs (at 31 and 77 hours) did not reduce the overall water surface slope because migration increased immediately after the cutoff balancing the loss of sinuosity. During the first 39 hours the sinuosity increased from 1.1-1.2 and the water surface slope decreased to 0.0055 from a high of 0.0059 (Figure 5.9). As the bend morphology became skewed, the water surface slope declined in two steps between 39 and 45 hours, and 60-68.5 hours. By 68.5 hours the slope had decreased to 0.0046 and the sinuosity was 1.6 (Figure 5.9). Once the cutoffs began, the channel steepened, and by the end of the experiment the water surface slope was 0.0055 and the sinuosity was 1.2 (Figure 5.9).

The mean water surface slope was calculated using a best-fit line to the water surface data to interpolate a water surface slope for the entire flume. The water surface slope is not constant and steepens downstream (Figure 5.13). The water surface slope at the downstream end of the flume declines until the slope is much more uniform at 68.5 hours, prior to the cutoffs, and the downstream slope increased relative to upstream following the cutoffs (Figure 5.15). The slope steepens within Bend 2. We therefore calculated the water surface slope and sinuosity separately for Bends 1-4 (Figure 5.14) to account for downstream steepening. The water surface slope in Bend 1 steadily declined from 0.0047 at 6 hours to 0.0029 at 68.5 hours as the bend sinuosity increased from 1.09 to 1.29. The water surface slopes for the other bends were more volatile. The slope in Bend 2 varied between 0.0038 to 0.0055 during the first 39 hours of the experiment. It then decreased to about 0.004 until increasing rapidly 77.5 hours as the bed aggraded and Bend 3 cut off. The sinuosity in Bend 2 increased to 2.4 as the bend skewness increased at 68.5 hours, but decreased rapidly to 1.3 when Bend 3 cut off (Figure 5.14b).

Much of the slope adjustment observed in Figure 5.8 was due to the dramatic decrease in slope in Bends 3 and 4, both of which had slopes decrease by half relative to their maximum value. The slope in Bend 3, decreased from 0.011 to 0.0048 at 68.5 hours prior to cutting off then increased again to 0.01 at 114 hours (Figure 5.14A). The water surface slope in Bend 4 decreased from 0.008 to 0.004 between 22 and 68.5 hours, and was steady until increasing again at 100 hours once it cut off and steepened (Figure 5.14A). The sinuosity increased to values greater than 2 as the water surface slope dropped in Bends 3 and 4 (Figure 5.14B). For Bends 2-4 the decrease in water surface slope is greater than the increase in sinuosity due to in-channel aggradation and backwater from the overbank flow on the floodplain.

### 5.3.5 Channel geometry

Channel geometry also varied during the experiments (Figure 5.9). The mean channel depth for the entire experiment was 2.8 cm, and varied from 2.5 to 3.3 cm. The average channel depth increased during the first 18 hours to 3.3 cm, then gradually decreased to 2.5 cm at 78 hours and stayed within 2.5 and 2.8 cm for the remainder of the experiment (Figure 5.9). The average bankfull channel width during the experiment was 30 cm, but the average width varied form 19-40 cm (Figure 5.9). The average channel width was relatively steady during the first 52 hours of the experiment (29-32 cm), but subsequently declined to 19 cm at 87 hours and did not increase until the cutoff of Bend 2 after which the width increased to a maximum of 40 cm at 108 hours.

The average width was highest for Bend 1 (34 cm) and lowest for Bend 4 (25 cm) during the first 52 hours of the experiment (Figure 5.15). The difference decrease in width between Bends 1 and 4 (26%) in the first 52 hours is identical the decrease in the slope of the basin from Bends 1 to 4 (26%, Figure 5.2). The width decline at 52 hours occurred first upstream and lastly in Bend 4 (Figure 5.15), but the width of Bends 1, 2, and 4 all increased rapidly once Bend 2 cut off.

Because the width and depth both decreased through time, the width depth ratio (B/H) remained relatively steady near 10 until it dropped to about 7.1 at 87 hours. B/H subsequently increased dramatically to about 40 due to large increases in width following the series of cutoffs (Figure 5.9).

### 5.3.6 Migration Rates

The bank erosion rate ranged from 0.3 to 3.6 cm/hr (Figure 5.16), with a mean outer bank erosion and inner bank accretion rate of 1.5 cm per hour (0.048 and 0.049 widths/hr). Erosion rates were highest at the beginning of the experiment as the channel began to develop curvature and bends lengthened. The erosion rate gradually declined from 2.5 cm/hr at 25 hours to 0.63 cm/hr at 60 hours and stayed below 1 cm/hr until Bend 2 cut off at 87 hours. Mean erosion and deposition rates were similar with the exception of 6, 25, and 39 hours, which corresponded to changes in channel width.

### 5.3.7 Summary of results

During the bend building phase of the experiment, the water surface slope declined slowly as sinuosity increased. The average width (30 cm) and depth (3 cm) were quasi steady as bends grew. During the bar growth phase the sediment transport rate at the downstream end of the flume exceeded the feed. At the downstream portion of the flume, it was steep and the banks were entirely coarse sediment. The bank erosion rate varied between 0.03-0.1 widths/hr.

The bends became skewed downstream when erosion focused over a short distance just downstream of the apex. The width decreased throughout the flume and observation suggest the depth decrease was greater downstream in the steeper reach of the flume where it aggraded. The portion of water depth over the floodplain increased. The decreased depth, water surface slope, and discharge through the channel decreased transport rates of coarse sediment, and the sediment flux declined until only about 10% of the material transported out of the flume was coarse sediment. The change in migration style (to localized bank erosion only) decreased the erosion rate to about 0.02-0.03 widths/hr and sediment eroded from banks was trapped upstream of the downstream bend apex.

The increased overbank flow and high groundwater levels associated with bed aggradation during irrigation flow limited alfalfa growth in some patches on the floodplain. These areas were the locus for overbank erosion and cutoff as each of the three downstream bends cut off over 25 hours. After the cutoff of Bend 2 at 87 hours, the channel steepened and the width and depth increased. Bank erosion rates increased and sediment transport increased at the flume outlet following the final cutoff at the distal end of the flume. In response to the high transport rates and rapidly adjusting channel, island bars developed as fine sediment deposition in the chute channel was limited. The slopes were particularly steep at the downstream end of the

flume, (which was much steeper than the upstream end) and may have limited fine deposition in chute channels.

## 5.4 Discussion

### 5.4.1 Comparison with 2009 experiment

Our experimental methods differed from the 2009 experiment in the inlet condition, sediment feed, alfalfa density, the intitial channel morphology, and flood hydrograph over the first 71 hours of the 2009 experiment (Table 5.1). In the 2009 experiment, bends developed from upstream to downstream, while bends developed simultaneously throughout the flume in 2012. This was likely because of the initial channel configuration, which was straight with the exception of a small bend at the upstream end of the flume in the 2009 experiment, versus a slightly sinuous channel in 2012 with small curvature perturbations throughout the length of the flume (Figure 5.1). Alternatively, it may have been a consequence of the steeper regions at the bottom of the flume. The 2012 experiments consequently developed a meandering planform much faster than the 2009 experiment. The sinuosity was 1.2 after 20 hours in the 2012 experiment versus 100 hours in the 2009 experiment. The faster development of sinuosity is particularly valuable in experiments with alfalfa, where experiments are slowed by the need periodically turn the flume off for a week so that alfalfa can be replanted. In both experiments, the upstream bend elongated through time as the upstream boundary condition moved downstream.

The three main differences between the 2009 and 2012 experiments—the increased alfalfa density in 2012–the higher sediment supply in 2012, and the difference in slope at the downstream end of the basin resulted in a channel that was deeper (2.8 cm versus 1.2 cm for the 2009 experiment) and narrower (30 cm versus 41 cm) (Table 5.3). The channel was also more sinuous, with the mean sinuosity in 2012 (1.3) exceeding the maximum sinuosity in the 2009 experiment (1.2). The smaller chutes in 2012 allowed the higher sinuosities to develop before chute cutoffs occurred, and cutoffs in the 2012 experiment mostly occurred when aggradation-induced ponding limited alfalfa growth on the floodplain. The alfalfa in 2012 was 3 times denser than 2009 but the average erosion rate in the 2012 experiment were very similar (1.5 cm/hr and 1.4-1.6 cm/hr, respectively) (Table 5.3). Because the 2012 experiments were narrower, the migration rate per unit channel width was higher in the 2012 experiments (0.048 widths/hr versus 0.032-0.039 widths/hr for the 2012 and 2009 experiment, respectively) (Table 5.3).

Because the coarse feed was turned off periodically in the 2009 experiment, aggradation at the upstream end of the flume was limited. For the 2012 experiment the sediment supply was held constant leading to aggradation in Bends 1-3. The supply was only constant in the upper portion of the flume. Upstream aggradation implies that the supply was diminished downstream. Downstream, where bank erosion was more variable, local supply varied substantially. Because the discharge was held constant, it was the bed aggradation that led to ponding on the floodplain, overbank flows and eventual chute cutoff.

### 5.4.2 Revised time scaling and comparison of migration rates

The average migration rate over the entire experiment was 0.048 channel widths/hr (0.015 m/hr). To compare this migration rate with field migration rates requires scaling both length and time between the flume and the field. The length scaling factor, λ, is equal to:

$$X_{flume} = \lambda X_{field} \tag{5.3}$$

where $X_{field}$ and $X_{flume}$ are length in the field and flume, respectively, and X can represent any length scale such as channel width, channel depth, and grain diameter [Yalin, 1971; Parker et al., 2003]. Comparing the inner-quartile range of width, depth, and $D_{50}$ from the field (From Chapter 2 and Appendix B–Table B1) with the average values in the 2012 experiment (Table 5.4) gives λ between 0.01-0.04 depending on the parameter of interest (Table 5.4).

Unlike length scales, time can be scaled in a variety of ways that provide very different results [Yalin, 1971; Peakall et al., 1996]. A further complication arises because experimental time is calculated for continuous bankfull flood and processes such as bank erosion are often measured in years where there are long periods when river discharge causes little to no bank erosion and sediment transport is minimal. Following Parker et al. [2003], we can account for the periods when erosion and sediment transport are minimal by including the intermittency of effective flows (I). Using Froude similarity [Yalin, 1971; Peakall et al., 1996, Parker et al., 2003], Braudrick et al. [2009] (Chapter 2) converted their experimental time to the equivalent time in the field using:

$$t_{field} = \frac{t_{flume}}{\sqrt{\lambda} I} \tag{5.4}$$

where $t_{field}$ and $t_{flume}$ are the scaled time for the field and flume, respectively. Following Braudrick et al. [2009] we use an intermittency of 0.022 assuming bankfull flow occurs 8 days/yr using data from the Rocky Mountains [Dunne and Leopold, 1979; Andrews and Nankervis, 1995]. Using Froude scaling, the 120-hour 2012 experiment corresponds to 3.1-6.2 years of channel evolution in the field. The bank erosion rate would therefore correspond to 0.59-0.93 channel widths/year, at least 6 times faster than observed in Appendix B–Table B1 (Figure 5.17). Braudrick et al. [2009] also found that Froude scaling yielded very fast migration rates relative to the field (see Chapter 2). Given their similar migration rates, it is not surprising that this scaling approach also yields fast migration rates for the 2012 experiments relative to the gravel meanders in Appendix B–Table B1. An alternative approach is to assume sediment transport similarity (that is the dimensionless sediment transport is similar in the flume and field). Combining the dimensional analysis of sediment transport time scaling from Yalin [1971] with an intermittency yields:

$$t_{field} = \frac{t_{flume}}{\lambda^{1.5} I} \tag{5.5}$$

Using sediment transport scaling is appropriate if migration is limited by the rate of removal of sediment from the toe of the bank, which must be a function of bedload transport. Using the same scaling factor (0.01 to 0.04) and intermittency as above, the 120-hour experiment represents 78-620 years. Our average migration rate of 0.048 widths/hr in the 2012 experiment

would therefore be equivalent to 0.0023-0.0092 widths/yr in the field using sediment transport similarity, this is at the low end of migration rates of gravel-bed meanders in Appendix B–Table B1 (Figure 5.17).

### 5.4.3 Controls on the change in the pattern of migration

Once the bends lengthened in the 2012 experiment, the pattern of channel migration changed from erosion over the majority of the bend length to erosion focused near the bend apex, creating downstream skewed meanders. In the 2009 experiment, such bends did not develop, perhaps due to the larger chutes that capture flow and led to bend cutoff at a lower sinuosity. Downstream-skewed bends are commonly observed in the field [e.g., Brice, 1974; Tanaka et al., 2011] and theory suggests that they occur when the width depth ratio exceeds a critical value determined by the Shields stress and bend wavelength [Zolezzi and Seminara, 2001; Zolezzi et al., 2009]. The critical width-depth ratio decreases for decreases in Shields stresses and increases in bend wavelength. By decreasing the water surface slope and hence Shields stress (assuming grain size and depth change less than slope) migration can adjust the critical width-depth ratio at which skewness develops, potentially leading to skewed bends. The conditions that support downstream-skewed bends commonly occur in gravel bed meanders in the field [Zolezzi et al., 2009].

### 5.4.4 Comparison with field channels

The meandering channel created in this experiment was dynamic and showed several features common to meanders in the field. The width to depth ratio was relatively low end compared to field observations from Chapter 3 (10 versus a median value of 22 for gravel meanders as a whole). Sediment was sorted with coarse sediment on the point bar deposited upstream of the bend apex and fines deposited downstream, similar to observations in the field [e.g., Bluck, 1971; Jackson III, 1977; Dietrich and Smith, 1984; Clayton and Pitlick, 2010]. Clusters of cutoffs following migration have been observed in the field [e.g., Hooke, 2004]. A temporal variation in sinuosity seems likely given our limited number of bends and their influence on one another.

One obvious difference between these experiments and rivers in the field is the lack of a flood hydrograph. This discharge was held constant at a value that, at least initially, just filled the channel bank, affirming the finding of Braudrick et al. [2009] that variable flood flows are not required for meandering. The effects of infrequent overbank flows relative to bankfull flows on channel planform are an area of uncertainty. In some channels with large floodplains, infrequent high flows may not increase sediment transport rates relative to bankfull conditions due to increased backwater effects from the floodplain [e.g., McKean and Tonina, 2013]. While other studies have observed large increases in bank erosion rates following high flows [e.g., Pizzuto, 1994]. Chute cutoffs are often associated with high floods rather than lower bankfull events [e.g., Gay et al., 2001; Constantine et al., 2010; Micheli and Larsen, 2010; Zinger et al., 2011] because they require erosion of floodplain surfaces that may be vegetated.

The absence of overbank flows in my experiments may therefore have reduced the migration rate and the frequency of cutoffs. Cutoffs in the 2012 experiments resulted from in-channel aggradation which reduced alfalfa coverage on the floodplain. Subsequent overbank flows could then more easily erode the floodplain because aggradation increased the discharge

on the floodplain relative to the channel, and also decreased the extent of erosion-resistant patches of vegetation. To our knowledge, a similar linkage between aggradation, vegetation growth, and cutoffs has not been observed in the field, and is at least partially an artifact of our experiments.

Similar to the 2009 experiment, cutoffs occurred through chute channels, but here channels were less extensive, and required more floodplain erosion for the channel to cut off. A variable flood discharge would likely have increased the frequency of cutoffs, steepening the channel and limiting in-channel aggradation. In channels with variable hydrographs, the decreased water surface slope associated with migration would periodically be counterbalanced by chute cutoffs occurring during high flows. The role of hydrographs could be explored in future studies using the same input conditions and alfalfa density, but incorporating overbank discharge. Despite these differences, this experiment behaved remarkably similar to channels in the field, and allow direct observation and measurements of changes to meander morphology through time.

## 5.5 Conclusions

Using experimental conditions similar to that described in Chapter 2 (and reported in Braudrick et al. [2009]), we were able to recreate a meandering channel in the laboratory using alfalfa to provide strength, and fine sediment to partially plug and infill chutes. This experiment had constant discharge and sediment supply at the upstream end of the flume, but the initial basin sediment surface steepened at two successive reaches downslope. The resulting water surface slope, width, depth, and migration rate varied significantly.

At the beginning of the experiment, the channel increased its sinuosity as it migrated and decreased sinuosity following cutoffs. As the channel migrated and the sinuosity increased, leading to a decline in the water surface slope. After 35-50 hours, the migration pattern of the bends changed from eroding the majority of their banks, to focused erosion downstream of the bend apex, creating locally distorted bends pointing sharply downstream. These bends lead to further decreases in slope, causing aggradation upstream of the bend apex as bank erosion decreased and could no longer accommodate the supply.

The aggradation eventually lead to cutoffs when in-stream aggradation increased the proportion of flow on the floodplain, and limited alfalfa growth by locally ponding water above the floodplain surface, decreasing alfalfa density and creating a weak location on the floodplain. If the experiment had variable flood flows, cutoffs may have occurred in the absence of aggradation, but given the strong bank strength. The zones of weak alfalfa growth were the locus for channelized floodplain flow, which eventually enlarged and connected to downstream chutes. Following the cutoffs the water surface slope increased causing both the sediment flux and bank erosion to increase.

The migration rate was very similar between these experiments and 2009 experiment in the same basin, despite the alfalfa density being 3 times lower in the previous experiment. The main effect of the denser alfalfa (and constant supply) in the current experiment is that the channel width was 25% narrower, and suppression of chutes and strengthening of the floodplain limited chute cutoffs, allowing the sinuosity to increase. The bends in the 2012 experiments

were skewed downstream, which was not observed in the 2009 experiments. Small-amplitude bends along the initial channel length led to more rapid bend development than the 2009 experiment, which had an initially straight channel.

Assuming that the dimensionless sediment transport rate was constant between the flume and field, and a scaling factor of 0.01-0.04 this experiment had an average migration rate of 0.0028-0.009 widths/yr, which is on the low end of the range of field observations. Our observations of decreased slope leading to a change in migration pattern support theory on the origins of bend skewness.

## 5.6 Tables

Table 5.1. Comparison of the 2012 experimental methods with the 2009 experiment [Chapter 2]

| | 2012 experiment | 2009 experiment (Chapter 2) |
|---|---|---|
| Bankfull discharge | 1.8 l/s | 1.8 l/s |
| High flow discharge | N/A | 2.7 l/s, but up to 4.4 l/s |
| Average initial width | 29 cm | 40 cm |
| Average initial depth | 2.7 cm | 1.9 cm |
| Coarse sediment feed rate | 1.4 kg/hr (constant) | 0.75 kg/hr (variable) |
| Fine sediment feed rate | 5 kg/hr | 3.4 kg/hr |
| Coarse sediment feed $D_{50}$ | 0.75 mm | 0.78 mm |
| Fine sediment feed $D_{50}$ | 0.35 mm | 0.35 mm |
| Fine sediment specific gravity | 1.36 | 1.5 (0-71 hours)<br>1.3 (71-136 hours) |

Table 5.2. Channel cutoffs during the 2012 experiment.

| Time (hrs) | Bend | Post-cutoff length (m) | Pre-cutoff length (m) | Length ratio |
|---|---|---|---|---|
| 12.5 | 5 | N/A | N/A | N/A |
| 31 | 4 | 0.6 | 1.7 | 0.3 |
| 77 | 3 | 1.6 | 5.6 | 0.3 |
| 87 | 2 | 4.8 | 8.9 | 0.5 |
| 102 | 4 | 1.7 | 5.4 | 0.3 |

Table 5.3. Comparison of the 2012 experimental results with the 2009 experiment [Braudrick et al., 2009, Chapter 2]. The steady hydrograph in the 2009 experiment represents data from the final 65 hours when the hydrograph was a bankfull discharge of 1.8 l/s, the same as the 2012 experiments.

| | **2012 experiment** | **2009 experiment (Chapter 2)** |
|---|---|---|
| Average width (cm) | 30 | 41 |
| Average depth (cm) | 2.8 | 1.2 |
| Water surface slope (minimum and maximum) | 0.0055 (0.0046-0.0064) | 0.0047 (0.0042-0.0055) |
| Sinuosity (minimum and maximum) | 1.3 (1.1-1.6) | 1.1 (1.0-1.2) |
| Migration rate (cm/hr) | 1.5 (erosion) 1.5 (deposition) | 1.6 (entire experiment) 1.4 (steady hydrograph) |
| Migration rate (widths/hr) | 0.048 (erosion) 0.049 (deposition) | 0.039 (entire experiment) 0.032 (steady hydrograph) |

Table 5.4. Comparison of average conditions in the 2012 experiment with the inner quartile range of gravel meanders in the field from Appendix B–Table B1.

| | **2012 experiment** | **Field inner quartile range** | **λ** |
|---|---|---|---|
| Bankfull discharge ($m^3/s$) | $1.8 \times 10^{-3}$ | 22.7-340 | N/A-time |
| Slope | 0.0055 | 0.00095-0.0036 | N/A-dimensionless |
| Average initial width (m) | 0.3 | 15-60 | 0.01-0.02 |
| Average initial depth | 0.027 | 0.8-2.4 | 0.01-0.04 |
| Coarse sediment feed $D_{50}$ (mm) | 0.75 mm | 18-53 mm | 0.01-0.04 |

## 5.7 Figures

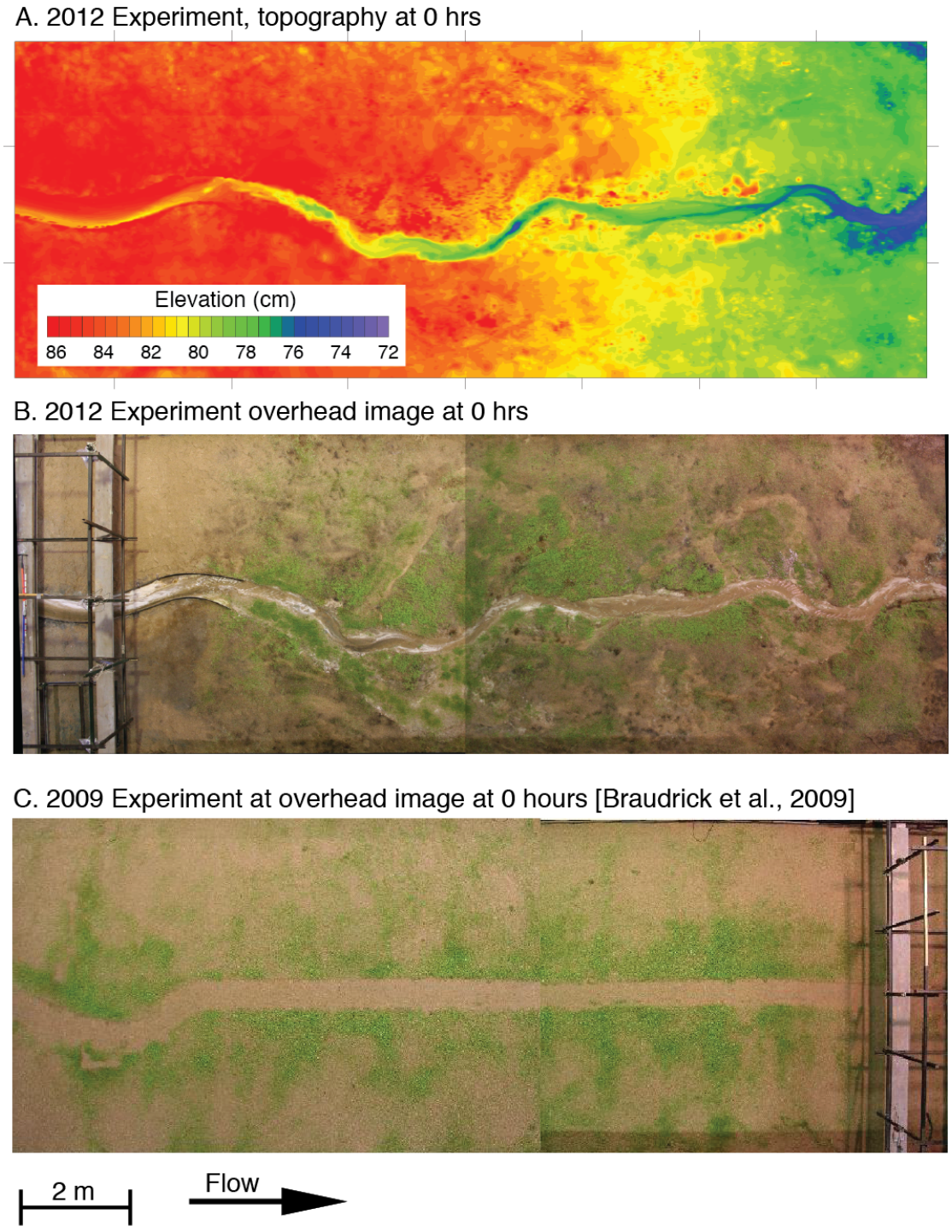


Figure 5.1. Initial channel morphology for the 2012 and 2009 experiments. A. Bed topography at 0 hours for the 2012 experiment. B. Overhead image at 0 hours for the 2012 experiment. C. Overhead image at 0 hours for the 2009 experiment.

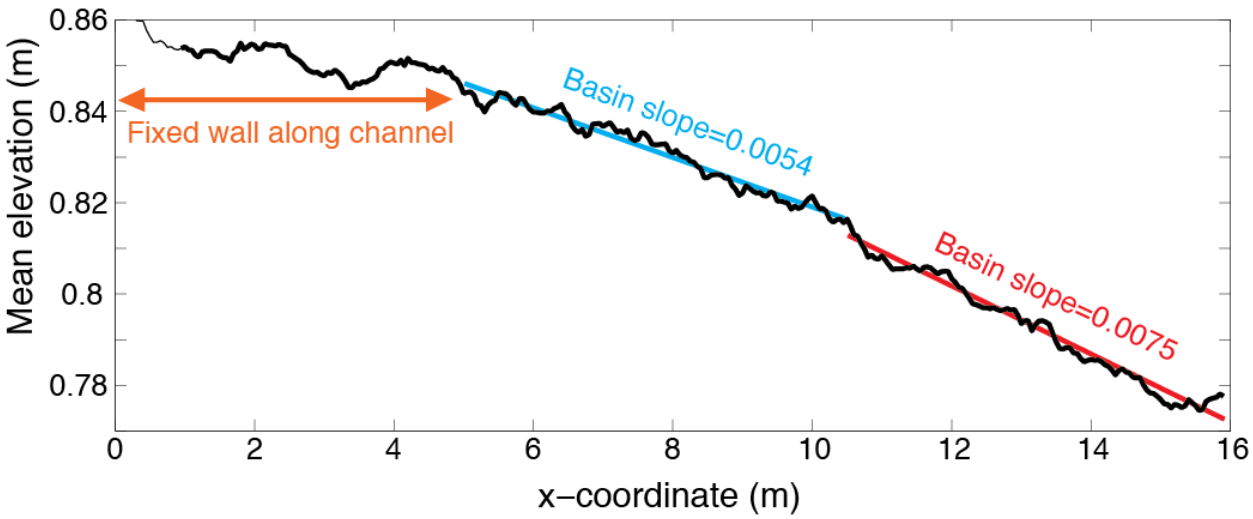


Figure 5.2. Mean basin slope at 0 hours, showing the steepening of the slope downstream. The blue and red lines are the linear best fit to the bed slope in the middle and lower sections of the flume. From the downstream end of the fixed wall inlet section to 10.5 m the slope is 0.0054 and from 10.5 m-15.9 m, the mean basin slope 0.0075.

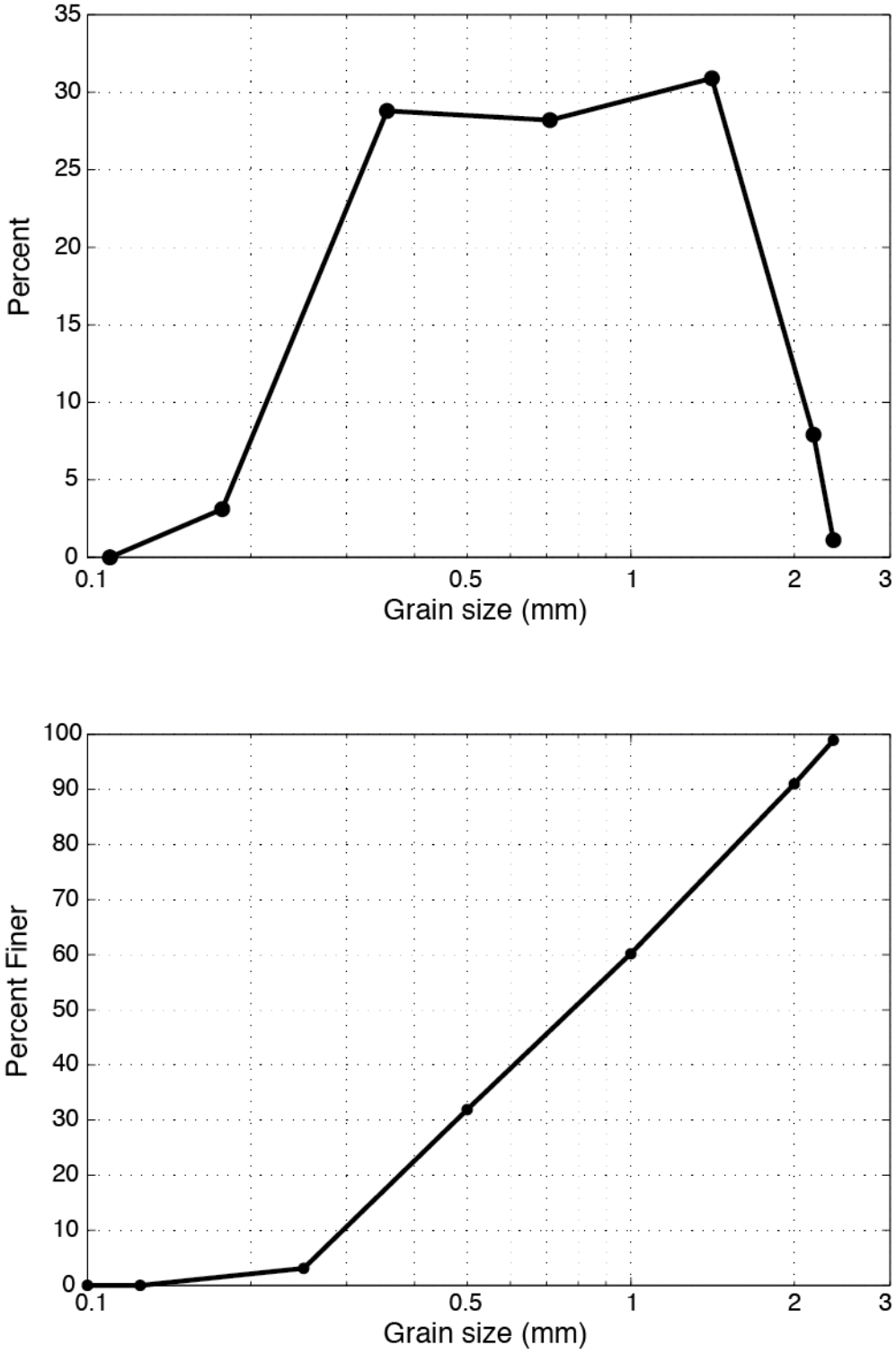


Figure 5.3. Grain size distribution of the coarse sediment feed. The coarse sediment that filled the basin had a similar distribution.

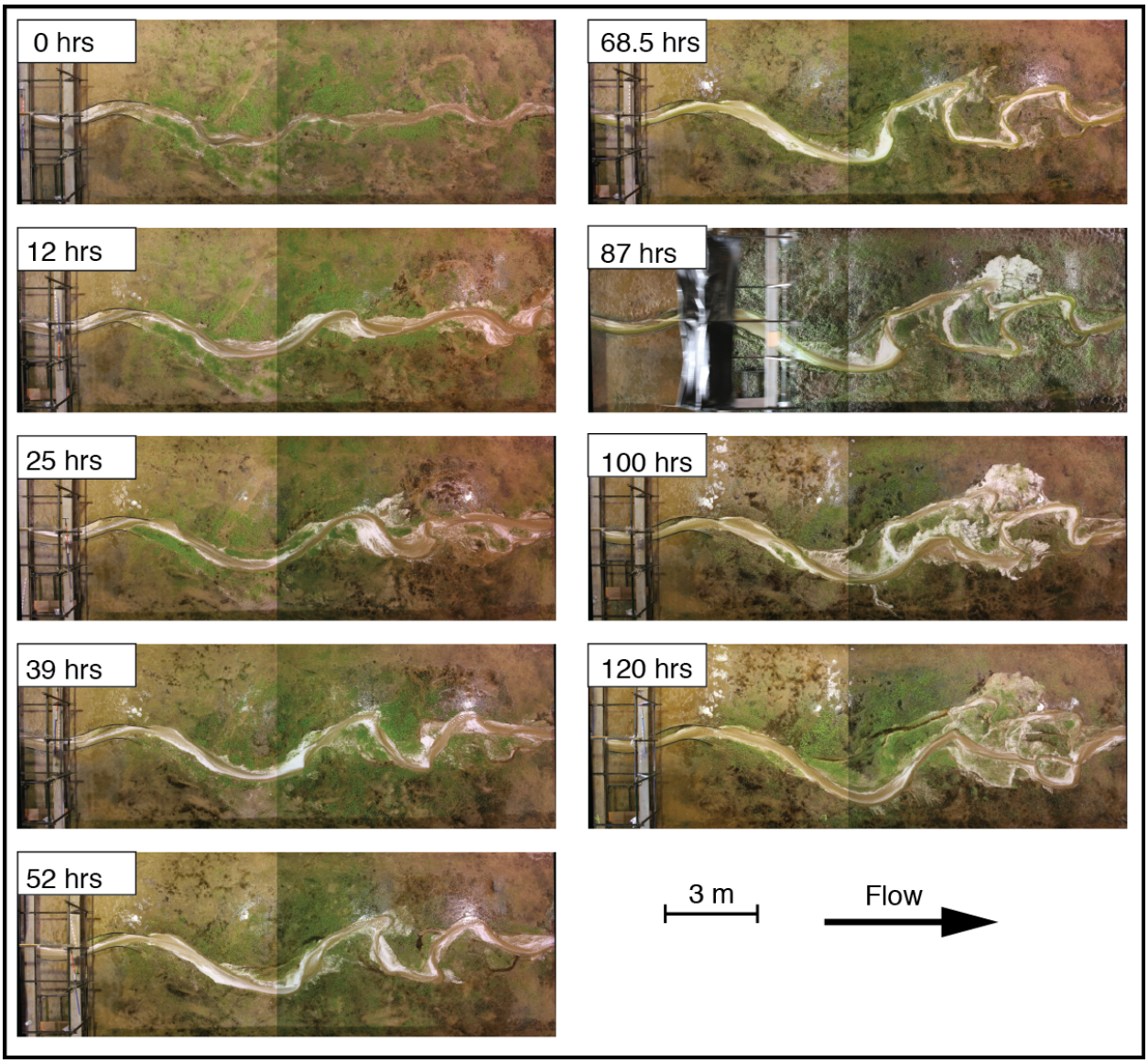


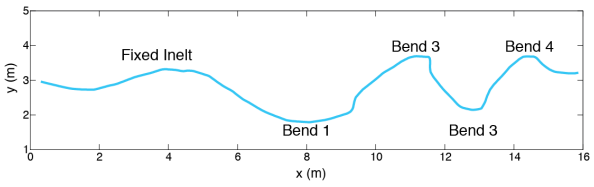


Figure 5.4. Overhead images of experiment through time. The plastic sediment is white and the floodplain and fed sediment are brown. The green is alfalfa. The bend names at 39 hours are shown along the centerline in the bottom panel.

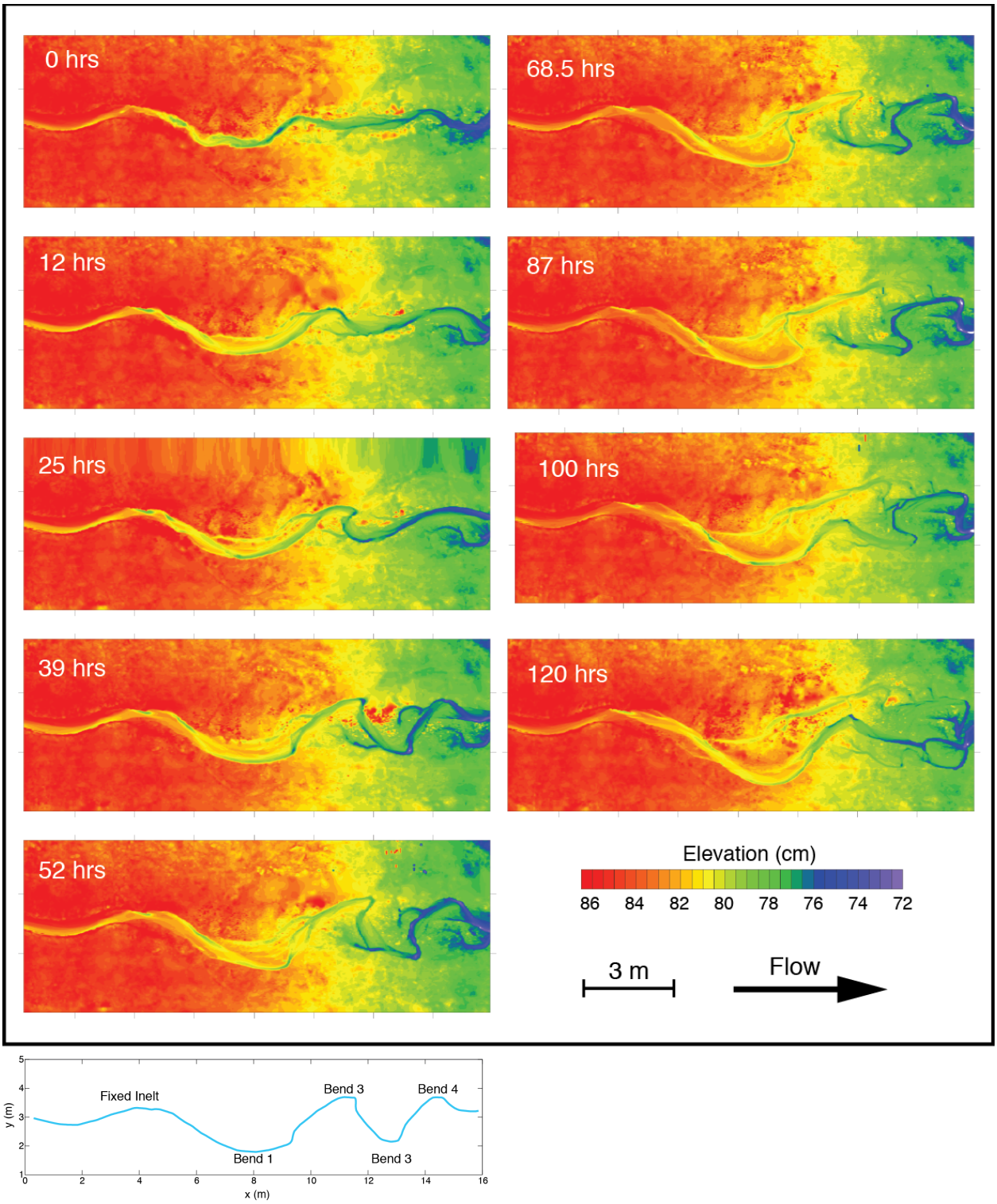


Figure 5.5. Topographic maps of the channel through time. Bend numbers discussed in the text are labeled at 25 hours. The bend names at 39 hours are shown along the centerline in the bottom panel. Enlarged versions of these maps for every survey are given in Appendix D.

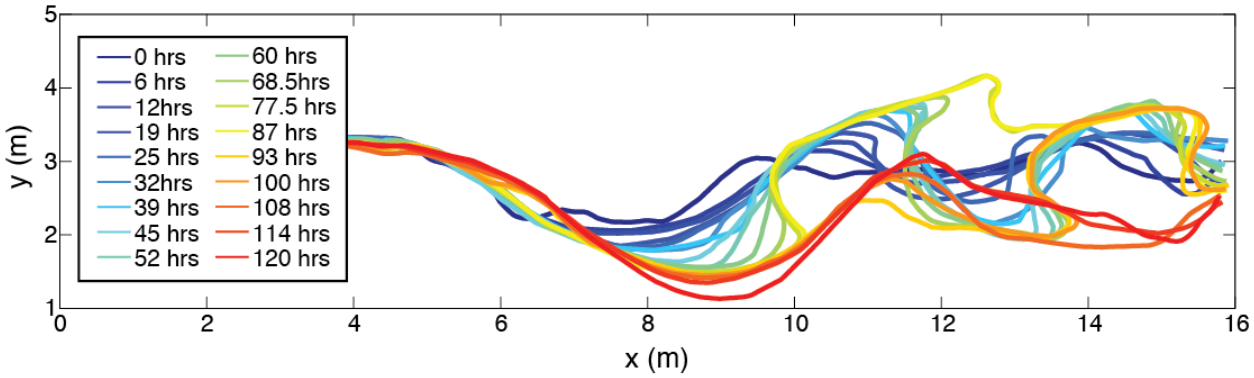


Figure 5.6. Channel centerline locations through time for all 18 topographic surveys.


Figure 5.7. Comparison of the 2012 and 2009 experiments. The bends numbers are shown in panel A. In the 2012 experiment, all sand (the coarse feed and floodplain material is brown, while the plastic sediment is white. In 2009, the colors of the floodplain and plastic are the same, but the fed sand was painted blue. Chutes are denoted with a C in both images.

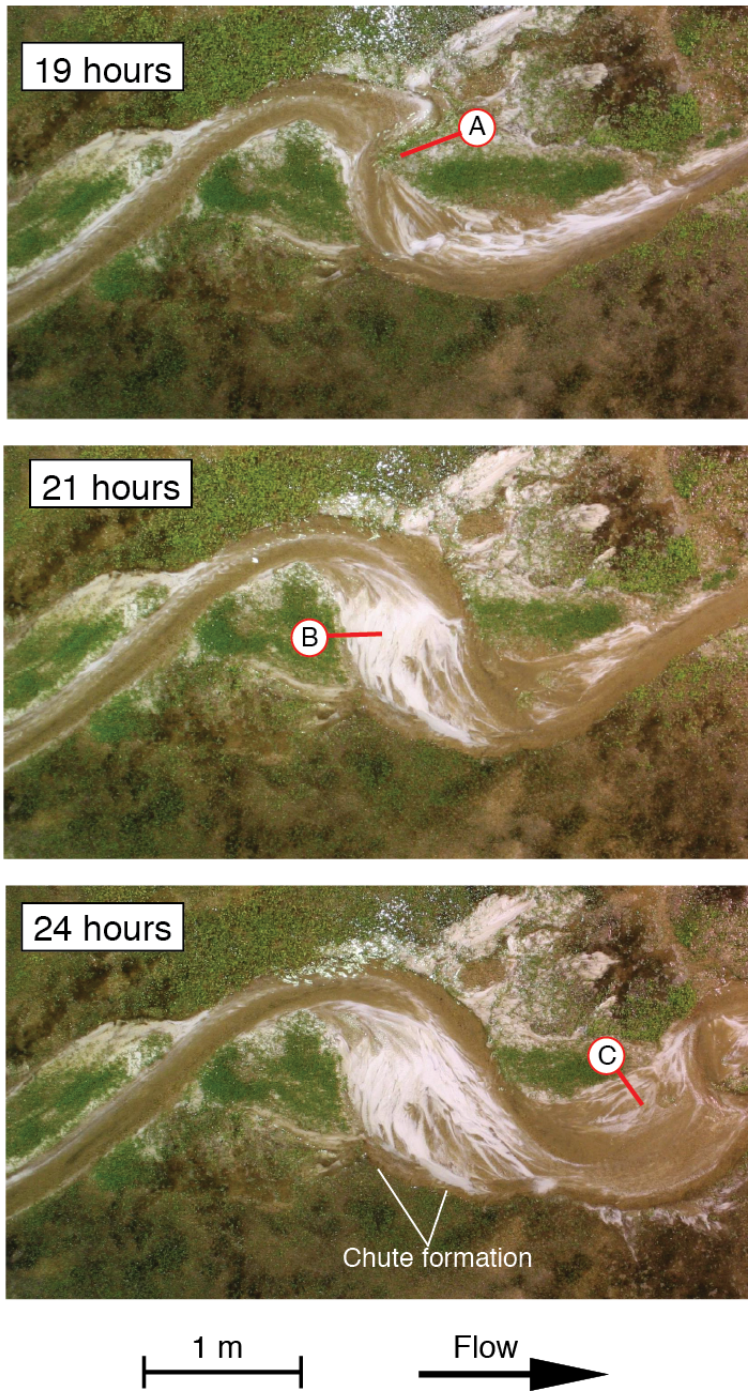


Figure 5.8. Rapid deposition of fine sediment downstream of the bend apex as the downstream limb of the bend. Point A (19 hours) shows a densely vegetated patch limiting downstream migration of the bend. Point B (21 hours) shows the rapid deposition of fine sediment in just 2 hours. Dune fronts show former channel location. Point C (24 hours) shows the rapid deposition of coarse sediment on the next point bar downstream. The rapid downstream migration formed a chute on the inside of the bend.

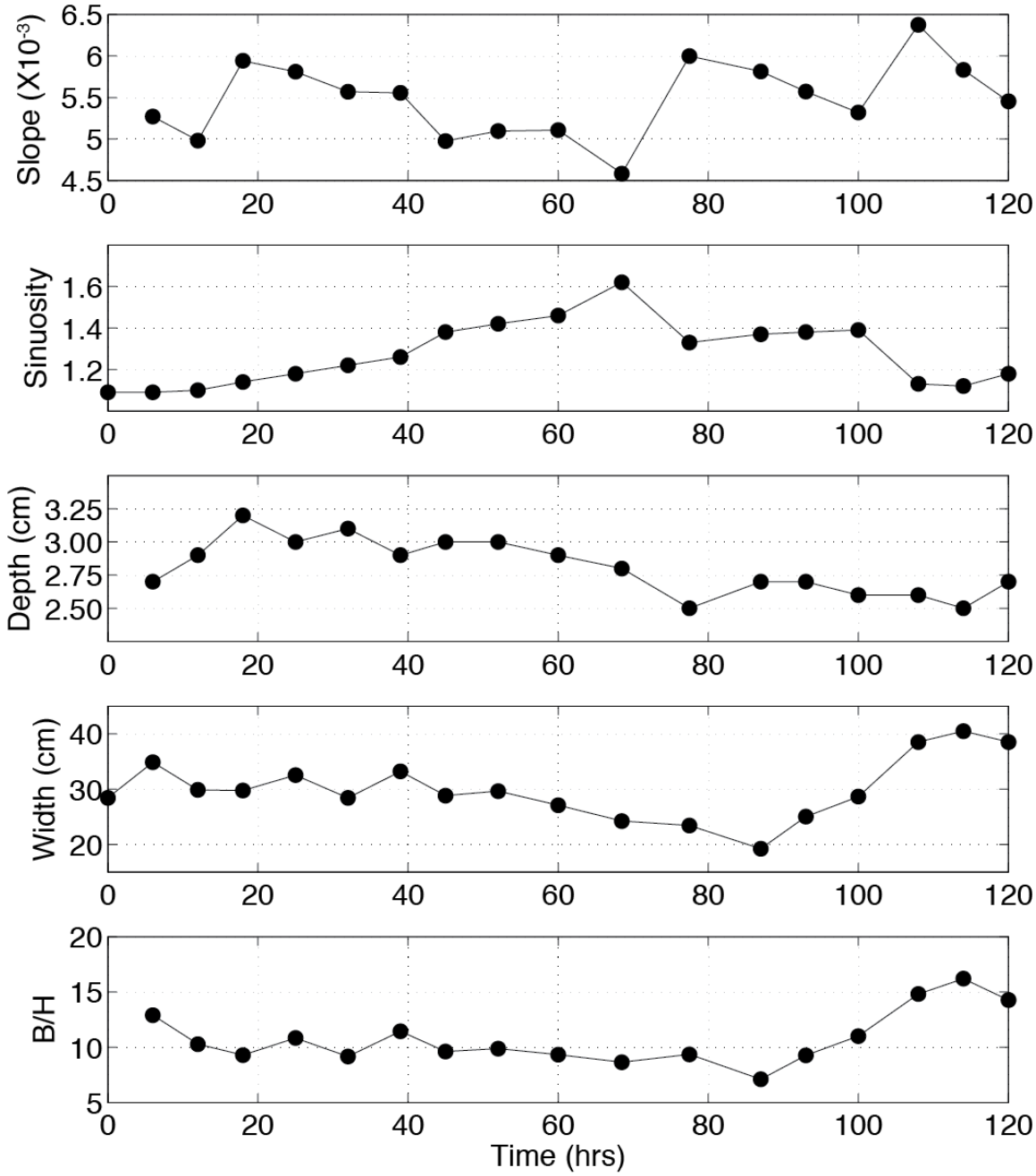


Figure 5.9. Reach-Average hydraulic characteristics from 6-15.9 m. Slope is the water surface slope and B/H is the width depth ratio.

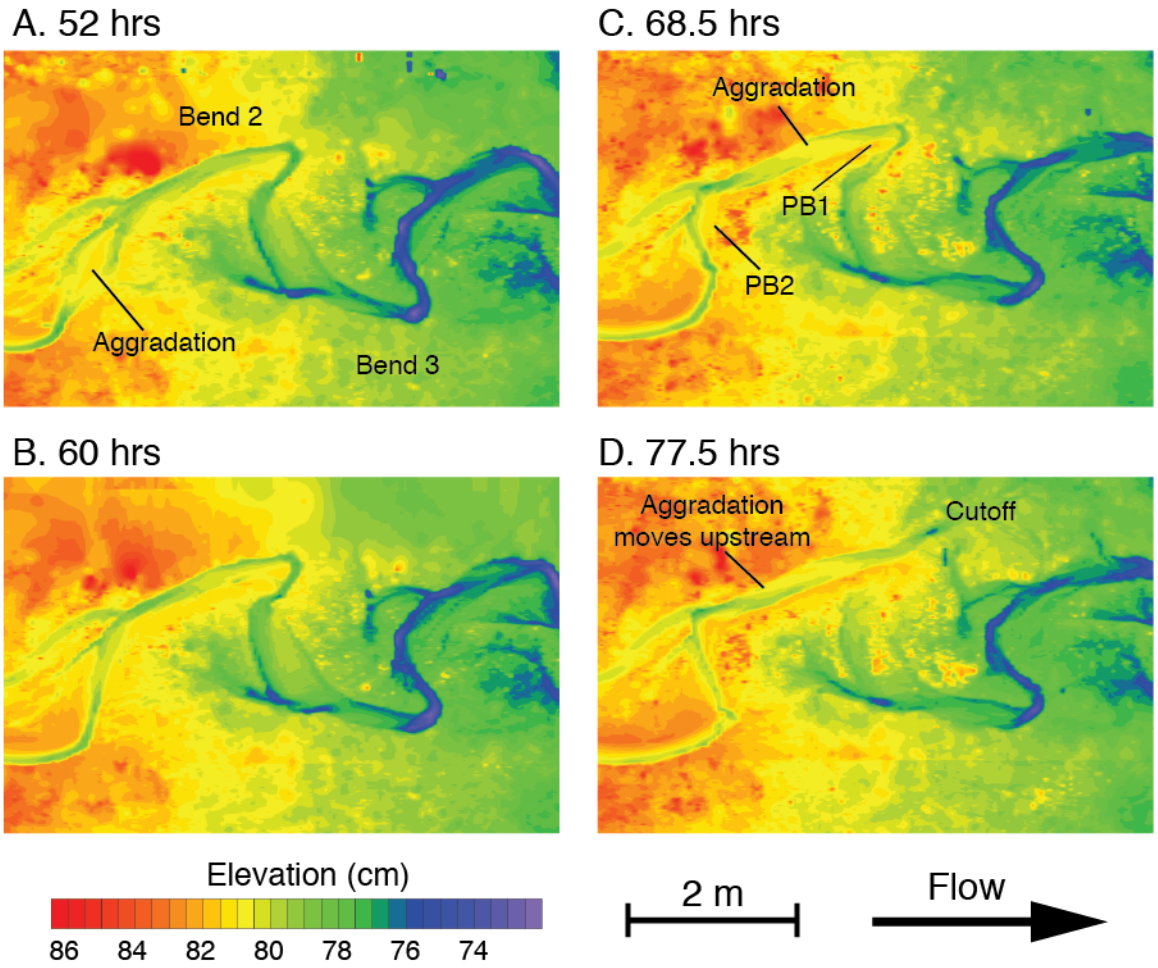


Figure 5.10. Evolution of channel from 8-15 at 52-77.5 hrs. Aggradation occurred at 52 and 68.5 hours, leading to the cutoff at 77.5 hrs. Panel C shows the development of a second point bar at the upstream end of Bend 2 (labeled PB2).

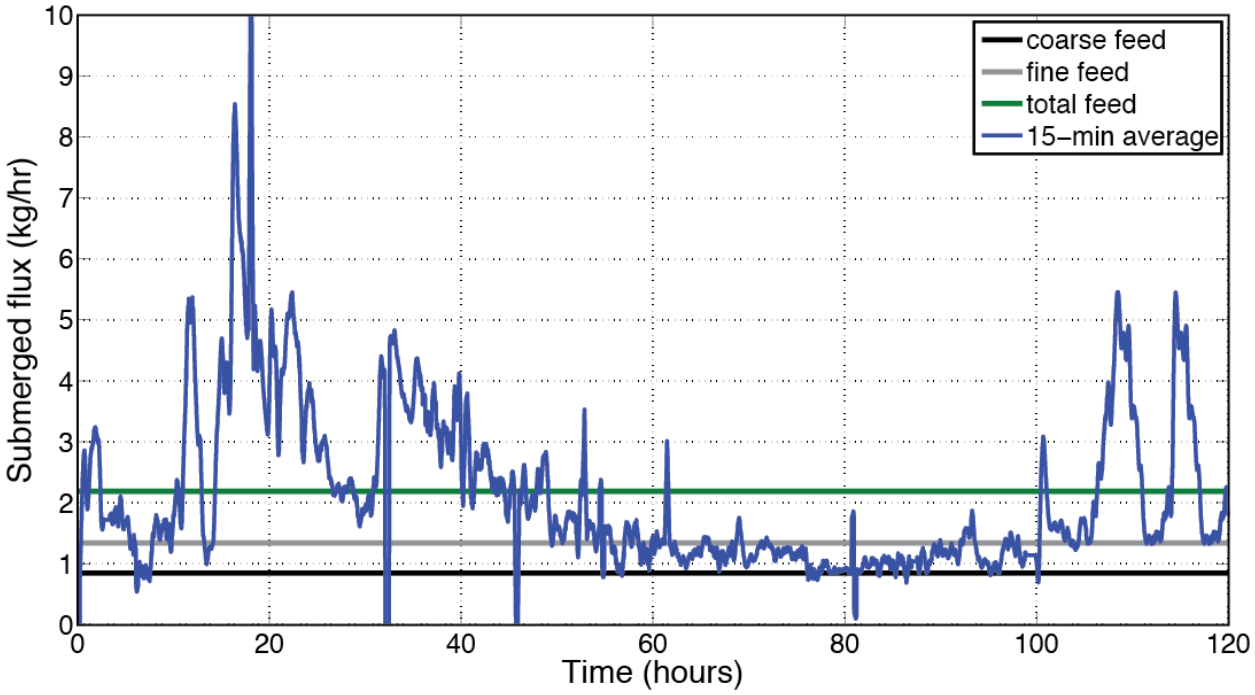


Figure 5.11. Submerged sediment flux measured at the flume outlet. The raw sediment flux data are filtered twice with a 15-minute running average filter.

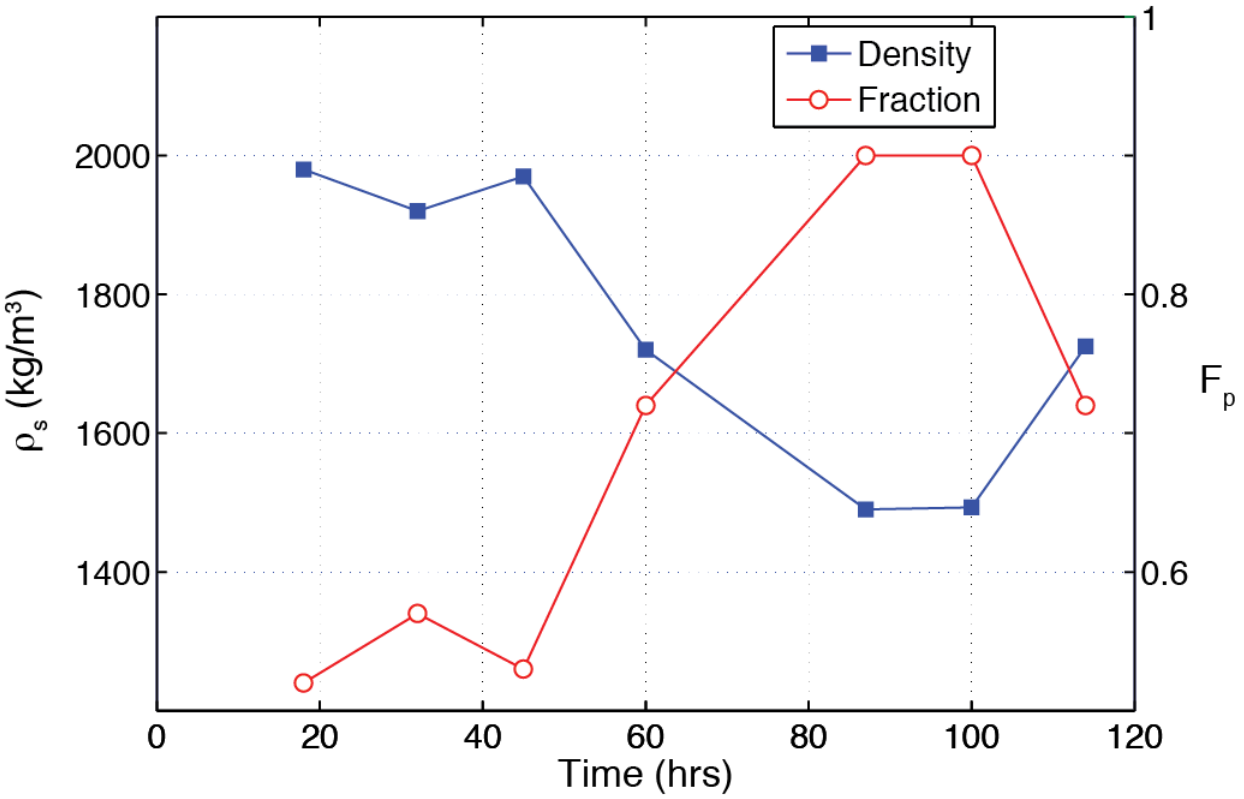


Figure 5.12. The density of sediment measured at the flume outlet ($\rho_s$) (left axis, blue) and the fraction of the flux at the outlet that is lightweight plastic ($F_p$) (right axis, red). The combined density of the feed is 1640 kg/m$^3$, and $F_p$ of the feed is 0.78.

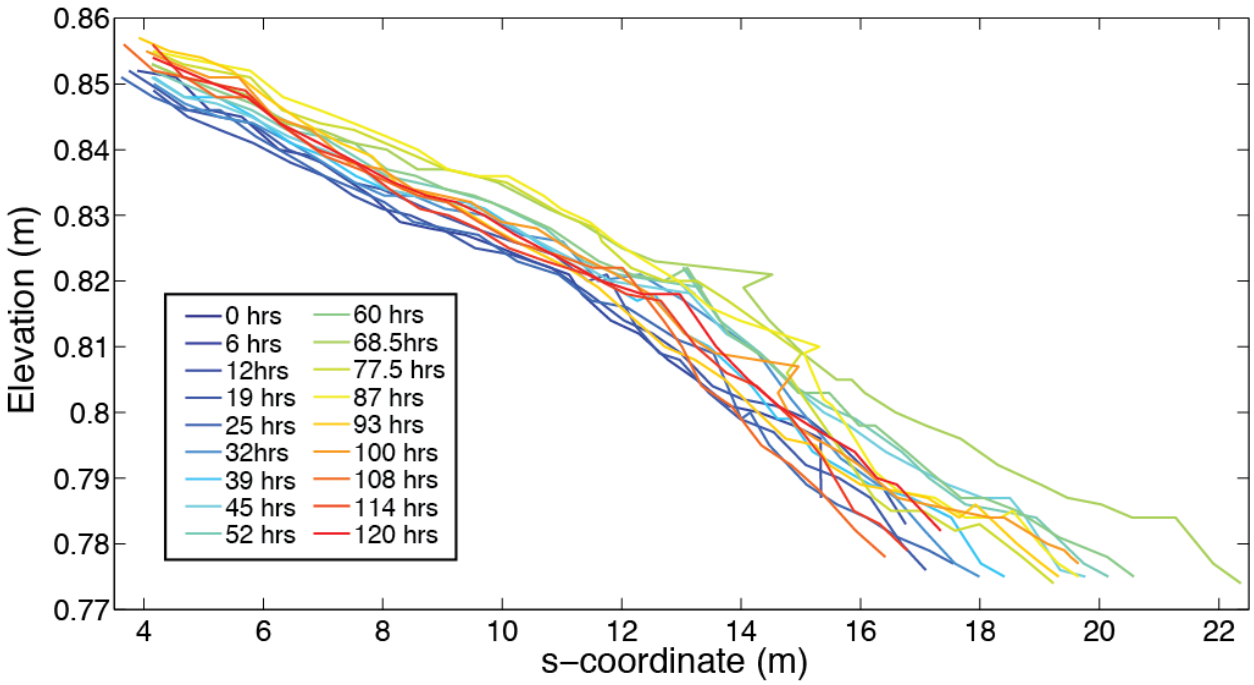


Figure 5.13 Water surface profiles through time. The steps in the profile are often associated with overbank flows.

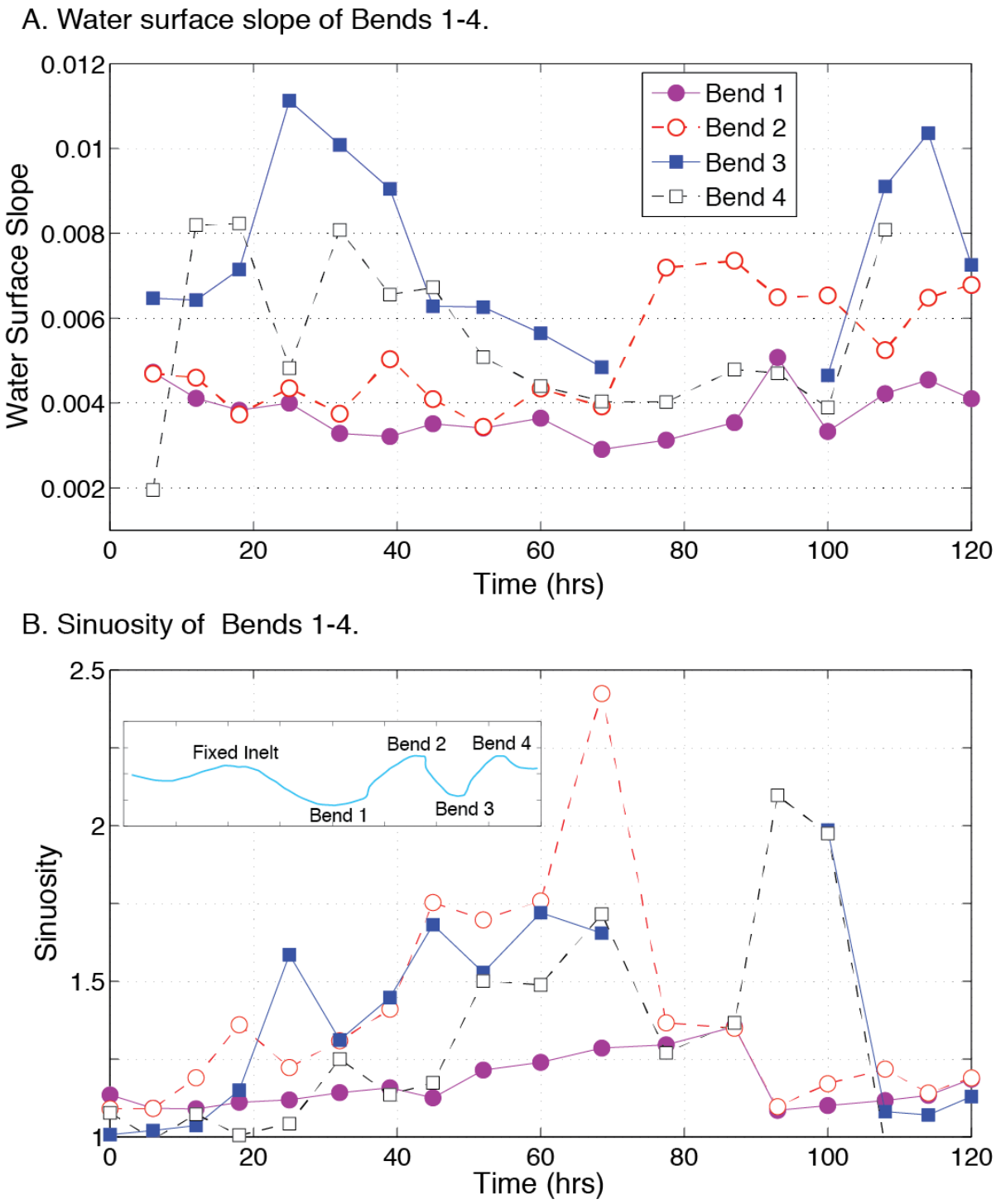


Figure 5.14. Water surface slope and sinuosity of Bends 1-4 through time. The location of the bends at 39 hours is shown in the inset figure. Missing data for Bend 3 reflects the period when it was cutoff.

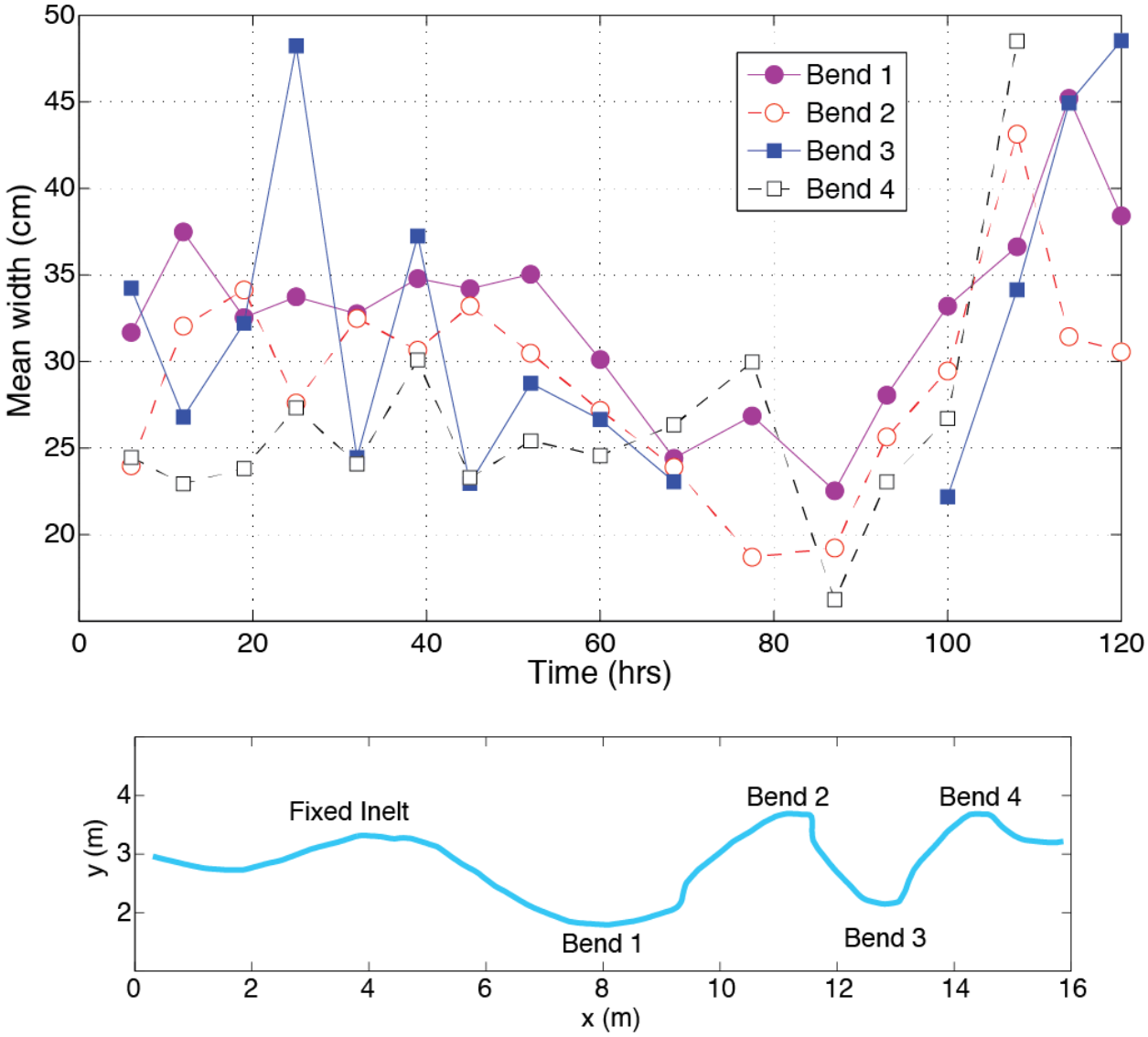


Figure 5.15. Mean width for each bend through time. The location of the bends at 39 hours is shown in the bottom panel.

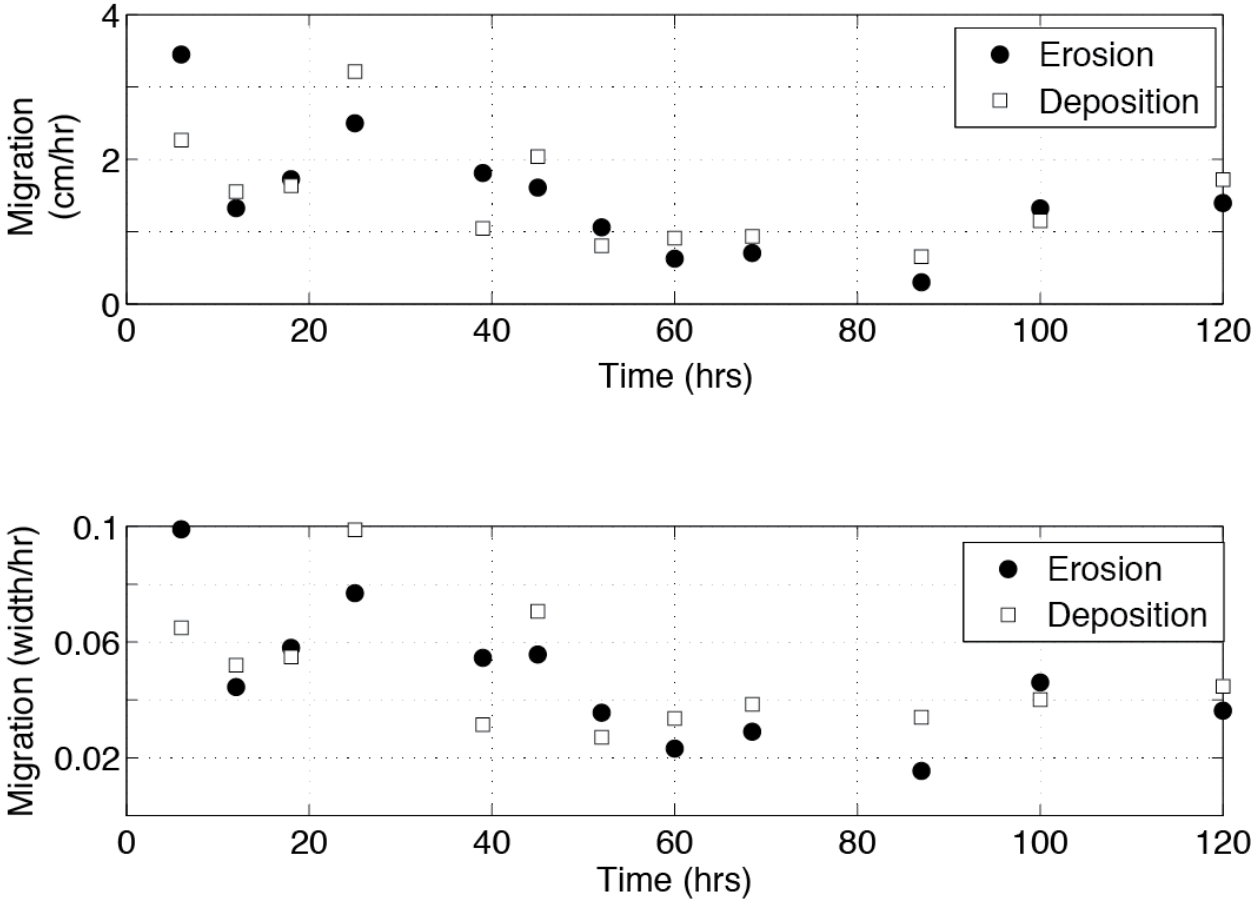


Figure 5.16. Average migration rate and through time downstream of x =6 m. Erosion and deposition rates are shown separately because the width changed through time. Migration rates are not included during surveys that include cutoffs.

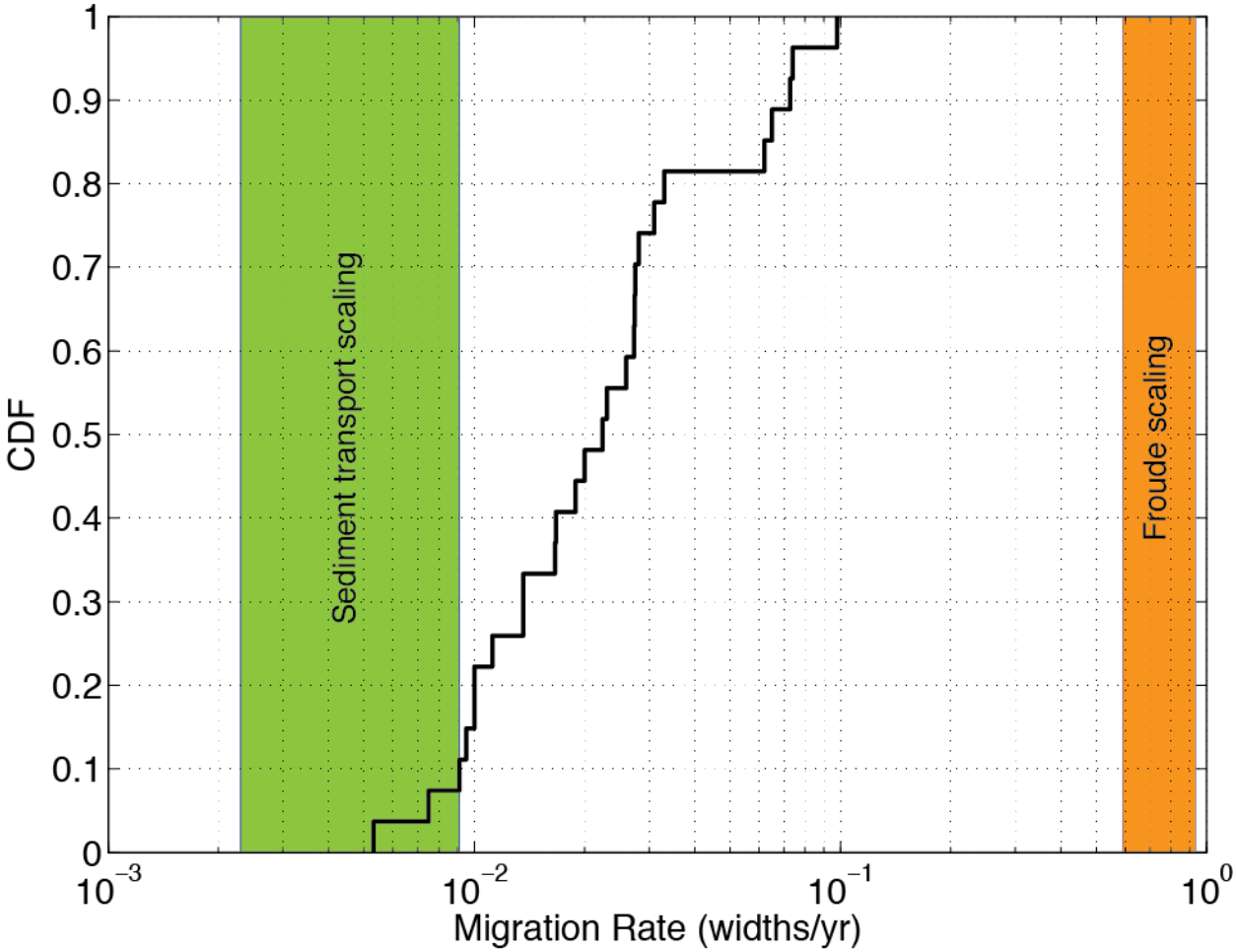


Figure 5.17. Comparison of migration rates for gravel-bed meanders with scaled migration rates from the experiment. The black line is the cumulative distribution function of channel migration rates in gravel-bed meanders from the database in Appendix B–Table B1. The shaded orange area shows the mean migration rate scaled to the field using Froude similarity (Equation 5.4) and the shaded green area shows mean migration rate scaled to the field using sediment transport similarity (Equation 5.5)

# 6 Bibliography


Alabyan, A. M. and Chalov, R. S. (1998). Types of river channel patterns and their natural controls. Earth Surface Processes and Landforms, 23(5), 467-474.

Allmendinger, N. E., Pizzuto, J. E., Potter, N., Johnson, T. E., and Hession, W. C. (2005). The influence of riparian vegetation on stream width, eastern Pennsylvania, USA. Geological Society of America Bulletin, 117(1), 229-243.

Amlin, N. M. and Rood, S. B. (2002). Comparative tolerances of riparian willows and cottonwoods to water-table decline. Wetlands, 22(2), 338-346.

Andrews, E. D. (1984). Bed-material entrainment and hydraulic geometry of gravel-bed rivers in colorado. Bulletin of the Geological Society of America, 95(3), 371-378.

Andrews, E. D. and Nankervis, J. M. (1995). Effective discharge and the design of channel maintenance flows for gravel bed rivers. In J. Costa (Ed.), Natural and anthropogenic influences in fluvial geomorphology, geophysical monograph 89. (pp. 151-64).

Asahi, K., Shimizu, Y., Nelson, J., and Parker, G. (2013). Numerical simulation of river meandering with self-evolving banks. Journal of Geophysical Research: Earth Surface, n/a.

ASCE Task Committee on Hydraulics, Bank Mechanics, and modelling of River Width Adjustment (1998). River width adjustment. I: Processes and mechanisms. Journal of Hydraulic Engineering, 124(9), 881-902.

Ashmore, P. E. and Church, M. (1998). Sediment transport and river morphology: A paradigm for study. Gravel-bed Rivers in the Environment, 115-148.

Barnard, P. L., Rubin, D. M., Harney, J., and Mustain, N. (2007). Field test comparison of an autocorrelation technique for determining grain size using digital 'beachball' camera versus traditional methods. Sedimentary Geology, 201, 180-195.

Beechie, T. J., Liermann, M., Pollock, M. M., Baker, S., and Davies, J. (2006). Channel pattern and river-floodplain dynamics in forested mountain river systems. Geomorphology, 78(1-2), 124-141.

Bellugi, D. (2012). What controls shallow landslide size across landscapes? PhD Thesis, UC Berkeley.

Bertoldi, W. and Tubino, M. (2005). Bed and bank evolution of bifurcating channels. Water Resources Research, 41, doi:10.1029/2004WR003333.

Blacknell, C. (1982). Morphology and surface sedimentary features of point bars in welsh gravel-bed rivers. Geological Magazine, 119(02), 181-192.

Blondeaux, P. and Seminara, G. (1985). A unified bar-bend theory of river meanders. Journal of Fluid Mechanics, 157, 449-470.

Bluck, B. J. (1971). Sedimentation in the meandering River Endrick. Scottish Journal of Geology, 7, 93-138.

Blum, M. D. and Törnqvist, T. E. (2000) Fluvial responses to climate and sea-level change: a review and look forward. Sedimentology, 47(s1), 2-48.

Braudrick, C. A., Dietrich, W. E., Leverich, G. T., and Sklar, L. S. (2009). Experimental evidence for the conditions necessary to sustain meandering in coarse-bedded rivers. Proceedings of the National Academy of Sciences, 106, 16936-16941.

Brice, J. C. (1964). Channel patterns and terraces of the Loup Rivers in Nebraska. Geological Survey Professional Paper, 422-D, D1-D41.

Brice, J. C. (1973). Meandering pattern of the White River in Indiana-an analysis. In M. Morisawa (Ed.), Fluvial geomorphology (M. Morisawa, Ed.). State University of New York, Binghampton.

Brice, J. C. (1974). Evolution of meander loops. Bulletin of the Geological Society of America, 85(4), 581-586.

Brownlie, W. R. (1981). Prediction of flow depth and sediment discharge in open channels. Report No. KH-R-43A, WM Keck Laboratory of Hydraulics and Water Resources, California Institute of Technology, Pasadena CA, 232.

Buffington, J. M. and Montgomery, D. R. (1997). A systematic analysis of eight decades of incipient motion studies, with special reference to gravel-bedded rivers. Water Resources Research, 33(8), 1993-2029.

Carson, M. A. (1984). The meandering-braided river threshold: A reappraisal. Journal of Hydrology, 73, 315-334.

Chang, H. H. (2006). Generalized computer program FLUVIAL-12, mathematical model for erodible channels, users manual. San Deigo State University, San Deigo, California.

Church, M. (2002). Geomorphic thresholds in riverine landscapes. Freshwater Biology, 47, 541-557.

Church, M. (2006). Bed material transport and the morphology of alluvial river channels. Annual Reviews of Earth and Planetary Science, 34, 325-354.

Church, M. and Rood, K. (1983). Catalogue of alluvial river channel regime data. In Department of geography, university of British Columbia. 99 p,

Clayton, J. A. (2010). Local sorting, bend curvature, and particle mobility in meandering gravel bed rivers. Water Resources Research, 56, W02601.

Clayton, J. A. and Pitlick, J. (2007). Spatial and temporal variations in bed load transport intensity in a gravel bed river bend. Water Resources Research, 43(2), W02426.

Colombini, M., Seminara, G., and Tubino, M. (1987). Finite-amplitude alternate bars. Journal of Fluid Mechanics, 181, 213-32.

Constantine, C. R. (2006). Quantifying the connection between flow, bar deposition, and meander migration in large gravel-bed rivers. Thesis, University of California, Santa Barbara.

Constantine, C. R., Dunne, T., and Hanson, G. J. (2009). Examining the physical meaning of the bank erosion coefficient used in meander migration modeling. Geomorphology, 106(3-4), 242-252.

Constantine, J. A., McLean, S. R., and Dunne, T. (2010). A mechanism of chute cutoff along large meandering rivers with uniform floodplain topography. Geological Society of America Bulletin, 122, 855-869.

Crosato, A. and Mosselman, E. (2009). Simple physics-based predictor for the number of river bars and the transition between meandering and braiding. Water Resources Research, 45, W03424.

Cui, Y., Parker, G., Lisle, T. E., Gott, J., Hansler-Ball, M. E., Pizzuto, J. E., et al. (2003). Sediment pulses in mountain rivers: 1. Experiments. Water Resources Research, 39(9), 1239.

Cui, Y. and Parker, G. (2005) Numerical model of sediment pulses and sediment-supply disturbances in mountain rivers. Journal of hydraulic engineering, 131, 646.

Cui, Y. and Wilcox, A. (2008). Development and application of numerical models of sediment transport associated with dam removal. Chapter, 23, 995-1020.

Davies, N. S. and Gibling, M. R. (2010). Paleozoic vegetation and the Siluro-Devonian rise of fluvial lateral accretion sets. Geology, 38, 51-54.

Dietrich, W. E. (1982). Settling velocity of natural particles. Water Resources Research, 18(6), 1615-1626.

Dietrich, W. E. and Smith, J. D. (1984). Bed load transport in a river meander. Water Resources Research, 20(10), 1355-1380.

Dietrich, W. E., Smith, J. D. and Dunne, T. (1984). Boundary shear stress, sediment transport and bed morphology in a sand-bedded river meander during high and low flow, River Meandering (C. M. Elliot, ed.). Proceedings of the Conference Rivers '83, 632-639.

Dietrich, W. E. (1987) Mechanics of flow and sediment transport in river bends. River Channels: Environment and Process, 179-227.

Dietrich, W. E., Kirchner, J. W., Ikeda, H., and Iseya, F. (1989). Sediment supply and the development of the coarse surface layer in gravel-bedded rivers. Nature, 340 (6230), 215-217.

Dietrich, W. E. and Whiting, P. (1989). Boundary shear stress and sediment transport in river meanders of sand and gravel. In S. Ikeda and G. Parker (Eds.), River meandering, American Geophysical Union Water Resources Monograph. (pp. 1-50). Washington DC: American Geophysical Union.

Dietrich, W. E., Day, G., and Parker, G. (1999). The Fly River, Papua New Guinea: Inferences about river dynamics, floodplain sedimentation and fate of sediment. Varieties of Fluvial Form, 345-376.

Dietrich, W. E., Nelson, P. A., Yager, E., Venditti, J. G., Lamb, M. P. and Collins, L. (2006). Sediment patches, sediment supply, and channel morphology. In G. Parker and M. H. Garcia (Eds.), River, Coastal and Estuarine: Morphodynamics, RCEM 2005, 79-90.

Doyle, M. W., Stanley, E. H., and Harbor, J. M. (2003). Channel adjustments following two dam removals in Wisconsin. Water Resources Research, 39(1), 1011.

Dunne, T. and Leopold, L. B. (1979). Water in Environmental Planning, 818 pp. WH Freeman, New York.

Dunne, T., Dietrich, W. E., Humphrey, N. F., and Tubbs, D. W. (1981). Geologic and geomorphic implications for gravel supply. In Proceedings of the conference on salmon-spawning gravel: A renewable resource in the Pacific Northwest.

Dunne, T., Constantine, J. A., and Singer, M. B. (2010). The role of sediment transport and sediment supply in the evolution of river channel and floodplain complexity. Transactions Japanese Geomorphological Union, 31, 155-170.

Eaton, B. C. and Church, M. (2004). A graded stream response relation for bed load-dominated streams. Journal of Geophysical Research, 109,1-18.

Eaton, B. C. and Church, M. (2009). Channel stability in bed load-dominated streams with nonerodible banks: Inferences from experiments in a sinuous flume. Journal of Geophysical Research, 114, F01024.

Eaton, B. C., Millar, R. G., and Davidson, S. (2010). Channel patterns: Braided, anabranching, and single-thread. Geomorphology, 120(3-4), 353-364.

Emmett, W. W. (1972). The hydraulic geometry of some Alaskan streams south of the Yukon River. US Geological Survey Open File Report, 102.

Erwin, S. O. (2012). Point bars and sediment supply. PhD Thesis, Utah State University.

Erwin, S. O., Braudrick, C. A., Wilcock, P. R., and Lightbody, A. (In preparation). Influence of sediment supply on point bar morphology in laboratory meander.

Federici, B. and Paola, C. (2003). Dynamics of channel bifurcations in noncohesive sediments. Water Resources Research, 39(6).

Federici, B. and Seminara, G. (2003). On the convective nature of bar instability. Journal of Fluid Mechanics, 487, 125-145.

Ferguson, R., Hoey, T., Wathen, S., and Werritty, A. (1996). Field evidence for rapid downstream fining of river gravels through selective transport: Geology, v. 24. Doi, 10, 0091-7613.

Ferguson, R. I. (1981). Channel form and channel changes. British Rivers, 90, 125.

Ferguson, R. I. (1987). Hydraulic and sedimentary controls of channel pattern. In River channels: Environment and process. (pp. 129-58). Blackwell: Oxford.

Fisk, H. N. (1944). Geological investigation of the alluvial valley of the Lower Mississippi River. Vicksburg, Mississippi: Mississippi River Commission.

Francalanci, S., Solari, L., Toffolon, M., and Parker, G. (2012). Do alternate bars affect sediment transport and flow resistance in gravel-bed rivers? Earth Surface Processes and Landforms, 37(8), 866-875.

Friedkin, J. F. (1945). A laboratory study of the meandering of alluvial rivers. United States Waterways Experiment Station.

Garcia, M. and Nino, Y. (1993). Dynamics of sediment bars in straight and meandering channels: Experiments on the resonance phenomenon. Journal of Hydraulic Research, 31(6), 739-761.

Garcia, M. H. (2008). Sediment transport and morphodynamics. In Sedimentation engineering: Processes, measurements, modeling and practice, edited by MH García. (pp. 21-164).

Gay, G. R., Gay, H. H., Gay, W. H., Martinson, H. A., Meade, R. E., and Moody, J. A. (1998). Evolution of cutoffs across meander necks in Powder River, Montana, USA. Earth Surface Processes and Landforms, 23, 651-662.

Gilbert, G. K. (1917). Hydraulic-mining debris in the Sierra Nevada: US geol. Survey Prof. Paper, 105, 154.

Gran, K. and Paola, C. (2001). Riparian vegetation controls on braided stream dynamics. Water Resources Research, 37(12), 3275-83.

Gustavson, T. C. (1978). Bed forms and stratification types of modern gravel meander lobes, Nueces River, Texas. Sedimentology, 25(3), 401-426.

Harrison, L. R., Legleiter, C. J., Wydzga, M. A. and Dunne, T. (2011) Channel dynamics and habitat development in a meandering, gravel bed river. Water Resources Research, 47(4).

Henderson, F. M. (1966). Open channel flow. New York, NY: MacMillan.

Hession, W. C., Pizzuto, J. E., Johnson, T. E., and Horwitz, R. J. (2003). Influence of bank vegetation on channel morphology in rural and urban watersheds. Geology, 31, 147-151.

Hey, R. D. and Thorne, C. R. (1986). Stable channels with mobile gravel beds. Journal of Hydraulic Engineering, 112(8), 671-689.

Hickin, E. J. (1984). Vegetation and river channel dynamics. The Canadian Geographer, 28(2), 111-126.

Hickin, E. J. and Nanson, G. C. (1984). Lateral migration rates of river bends. Journal of Hydraulic Engineering, 110(11), 1557-1567.

Hoffman, D. F. and Gabet, E. J. (2007). Effects of sediment pulses on channel morphology in a gravel-bed river. Geological Society of America Bulletin, 119, 116-125.

Hooke, J. M. (1995). River channel adjustment to meander cutoffs on the River Bollin and River Dane, northwest England. Geomorphology, 14(3), 235-253.

Hooke, J. M. (2003). River meander behaviour and instability: A framework for analysis. Transactions of the Institute of British Geographers, 28(2), 238-253.

Hooke, J. M. (2004). Cutoffs galore!: Occurrence and causes of multiple cutoffs on a meandering river. Geomorphology, 61(3-4), 225-238.

Hooke, J. M. (2007). Complexity, self-organisation and variation in behaviour in meandering rivers. Geomorphology, 91(3-4), 236-258.

Howard, A. D. (1992). Modeling channel migration and floodplain sedimentation in meandering streams. In P. A. Carling and G. E. Petts (Eds.), Lowland floodplain rivers. (pp. 1-41). John Wiley and Sons.

Hudson, P. F. and Kesel, R. H. (2000). Channel migration and meander-bend curvature in the lower Mississippi River prior to major human modification. Geology, 28, 531-534.

Ikeda, H. (1983). Experiments on bedload transport, bed forms, and sedimentary structures using fine gravel in the 4-meter-wide flume. Environmental Research Center Papers, 2, 1-78.

Ikeda, H. (1989). Sedimentary controls on channel migration and origin of point bars in sand-bedded meandering rivers. Water Resources Monograph, 12, 51-68.

Ikeda, H. and Iseya, F. (1988). Experimental study of heterogeneous sediment transport. Environmental Research Center Papers, 12, 1-51.

Ikeda, S., Parker, G., and Sawai, K. (1981). Bend theory of river meanders. Part 1. Linear development. Journal of Fluid Mechanics, 112, 363-377.

Jackson, R. G.II (1976). Depositional model of point bars in the lower Wabash River. Journal of Sedimentary Petrology, 46, 579-594.

Jang, C. L. and Shimizu, Y. (2007). Vegetation effects on the morphological behavior of alluvial channels. Journal of Hydraulic Research, 45(6), 763-772.

Johannesson, H. and Parker, G. (1989). Linear theory of river meanders. In S. Ikeda and G. Parker (Eds.), River Meandering. (pp. 181-213). American Geophysical Union.

Juracek, K. E. and Perry, C. A. (2005). Gravel sources for the Neosho River in Kansas, 2004. USGS Scientific Investigations Report, 2005–5282.

Kellerhals, R., Church, M. and Bray, D. I. (1976) Classification and analysis of river processes. ASCE Journal of the Hydraulics Division, 102, 813-830.

Kleinhans, M. G. (2010). Sorting out river channel patterns. Progress in Physical Geography, 34(3), 287.

Kleinhans, M. G. and van den Berg, J. H. (2010). River channel and bar patterns explained and predicted by an empirical and physics-based method. Earth Surface Proceses and Landforms.

Knighton, A. D. (1998). Fluvial forms and processes. Arnold London.

Kondolf, G. M. (2006). River restoration and meanders. Ecology and Society, 11(2), 42.

Kondolf, G. M., Smeltzer, M. W., and Railsback, S. F. (2001). Design and performance of a channel reconstruction project in a coastal California gravel-bed stream. Environmental Management, 28(6), 761-776.

Kreig, R. A. (1977). Terrain analysis for the Trans-Alaska Pipeline. Civil Engineering Magazine, 47(7), 61-65.

Lamb, M. P., Dietrich, W. E. and Venditti, J. G. (2008) Is the critical Shields stress for incipient sediment motion dependent on channel-bed slope? Journal of Geophysical Research F, 113(F2), F02008.

Lanzoni, S. (2000a) Experiments on bar formation in a straight flume, 1. Uniform sediment. Water Resources Research, 36(11), 3337-3349.

Lanzoni, S. (2000b). Experiments on bar formation in a straight flume 2. Graded sediment. Water Resources Research, 36(11), 3351-3363.

Lauer, J. W. and Parker, G. (2008). Net local removal of floodplain sediment by river meander migration. Geomorphology, 96(1-2), 123-149.

Legleiter, C. J. and Kyriakidis, P. C. (2006). Forward and inverse transformations between Cartesian and channel-fitted coordinate systems for meandering rivers. Mathematical Geology, 38(8), 927-958.

Legleiter, C. J., Harrison, L. R. and Dunne, T. (2011) Effect of point bar development on the local force balance governing flow in a simple, meandering gravel bed river. Journal of Geophysical Research, 116 (F1).

Leopold, L. B. and Wolman, M. G. (1957). River channel patterns: Braided, meandering and straight. US Geological Survey Professional Paper 282-B, 282-B, 85 pp.

Leopold, L. B. and Wolman, M. G. (1960). River meanders. Geological Society of America Bulletin, 71, 769-794.

Leopold, L. B. (1992). Sediment size that determines channel morphology. In P. Billi, R. D. Hey, C. R. Thorne, and P. Taconi (Eds.), Dynamics of gravel-bed rivers. (pp. 297-311). John Wiley and Sons Ltd.

Leopold, L. B. and Emmett, W. W. (1997) Bedload and River Hydraulics: Inferences from the East Fork River, Wyoming. US Geological Survey Professional Paper, 1583, 52 p.

Levey, R. A. (1977). Bed-form distribution and internal stratification of coarse-grained point bars, Upper Congaree River, SC. Canadian Society of Petroleum Geologists, Memoir 5, 105-127.

Lisle, T. E. (1982). Effects of aggradation and degradation on riffle-pool morphology in natural gravel channels, Northwestern California. Water Resources Research, 18(6), 1643-1651.

Lisle, T. E. and Hilton, S. (1992). The volume of fine sediment in pools: An index of sediment supply in gravel-bed streams. Water Resources Bulletin, 26.

Lisle, T. E., Iseya, F., and Ikeda, H. (1993). Response of a channel with alternate bars to decrease in supply of mixed-size bedload: A flume experiment. Water Resources Research, 29, 3623-3629.

Luchi, R., Zolezzi, G., and Tubino, M. (2010a). Modelling mid-channel bars in meandering channels. Earth Surface Processes and Landforms, 35(8), 902-917.

Luchi, R., Hooke, J. M., Zolezzi, G., and Bertoldi, W. (2010b). Width variations and mid-channel bar inception in meanders: River Bollin (UK). Geomorphology, 119(1-2), 1-8.

Mackin, J. H. (1948). Concept of the graded river. Geological Society of America Bulletin, 59(5), 463-512.

Madej, M. A. (1978). Response of a stream channel to increased sediment load. In M.S. Thesis, University of Washington. Thesis,

Madej, M. A. and Ozaki, V. (1996). Channel response to sediment wave propagation and movement, Redwood Creek, California, USA. Earth Surface Processes and Landforms, 21, 911-927.

Madej, M. A., Sutherland, D. G., Lisle, T. E., and Pryor, B. (2009). Channel responses to varying sediment input: A flume experiment modeled after Redwood Creek, California. Geomorphology, 103, 507-519.

Major, J. J., OConnor, J. E., Podolak, C. J., Keith, M. K., Grant, G. E., Spicer, K. R., et al. (2012). Geomorphic response of the Sandy River, Oregon, to removal of Marmot Dam. US Department of the Interior, US Geological Survey.

Manga, M. and Kirchner, J. W. (2000). Stress partitioning in streams by large woody debris. Water Resources Research, 36(8), 2373-2379.

McGowen, J. H. and Garner, L. E. (1970). Physiographic features and stratification types of coarse grained point bars: Modern and ancient examples. Sedimentology, 14, 77-111.

McKean, J. A., Isaak, D. J., and Wright, C. W. (2008). Geomorphic controls on salmon nesting patterns described by a new, narrow-beam terrestrial–aquatic lidar. Frontiers in Ecology and the Environment, 6(3), 125-130.

McKean, J. and Tonina, D. (2013). Bed stability in unconfined gravel bed mountain streams: With implications for salmon spawning viability in future climates. Journal of Geophysical Research: Earth Surface, n/a.

Meyer-Peter, E. and Müller, R. (1948). Formulas for bed-load transport. In Proceedings of the 2nd meeting of the international association for hydraulic structures research.

Métivier, F. and Barrier, L. (2012). Alluvial landscape evolution: What do we know about metamorphosis of gravel-bed meandering and braided streams? In M. Church, P. M. Biron, and A. G. Roy (Eds.), Gravel-bed rivers: Processes, tools, environments. (pp. 474-501). Wiley Online Library.

Micheli, E. R. and Kirchner, J. W. (2002). Effects of wet meadow riparian vegetation on streambank erosion. 1. Remote sensing measurements of streambank migration and erodibility. Earth Surface Processes and Landforms, 27, 627-639.

Micheli, E. R. and Larsen, E. W. (2010). River channel cutoff dynamics, Sacramento River, California, USA. River Research and Applications.

Millar, R. G. (2000). Influence of bank vegetation on alluvial channel patterns. Water Resources Research, 36, 1109-1118.

Miwa, H., Daido, A., and Katayama, T. (2005). Effect of river bed degradation and aggradation on transformation of alternate bar morphology. River, Coastal, and Estuarine Morphodynamics, 1, 471.

Montefusco, L. and Tacconi, P. (1984). Effects of river meander stabilization. In River meandering.

Moore, J. M., Howard, A. D., Dietrich, W. E. and Schenk, P. M. (2003). Martian Layered Fluvial Deposits: Implications for Noachian Climate Scenarios. Geophysical Research Letters, 30(24).

Mueller, E. R. and Pitlick, J. (2005). Variation in the reference shields stress for bed load transport in gravel-bed streams and rivers. Water Resources Research, 41(4).

Mueller, E. R. and Pitlick, J. (2013). Sediment supply and channel morphology in mountain river systems: 1. Relative importance of lithology, topography and climate. Journal of Geophysical Research: Earth Surface, n/a.

Nanson, G. C. (1980). Point bar and floodplain formation of the meandering Beatton River, northeastern British Columbia, Canada. Sedimentology, 27(1), 3-29.

Nanson, G. C. and Hickin, E. J. (1986). A statistical analysis of bank erosion and channel migration in western Canada. Bulletin of the Geological Society of America, 97(4), 497-504.

Neill, C. R. (1984). Bank erosion vs bedload transport in a gravel river. River Meandering: Proceedings of the Conference on Rivers '83, New Orleans, LA, 204-211.

Nelson, J. M. and Smith, J. D. (1989). Flow in meandering channels with natural topography. River Meandering, 69-102.

Nelson, P. A., Venditti, J. G., Dietrich, W. E., Kirchner, J. W., Ikeda, H., Iseya, F., et al. (2009). Response of bed surface patchiness to reductions in sediment supply. J. Geophys. Res, 114.

Nixon, M. (1959) A study of the bank-full discharges of rivers in England and Wales. Proceedings of the Institute of Civil Engineering, 12(2), 157-174.

Parker, G. (1976). On the cause and characteristic scales of meandering and braiding in rivers. Journal of Fluid Mechanics, 76.

Parker, G. (1979). Hydraulic geometry of active gravel rivers. Journal of the Hydraulics Division, 105(9), 1185-1201.

Parker, G. and Klingeman, P. C. (1982). On why gravel bed streams are paved. Water Resources Research, 18(5), 1409-1423.

Parker, G., Toro-Escobar, C. M., Ramey, M., and Beck, S. (2003). Effect of floodwater extraction on mountain stream morphology. Journal of Hydraulic Engineering, 129, 885-895.

Parker, G., Wilcock, P. R., Paola, C., Dietrich, W. E., and Pitlick, J. (2007). Physical basis for quasi-universal relations describing bankfull hydraulic geometry of single-thread gravel bed rivers. Journal of Geophysical Research, 112(F4).

Parker, G., Shimizu, Y., Wilkerson, G. V., Eke, E. C., Abad, J. D., Lauer, J. W., et al. (2011). A new framework for modeling the migration of meandering rivers. Earth Surface Processes and Landforms, 36(1), 70-86.

Peakall, J., Ashworth, A., and Best, J. (1996). Physical modelling in fluvial geomorphology: Principles, applications, and unresolved issues. In B. L. Rhoads and C. E. Thorn (Eds.), The scientific nature of geomorphology: Proceedings of the 27th Binghamton Symposium in Geomorphology held 27-29 September 1995. (pp. 221-53).

Peakall, J., Ashworth, P. J., and Best, J. L. (2007). Meander-bend evolution, alluvial architecture, and the role of cohesion in sinuous river channels: A flume study. Journal of Sedimentary Research, 77, 197-212.

Pickup, G. and Cui, Y. (2008). Modeling the impact of tailings and waste rock disposal on the fly river system. Developments in Earth and Environmental Sciences, 9, 257-289.

Pitlick, J., Mueller, E. R., and Segura, C. (2012). Differences in sediment supply to braided and single-thread river channels: What do the data tell us? In M. Church, P. M. Biron, and A. G. Roy (Eds.), Gravel-bed rivers: Processes, tools, environments. (pp. 502-10). Wiley.

Pizzuto, J. E. (1994). Channel adjustments to changing discharges, Powder River, Montana. Geological Society of America Bulletin, 106, 1494-1501.

Podolak, C. J. P. and Wilcock, P. R. (2013). Experimental study of the response of a gravel streambed to increased sediment supply. Earth Surface Processes and Landforms, 38(14), 1748-1764.

Pollen, N. and Simon, A. (2006). Geotechnical implications for the use of alfalfa in experimental studies of alluvial-channel morphology and planform. In AGU fall meeting abstracts.

Pryor, B. S., Lisle, T., Montoya, D. S., and Hilton, S. (2011). Transport and storage of bed material in a gravel-bed channel during episodes of aggradation and degradation: A field and flume study. Earth Surface Processes and Landforms, 36(15), 2028-2041.

Rowland, J. C. (2007). Tie Channels. PhD Dissertation, UC Berkeley

Rozovskii, I. L. (1957). Flow of water in bends of open channels. Academy of Sciences of the Ukrainian SSR.

Rubin, D. M. (2004). A simple autocorrelation technique for determining grain size from images of sediment. Journal of Sedimentary Research, 74, 160-165.

Schattner, I. (1962). The lower Jordan Valley: A study in the fluviomorphology of an arid region. Magnes Press, Hebrew University.

Schumm, S. A. (1963). A tentative classification of alluvial river channels. US Geological Survey Circular, 477(10).

Schumm, S. A. and Khan, H. R. (1972). Experimental study of channel patterns. Bulletin of the Geological Society of America, 83(6), 1755-1770.

Schumm, S. A. (1968). River adjustment to altered hydrologic regimen—: Murrumbidgee River and paleochannels, Australia. US Geol. Survey Prof. Paper, 598, 65.

Schumm, S. A. (1985). Patterns of alluvial rivers. Annual Reviews in Earth and Planetary Sciences, 13(1), 5-27.

Self, R. P. (1983). Petrologic variation in Pliocene to Quaternary gravels of southeastern Louisiana. Transactions of the Gulf Coast Association of Geological Societies, 33, 407-415.

Seminara, G. (2006). Meanders. Journal of Fluid Mechanics, 554, 271-297.

Seminara, G. and Tubino, M. (1989). Alternate bars and meandering: Free, forced and mixed interactions. Water Resources Monograph, 12, 267-320.

Simon, A., Dickerson, W., and Heins, A. (2004). Suspended-sediment transport rates at the 1.5-year recurrence interval for ecoregions of the United States: Transport conditions at the bankfull and effective discharge? Geomorphology, 58(1-4), 243-262.

Smith, J. D. (2004). The role of riparian shrubs in preventing floodplain unraveling along the Clark Fork of the Columbia river in the Deer Lodge Valley, Montana. In S. J. Bennett and A. Simon (Eds.), Riparian vegetation and fluvial geomorphology, Water Sci. Appl. Vol 8. (pp. 71-85).

Smith, N. D., Cross, T. A., Dufficy, J. P., and Clough, S. R. (1989). Anatomy of an avulsion. Sedimentology, 36(1), 1-23.

Smith, C. E. (1998) Modeling high sinuosity meanders in a small flume. Geomorphology, 25, 19-30.

Smith, S. M. and Prestegaard, K. L. (2005). Hydraulic performance of a morphology-based stream channel design. Water Resources Research, 41(11), W11413.

Sun, T., Meakin, P., and Jøssang, T. (2001). A computer model for meandering rivers with multiple bed load sediment sizes 1. Theory. Water Resources Research, 37(8), 2227-2241.

Sun, T., Meakin, P., Jossang, T., and Schwarz, K. (1996). A simulation model for meandering river. Water Resources Research, 32, 2937-2954.

Tal, M. and Paola, C. (2007). Dynamic single-thread channels maintained by the interaction of flow and vegetation. Geology, 35(4), 347.

Tal, M. and Paola, C. (2010). Effects of vegetation on channel morphodynamics: Results and insights from laboratory experiments. Earth Surface Processes and Landforms, 35(9), 1014-1028.

Tanaka, K., Shimizu, Y., Yamaguchi, S., Iwaskai, T., Kimura, I. and Tanaka, G. (2011) Geomorphological characteristics of female and male-type meanders. River, Coastal and Estuarine Morphodynamics: RCEM2011.

Torizzo, M. and Pitlick, J. (2004). Magnitude-frequency of bed load transport in mountain streams in Colorado. Journal of Hydrology, 290(1-2), 137-151.

Trush, W. J., McBain, S. M., and Leopold, L. B. (2000). Attributes of an alluvial river and their relation to water policy and management. Proceedings of the National Academy of Sciences, 97(22), 11858.

van den Berg, J. H. (1995). Prediction of alluvial channel pattern of perennial rivers. Geomorphology, 12(4), 259-279.

van Dijk, W. M., van de Lageweg, W. I., and Kleinhans, M. G. (2012). Experimental meandering river with chute cutoffs. Journal of Geophysical Research, 117(F3).

van Dijk, W. M., van de Lageweg, W. I., and Kleinhans, M. G. (2013). Formation of a cohesive floodplain in a dynamic experimental meandering river. Earth Surface Processes and Landforms,.

Venditti, J. G., Dietrich, W. E., Nelson, P. A., Wydzga, M. A., Fadde, J., and Sklar, L. (2010). Effect of sediment pulse grain size on sediment transport rates and bed mobility in gravel bed rivers. Journal of Geophysical Research, 115(F3).

Venditti, J. G., Nelson, . P. A., Minear, J. T., Wooster, J., and Dietrich, W. E. (2012). Alternate bar response to sediment supply termination. Journal of Geophysical Research, 117(F2).

Viereck, L. A. (1970). Forest succession and soil development adjacent to the Chena River in interior Alaska. Arctic and Alpine Research, 2(1), 1.

Walling, D. E. and Webb, B. W. (1987). Suspended load in gravel-bed rivers: UK experience. Sediment Transfer in Gravel-Bed Rivers. John Wiley and Sons New York. 1987. P 691-723, 8 Tab, 11 Fig, 54 Ref.

Wathen, S. J. and Hoey, B. (1998). Morphological controls on the downstream passage of a sediment wave in a gravel-bed stream. Earth Surface Processes and Landforms, 23, 715-730.

Whiting, P. J. and Dietrich, W. E. (1993a). Experimental Studies of Bed Topography and Flow Patterns in Large-amplitude Meanders: 1. Observations, 29, 3605-3614.

Whiting, P. J. and Dietrich, W. E. (1993b). Experimental constraints on bar migration through bends: Implications for meander wavelength selection. Water Resources Research, 29, 1091-1102.

Wilcock (1998). Two-Fraction model of initial sediment motion in gravel-bed rivers. Science (New York, N.Y.), 280, 410-412.

Wilcock, P. R. and Kenworthy, S. T. (2002). A two-fraction model for the transport of sand/gravel mixtures. Water Resources Research, 38(10).

Wilcock, P. R. and McArdell, B. W. (1997). Partial transport of a sand/gravel sediment. Water Resources Research, 33(1), 235-245.

Wilkerson, G. V. and Parker, G. (2011). Physical basis for quasi-universal relationships describing bankfull hydraulic geometry of sand-bed rivers. Journal of Hydraulic Engineering, 137(7), 739-753.

Wolman, M. G. and Brush, L. M. (1961). Factors controlling the size and shape of stream channels in coarse noncohesive sands. U.S. Geol. Surv. Prof. Paper , 282-G, 183-210.

Xu, J. (2008). Discrimination of channel patterns for gravel- and sand-bed rivers. Zeitschrift Für Geomorphologie, 52(4), 503-523.

Yalin, M. S. (1971). Theory of hydraulic models. The MacMillan Press, Ltd.

Zinger, J. A., Rhoads, B. L., and Best, J. L. (2011). Extreme sediment pulses generated by bend cutoffs along a large meandering river. Nature Geoscience, 4, 675-678.

Zolezzi, G. and Seminara, G. (2001). Downstream and upstream influence in river meandering. Part 1. General theory and application to overdeepening. Journal of Fluid Mechanics, 438, 183-211.

Zolezzi, G., Luchi, R., and Tubino, M. (2009). Morphodynamic regime of gravel bed, single-thread meandering rivers. Journal of Geophysical Research, 114(F1), F01005.

# Appendix A-Supplemental Video 1

Supplemental Video 1. The video consists of overhead photographs of the flume every 30 minutes and the experimental hydrograph. On the overhead photographs, Flow is from left to right and the entire flume width is shown. The brown sediment is sorted coarse sediment that made up the bed and floodplain prior to the experiments, the white sediment is fine sediment, and the blue sediment is identical to the brown, but fed from the upstream end of the flume.

# Appendix B-Morphologic river data used in Chapter 3

This appendix contains tables of the data used in Chapter 3.

## List of Tables

Table B1a. The location, data source, and planform characteristics of gravel-bed meanders in Chapter 3 ..... 145
Table B1b. Physical characteristics of gravel-bed meanders in Chapter 3. ..... 155
Table B2a. The location, data source, and planform characteristics of sand meanders in Chapter 3 ..... 161
Table B2b. Hydraulic characteristics of sand meanders in Chapter 3. ..... 155
Table B3a. The location, data source, and planform characteristics of gravel braided rivers in Chapter 3 ..... 145
Table B3b. Hydraulic characteristics of gravel braided rivers in Chapter 3. ..... 155

**Table B1a. The location, data source, and planform characteristics of gravel bed meanders in Chapter 3. Sources are listed at the end of the table. Hydraulic characteristics are given Table B1b.**

| River | Source Number | Location | Latitude (dd) | Longitude (dd) | Elevation (m) | Islands[a] | Cutoffs[b] | Land Use Code[c] | Veg. Code[d] | notes |
|---|---|---|---|---|---|---|---|---|---|---|
| East Fork | 1 | Clothesline Reach | 42.68 | -109.57 | 2160 | 3 | 1 | 4 | 2 | - |
| Frazer | 2 | Near Winter Park | 39.90 | -105.77 | 2744 | 1 | 0 | 2 | 3 | - |
| East Inlet | 2 | Near Grand Lake | 40.24 | -105.80 | 2592 | 0 | 1 | 4 | 2 | - |
| North Platte | 2 | near North Gate | 40.94 | -106.34 | 2383 | 0 | 1 | 4 | 2 | - |
| Stillwater | 2 | above Granby Reservoir | 40.19 | -105.90 | 2538 | 2 | 1 | 4 | 1 | - |
| Williams Fork | 2 | at mouth near Hamilton | 39.83 | -106.06 | 2678 | 0 | 1 | 4 | 2 | - |
| Little Muddy | 2 | near Parshall | 39.76 | -105.70 | 2632 | 0 | 0 | 2 | 4 | - |
| Little Grizzly | 2 | above Hebron | 40.58 | -106.45 | 2485 | 0 | 1 | 4 | 2 | - |
| Little Snake | 2 | near Slater, CO, USA | 41.00 | -107.14 | 2082 | 3 | 1 | 4 | 2 | - |
| Little Snake | 2 | near Dixon, CO, USA | 41.03 | -107.55 | 1934 | 3 | 1 | 1 | 2 | - |
| Elk | 2 | near Trull, CO, USA | 40.52 | -106.93 | 2017 | 2 | 1 | 1 | 2 | - |
| Yampa | 2 | near Hayden, CO, USA | 40.50 | -107.20 | 1945 | 3 | 1 | 1 | 3 | - |
| Yampa | 2 | near Maybell, CO, USA | 40.53 | -108.08 | 1797 | 3 | 1 | 1 | 3 | - |
| Sagehen | 3 | Near gauge | 39.43 | -120.24 | 1936 | 1 | 0 | 3 | 2 | - |
| WF Humptulips | 4 | - | 47.29 | -123.83 | 80 | 1 | 1 | 3 | 4 | Estimated location subtle cutoffs |
| Wynoochee | 4 | - | 47.17 | -123.63 | 68 | 3 | 1 | 1 | 3 | Estimated location |
| Chehalis | 4 | - | 46.82 | -123.22 | 25 | 3 | 1 | 1 | 3 | - |
| Nisqually W | 4 | - | 47.00 | -122.63 | 29 | 2 | 1 | 3 | 4 | - |
| Snoqualmie | 4 | at Carnation | 47.67 | -121.92 | 14 | 1 | 1 | 1 | 3 | - |
| Chehalis | 4 | at Porter | 46.94 | -123.31 | 9 | 1 | 1 | 1 | 4 | - |
| Willapa | 4 | at Willapa | 46.67 | -123.67 | 1 | 0 | 0 | 1 | 2 | - |
| Chehalis | 4 | at Doty | 46.63 | -123.28 | 99 | 0 | 0 | 1 | 4 | - |
| Green | 4 | - | 47.27 | -122.10 | 44 | 1 | 1 | 3 | 4 | Estimated location |

| River | Source Number | Location | Latitude (dd) | Longitude (dd) | Elevation (m) | Islands[a] | Cutoffs[b] | Land Use Code[c] | Veg. Code[d] | notes |
|---|---|---|---|---|---|---|---|---|---|---|
| Salmon | 5 | at mouth | 50.70 | -119.32 | 347 | 0 | 1 | 1 | 3 | - |
| Bonaparte | 5 | at Cache Creek | 50.83 | -121.34 | 464 | 3 | 1 | 1 | 3 | - |
| Chase | 5 | at Turtle Valley Road | 50.78 | -119.65 | 601 | 0 | 0 | 1 | 3 | - |
| Deadman | 5 | - | 50.85 | -120.95 | 483 | 3 | 1 | 1 | 2 | - |
| Tywi | 6 | Dryslwyn reach | 51.87 | -4.11 | 15 | 3 | 1 | 1 | 2 | Channel slope calculated from valley slope and sinuosity |
| Endrick | 7 | - | 56.06 | -4.48 | 11 | 0 | 1 | 1 | 2 | 1 island associated with bridge |
| Squamish | 8 | Southwest BC | 49.86 | -123.23 | 23 | 3 | 1 | 3 | 4 | - |
| Selwyn | 9 | near Malvern Hills | -43.46 | 171.90 | 300 | 3 | 1 | 1 | 2 | Location approximate |
| Little Eachaig | 10 | at Dalinlongart, UK | 56.00 | -4.98 | 12 | 3 | 1 | 1 | 3 | Reach 1 bend long |
| Lune | 10 | - | 54.08 | -2.73 | 14 | 1 | 0 | 1 | 1 | - |
| Arrow | 11 | Titley UK | 52.22 | -2.98 | 129 | 0 | 0 | 1 | 4 | - |
| Irfon (1) | 11 | - | 52.13 | -3.51 | 157 | 0 | 0 | 1 | 4 | - |
| Irfon (2) | 11 | - | 52.13 | -3.51 | 157 | 0 | 0 | 1 | 4 | - |
| Klondike | 12 | upstr. Bonanza Creek, YT, Canada | 64.03 | -139.23 | 319 | 3 | 0 | 4 | 2 | Cutoffs not visible, floodplain dredger mined |
| Yukon | 12 | at Carmacks, YT, Canada | 62.07 | -136.02 | 498 | 2 | 0 | 3 | 4 | Narrow valley |
| Pelly | 12 | at Pelly Crossing, YT, Canada | 62.82 | -136.50 | 476 | 3 | 1 | 3 | 4 | - |
| Stewart | 12 | at Mayo, YT, Canada | 63.58 | -135.95 | 519 | 3 | 1 | 3 | 4 | - |
| Fall (1) | 13 | Reach 4 | 40.40 | -105.62 | 2598 | 1 | 1 | 4 | 1 | Location approximate |
| Fall (2) | 13 | Reach 5 | 40.40 | -105.62 | 2598 | 1 | 1 | 4 | 1 | Location approximate |

| River | Source Number | Location | Latitude (dd) | Longitude (dd) | Elevation (m) | Islands[a] | Cutoffs[b] | Land Use Code[c] | Veg. Code[d] | notes |
|---|---|---|---|---|---|---|---|---|---|---|
| Colorado | 14 | Colorado National Park | 40.32 | -105.86 | 2670 | 1 | 1 | 4 | 1 | - |
| Sacramento | 15 | (RM 195-170) | 39.67 | -121.98 | 38 | 3 | 1 | 1 | 4 | - |
| Sacramento | 15 | (RM 170-144) | 39.39 | -122.00 | 20 | 3 | 1 | 1 | 4 | - |
| Sieve | 16 | - | 43.8 | 11.47 | 99 | 0 | 0 | 1 | 3 | Width from Google Earth |
| Tributary to Rio Grande Del Ranchos | 17 | | 36.31 | -105.58 | 2199 | 0 | 1 | 3 | 2 | - |
| Green | 18 | at Auburn | 47.25 | -122.13 | 23 | 3 | 1 | 3 | 4 | - |
| Skykomish | 18 | upstream of Snoqualamie junction | 47.84 | -121.98 | 14 | 3 | 1 | 1 | 3 | - |
| Elkhead | 19 | - | 40.54 | -107.41 | 1910 | 2 | 1 | 1 | 1 | Authors report channel incising upstream |
| Little Chena | 20 | - | 64.89 | -147.25 | 151 | 0 | 1 | 3 | 4 | Channel narrower than measured |
| McLaren | 20 | - | 63.12 | -146.53 | 882 | 2 | 0 | 3 | 4 | Nearly anastamosing |
| Little Tonsina | 21 | - | 61.53 | -145.25 | 545 | 0 | 1 | 3 | 4 | - |
| Gakona | 22 | at Gakona, AK, USA | 62.32 | -145.27 | 448 | 2 | 1 | 3 | 4 | - |
| Gulkana | 22 | at Gulkana, AK, USA | 62.28 | -145.38 | 426 | 3 | 1 | 3 | 4 | - |
| Chatanika | 22 | near Fairbanks, AK, USA | 65.08 | -147.72 | 163 | 1 | 1 | 3 | 4 | Measured sinuosity on Google Earth |
| Salcha | 22 | near Salcha, AK, USA | 64.47 | -146.88 | 212 | 1 | 1 | 3 | 4 | - |
| Alt Dubhaig Reach C | 23 | Scotland | 56.83 | -4.23 | 420 | 1 | 0 | 4 | 1 | - |
| Alt Dubhaig Reach D | 23 | Scotland | 56.83 | -4.23 | 417 | 1 | 0 | 4 | 1 | - |

| River | Source Number | Location | Latitude (dd) | Longitude (dd) | Elevation (m) | Islands[a] | Cutoffs[b] | Land Use Code[c] | Veg. Code[d] | notes |
|---|---|---|---|---|---|---|---|---|---|---|
| Lower Babbage | 24 | Downstream of Tulugaq confluence, YT, Canada | 69.15 | -138.32 | 17 | 1 | 1 | 4 | 1 | - |
| Powder | 25 | Montana | 45.25 | -105.66 | 977 | 0 | 1 | 1 | 2 | - |
| Clyde | 26 | near Carstairs | 55.68 | -3.64 | 189 | 3 | 1 | 1 | 1 | - |
| Medwin | 26 | near Carstairs | 55.68 | -3.63 | 190 | 0 | 1 | 1 | 1 | - |
| Derry Burn | 26 | - | 57.05 | -3.59 | 499 | 1 | 1 | 4 | 1 | - |
| Nueces | 27 | - | 29.09 | -99.86 | 228 | 1 | 0 | 1 | 1 | Used mean grain size, Width from Google Earth, |
| Beaver Run | 28 | - | 40.57 | -76.18 | 189 | 0 | 0 | 2 | 3 | Location approximate |
| Beaver Run | 28 | - | 40.57 | -76.18 | 189 | 0 | 0 | 2 | 2 | Location approximate |
| Rocky Run | 28 | - | 39.97 | -75.65 | 93 | 0 | 0 | 2 | 1 | Location approximate |
| Towamencin | 28 | - | 40.23 | -75.33 | 66 | 1 | 0 | 2 | 1 | Location approximate, veg & island characteristics from paper. |
| Otter | 29 | Dotton | 50.69 | -3.29 | 17 | 2 | 0 | 1 | 2 | - |
| Lugg | 29 | Byton (2) | 52.28 | -2.93 | 148 | 0 | 0 | 1 | 4 | - |
| Esk | 29 | Cropple How (average) | 54.37 | -3.34 | 10 | 0 | 0 | 1 | 4 | - |
| Usk | 29 | Llandetty | 51.88 | -3.27 | 113 | 0 | 0 | 1 | 3 | - |
| Alwin | 29 | Clennel | 55.35 | -2.12 | 153 | 1 | 1 | 1 | 1 | - |
| Eden | 29 | Temple Sowerby | 54.65 | -2.61 | 98 | 0 | 0 | 1 | 2 | - |
| North Tyne | 29 | Tarset | 55.17 | -2.35 | 122 | 0 | 0 | 1 | 3 | - |
| Hirnant | 29 | Rhiwedog | 52.90 | -3.57 | 163 | 0 | 0 | 1 | 4 | - |
| Hodder | 29 | Hodder Place | 53.85 | -2.45 | 47 | 0 | 0 | 1 | 3 | - |
| Hindurn | 29 | Wray (2) | 54.11 | -2.60 | 39 | 0 | 0 | 1 | 3 | - |
| Asker | 29 | Bridport | 50.73 | -2.75 | 6 | 0 | 0 | 2 | 2 | - |
| Chitterne Brook | 29 | Codford | 51.16 | -2.04 | 79 | 0 | 0 | 1 | 2 | - |

| River | Source Number | Location | Latitude (dd) | Longitude (dd) | Elevation (m) | Islands[a] | Cutoffs[b] | Land Use Code[c] | Veg. Code[d] | notes |
|---|---|---|---|---|---|---|---|---|---|---|
| Teign | 29 | Preston | 50.56 | -3.62 | 9 | 0 | 0 | 1 | 4 | - |
| Eden | 29 | Warwick Bridge | 54.90 | -2.83 | 23 | 0 | 0 | 1 | 3 | - |
| Kielder Burn | 29 | Kielder | 55.25 | -2.56 | 234 | 0 | 0 | 3 | 3 | - |
| Churnet | 29 | Rocester | 52.95 | -1.85 | 87 | 0 | 0 | 1 | 3 | - |
| Wylye | 29 | Norton Bavant | 51.19 | -2.13 | 99 | 0 | 0 | 1 | 2 | - |
| Pinsley Brook | 29 | Cholstrey Mill | 52.24 | -2.79 | 80 | 0 | 0 | 1 | 4 | - |
| Hamps | 29 | Waterhouses | 53.05 | -1.88 | 221 | 0 | 0 | 1 | 2 | - |
| Rye | 29 | Broadway Foot | 54.29 | -1.14 | 101 | 0 | 0 | 1 | 3 | Average of two reaches |
| Irthing | 29 | Greenholme | 54.92 | -2.80 | 22 | 0 | 0 | 1 | 3 | - |
| Exe | 29 | Thorverton | 50.80 | -3.51 | 31 | 0 | 0 | 1 | 2 | - |
| Glendaremeken | 29 | Threlkeld | 54.61 | -3.05 | 137 | 0 | 0 | 1 | 2 | - |
| Manifold | 29 | Hulme End (1 and 2) | 53.13 | -1.84 | 216 | 0 | 1 | 1 | 2 | Average of two reaches |
| Beatton | 30 | - | 57.28 | -121.58 | 707 | 0 | 1 | 3 | 4 | - |
| Notikewan | 31 | - | 56.9 | -118.23 | 602 | 0 | 1 | 4 | 3 | Location approximate |
| Sikanni Chief | 31 | - | 58.06 | -121.52 | 376 | 3 | 1 | 4 | 4 | Location approximate |
| Prophet River | 31 | - | 58.62 | -122.81 | 321 | 3 | 1 | 4 | 4 | Location approximate |
| Shushwump | 31 | - | 50.54 | -119.11 | 360 | 3 | 1 | 1 | 2 | Location approximate |
| Eagle River Upper | 31 | - | 50.93 | -118.8 | 366 | 3 | 1 | 1 | 2 | Location approximate |
| Little Smoky | 31 | - | 54.24 | -117.2 | 969 | 2 | 1 | 4 | 4 | Location approximate |
| Belly River | 32 | - | 49.49 | -113.3 | 1064 | 0 | 1 | 2 | 1 | Valley lined by terraces |
| River Bollin | 33 | - | 53.32 | -2.19 | 76 | 3 | 1 | 4 | 1 | - |
| River Dane | 34 | - | 53.18 | -2.25 | 72 | 0 | 1 | 1 | 3 | Only 2 islands in long reach |
| Nuporomaporo | 35 | Hokkaido, Japan | 44.93 | 142.06 | 18 | 0 | 1 | 4 | 1 | - |
| Nebosho | 36 | near Emporia, KS | 38.46 | -96.23 | 342 | 0 | 1 | 1 | 3 | - |
| Paddle | 37 | - | 53.90 | -115.04 | 679 | 0 | 1 | 4 | 3 | - |

| River | Source Number | Location | Latitude (dd) | Longitude (dd) | Elevation (m) | Islands[a] | Cutoffs[b] | Land Use Code[c] | Veg. Code[d] | notes |
|---|---|---|---|---|---|---|---|---|---|---|
| Little Paddle | 37 | - | 53.96166667 | -115.1483333 | 701 | 0 | 1 | 1 | 2 | - |
| Sheep | 37 | Okotoks | 50.72 | -113.98 | 1059 | 3 | 1 | 1 | 4 | - |
| Freeman | 37 | near Fort Assiniboine, AB, Canada | 54.32 | -114.88 | 612 | 2 | 1 | 1 | 4 | - |
| Sheep | 37 | At Black Diamond, AB Canada | 50.68 | -114.24 | 1181 | 1 | 1 | 1 | 3 | Post 2004 flood, increase in width and bar area |
| Waterton | 37 | near Stand Off, AB, Canada | 49.50 | -113.33 | 982 | 1 | 1 | 1 | 3 | - |
| Little Smoky | 37 | at Little Smokey, AB, Canada | 54.80 | -117.22 | 648 | 1 | 1 | 3 | 4 | - |
| Salmon | 38 | near Obsidian | 43.97 | -114.807 | 2120 | 3 | 1 | 2 | 1 | - |
| Valley | 38 | - | 44.22 | -114.93 | 1902 | 2 | 1 | 4 | 4 | - |
| Mataura | 39 | at Gore, S. Island, New Zealand | -46.15 | 168.92 | 65 | 3 | 1 | 1 | 3 | - |
| Squamish | 39 | downstr. confl. Ashlu, BC, Canada | 49.87 | -123.25 | 23 | 2 | 1 | 3 | 4 | - |
| Cecina | 39 | downstr. Ponti di Monterufoli, Italy | 43.32 | 10.68 | 36 | 3 | 0 | 1 | 4 | - |
| Allier | 39 | reach Les Echerolles Bressolles, France | 46.45 | 3.33 | 217 | 3 | 1 | 1 | 3 | - |
| Sinu | 39 | reach Urra dam-Tierralta, Colombia | 8.15 | -76.10 | 48 | 3 | 1 | 1 | 3 | - |
| Sinu | 39 | reach Tierralta-Guasimal, Colombia | 9.17 | -75.83 | 4 | 0 | 0 | 1 | 3 | - |
| White | 39 | at Petersburg, IN, USA (Reach M) | 38.53 | -87.43 | 124 | 0 | 1 | 1 | 3 | - |

| River | Source Number | Location | Latitude (dd) | Longitude (dd) | Elevation (m) | Islands[a] | Cutoffs[b] | Land Use Code[c] | Veg. Code[d] | notes |
|---|---|---|---|---|---|---|---|---|---|---|
| White | 39 | at Edwardsport, IN, USA (Reach W) | 38.75 | -87.23 | 135 | 0 | 1 | 1 | 3 | - |
| White | 39 | Upstr. confl. Muscatatuck, IN, USA (Reach E) | 38.82 | -86.15 | 158 | 0 | 1 | 1 | 3 | - |
| Big Fork | 39 | at Koochiching County, MN, USA | 48.43 | -93.73 | 330 | 2 | 1 | 1 | 3 | - |
| Tomichi | 39 | at Gunnison, CO, USA | 38.53 | -106.92 | 2335 | 2 | 1 | 4 | 1 | - |
| Blacks Fork | 39 | near Little America, Wyoming, USA | 41.63 | -109.80 | 1888 | 0 | 1 | 4 | 3 | - |
| Brandywine | 39 | at Embreeville, PA, USA | 39.93 | -75.73 | 65 | 0 | 0 | 1 | 4 | - |
| Paddle | 39 | near Rochfort Bridge, AB, Canada | 53.90 | -115.05 | 681 | 0 | 1 | 4 | 4 | - |
| Pole | 40 | Wyoming | 42.85 | -109.76 | 2171 | 0 | 1 | 4 | 2 | - |
| Ain | 41 | France | 45.98 | 5.28 | 254 | 0 | 1 | 1 | 4 | - |
| Pearl | 42 | Louisiana | 30.82 | -89.78 | 23 | 0 | 1 | 3 | 4 | - |
| Bogue Chito | 42 | Louisiana | 30.63 | -89.92 | 16 | 0 | 1 | 3 | 4 | - |
| Clark Fork | 43 | - | 46.4 | -112.74 | 1374 | 1 | 1 | 2 | 1 | Discharge from Deer Lodge, $D_{50}$ at Galen, everything else reach-average |
| Watts Branch | 44 | Maryland | 39.08 | -77.18 | 99 | 0 | 0 | 2 | 4 | - |
| Watts Branch | 45 | Viers Pasture near Rockville, MD | 39.08 | -77.18 | 99 | 0 | 0 | - | 1 | - |
| Christian's | 45 | Orange bridge near Staunton VA | 38.10 | -79.00 | 390 | 0 | 0 | 2 | 2 | - |

| River | Source Number | Location | Latitude (dd) | Longitude (dd) | Elevation (m) | Islands[a] | Cutoffs[b] | Land Use Code[c] | Veg. Code[d] | notes |
|---|---|---|---|---|---|---|---|---|---|---|
| Middle | 45 | Bethlehem Church, near Staunton VA | 38.13 | -79.22 | 492 | 0 | 1 | 1 | 1 | - |
| Cottonwood | 45 | Daniel, Wyoming | 42.75 | -110.09 | 2172 | 2 | 1 | 4 | 2 | - |
| Buffalo Fork | 45 | Flybox Ranch near Jackson, WY | 43.83 | -110.45 | 2069 | 3 | 1 | 4 | 1 | - |
| Wind | 45 | Dumb Cowboy Reach above Dubois, WY | 43.79 | -110.15 | 2637 | 2 | 1 | 4 | 1 | Estimated location |
| Du Noir | 45 | Above Dubois WY | 43.61 | -109.78 | 2225 | 1 | 1 | 4 | 2 | - |
| Middle Piney | 45 | below South Fork near Big Piney, WY | 42.60 | -110.46 | 2438 | 0 | 1 | 2 | 4 | Located site near gage |
| Upper Congaree | 46 | 11-22 km downstr. Columbia, SC | 33.88 | -81.00 | 30 | 0 | 1 | 1 | 4 | - |
| Ystwyth | 47 | Wales | 52.36 | -4.02 | 29 | 0 | 0 | 1 | 3 | - |
| Rheidol | 48 | near Lovesgrove, Wales | 52.41 | -4.03 | 13 | 0 | 1 | 1 | 3 | - |
| Hawk | 49 | - | 44.85 | -95.42 | 304 | 0 | 1 | 1 | 2 | - |
| Amite | 49 | - | 30.69 | -90.87 | 23 | 0 | 1 | 2 | 3 | Median particle size from point bar. |
| Bear Valley | 50 | ID | 44.41 | -115.38 | 1949 | 2 | 1 | 4 | 2 | - |
| South Fork Kern | 51 | - | 36.19 | -118.17 | 2397 | 0 | 1 | 4 | 2 | - |
| Sacramento | 52 | RM 243-211 | 39.93 | -122.07 | 57 | 3 | 1 | 1 | 4 | - |
| Taieri | 53 | - | -45.45 | 169.86 | 543 | 0 | 1 | 1 | 1 | Estimated location |
| Loganburn | 53 | - | -45.45 | 169.89 | 548 | 0 | 1 | 1 | 1 | Estimated location |
| Otapiri | 53 | - | -46.06 | 168.45 | 95 | 1 | 1 | 1 | 3 | Estimated location |
| Cobb | 53 | near Trilobite, NZ | -41.12 | 172.61 | 838 | 1 | 1 | 3 | 4 | - |
| Inangahua | 53 | Inangahua | -41.88 | 171.92 | 59 | 0 | 0 | 1 | 1 | - |

| River | Source Number | Location | Latitude (dd) | Longitude (dd) | Elevation (m) | Islands[a] | Cutoffs[b] | Land Use Code[c] | Veg. Code[d] | notes |
|---|---|---|---|---|---|---|---|---|---|---|
| North Fork Big | 54 | near Victoria, KS | 38.85 | -99.15 | 583 | 0 | 0 | 1 | 2 | Estimated location |
| Fall | 54 | near Eureka, KS | 37.81 | -96.30 | 316 | 0 | 0 | 1 | 2 | Estimated location |
| Birch | 55 | Alaska | 65.90 | -144.30 | 179 | 1 | 1 | 3 | 3 | - |
| Lower Jordan | 56 | - | 32.17 | 35.56 | 348 | 0 | 1 | 1 | 2 | - |
| Jefferson | 57 | downstream Silver Star, MT, USA | 45.70 | -112.25 | 1368 | 3 | 1 | 1 | 3 | - |
| Wind | 58 | - | 43.01 | -108.37 | 1501 | 3 | 1 | 4 | 3 | Sinuosity from Google Earth, relatively short reach |
| Strickland | 59 | RKM 265 | -6.91 | 142.06 | 33 | 2 | 1 | 3 | 4 | - |
| Skirden Beck | 60 | near Bolton by Bowland, UK | 53.93 | -2.33 | 83 | 1 | 1 | 1 | 2 | - |
| Severn | 61 | - | 52.51 | -3.43 | 123 | 0 | 1 | 1 | 2 | - |
| Solfatara | 62 | - | 44.74 | -110.69 | 2283 | 2 | 0 | 4 | 2 | - |
| Thomas | 63 | near Scio, OR | 44.71 | -122.77 | 115 | 3 | 0 | 1 | 3 | - |



Notes:

a. Islands: 0=no islands, 1=unvegetated islands, 2=vegetated islands, 3=vegetated and unvegetated islands.
b. Cutoffs: 0=no cutoff scars, 1=cutoff scars visible
c. Land Use Code: 1=Agricultural, 2=Urban/Industrial, 3=Forested, 4=Rangelands
d. Vegetation Code: 1=Grass/shrubs, 2=Predominantly Grass/shrubs with trees, 3=Predominantly trees with grass/shrubs, 4=Forested

Sources

1. Andrews [1979]; 2. Andrews [1984]; 3. Andrews and Erman [1986]; 4. Beechie et al. [2006]; 5. Beeson and Doyle [1995]; 6. Blacknell [1982]; 7. Bluck [1971], Sambrook Smith and Ferguson [1995], Sinuosity measured from Google Earth; 8. Brierly and Hickin [1991]; 9. Carson [1984]; 10. Charlton et al. [1978]; 11. Church and Rood [1983]; 12. Church and Rood [1983], location from Kleinhans and van den Berg [2010]; 13. Clayton [2010]; 14. Clayton and Pitlick [2007]; 15. Constantine et al. [2009]; 16. Darby et al. [2007]; 17. Dietrich and Whiting [1989]; 18. Dunne et al. [1981]; 19. Elliot and Gyetvai [1999]; 20. Emmett [1972].

21. Emmett [1972], sinuosity from Google Earth; 22. Emmett [1972], Sinuosity from Kleinhans and Van den Berg [2010]; 23.Ferguson and Ashworth [1991]; 24. Forbes [1983]; 25. Gay et al [1998]; 26. Gregory et al. [1997]; 27. Gustavson [1970]; 28. Hession et al. [2003], Allmendinger et al. [2005]; 29. Hey and Thorne [1986]; 30. Hickin and Nanson [1975], Nanson [1980]; 31. Hickin and Nanson [1984], Hickin [1988]; 32. Hickin and Nanson [1984], Hickin [1988], grain size from Kellerhals et al. [1972]; 33. Hooke [1995], Luchi et al. [2010]; 34. Hooke [2003]; 35. Ikeda [1989]; 36. Juracek and Perry [2005], Juracek [1999]; 37. Kellerhals et al. [1972]; 38. King et al. [2004]; 39. Kleinhans and van den Berg [2010]; 40. Larsen [1995]; 41. Lassettre et al. [2008], Piegay and Gurnell [1997], Marston et al. [1995]; 42. Lauer and Parker [2008a]; 43.Lauer and Parker [2008b], Smith [2004], Griffin and Smith [2001]; 44. Leopold [1973]; 45. Leopold and Wolman [1957]; 46. Levey [1977]; 47. Lewin [1976]; 48. Lewin [1978], Sinuosity measured from Google Earth over the 1700 m reach above Lovesgrove; 49. MacDonald et al. [1991]; 50. McGowen and Garner [1970]; 51. McKean et al. [2008], Tonina and McKean [2010]; 51. Micheli and Kirchner [2002]; 52. Micheli et al. [2004]; 53. Mosely personal communication to from van den berg [1995]; 54. Osterkamp [1978]; 55. Rowland et al. [2009] used two year flow from Kostohrys and Sterin [1996]; 56. Schattner [1967]; 57. Schumm et al. [2000]; 58. Smalley et al. [1994]; 59. Swanson et al. [2008], Aalto et al. [2008], Parker et al. [2008]; 60. Thompson [1986] location from Kleinhans and van den Berg [2010]; 61. Thorne and Lewin [1979]; 62. Whiting and Dietrich [1991]; 63. Williams [1978], Williams [1986]. References provided at the end of Table B1

**Table B1b. Physical characteristics of gravel-bed meanders in Chapter 3.**

| River | Drainage Area ($km^2$) | $Q_{bf}$ ($m^3/s$) | Channel Slope ($X10^{-3}$) | Sinu-osity | Valley Slope ($X10^{-3}$) | B (m) | H (m) | H/B | $R_h$ (m) | $D_{50}$ (m) | λ (m) | Migration Rate (m/yr) |
|---|---|---|---|---|---|---|---|---|---|---|---|---|
| East Fork | 470 | 16 | 0.70 | - | - | 18.0 | 0.60 | 30 | 0.56 | 0.005 | - | - |
| Frazer | 27 | 3 | 14.00 | 1.34 | 19.00 | 7.0 | 0.29 | 24.1 | 0.27 | 0.034 | - | - |
| East Inlet | 71 | 12 | 4.60 | 1.36 | 6.26 | 11.9 | 0.73 | 16.3 | 0.65 | 0.061 | - | - |
| North Platte | 3706 | 85 | 1.40 | 1.43 | 2.00 | 47.2 | 0.97 | 48.6 | 0.93 | 0.024 | - | - |
| Stillwater | 45 | 2 | 11.00 | 1.45 | 15.95 | 7.3 | 0.34 | 21.5 | 0.31 | 0.052 | - | - |
| Williams Fork | 883 | 47 | 2.00 | 1.51 | 3.02 | 24.4 | 1.62 | 15.1 | 1.43 | 0.045 | - | - |
| Little Muddy | 17 | 2 | 6.10 | 1.60 | 9.76 | 5.2 | 0.31 | 17.1 | 0.27 | 0.024 | - | - |
| Little Grizzly | 135 | 7 | 2.30 | 1.89 | 4.35 | 10.4 | 0.48 | 21.7 | 0.44 | 0.023 | - | - |
| Little Snake | - | 72 | 7.10 | - | - | 30.5 | 1.13 | 27.0 | 1.05 | 0.122 | - | - |
| Little Snake | 2559 | 114 | 2.40 | 1.43 | 3.43 | 36.6 | 1.65 | 22.2 | 1.51 | 0.070 | - | - |
| Elk | 1075 | 101 | 3.70 | 1.35 | 5.00 | 36.6 | 1.45 | 25.2 | 1.34 | 0.064 | - | - |
| Yampa | - | 167 | 1.53 | 1.31 | 2.00 | 53.3 | 1.63 | 32.7 | 1.54 | 0.058 | - | - |
| Yampa | 8832 | 255 | 0.88 | 1.98 | 1.74 | 83.8 | 1.85 | 45.3 | 1.77 | 0.034 | - | - |
| Sagehen | 27.2 | 2 | 11.50 | - | - | 4.9 | 0.41 | 12.0 | 0.35 | 0.058 | - | - |
| WF Humptulips | 125 | 198 | 1.65 | 1.67 | 2.76 | - | - | - | - | - | - | - |
| Wynoochee | 229 | 303 | 2.52 | 1.88 | 4.73 | - | - | - | - | - | - | - |
| Chehalis | 2542 | 941 | 0.84 | 1.85 | 1.56 | - | - | - | - | - | - | - |
| Nisqually W | 1818 | 407 | 3.43 | 1.27 | 4.36 | - | - | - | - | - | - | - |
| Snoqualmie | - | 860 | 0.40 | - | - | - | - | - | - | - | - | - |
| Chehalis | - | 831 | 0.60 | - | - | - | - | - | - | - | - | - |
| Willapa | - | 238 | 1.30 | - | - | - | - | - | - | - | - | - |
| Chehalis | - | 274 | 0.70 | - | - | - | - | - | - | - | - | - |
| Green | 690 | 279 | 3.39 | 1.42 | 4.81 | - | - | - | - | 0.017 | - | - |
| Salmon | 1510 | - | 0.90 | - | - | 32.5 | 2.00 | - | 1.78 | - | - | - |
| Bonaparte | 5020 | - | 3.00 | - | - | 35.0 | 2.00 | 17.5 | 1.79 | - | - | - |
| Chase | 279 | - | 3.00 | - | - | 20.0 | 1.50 | 13.3 | 1.30 | - | - | - |
| Deadman | - | - | 8.00 | - | - | 32.5 | 1.50 | 21.7 | 1.37 | - | - | - |
| Tywi | 748 | - | 1.00 | 2.00 | 2.00 | 35.5 | 1.76 | 20.2 | 1.60 | 0.005 | - | - |
| Endrick | - | 7 | 2.00 | 1.97 | 3.94 | 25.0 | 0.85 | 29.4 | 0.80 | 0.025 | 457 | 0.50 |
| Squamish | - | 500 | 1.30 | 1.43 | 1.86 | 105.0 | 3.60 | 29.2 | 3.37 | 0.095 | - | - |

| River | Drainage Area ($km^2$) | $Q_{bf}$ ($m^3/s$) | Channel Slope ($X10^{-3}$) | Sinu-osity | Valley Slope ($X10^{-3}$) | B (m) | H (m) | H/B | $R_h$ (m) | $D_{50}$ (m) | λ (m) | Migration Rate (m/yr) |
|---|---|---|---|---|---|---|---|---|---|---|---|---|
| Selwyn | - | 23 | 5.67 | 1.50 | 8.50 | 22.0 | 1.47 | 15.0 | 1.29 | 0.050 | - | - |
| Little Eachaig | - | 58 | 5.70 | 1.50 | 8.55 | 18.0 | 1.36 | 13.2 | 1.18 | 0.074 | - | - |
| Lune | - | 260 | 0.70 | 1.5 | 1.05 | 56 | 2.8 | 20.0 | 2.55 | 0.075 | - | - |
| Arrow | - | 30 | 4.50 | 1.65 | 7.43 | 14.0 | 1.37 | 10.2 | 1.15 | 0.041 | - | - |
| Irfon (1) | - | 66 | 2.40 | 1.38 | 3.31 | 26.0 | 1.16 | 22.4 | 1.06 | 0.039 | - | - |
| Irfon (2) | - | 81 | 1.40 | 1.52 | 2.13 | 29.0 | 1.63 | 17.8 | 1.47 | 0.055 | - | - |
| Klondike | - | 354 | 1.59 | 1.40 | 2.23 | 87.0 | 1.98 | 43.9 | 1.89 | 0.050 | - | - |
| Yukon | - | 2890 | 0.47 | 2.00 | 0.94 | 311.0 | 4.63 | 67.2 | 4.50 | 0.067 | - | - |
| Pelly | - | 2661 | 0.56 | 1.90 | 1.06 | 242.0 | 4.60 | 52.6 | 4.43 | 0.057 | - | - |
| Stewart | - | 2280 | 0.26 | 2.71 | 0.70 | 333.0 | 4.64 | 71.8 | 4.51 | 0.022 | - | - |
| Fall (1) | - | - | 2.00 | - | - | 10.0 | 0.60 | 16.7 | 0.54 | 0.016 | - | - |
| Fall (2) | - | - | 2.00 | - | - | 12.0 | 0.60 | 20.0 | 0.55 | 0.014 | - | - |
| Colorado | 140 | 11 | 1.70 | 2.10 | 3.57 | 19.0 | 0.61 | 31.2 | 0.57 | 0.022 | - | - |
| Sacramento | - | 2400 | 0.35 | 1.33 | 0.47 | 315.0 | 4.70 | 67.0 | 4.56 | 0.020 | - | - |
| Sacramento | - | 2000 | 0.20 | 1.50 | 0.30 | 210.0 | 6.30 | 33.3 | 5.94 | 0.015 | - | - |
| Sieve | 830 | 410 | 3.00 | - | - | - | - | - | - | - | - | - |
| Tributary to Rio Grande Del Ranchos | - | - | 6.60 | - | - | 4.0 | 0.40 | 10.0 | 0.33 | 0.032 | - | - |
| Green | - | 340 | - | - | - | - | - | - | - | 0.017 | - | - |
| Skykomish | - | - | - | - | - | - | - | - | - | 0.016 | - | - |
| Elkhead | 550 | 26.9 | 2.30 | 2.2 | 5.06 | 22.86 | 1.37 | 16.7 | 1.22 | 0.04 | 179 | - |
| Little Chena | 2437 | 73 | 2.00 | - | - | 37 | 3.51 | 10.5 | 2.95 | 0.0135 | - | - |
| McLaren | 725 | 161 | 0.70 | - | - | 90 | 1.19 | 75.6 | 1.16 | 0.0085 | - | - |
| Little Tonsina | 85 | 6.2 | 4.00 | 1.76 | 7.04 | 13.72 | 0.73 | 18.8 | 0.66 | 0.0083 | - | - |
| Gakona | 1606 | 127 | 4.10 | 2.25 | 1.82 | 61.0 | 1.17 | 52.1 | 1.13 | 0.021 | - | - |
| Gulkana | 5092 | 510 | 4.20 | 1.80 | 2.33 | 152.4 | 1.01 | 151 | 1.00 | 0.021 | - | - |
| Chatanika | 1269 | 110 | 1.70 | 2.90 | 0.59 | 46.3 | 1.04 | 44.5 | 1.00 | 0.018 | - | - |
| Salcha | 5620 | 368 | 0.80 | 1.56 | 0.51 | 99.0 | 2.79 | 35.5 | 2.64 | 0.019 | - | - |
| Alt Dubhaig Reach C | - | 6 | 11.00 | 1.30 | 14.30 | 14.0 | 0.57 | 24.6 | 0.53 | 0.041 | - | - |
| Alt Dubhaig Reach D | - | 6 | 8.00 | 1.50 | 12.00 | 24.0 | 0.48 | 50.0 | 0.46 | 0.042 | - | - |
| Lower | - | 500 | 0.56 | 1.31 | 0.74 | 62.0 | - | - | - | 0.015 | - | - |

| River | Drainage Area ($km^2$) | $Q_{bf}$ ($m^3/s$) | Channel Slope ($X10^{-3}$) | Sinu-osity | Valley Slope ($X10^{-3}$) | B (m) | H (m) | H/B | $R_h$ (m) | $D_{50}$ (m) | λ (m) | Migration Rate (m/yr) |
|---|---|---|---|---|---|---|---|---|---|---|---|---|
| Babbage | | | | | | | | | | | | |
| Powder | 21500 | - | 1.00 | 1.45 | 1.45 | 50.0 | - | - | - | - | - | - |
| Clyde | - | - | - | - | - | - | - | - | - | - | - | - |
| Medwin | - | - | - | - | - | - | - | - | - | - | - | - |
| Derry Burn | - | - | - | - | - | - | - | - | - | - | - | - |
| Nueces | 5050 | 340 | 1.80 | 1.3 | 2.34 | 77 | 1 | 77.0 | 0.97 | 0.023 | - | - |
| Beaver Run | 12 | - | 11.50 | 1.50 | - | 7.4 | 0.32 | 23.1 | 0.29 | 0.064 | 154 | 0.14 |
| Beaver Run | 12 | - | 8.10 | 1.50 | - | 6.0 | 0.33 | 18.2 | 0.30 | 0.045 | 158 | 0.39 |
| Rocky Run | 8 | - | 6.30 | 1.30 | - | 4.5 | 0.39 | 11.5 | 0.33 | 0.045 | 108 | 0.15 |
| Towamencin | 5 | - | 7.40 | - | - | 4.7 | 0.32 | 14.7 | 0.28 | 0.023 | 47 | 0.46 |
| Otter | 203 | 104 | 3.53 | 1.43 | 5.03 | 25.2 | 1.58 | 16.0 | 1.50 | 0.057 | - | - |
| Lugg | 203 | 24 | 3.44 | 1.47 | 5.07 | 21.1 | 0.96 | 22.0 | 0.92 | 0.035 | - | - |
| Esk | 70 | 61 | 2.68 | 1.53 | 4.10 | 25.3 | 1.30 | 19.5 | 1.25 | 0.041 | - | - |
| Usk | 543.90 | 304.00 | 1.33 | 1.25 | 1.66 | 48.50 | 2.59 | 18.7 | 2.49 | 0.07 | - | - |
| Alwin | 27.70 | 9.70 | 10.86 | 1.26 | 13.65 | 12.30 | 0.50 | 24.6 | 0.48 | 0.07 | - | - |
| Eden | 616.40 | 237.00 | 1.46 | 1.26 | 1.84 | 57.80 | 2.69 | 21.5 | 2.60 | 0.06 | - | - |
| North Tyne | 284.90 | 192.30 | 2.51 | 1.28 | 3.22 | 45.20 | 2.14 | 21.1 | 2.08 | 0.09 | - | - |
| Hirnant | 33.90 | 50.00 | 13.33 | 1.29 | 17.14 | 18.40 | 1.14 | 16.1 | 1.07 | 0.06 | - | - |
| Hodder | 261.00 | 348.00 | 2.96 | 1.29 | 3.77 | 46.60 | 2.61 | 17.9 | 2.51 | 0.07 | - | - |
| Hindurn | - | 120.00 | 6.70 | 1.32 | 8.81 | 41.70 | 1.28 | 32.6 | 1.25 | 0.09 | - | - |
| Asker | 49.10 | 19.00 | 2.41 | 1.33 | 3.21 | 11.60 | 1.22 | 9.51 | 1.05 | 0.02 | - | - |
| Chitterne Brook | - | 3.90 | 1.94 | 1.42 | 2.75 | 6.50 | 0.68 | 9.56 | 0.59 | 0.02 | - | - |
| Teign | 381.00 | 148.00 | 1.40 | 1.51 | 2.11 | 29.40 | 2.07 | 14.2 | 1.94 | 0.04 | - | - |
| Eden | 1367.00 | 424.00 | 1.70 | 1.63 | 2.77 | 76.50 | 3.21 | 23.8 | 3.10 | 0.05 | - | - |
| Kielder Burn | 58.80 | 36.50 | 5.70 | 1.68 | 9.60 | 28.00 | 1.05 | 26.7 | 0.99 | 0.06 | - | - |
| Churnet | 236.00 | 34.00 | 1.34 | 1.74 | 2.33 | 14.40 | 1.96 | 7.35 | 1.61 | 0.03 | - | - |
| Wylye | 112.40 | 7.10 | 1.57 | 1.78 | 2.80 | 9.60 | 0.82 | 11.7 | 0.75 | 0.02 | - | - |
| Pinsley Brook | 24.20 | 14.00 | 3.92 | 1.79 | 7.00 | 10.60 | 0.82 | 12.9 | 0.75 | 0.01 | - | - |
| Hamps | 35.10 | 27.00 | 4.82 | 2.05 | 9.86 | 15.00 | 1.07 | 14.0 | 0.95 | 0.05 | - | - |
| Rye | 131.70 | 100.00 | 3.20 | 1.59 | 5.07 | 24.50 | 1.79 | 13.7 | 1.61 | 0.08 | - | - |
| Irthing | 334.60 | 60.40 | 1.19 | 2.14 | 2.55 | 32.20 | 1.34 | 24.0 | 1.31 | 0.04 | - | - |
| Exe | 600.90 | 154.00 | 3.16 | 2.38 | 7.52 | 42.70 | 1.46 | 29.3 | 1.40 | 0.06 | - | - |
| Glendareme ken | 64.50 | 45.00 | 4.69 | 2.42 | 11.35 | 18.60 | 1.22 | 15.3 | 1.12 | 0.04 | - | - |

| River | Drainage Area ($km^2$) | $Q_{bf}$ ($m^3/s$) | Channel Slope ($X10^{-3}$) | Sinu-osity | Valley Slope ($X10^{-3}$) | B (m) | H (m) | H/B | $R_h$ (m) | $D_{50}$ (m) | λ (m) | Migration Rate (m/yr) |
|---|---|---|---|---|---|---|---|---|---|---|---|---|
| Manifold | 46.00 | 28.00 | 2.80 | 1.77 | 5.56 | 14.65 | 1.22 | 12.0 | 1.07 | 0.05 | - | - |
| Beatton | 16070 | 222 | 0.30 | 2.22 | 0.66 | 55.0 | 3.00 | 18.3 | 2.70 | 0.004 | 908 | 0.48 |
| Notikewan | - | 388 | 0.74 | - | - | 54 | 4.5 | 12.0 | 3.86 | - | 918 | 1.21 |
| Sikanni Chief | - | 1259 | 0.45 | - | - | 217 | 8.3 | 26.1 | 7.71 | - | 2793 | 2.92 |
| Prophet River | - | 830 | 1.60 | - | - | 141 | 6 | 23.5 | 5.53 | - | 2333 | 2.34 |
| Shushwump | - | 454 | 0.27 | - | - | 92 | 2.5 | 36.8 | 2.37 | - | 1078 | 1.73 |
| Eagle River Upper | - | 272 | 1.09 | - | - | 49 | 3.5 | 14.00 | 3.06 | - | 512 | 1.34 |
| Little Smoky | - | 44 | 1.70 | 1.7 | - | 39 | 2.5 | 15.6 | 2.22 | - | 741 | 0.53 |
| Belly River | - | 101 | 1.90 | 1.7 | 3.23 | 28.7 | 1.01 | 28.5 | 0.94 | 0.03 | 503 | 0.81 |
| River Bollin | 55 | 15 | 3.00 | 1.50 | 5.00 | 15.0 | 0.80 | 18.8 | 0.72 | 0.030 | - | - |
| River Dane | 152 | 30 | 1.80 | 2.05 | 3.69 | 20.0 | 1.30 | 15.4 | 1.15 | 0.075 | 211 | 1.24 |
| Nuporomapo ro | - | - | - | - | - | - | - | - | - | - | - | - |
| Nebosho | - | - | 0.23 | - | - | - | - | - | - | 0.017 | - | - |
| Paddle | 883 | 55 | 1.40 | 1.50 | 2.10 | 17.0 | 1.10 | 15.5 | 0.97 | 0.005 | - | - |
| Little Paddle | - | 29.5 | 2.00 | 1.6 | 3.20 | 16.2 | 1.25 | 13.0 | 1.08 | 0.054 | - | - |
| Sheep | 1626.52 | 65 | 5.00 | 1.3 | 3.85 | 45 | 0.76 | 59.2 | 0.74 | 0.031 | - | - |
| Freeman | - | 203 | 3.30 | 1.80 | 5.94 | 79.9 | 1.37 | 58.2 | 1.33 | 0.070 | - | - |
| Sheep | 601 | 47 | 5.90 | 1.30 | 4.94 | 46.6 | 0.58 | 80.5 | 0.57 | 0.043 | - | - |
| Waterton | - | 153 | 2.50 | 1.30 | 3.25 | 94.8 | 1.25 | 75.9 | 1.22 | 0.046 | - | - |
| Little Smoky | - | - | 0.94 | 1.70 | 1.60 | 111.0 | 3.80 | 29.2 | 3.56 | 0.073 | 1376 | 0.53 |
| Salmon | 243 | 12.69 | 6.60 | - | - | 12.8 | 0.8 | 16.0 | 0.71 | 0.061 | - | - |
| Valley | 386 | 24.07 | 4.00 | - | - | 24.7 | 0.79 | 31.3 | 0.74 | 0.04 | - | - |
| Mataura | - | 511 | 1.40 | 1.33 | 1.86 | 142.0 | 2.24 | 63.4 | 2.17 | 0.026 | - | - |
| Squamish | - | 670 | 1.33 | 1.43 | 1.90 | - | - | - | - | 0.050 | - | - |
| Cecina | - | 250 | 1.36 | 1.36 | 1.85 | - | - | - | - | 0.040 | - | - |
| Allier | - | 800 | 0.63 | 1.33 | 0.84 | 260.0 | 1.40 | - | 1.39 | 0.006 | - | - |
| Sinu | - | - | 0.60 | 1.60 | 0.96 | 160.0 | 3.20 | 50.0 | 3.08 | 0.006 | - | - |
| Sinu | - | 980 | 0.30 | 2.50 | 0.75 | 145.0 | 3.50 | 41.4 | 3.34 | 0.005 | - | - |
| White | - | 850 | 0.18 | 1.48 | 0.26 | 140.0 | 6.50 | 21.5 | 5.95 | - | - | - |
| White | - | 439 | 0.20 | 1.65 | 0.33 | 85.0 | 4.50 | 18.9 | 4.07 | - | - | - |
| White | - | 382 | 0.29 | 1.70 | 0.49 | 60.0 | 3.00 | 20.0 | 2.73 | - | 801 | 0.67 |
| Big Fork | - | 155 | 0.63 | 2.39 | 1.51 | 54.9 | 1.71 | 32.1 | 1.61 | 0.006 | 1148 | - |

| River | Drainage Area ($km^2$) | $Q_{bf}$ ($m^3/s$) | Channel Slope ($X10^{-3}$) | Sinu-osity | Valley Slope ($X10^{-3}$) | B (m) | H (m) | H/B | $R_h$ (m) | $D_{50}$ (m) | λ (m) | Migration Rate (m/yr) |
|---|---|---|---|---|---|---|---|---|---|---|---|---|
| Tomichi | - | 28 | 3.58 | 1.93 | 6.90 | 23.5 | 0.70 | 33.6 | 0.66 | 0.042 | - | - |
| Blacks Fork | - | 226 | 0.80 | 1.90 | 1.52 | 57.9 | 1.78 | 32.5 | 1.68 | 0.018 | - | - |
| Brandywine | - | - | 0.45 | 1.57 | 0.71 | - | - | - | - | 0.02 | 0 | 0.00 |
| Paddle | - | 46.20 | 1.40 | 1.50 | 2.10 | 22.90 | 2.04 | 11.2 | 1.73 | 0.05 | 0 | 0.00 |
| Pole | | 24 | 1.50 | - | - | 21.2 | 0.95 | 22.3 | 0.87 | 0.052 | - | - |
| Ain | 3672 | - | 1.50 | 1.26 | 1.89 | 60.0 | - | - | - | - | - | - |
| Pearl | 17030 | 570 | 0.19 | 1.90 | 0.36 | 117.0 | 5.30 | 22.1 | 4.86 | 0.015 | 1512 | 0.88 |
| Bogue Chito | 3140 | 150 | 0.39 | 1.70 | 0.66 | 54.0 | 3.30 | 16.4 | 2.94 | 0.015 | 371 | 0.49 |
| Clark Fork | 2577 | 54 | 1.90 | 1.6 | 1.19 | 18 | 0.7 | 25.7 | 0.65 | 0.03 | 306 | 0.18 |
| Watts Branch | 10 | - | 8.10 | - | - | 7.6 | - | - | - | 0.016 | - | - |
| Watts Branch | 10 | 7 | 3.10 | - | - | 13.1 | 0.52 | 25.2 | 0.48 | 0.025 | - | - |
| Christian's | 62 | 20 | 1.50 | - | - | - | - | - | - | 0.023 | - | - |
| Middle | 47 | 23 | 2.10 | - | - | | - | - | - | 0.023 | - | - |
| Cottonwood | 528 | 23 | 1.10 | - | - | - | - | - | - | 0.015 | - | - |
| Buffalo Fork | 894 | 34 | 0.45 | - | - | - | - | - | - | 0.037 | - | - |
| Wind | 142 | 10 | 3.70 | 1.50 | - | 9.1 | - | - | - | 0.043 | - | - |
| Du Noir | 241 | 13 | 0.98 | - | - | 13.0 | - | - | - | 0.040 | - | - |
| Middle Piney | 88 | 6 | 9.10 | - | - | 23.0 | 0.67 | 34.3 | 0.63 | 0.094 | - | - |
| Upper Congaree | - | - | 0.29 | 1.75 | 0.50 | - | - | - | - | 0.010 | - | - |
| Ystwyth | 152 | - | 3.70 | - | - | - | - | - | - | 0.020 | - | - |
| Rheidol | 179 | - | 3.51 | 1.14 | 4.00 | 24.0 | - | - | - | - | 308 | 1.75 |
| Hawk | - | 40.7 | 0.63 | 1.7 | 0.37 | 22.86 | 1.31 | 17.4 | 1.18 | 0.012 | 439 | - |
| Amite | 7800 | 606 | 0.61 | 1.55 | 0.95 | 68 | 4 | 17.0 | 3.58 | 0.0021 | - | - |
| Bear Valley | - | 7 | 3.00 | - | - | 15.0 | 1.00 | 15.0 | 0.88 | 0.052 | - | - |
| South Fork Kern | 380 | 7 | 1.00 | 1.53 | 1.53 | 30.0 | 1.00 | 30.0 | 0.94 | 0.004 | 202 | - |
| Sacramento | - | 2270 | 0.50 | - | - | 372.0 | - | - | - | 0.035 | 2840 | - |
| Taieri | - | 12 | 1.50 | 1.77 | 2.66 | 17.8 | 0.86 | 20.7 | 0.78 | 0.011 | - | - |
| Loganburn | - | 8 | 3.21 | 1.68 | 5.40 | 10.6 | 0.63 | 16.8 | 0.56 | 0.030 | - | - |
| Otapiri | - | 20 | 3.20 | 1.69 | 5.41 | 13.5 | 0.96 | 14.1 | 0.84 | 0.061 | - | - |
| Cobb | - | 33 | 6.50 | 1.40 | 9.10 | 44.4 | 0.69 | 64.4 | 0.67 | 0.052 | - | - |
| Inangahua | - | 1018.00 | 3.58 | 1.48 | 5.30 | 116.00 | 2.93 | 39.6 | 2.79 | 0.09 | 0 | 0.00 |

| River | Drainage Area ($km^2$) | $Q_{bf}$ ($m^3/s$) | Channel Slope ($X10^{-3}$) | Sinu-osity | Valley Slope ($X10^{-3}$) | B (m) | H (m) | H/B | $R_h$ (m) | $D_{50}$ (m) | λ (m) | Migration Rate (m/yr) |
|---|---|---|---|---|---|---|---|---|---|---|---|---|
| North Fork Big | 140 | 8 | 1.20 | 1.90 | 2.28 | - | - | - | - | 0.004 | - | - |
| Fall | - | 331 | 1.70 | 1.60 | 1.06 | - | - | - | - | 0.012 | - | - |
| Birch | 6500 | 334 | 0.26 | 2.60 | - | - | - | - | - | - | - | - |
| Lower Jordan | - | - | - | - | - | - | - | - | - | - | - | - |
| Jefferson | - | 209 | 1.20 | 1.83 | 2.20 | 92.0 | 2.60 | 35.4 | 2.46 | 0.053 | - | - |
| Wind | 5980 | 141.6 | 1.00 | 1.46 | 1.46 | 41.8 | 1.68 | 24.9 | 1.56 | 0.021 | - | - |
| Strickland | - | 5700 | 0.37 | 1.72 | 0.37 | 342 | 7.6 | 45.0 | 7.28 | - | 4280 | 1.80 |
| Skirden Beck | - | 19 | 4.80 | 1.45 | 6.96 | 12.0 | 1.00 | 12.0 | 0.86 | 0.045 | - | - |
| Severn | - | 70 | 1.75 | 1.83 | 3.20 | 30.0 | 1.00 | 30.0 | 0.94 | 0.040 | 457 | 0.70 |
| Solfatara | 62 | 2 | 1.00 | - | - | 5.2 | 0.50 | 10.4 | 0.42 | 0.008 | - | - |
| Thomas | 282 | 365 | 3.00 | 1.32 | 3.96 | 24.7 | 0.71 | 34.8 | 0.67 | 0.048 | 626 | - |

$Q_{bf}$=bankfull discharge, B=bankfull width, H=bankfull depth, B/H=width depth ratio, $R_h$=hydraulic radius, $D_{50}$=median surface diameter, λ=bend wavelength.

**Table B2a. , location, data sources, and planform characteristics of sand meanders used in Chapter 3. Sources are listed at the end of the table.**

| Source | River | Latitude (dd) | Longitude (dd) | Elevation (m) | Islands[a] | Cutoffs[b] | Land Use Code[c] | Vegetation Code[d] |
|---|---|---|---|---|---|---|---|---|
| 1 | Strickland | -7.28 | 141.7 | 39 | 2 | 1 | 4 | 4 |
| 2 | Genesee | 42.78 | -77.83 | 208 | 0 | 1 | 1 | 3 |
| 3 | Little Tallahatchie | 34.4 | -89.85 | 61 | 0 | 1 | 1 | 2 |
| 4 | South Esk | 56.79 | -3.03 | 217 | 0 | 0 | 1 | 4 |
| 5 | Muddy | 42.65 | -109.55 | 2168 | 0 | 1 | 4 | 2 |
| 6 | Lower Teshio | 44.94 | 141.88 | 3 | 0 | 1 | 1 | 2 |
| 7 | Assiniboine | 49.97 | -98.17 | 251 | 0 | 1 | 1 | 2 |
| 7 | Athabasca | 58.33 | -111.65 | 215 | 1 | 1 | 3 | 4 |
| 7 | Beaver | 54.35 | -110.22 | 497 | 0 | 1 | 3 | 4 |
| 7 | Colorado | 29.6 | -96.45 | 44 | 0 | 1 | 1 | 2 |
| 7 | Fly | -6.32 | 141.07 | 19 | 0 | 1 | 3 | 4 |
| 7 | Gels Aa | 55.32 | 8.9 | 6 | 0 | 1 | 1 | 1 |
| 7 | Humboldt | 40.8 | -118.03 | 1282 | 1 | 1 | 4 | 1 |
| 7 | Ica | -2.9 | -69.65 | 58 | 1 | 1 | 3 | 4 |
| 7 | Juru (1) | -6.75 | -69.92 | 117 | 0 | 1 | 3 | 4 |
| 7 | Juru (2) | -6.52 | -68.32 | 92 | 0 | 1 | 3 | 4 |
| 7 | Kanaranzi | 43.52 | -96.07 | 426 | 0 | 1 | 1 | 1 |
| 7 | Lachlan | -33.82 | 148.63 | 286 | 0 | 1 | 1 | 2 |
| 7 | Lesser Slave | 55.3 | -114.75 | 577 | 0 | 1 | 1 | 3 |
| 7 | Mamore | -11.68 | -65.08 | 127 | 1 | 1 | 3 | 4 |
| 7 | Milk | 48.98 | -110.47 | 820 | 1 | 1 | 3 | 2 |
| 7 | Minnesota (1) | 44.2 | -94.23 | 234 | 0 | 1 | 1 | 4 |
| 7 | Minnesota (2) | 44.63 | -93.78 | 212 | 0 | 1 | 1 | 4 |
| 7 | Murrumbidgee (1) | -35.1 | 147.32 | 182 | 0 | 1 | 1 | 2 |
| 7 | Murrumbidgee (2) | -34.73 | 146.5 | 149 | 0 | 1 | 1 | 3 |
| 7 | Murrumbidgee (3) | -34.63 | 146.12 | 132 | 0 | 1 | 1 | 3 |
| 7 | Okavango (1) | -18.4 | 21.88 | 995 | 0 | 1 | 3 | 3 |
| 7 | Okavango (2) | -18.43 | 22.02 | 991 | 0 | 1 | 4 | 2 |
| 7 | Okavango (3) | -18.8 | 22.27 | 985 | 0 | 1 | 4 | 3 |
| 7 | Okavango (4) | -18.85 | 22.42 | 983 | 0 | 1 | 4 | 3 |
| 7 | Pembina (1) | 53.13 | -115.3 | 848 | 0 | 1 | 1 | 2 |
| 7 | Pembina (2) | 54.45 | -113.98 | 603 | 0 | 1 | 1 | 2 |
| 7 | Purus (1) | -8.33 | -67.33 | 90 | 0 | 1 | 3 | 4 |
| 7 | Purus (2) | -8.65 | -67.37 | 104 | 0 | 1 | 3 | 4 |
| 7 | Purus (3) | -7.23 | -64.8 | 51 | 0 | 1 | 3 | 4 |
| 7 | Root | 43.77 | -91.65 | 210 | 0 | 1 | 1 | 3 |
| 7 | Sinu | 9.08 | -75.83 | 8 | 0 | 0 | 1 | 2 |
| 7 | Smoky Hill | 38.88 | -97.25 | 342 | 0 | 1 | 1 | 2 |
| 7 | Sutlej | 30.75 | 74.23 | 182 | 0 | 1 | 1 | 1 |
| 7 | Swan | 55.32 | -115.4 | 590 | 0 | 1 | 1 | 3 |
| 7 | Vermilion | 53.37 | -111.17 | 585 | 0 | 1 | 1 | 4 |
| 7 | West Prairie | 55.43 | -116.5 | 599 | 0 | 1 | 1 | 2 |
| 7 | Zumbro | 44.32 | -92.05 | 207 | 0 | 1 | 1 | 3 |
| 8 | Po | 45.14 | 9.97 | 29 | 1 | 1 | 1 | 2 |

| Source | River | Latitude (dd) | Longitude (dd) | Elevation (m) | Islands[a] | Cutoffs[b] | Land Use Code[c] | Vegetation Code[d] |
|---|---|---|---|---|---|---|---|---|
| 9 | Desna | 51.29 | 31.1 | 108 | 0 | 1 | 1 | 3 |
| 9 | Snov | 52.59 | 31.62 | 109 | 0 | 1 | 1 | 2 |
| 10 | Trinity | 30.12 | -94.81 | 9 | 0 | 1 | 3 | 4 |
| 11 | Klip River | -27.65 | 29.58 | 1702 | 0 | 1 | 1 | 2 |
| 12 | Barwon | - | - | - | - | - | - | - |
| 12 | Big | - | - | - | - | - | - | - |
| 12 | Black Vermillion | - | - | - | - | - | - | - |
| 12 | Coleto | - | - | - | - | - | - | - |
| 12 | East Prairie | - | - | - | - | - | - | - |
| 12 | Guadelupe | - | - | - | - | - | - | - |
| 12 | Little Blue | - | - | - | - | - | - | - |
| 12 | Makarewa | - | - | - | - | - | - | - |
| 12 | Marais des Cignes | - | - | - | - | - | - | - |
| 12 | Medicine | - | - | - | - | - | - | - |
| 12 | Mill | - | - | - | - | - | - | - |
| 12 | Mississippi (1) | - | - | - | - | - | - | - |
| 12 | Mississippi (2) | 36.53 | -89.56 | 83 | 1 | 1 | 1 | 2 |
| 12 | N. Fork Solomon (1) | - | - | - | - | - | - | - |
| 12 | N. Fork Solomon (2) | - | - | - | - | - | - | - |
| 12 | Potawatomie | - | - | - | - | - | - | - |
| 12 | Prairie Dog | - | - | - | - | - | - | - |
| 12 | Republican | - | - | - | - | - | - | - |
| 12 | S. Fork Solomon | - | - | - | - | - | - | - |
| 12 | Saline | - | - | - | - | - | - | - |
| 12 | Salt | - | - | - | - | - | - | - |
| 12 | San Antonio | - | - | - | - | - | - | - |
| 12 | Smoky Hill | - | - | - | - | - | - | - |
| 12 | Solomon | - | - | - | - | - | - | - |
| 12 | Stranger | - | - | - | - | - | - | - |
| 12 | Turkey | - | - | - | - | - | - | - |

Notes:

a. Islands: 0=no islands, 1=unvegetated islands, 2=vegetated islands, 3=vegetated and unvegetated islands.
b. Cutoffs: 0=no cutoff scars, 1=cutoff scars visible
c. Land Use Code: 1=Agricultural, 2=Urban/Industrial, 3=Forested, 4=Rangelands
d. Vegetation Code: 1=Grass/shrubs, 2=Predominantly Grass/shrubs with trees, 3=Predominantly trees with grass/shrubs, 4=Forested

Sources: 1. Aalto et al. [2008], Swanson et al. [2008], Parker et al. [2008]; 2. Beck et al. [1984]; 3. Biedenharn [1984]; 4. Bridge and Jarvis [1976]; 5. Dietrich and Smith [1983]; 6. Iseya and Ikeda [1989]; 7. Kleinhans and van den Berg [2010]; 8. Montefusco and Taconi [1984]; 9. Rosovski [1959]; 10. Smith [2012]; 11. Tooth et al. [2012]; 12. van den Berg [1995].

**Table B2b. Hydraulic characteristics of sand meanders in Chapter 3.**

| River | Bankfull Discharge ($m^3/s$) | Bankfull Width (m) | Bankfull Depth (m) | $D_{50}$ (m) | Channel Slope | Valley Slope | Sinuosity | Width Depth Ratio |
|---|---|---|---|---|---|---|---|---|
| Strickland | 5700 | 350 | - | 0.00022 | 0.0001 | 0.00025 | 2 | - |
| Genesee | - | 74 | 3.8 | - | 0.000201 | - | - | 19.5 |
| Little Tallahatchie | - | - | - | - | 0.00025 | - | - | - |
| South Esk | 22 | - | - | - | - | - | - | - |
| Muddy | - | - | - | 0 | - | - | - | - |
| Lower Teshio | 1500 | 125 | 6.5 | 0.0012 | 0.00025 | - | - | 19.2 |
| Assiniboine | 626 | 150 | 4.2 | 0.0004 | 0.00025 | 0.0005 | 2 | 35.7 |
| Athabasca | 2605.4 | 442 | 5.3 | 0.00019 | 0.000089 | 0.00012 | 1.4 | 83.4 |
| Beaver | 141.6 | 54 | 2.9 | 0.00056 | 0.000205 | 0.00027 | 1.3 | 18.7 |
| Colorado | 4250 | - | - | 0.001 | 0.000194 | 0.00032 | 1.7 | - |
| Fly | 3018 | - | - | 0.0002 | 0.000065 | 0.00011 | 1.7 | - |
| Gels Aa | 10 | 15 | 1.5 | 0.00051 | 0.0005 | 0.00088 | 1.8 | 10 |
| Humboldt | 109 | 15 | 3.86 | 0.0007 | 0.000372 | 0.00054 | 1.5 | 3.9 |
| Ica | 10213 | - | - | 0.0003 | 0.000082 | 0.00015 | 1.8 | - |
| Juru (1) | 3000 | - | - | 0.0003 | 0.000072 | 0.00017 | 2.3 | - |
| Juru (2) | 7700 | - | - | 0.0003 | 0.00008 | 0.00018 | 2.3 | - |
| Kanaranzi | 23.4 | 8 | 1.4 | 0.00045 | 0.000711 | 0.0014 | 2 | 5.4 |
| Lachlan | 620 | - | - | 0.0007 | 0.000382 | 0.0006 | 1.6 | - |
| Lesser Slave | 107.3 | 59 | 2.6 | 0.0002 | 0.00011 | 0.00022 | 2 | 22.8 |
| Mamore | 14700 | - | - | 0.0003 | 0.00009 | 0.00013 | 1.5 | - |
| Milk | 150 | 47 | - | 0.00023 | 0.0005 | 0.0011 | 2.3 | - |
| Minnesota (1) | 313.9 | 43 | 4.69 | 0.0005 | 0.000242 | 0.00047 | 1.9 | 9.1 |
| Minnesota (2) | 427 | 88 | 4.5 | 0.0005 | 0.000102 | 0.0002 | 2 | 19.6 |
| Murrumbidgee (1) | 708 | - | - | 0.0004 | 0.00017 | 0.00039 | 2.3 | - |
| Murrumbidgee (2) | 566 | - | - | 0.0009 | 0.000212 | 0.00036 | 1.7 | - |
| Murrumbidgee (3) | 311 | - | - | 0.00071 | 0.000132 | 0.00025 | 1.9 | - |
| Okavango (1) | 163.1 | 85 | 2.79 | 0.0003 | 0.000107 | 0.00018 | 1.7 | 30.5 |
| Okavango (2) | 90.3 | 53 | 2.8 | 0.0003 | 0.000079 | 0.00018 | 2.3 | 18.9 |
| Okavango (3) | 91.7 | 51 | 3.21 | 0.0003 | 0.000091 | 0.00018 | 2 | 15.9 |
| Okavango (4) | 97.4 | 49 | 3.98 | 0.0003 | 0.000102 | 0.00018 | 1.8 | 12.3 |
| Pembina (1) | 566 | 79 | 4.1 | 0.00027 | 0.000329 | 0.00056 | 1.7 | 19.3 |
| Pembina (2) | 608.9 | 95 | 5 | 0.00032 | 0.00011 | 0.00022 | 2 | 19 |
| Purus (1) | 16711 | - | - | 0.0003 | 0.000032 | 0.00005 | 1.6 | - |
| Purus (2) | 6000 | - | - | 0.0003 | 0.000093 | 0.00016 | 1.7 | - |
| Purus (3) | 10550 | - | - | 0.0003 | 0.000065 | 0.00014 | 2.1 | - |
| Root | - | 34 | 2.9 | 0.00045 | 0.000611 | 0.00088 | 1.4 | 11.6 |
| Sinu | 1200 | 140 | 5 | 0.0004 | 0.0002 | 0.0003 | 1.5 | 28 |
| Smoky Hill | - | - | - | 0.00046 | 0.000361 | 0.00065 | 1.8 | - |
| Sutlej | 2100 | - | - | 0.00023 | 0.0002 | 0.00028 | 1.4 | - |
| Swan | 149 | 42 | 3.78 | 0.00029 | 0.000318 | 0.00054 | 1.7 | 11.1 |
| Vermilion | 7.9 | 19 | 1.1 | 0.00026 | 0.000359 | 0.00079 | 2.2 | 16.9 |
| West Prairie | 164 | 31 | 3.3 | 0.00043 | 0.000689 | 0.0012 | 1.8 | 9.4 |
| Zumbro | - | 49 | 3.11 | 0.0008 | 0.000532 | 0.00099 | 1.9 | 15.7 |
| Po | - | - | - | 0.00055 | 0.0021 | - | - | - |
| Desna | - | 130 | 3.2 | - | 0.000027 | 0.000050 | 1.84 | 40.625 |
| Snov | - | 25 | 0.5 | - | 0.000382 | 0.00061 | 1.6 | 50 |

| River | Bankfull Discharge ($m^3/s$) | Bankfull Width (m) | Bankfull Depth (m) | $D_{50}$ (m) | Channel Slope | Valley Slope | Sinuosity | Width Depth Ratio |
|---|---|---|---|---|---|---|---|---|
| Trinity | - | - | - | - | - | - | - | - |
| Klip River | - | - | - | 0.0014 | 0.001 | 0.0016 | 1.6 | - |
| Barwon | 210 | 40 | 5 | 0.00015 | 0.000022 | 0.00005 | 2.3 | 8 |
| Big | - | - | - | 0.00081 | 0.000812 | 0.0020 | 2.5 | - |
| Black Vermillion | - | - | - | 0.0004 | 0.00049 | 0.00098 | 2 | - |
| Coleto | - | 122 | 7.6 | 0.0003 | 0.000737 | 0.00101 | 1.4 | 16.1 |
| East Prairie | 396.5 | 39 | 7.2 | 0.00033 | 0.0005 | 0.0007 | 1.4 | 5.4 |
| Guadelupe | - | 57 | 7 | 0.00045 | 0.00033 | 0.00074 | 2.2 | 8.1 |
| Little Blue | - | - | - | 0.00077 | 0.000521 | 0.00073 | 1.4 | - |
| Makarewa | 129 | 29 | 2.47 | 0.001 | 0.000898 | 0.0017 | 1.9 | 11.6 |
| Marais des Cignes | - | - | - | 0.00023 | 0.000389 | 0.0007 | 1.8 | - |
| Medicine | 130.3 | 47 | 3.2 | 0.00031 | 0.00051 | 0.00071 | 1.4 | 14.6 |
| Mill | - | - | - | 0.00043 | 0.00062 | 0.0019 | 3 | - |
| Mississippi (1) | 28000 | 1975 | 10.6 | 0.00035 | 0.000045 | 0.00011 | 2.3 | 186.3 |
| Mississippi (2) | 28320 | - | - | 0.00037 | 0.000093 | 0.00013 | 1.4 | - |
| N. Fork Solomon (1) | - | - | - | 0.00075 | 0.000538 | 0.00086 | 1.6 | - |
| N. Fork Solomon (2) | - | - | - | 0.00046 | 0.001306 | 0.0021 | 1.6 | - |
| Potawatomie | - | - | - | 0.00119 | 0.0002 | 0.00034 | 1.7 | - |
| Prairie Dog | - | - | - | 0.00169 | 0.000638 | 0.00102 | 1.6 | - |
| Republican | - | - | - | 0.00047 | 0.000662 | 0.00086 | 1.3 | - |
| S. Fork Solomon | - | - | - | 0.00115 | 0.001 | 0.0014 | 1.4 | - |
| Saline | - | - | - | 0.0007 | 0.000581 | 0.00093 | 1.6 | - |
| Salt | - | - | - | 0.00026 | 0.00038 | 0.00076 | 2 | - |
| San Antonio | - | - | - | 0.00013 | 0.000191 | 0.00033 | 1.7 | - |
| Smoky Hill | - | - | - | 0.00035 | 0.00021 | 0.00042 | 2 | - |
| Solomon | - | - | - | 0.00064 | 0.000171 | 0.00048 | 2.8 | - |
| Stranger | - | - | - | 0.00017 | 0.000178 | 0.00032 | 1.8 | - |
| Turkey | - | 9 | 1.83 | 0.00046 | 0.000729 | 0.0010 | 1.4 | 5 |

**Table B3a. Location, data sources, and floodplain characteristics of gravel braided rivers in Chapter 3. Sources are listed at the end of the table.**

| Source | River | Location | Latitude (dd) | Longitude (dd) | Elevation (m) | Land Use Code[c] | Vegetation Code[d] |
|---|---|---|---|---|---|---|---|
| 1 | Ahuriri | at South Diadem, S. Island, New Zealand | -44.50 | 169.77 | 553 | 4 | 1 |
| 1 | Athabasca | at Jasper, AB, Canada | 52.87 | -118.07 | 1041 | 3 | 4 |
| 1 | Elbow | at Fullertons Ranch, AB, Canada | 50.92 | -114.62 | 1340 | 3 | 4 |
| 1 | Haast | at Roaring Billy, S. Island, New Zealand | -43.95 | 169.35 | 52 | 3 | 3 |
| 1 | Hokitika (1) | at Colliers Creek, S. Island, New Zealand | -42.98 | 171.00 | 71 | 4 | 4 |
| 1 | Hokitika (2) | at Kaniere Br, S. Island, New Zealand | -42.75 | 171.00 | 12 | 1 | 1 |
| 1 | Hooker | at Ball Hut riv. bridge, S. Island, New Zealand | -43.75 | 170.13 | 624 | 4 | 2 |
| 1 | Ngaruroro | near Whanawhana, N Island NZ | -39.57 | 176.50 | 129 | 1 | 2 |
| 1 | Opihi | at Rockwood, S. Island, New Zealand | -44.17 | 170.97 | 146 | 1 | 2 |
| 1 | Rakaia | in the gorge, S. Island, New Zealand | -43.55 | 171.72 | 236 | 1 | 2 |
| 1 | Wairau | at Hells Gate, S. Island, New Zealand | -42.03 | 172.90 | 807 | 3 | 3 |
| 1 | Wairoa | at Tuamarina, S. Island, New Zealand | -41.43 | 173.92 | 1 | 1 | 2 |
| 1 | West Banas | near Abu Road, Gujarat, India | 24.47 | 72.75 | 239 | 1 | 2 |
| 1 | Yukon | above White River, YT, Canada | 63.12 | -139.50 | 356 | 3 | 4 |
| 2 | Allt Dubhaig | Reach B | 56.84 | -4.24 | 569 | 4 | 1 |
| 2 | Banas | - | - | - | - | - | - |
| 2 | Grey | - | - | - | - | - | - |
| 2 | Orari | - | - | - | - | - | - |
| 2 | Otekaieke | - | - | - | - | - | - |
| 2 | Hakataramea | - | - | - | - | - | - |
| 2 | Hurunui | - | - | - | - | - | - |
| 2 | Inangahua | - | - | - | - | - | - |
| 2 | Kootenay | - | - | - | - | - | - |
| 2 | Lleddam | - | - | - | - | - | - |
| 2 | Maerewhemta | - | - | - | - | - | - |
| 2 | Ohau | - | - | - | - | - | - |
| 2 | Opuha | - | - | - | - | - | - |
| 2 | Otematata | - | - | - | - | - | - |
| 2 | Pipestone | - | - | - | - | - | - |
| 2 | Rangitata | - | - | - | - | - | - |
| 2 | S. Ashburton | - | - | - | - | - | - |
| 2 | Squamish | - | - | - | - | - | - |
| 2 | Waiau-Uha | - | - | - | - | - | - |
| 2 | Yashwantgur | - | - | - | - | - | - |

Sources: 1. Kleinhans and van den Berg [2010]; 2. van den Berg [1995]

## Table B3b. Hydraulic characteristics of gravel braided rivers in Chapter 3

| River | Bankfull Discharge ($m^3/s$) | Bankfull Width (m) | Bankfull Depth (m) | $D_{50}$ (m) | Channel Slope | Valley Slope | Sinuosity | Width Depth Ratio |
|---|---|---|---|---|---|---|---|---|
| Ahuriri | 228 | 252 | 0.49 | 0.027 | - | 0.009 | - | 514 |
| Athabasca | 878 | 146 | 2.26 | 0.060 | 0.00590 | 0.00649 | 1.1 | 65 |
| Elbow | - | - | - | 0.041 | 0.00720 | 0.00792 | 1.1 | - |
| Haast | 2576 | 910 | 1.57 | 0.040 | - | 0.0016 | - | 580 |
| Hokitika (1) | 975 | 541 | 0.84 | 0.077 | 0.00590 | 0.00608 | 1.03 | 644 |
| Hokitika (2) | 740 | 314 | 1.49 | 0.021 | 0.00177 | 0.002 | 1.13 | 211 |
| Hooker | 1112 | 270 | 1.13 | 0.067 | 0.01820 | 0.01947 | 1.07 | 239 |
| Ngaruroro | - | - | - | 0.055 | 0.00400 | 0.0042 | 1.05 | - |
| Opihi | 214 | 140 | 0.87 | 0.033 | 0.00610 | 0.00634 | 1.04 | 161 |
| Rakaia | 1813 | 1753 | 0.84 | 0.025 | 0.00404 | 0.00404 | 1 | 2087 |
| Wairau | 248 | 229 | 0.64 | 0.031 | 0.01060 | 0.01092 | 1.03 | 358 |
| Wairoa | 1536 | 1137 | 0.97 | 0.055 | - | 0.0032 | - | 1172 |
| West Banas | 2407 | - | - | 0.005 | 0.00217 | 0.0023 | 1.06 | - |
| Yukon | 6478 | 582 | 4.55 | 0.036 | 0.00040 | 0.00044 | 1.1 | 128 |
| Allt Dubhaig | 6 | - | - | 0.046 | 0.01500 | 0.018 | 1.2 | - |
| Banas | 2407 | - | - | 0.005 | - | 0.0023 | - | - |
| Grey | 486 | 124 | 1.86 | 0.070 | 0.00310 | 0.00341 | 1.1 | 67 |
| Orari | 175 | 255 | 0.52 | 0.024 | 0.00830 | 0.0083 | 1 | 490 |
| Otekaieke | 93 | 162 | 0.42 | 0.016 | 0.01000 | 0.0102 | 1.02 | 386 |
| Hakataramea | 377 | 390 | 0.67 | 0.030 | 0.00570 | 0.00593 | 1.04 | 582 |
| Hurunui | 381 | 316 | 0.74 | 0.035 | 0.00630 | 0.0068 | 1.08 | 427 |
| Inangahua | 347 | 324 | 0.80 | 0.087 | 0.00470 | 0.00503 | 1.07 | 405 |
| Kootenay | - | 104 | 1.87 | 0.088 | - | 0.00231 | - | 56 |
| Lleddam | 562 | 73 | 2.53 | 0.080 | 0.00730 | 0.00767 | 1.05 | 29 |
| Maerewhemta | 271 | 94 | 1.17 | 0.031 | 0.00791 | 0.00854 | 1.08 | 80 |
| Ohau | 189 | 109 | 0.84 | 0.045 | 0.00650 | 0.00696 | 1.07 | 130 |
| Opuha | 197 | 171 | 0.63 | 0.031 | 0.01000 | 0.0104 | 1.04 | 271 |
| Otematata | 385 | 244 | 0.72 | 0.034 | 0.01200 | 0.01308 | 1.09 | 339 |
| Pipestone | 52 | 35 | 0.76 | 0.145 | 0.01500 | 0.0165 | 1.1 | 46 |
| Rangitata | 1372 | 125 | 2.96 | 0.069 | 0.00520 | 0.00749 | 1.44 | 42 |
| S. Ashburton | 347 | 137 | 1.12 | 0.037 | 0.01160 | 0.01322 | 1.14 | 122 |
| Squamish | 500 | - | - | 0.095 | 0.00576 | 0.0069 | 1.197 | - |
| Waiau-Uha | 1149 | 1156 | 0.78 | 0.036 | 0.00458 | 0.0049 | 1.07 | 1482 |
| Yashwantgur | 283 | - | - | 0.002 | - | 0.0045 | - | - |

# Appendix C-Enlarged Depth and Facies Maps for Chapter 4

This Appendix contains enlarged depth and facies maps from the experiments in Chapter 4.

## List of Figures

Figure C1. Flow depth at -27.5 hours. ..... 168
Figure C2. Flow depth at -19.5 hours ..... 169
Figure C3. Flow depth at -9 hours. ..... 170
Figure C4. Flow depth at 0 hours..... 171
Figure C5. Flow depth at 12 hours..... 172
Figure C6. Flow depth at 20 hours..... 173
Figure C7. Flow depth at 29 hours..... 174
Figure C8. Flow depth at 38 hours..... 175
Figure C9. Flow depth at 48 hours..... 176
Figure C10. Flow depth at 55 hours..... 177
Figure C11 Flow depth at 64 hours..... 178
Figure C12. Flow depth at 71 hours..... 179
Figure C13. Flow depth at 80 hours..... 180
Figure C14. Flow depth at 100 hours..... 181
Figure C15. Facies Maps from -9 to 11.8 hours ..... 182
Figure C16 Facies Maps from 20 to 55 hours..... 183
Figure C17 Facies Maps from 80 to 100 hours..... 184

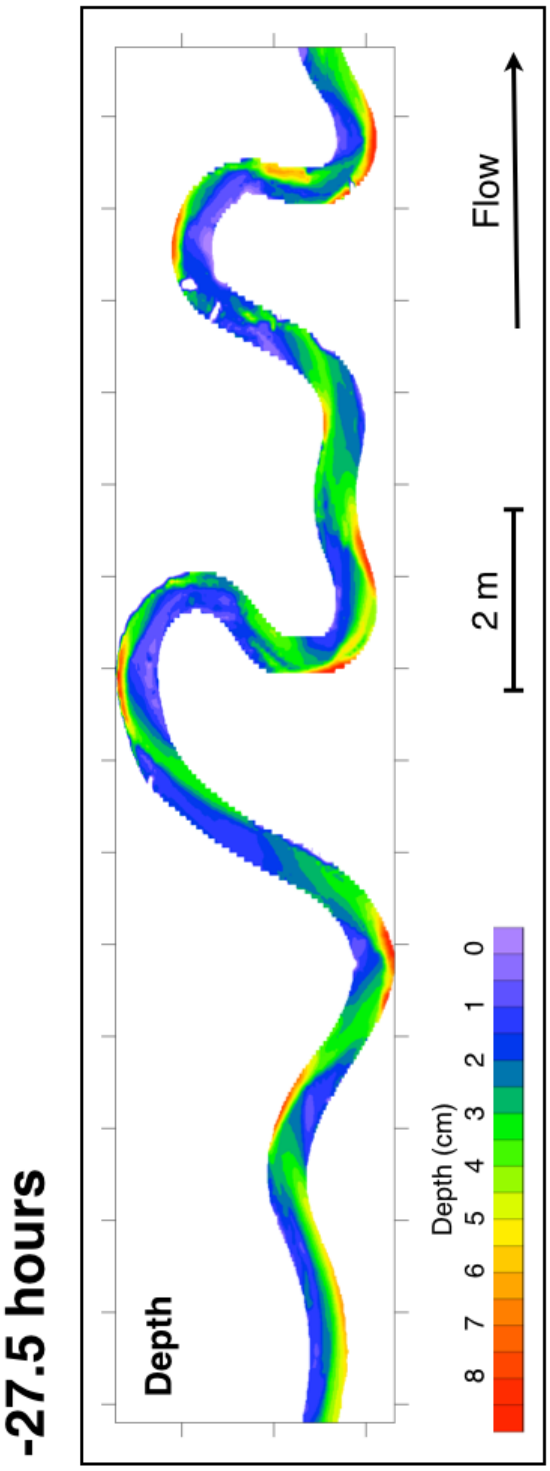


Figure C1. Flow depth  at -27.5 hours.

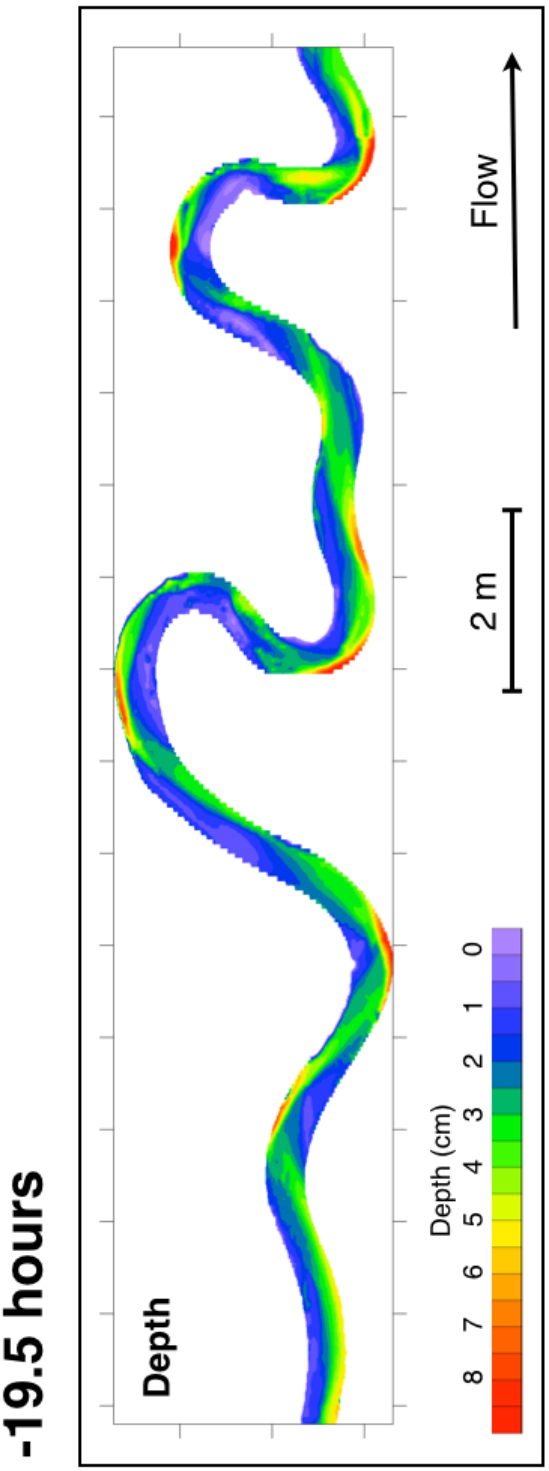


Figure C2. Flow depth  at -19.5 hours

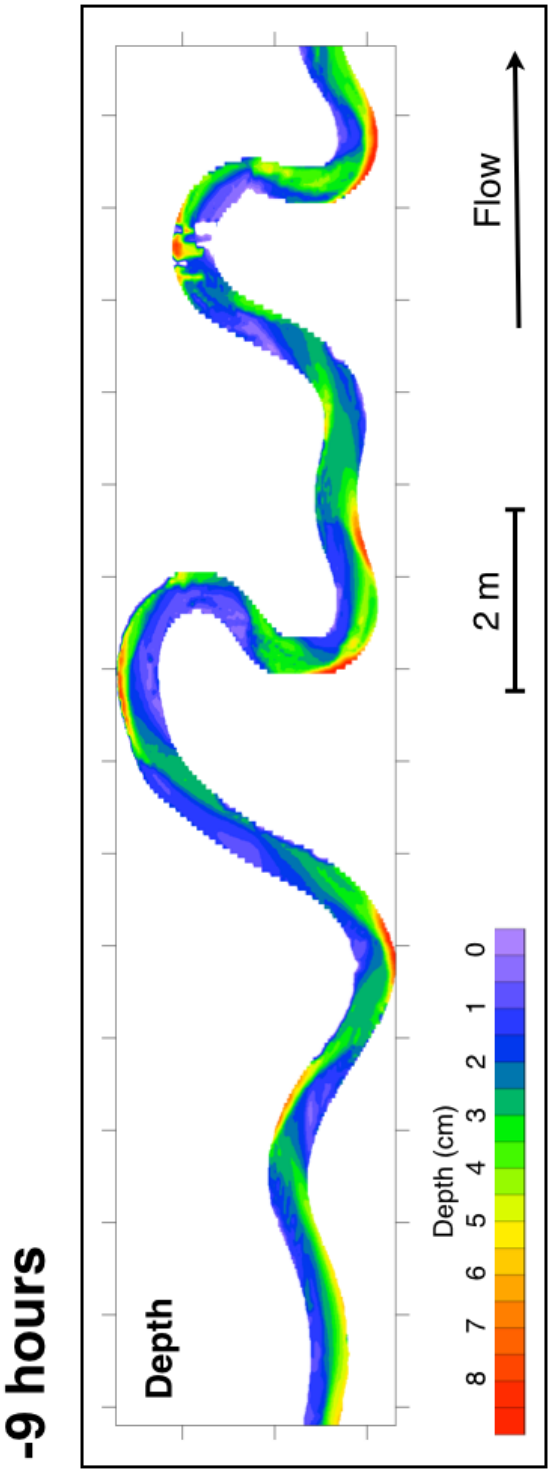


Figure C3. Flow depth  at -9 hours.

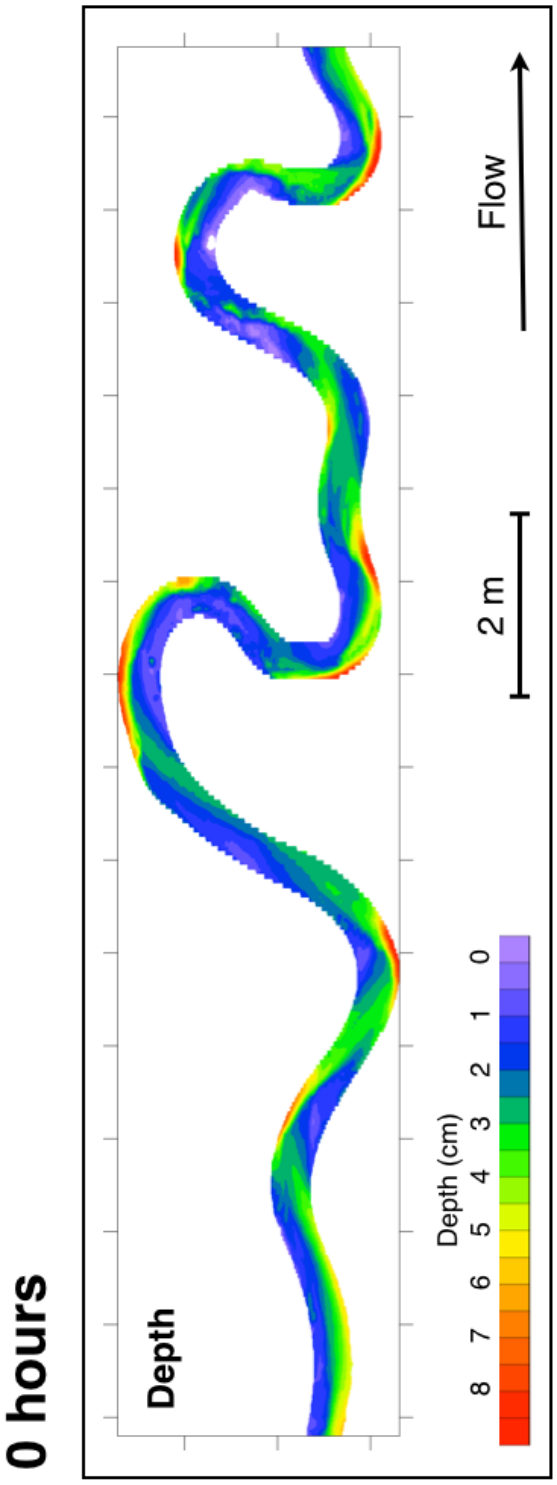


Figure C4. Flow depth  at 0 hours

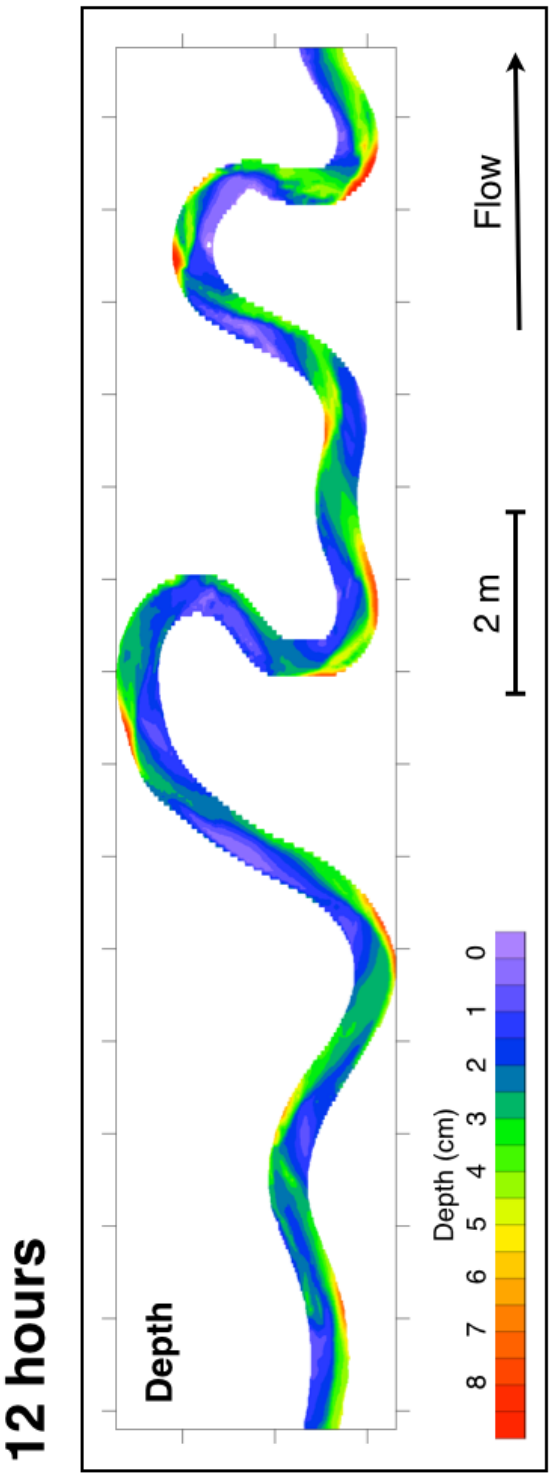


Figure C5. Flow depth  at 12 hours

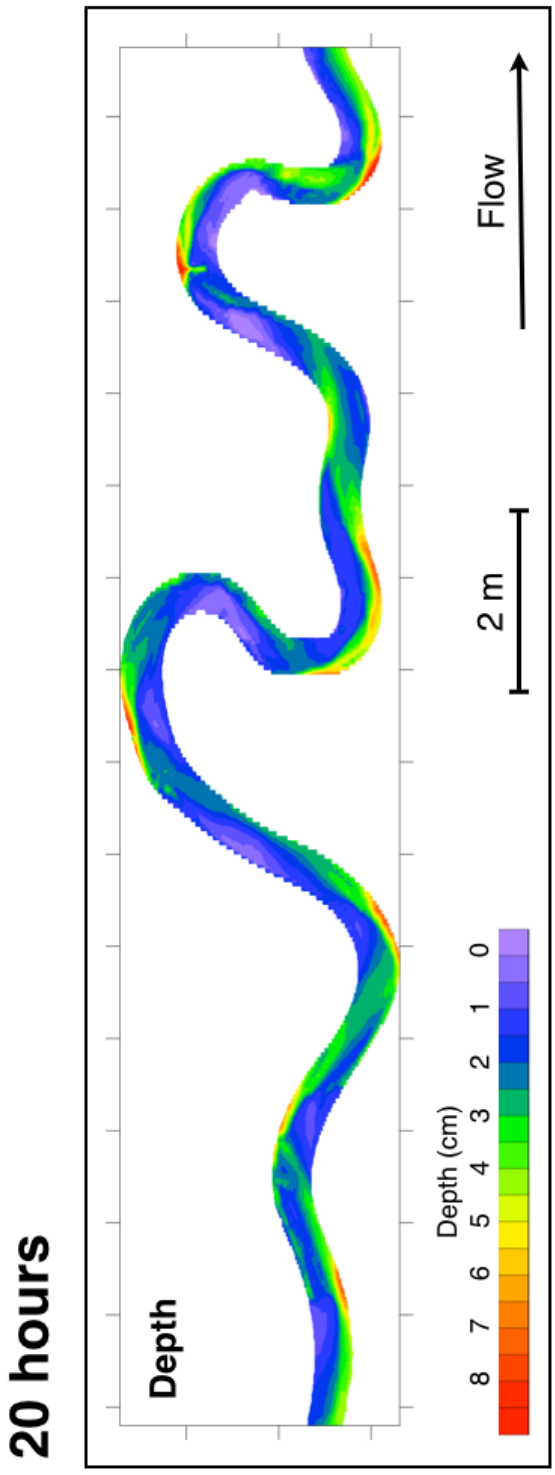


Figure C6. Flow depth  at 20 hours

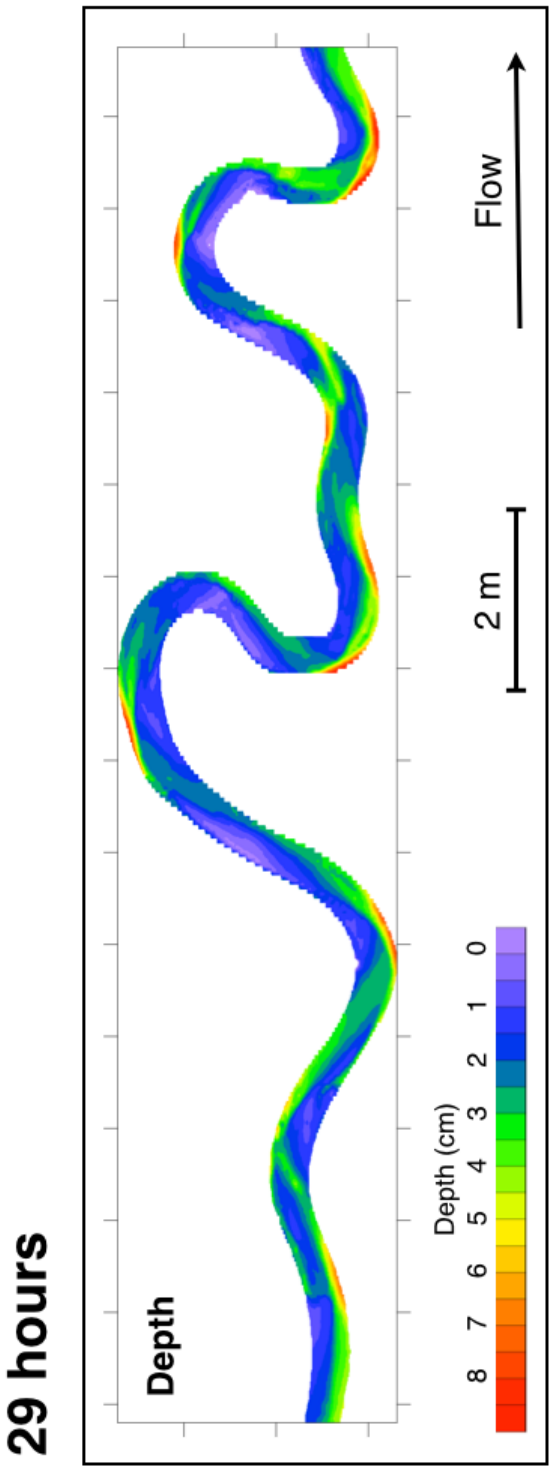


Figure C7. Flow depth  at 29 hours

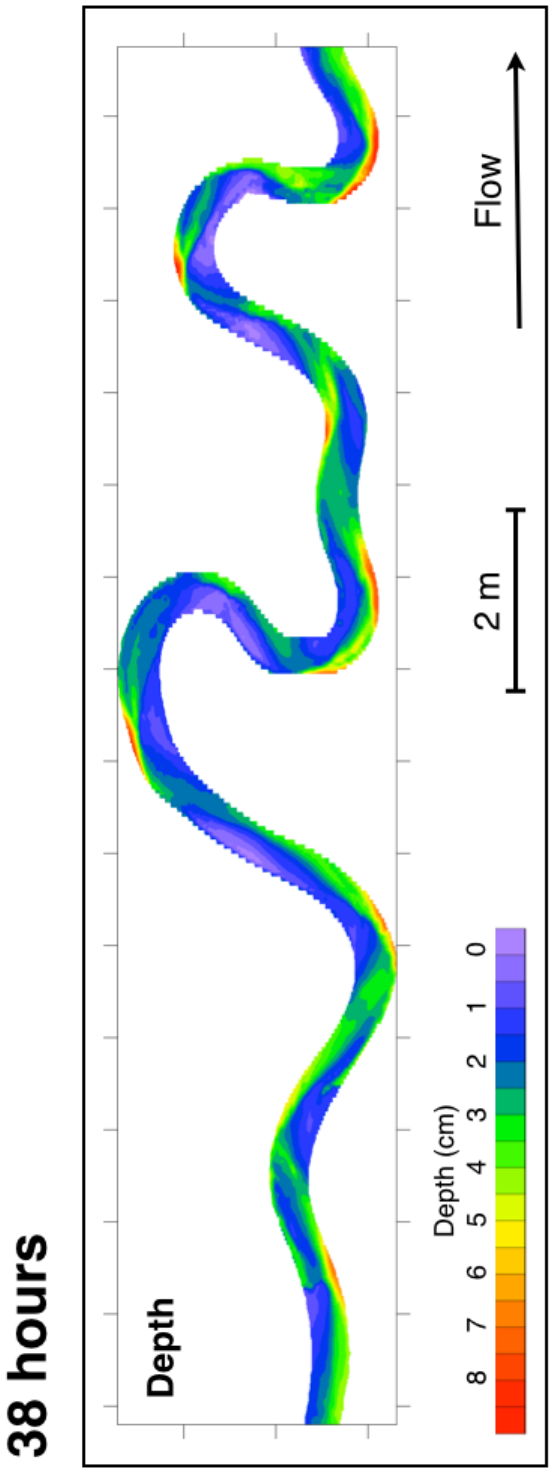


Figure C8. Flow depth  at 38 hours

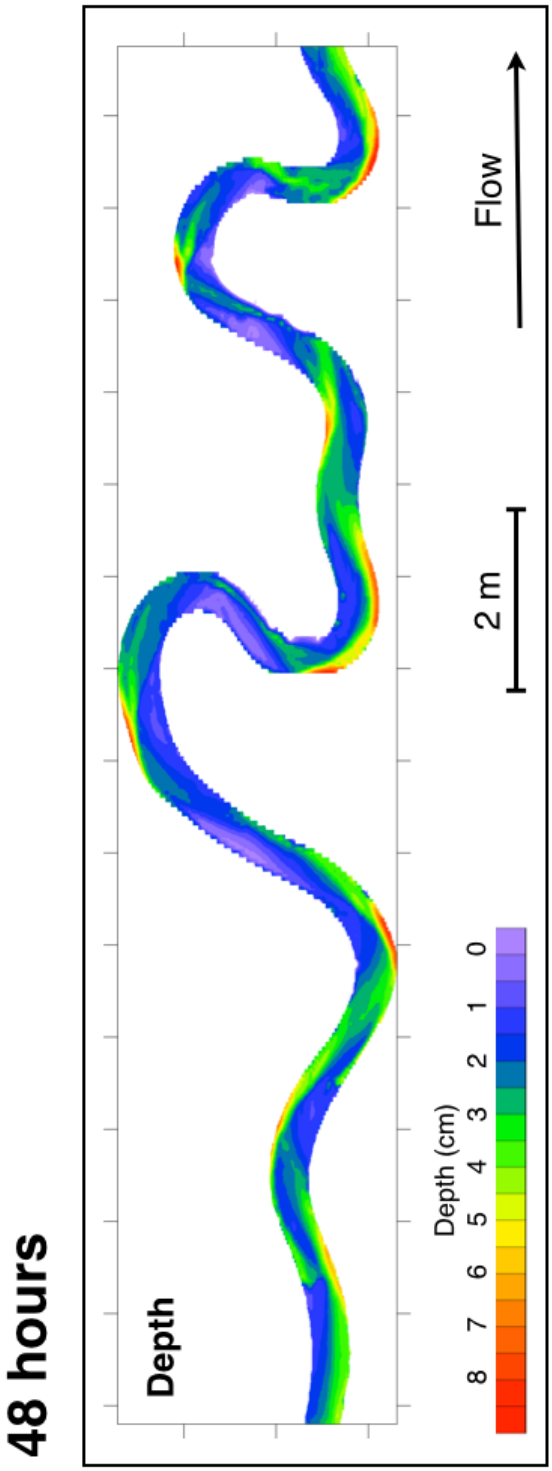


Figure C9. Flow depth  at 48 hours

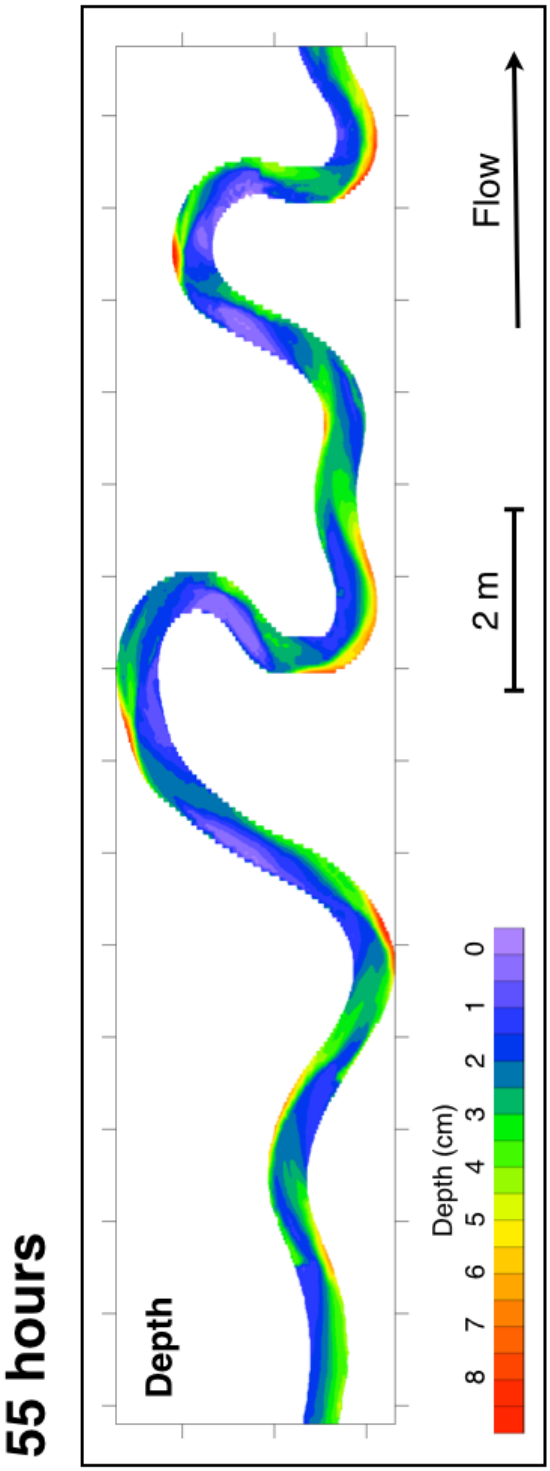


Figure C10. Flow depth  at 55 hours

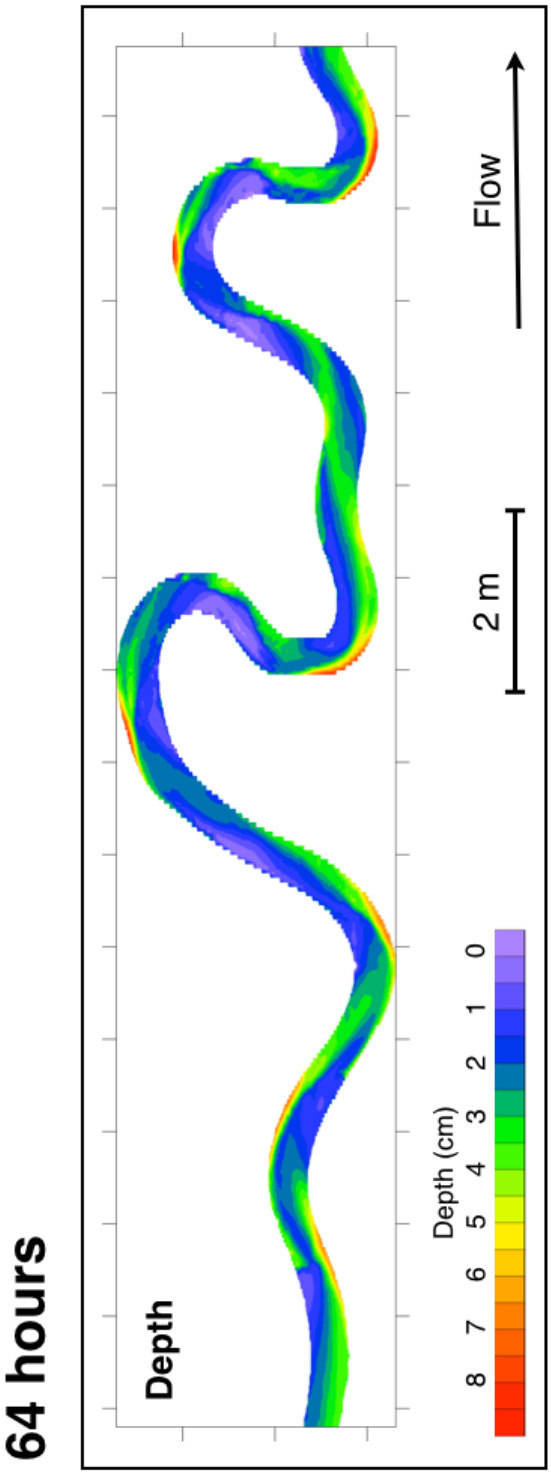


Figure C11 Flow depth  at 64 hours

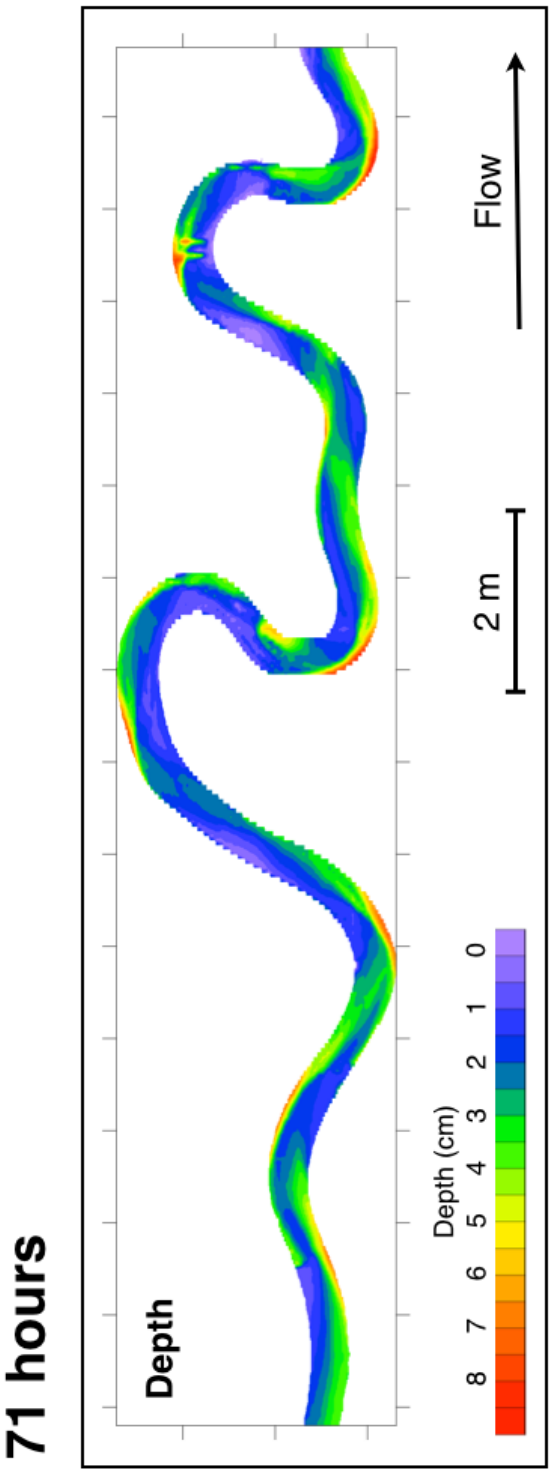


Figure C12. Flow depth  at 71 hours

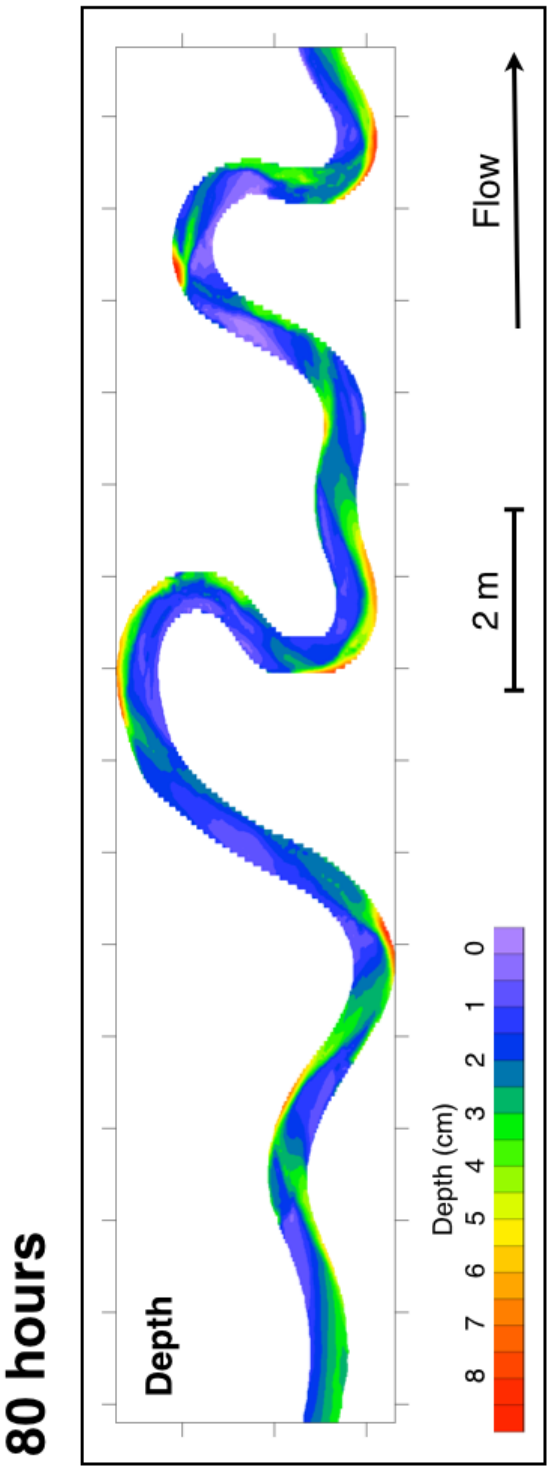


Figure C13. Flow depth  at 80 hours

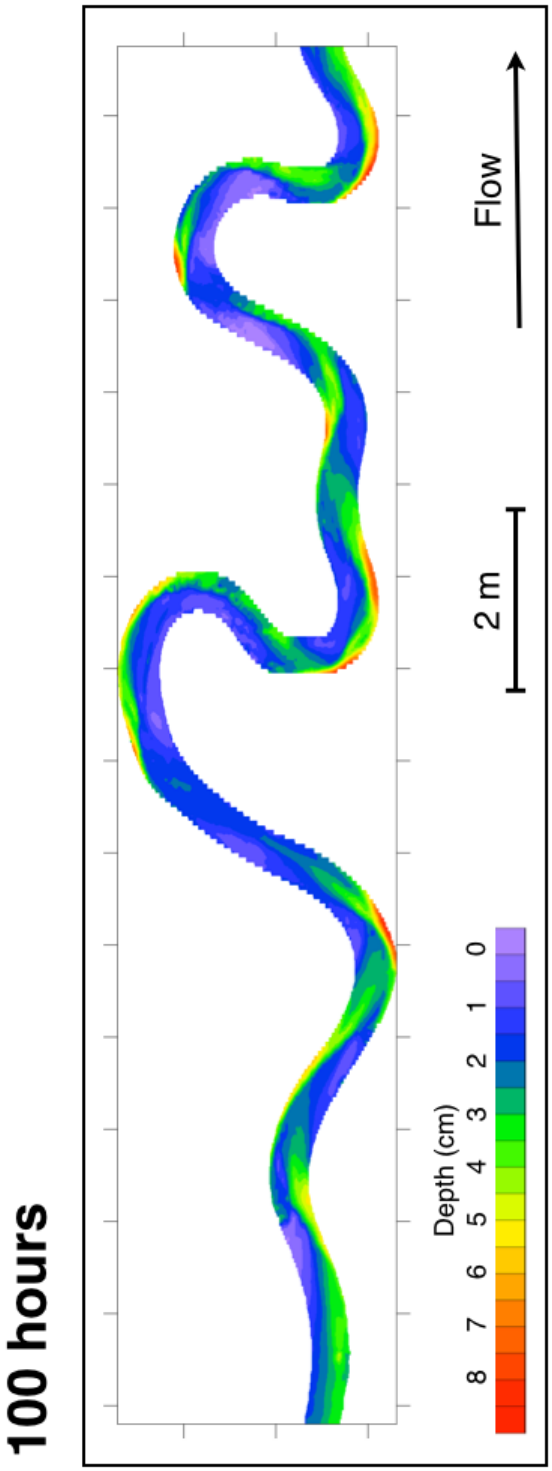


Figure C14. Flow depth  at 100 hours

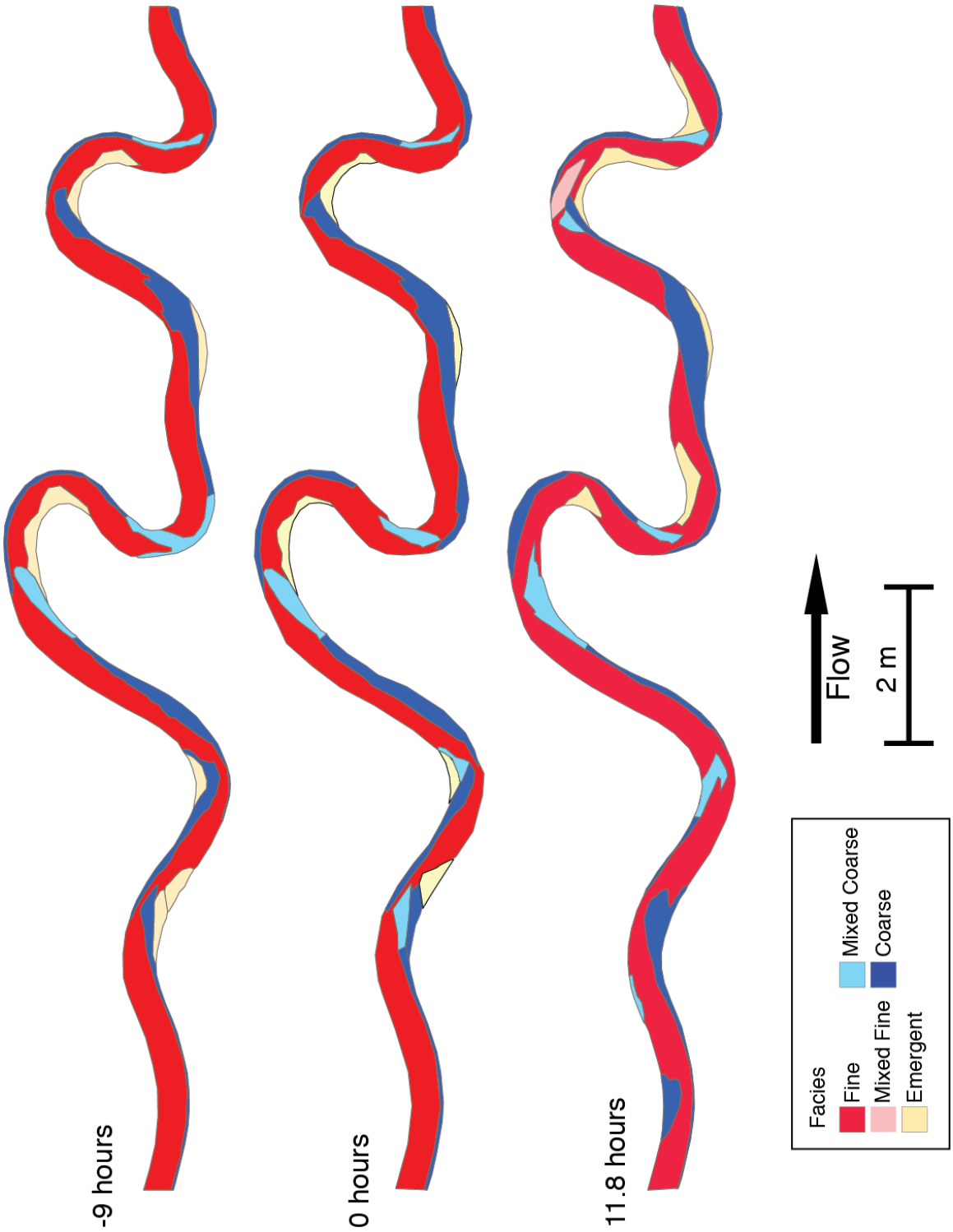


Figure C15. Facies Maps from -9 to 11.8 hours

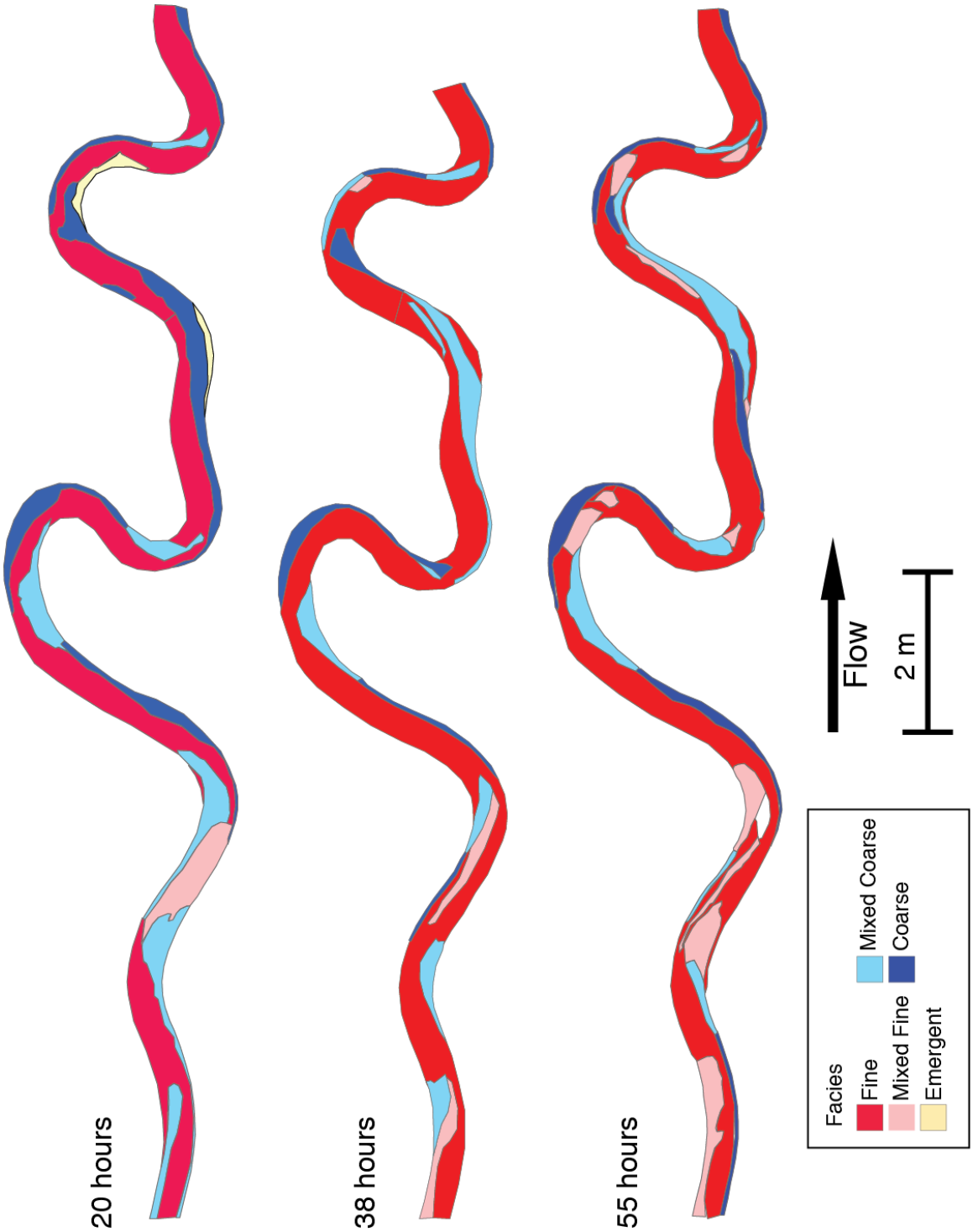


Figure C16 Facies Maps from 20 to 55 hours

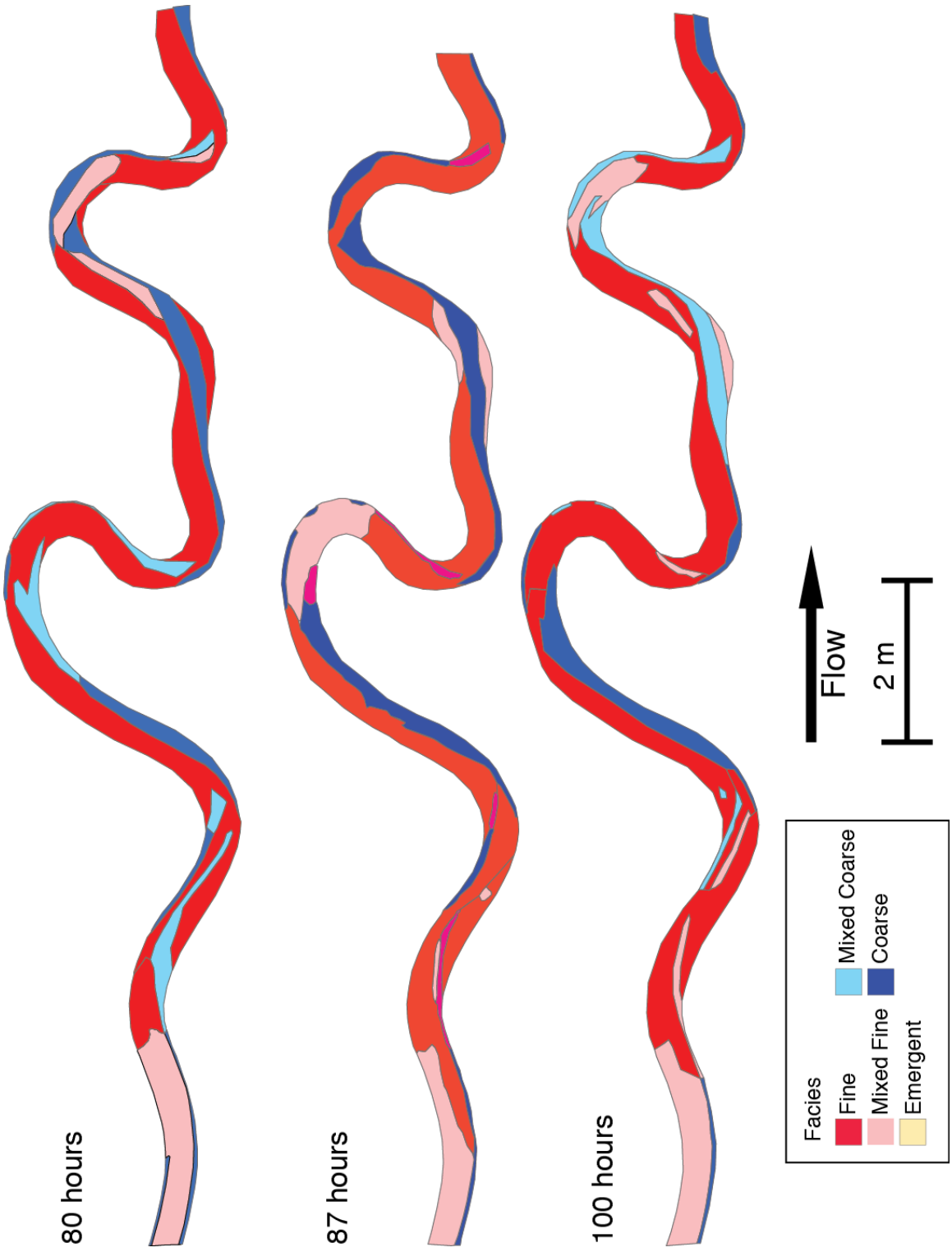


Figure C17 Facies Maps from 80 to 100 hours

# Appendix D-Enlarged Topographic maps from Chapter 5

This Appendix describes two attached video files and includes enlarged topographic maps and overhead photographs from the experiments in Chapter 5.

Supplemental Video 2 shows overhead photographs of the flume every 30 minutes. Flow is from left to right. The white is plastic, the tan colors are sand, and the green is alfalfa. Every second in the video shows 5 hours of evolution of the experiment.

Supplemental Video 3 shows the topographic evolution of the experiment through time. Flow is from left to right.

## List of Figures

Figure D.1. Bed topography and overhead image at 0 hours..... 186
Figure D.2. Bed topography and overhead image at 6 hours..... 187
Figure D.3. Bed topography and overhead image at 12 hours..... 188
Figure D.4. Bed topography and overhead image at 18 hours..... 189
Figure D.5. Bed topography and overhead image at 25 hours..... 190
Figure D.6. Bed topography and overhead image at 32 hours..... 191
Figure D.7. Bed topography and overhead image at 39 hours..... 192
Figure D.8. Bed topography and overhead image at 45 hours..... 193
Figure D.9. Bed topography and overhead image at 52 hours..... 194
Figure D.10. Bed topography and overhead image at 60 hours..... 195
Figure D.11. Bed topography and overhead image at 68.5 hours..... 196
Figure D.12. Bed topography and overhead image at 77.5 hours..... 197
Figure D.13. Bed topography and overhead image at 87 hours..... 198
Figure D.14. Bed topography and overhead image at 93 hours..... 199
Figure D.15. Bed topography and overhead image at 100 hours..... 200
Figure D.16. Bed topography and overhead image at 108 hours..... 201
Figure D.17. Bed topography and overhead image at 114 hours..... 202
Figure D.18. Bed topography and overhead image at 120 hours..... 203

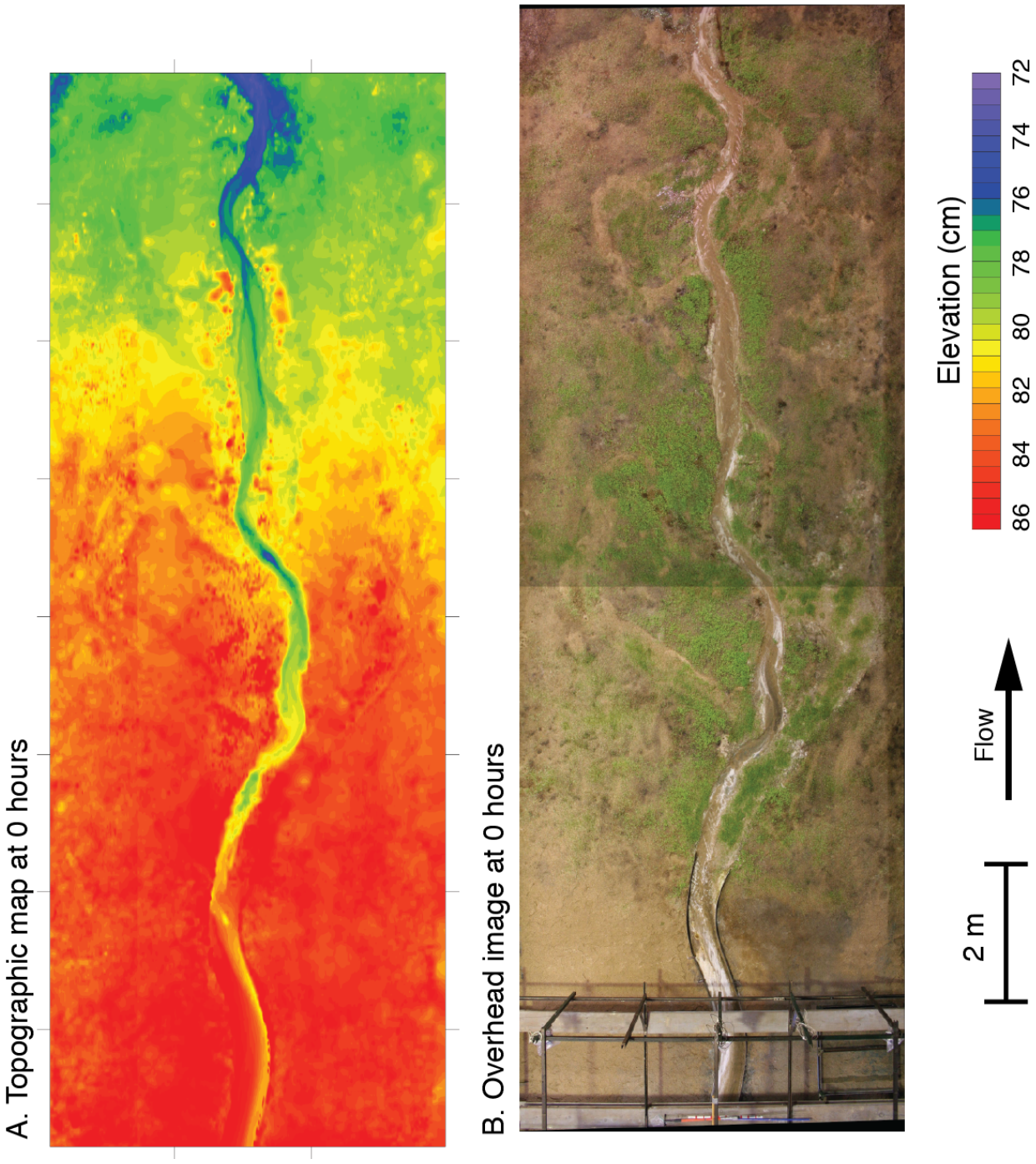


Figure D.1. Bed topography and overhead image at 0 hours.

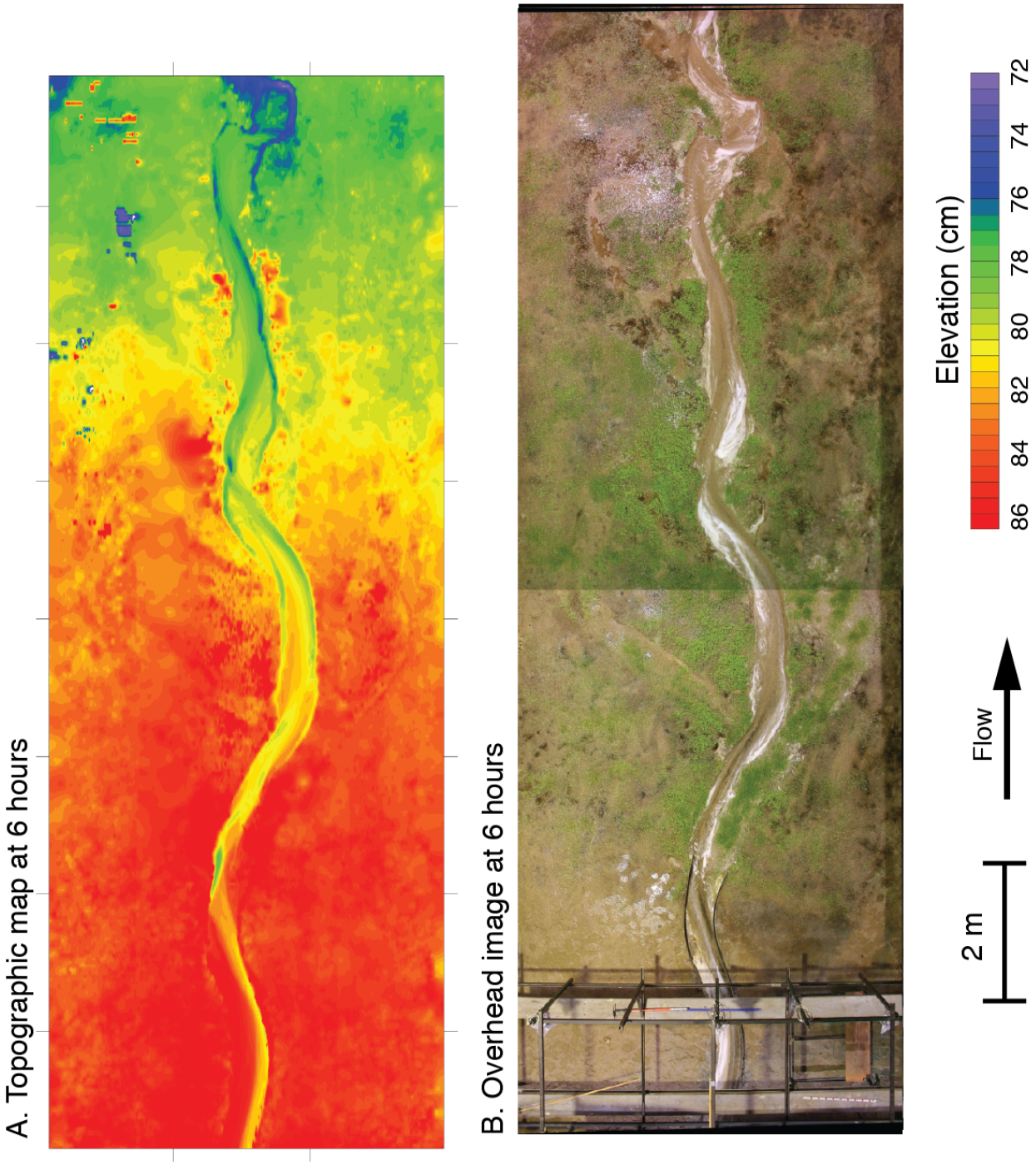


Figure D.2. Bed topography and overhead image at 6 hours.

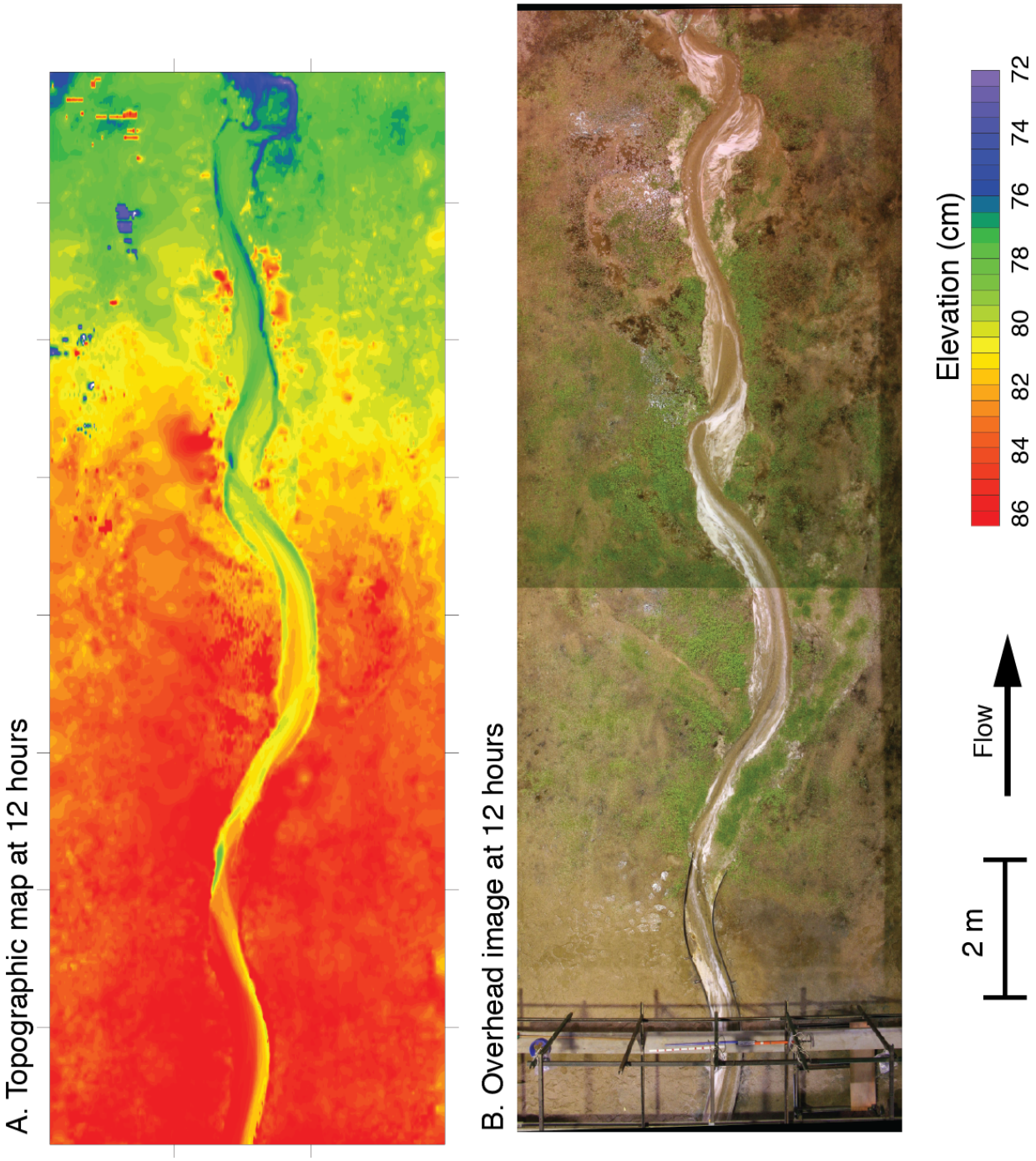


Figure D.3. Bed topography and overhead image at 12 hours.

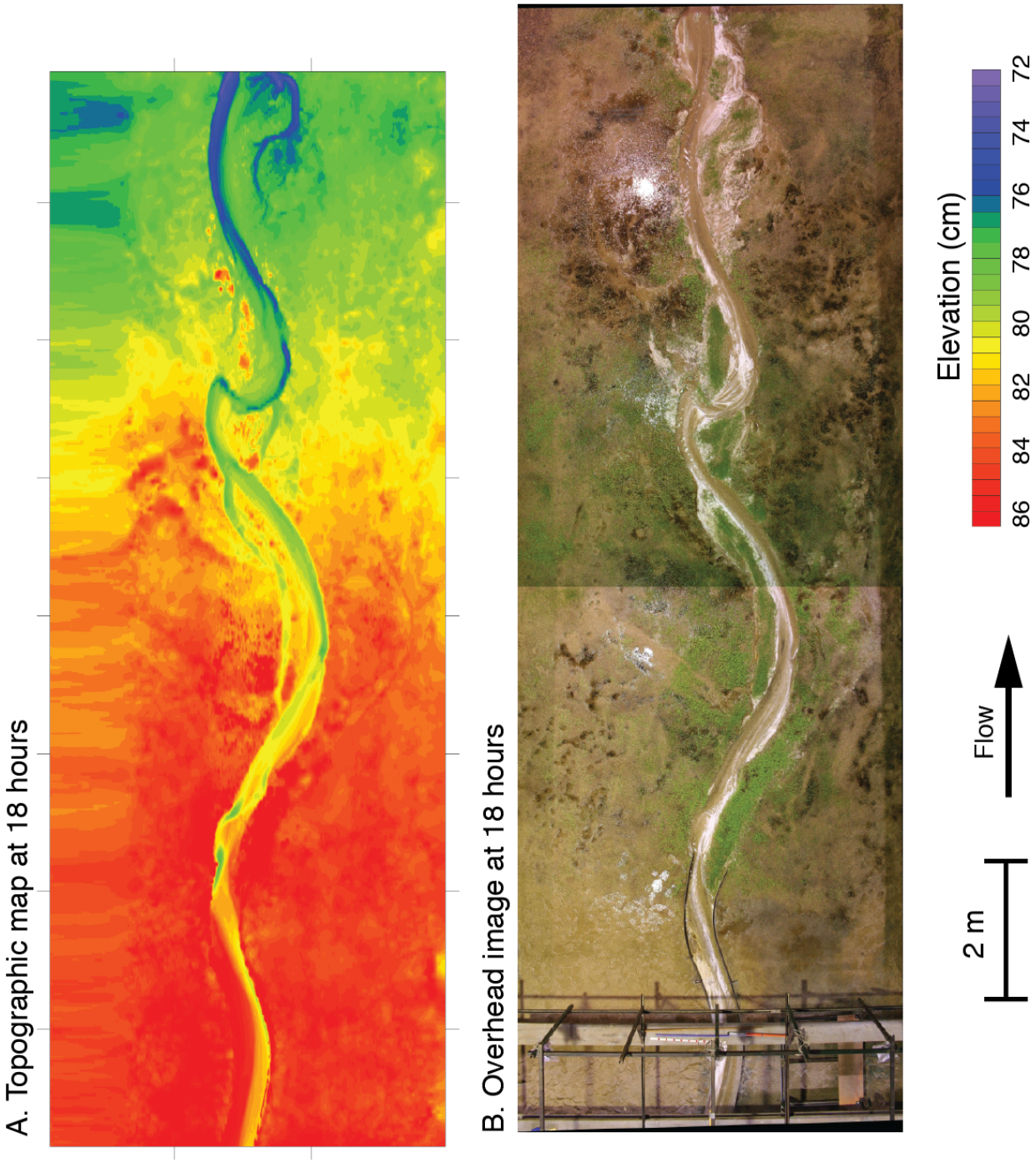


Figure D.4. Bed topography and overhead image at 18 hours.

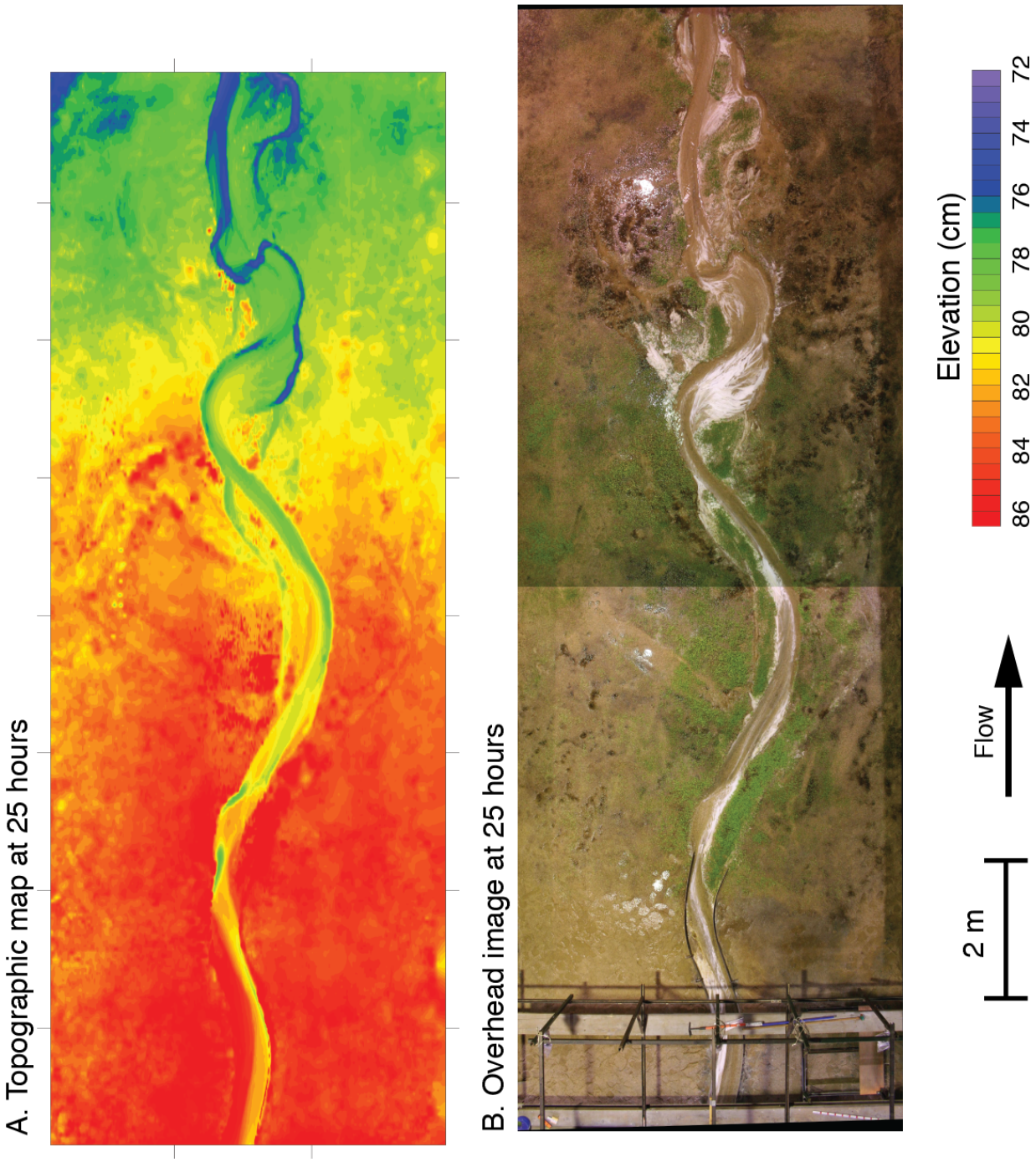


Figure D.5. Bed topography and overhead image at 25 hours.

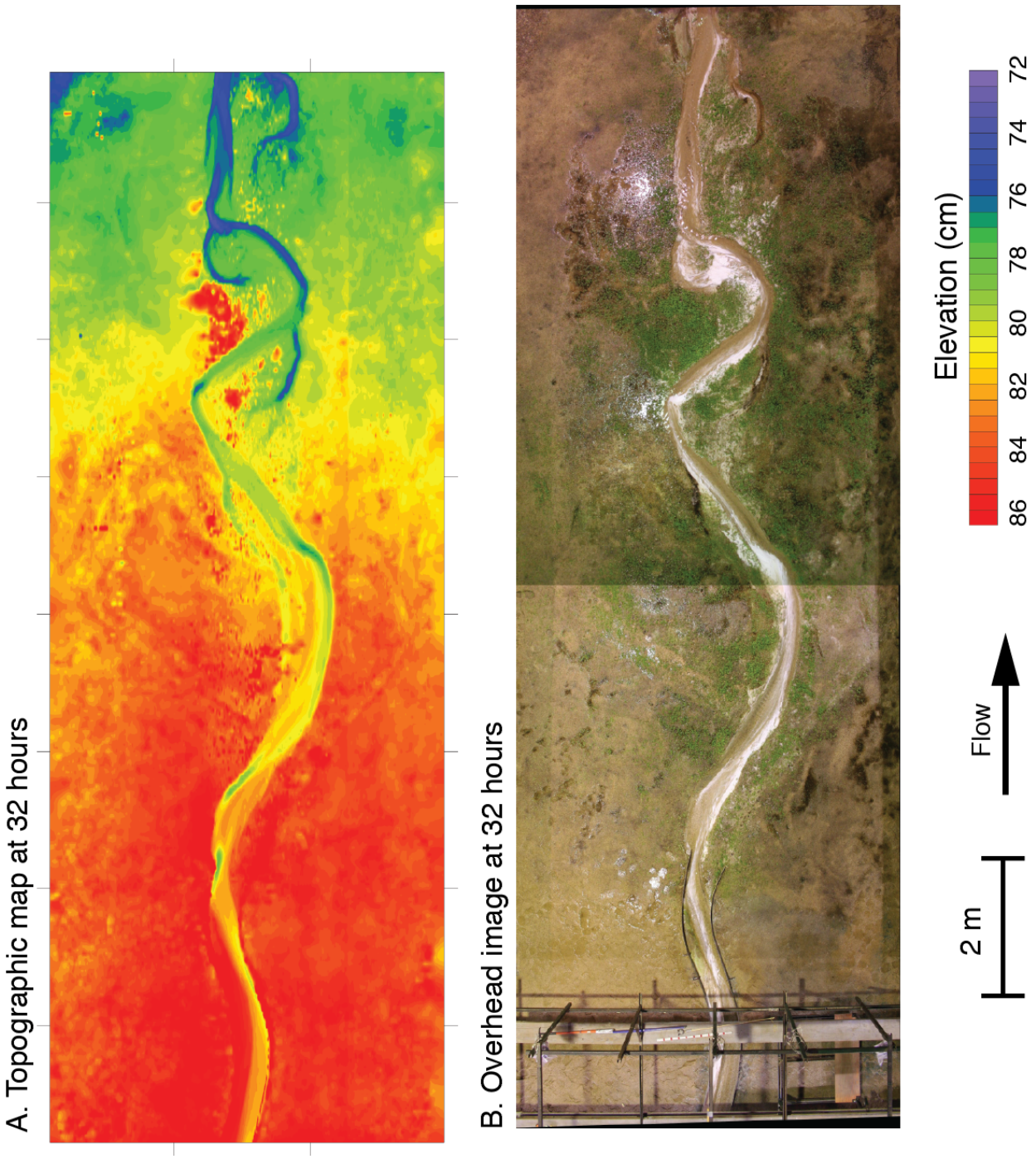


Figure D.6. Bed topography and overhead image at 32 hours.

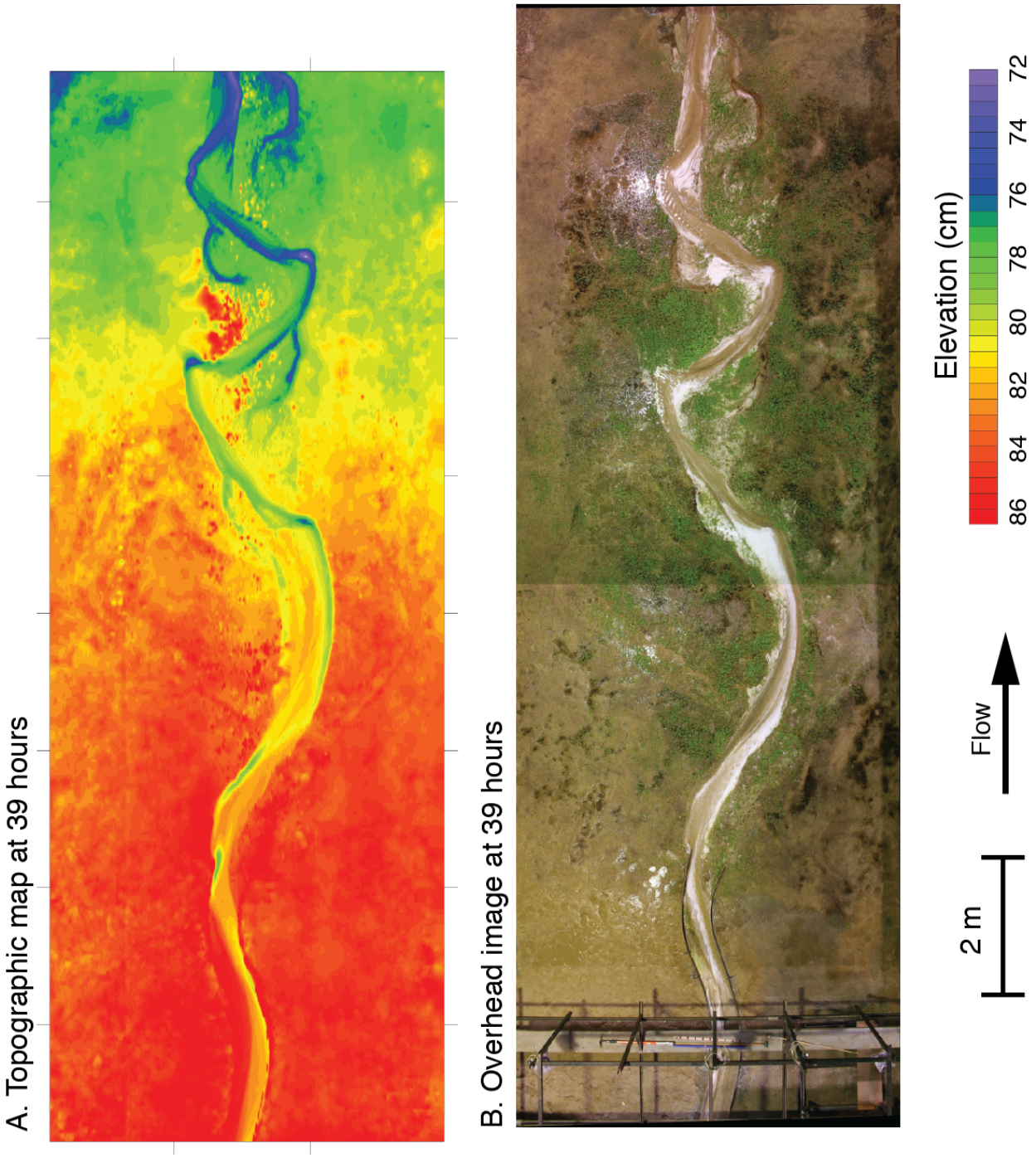


Figure D.7. Bed topography and overhead image at 39 hours.

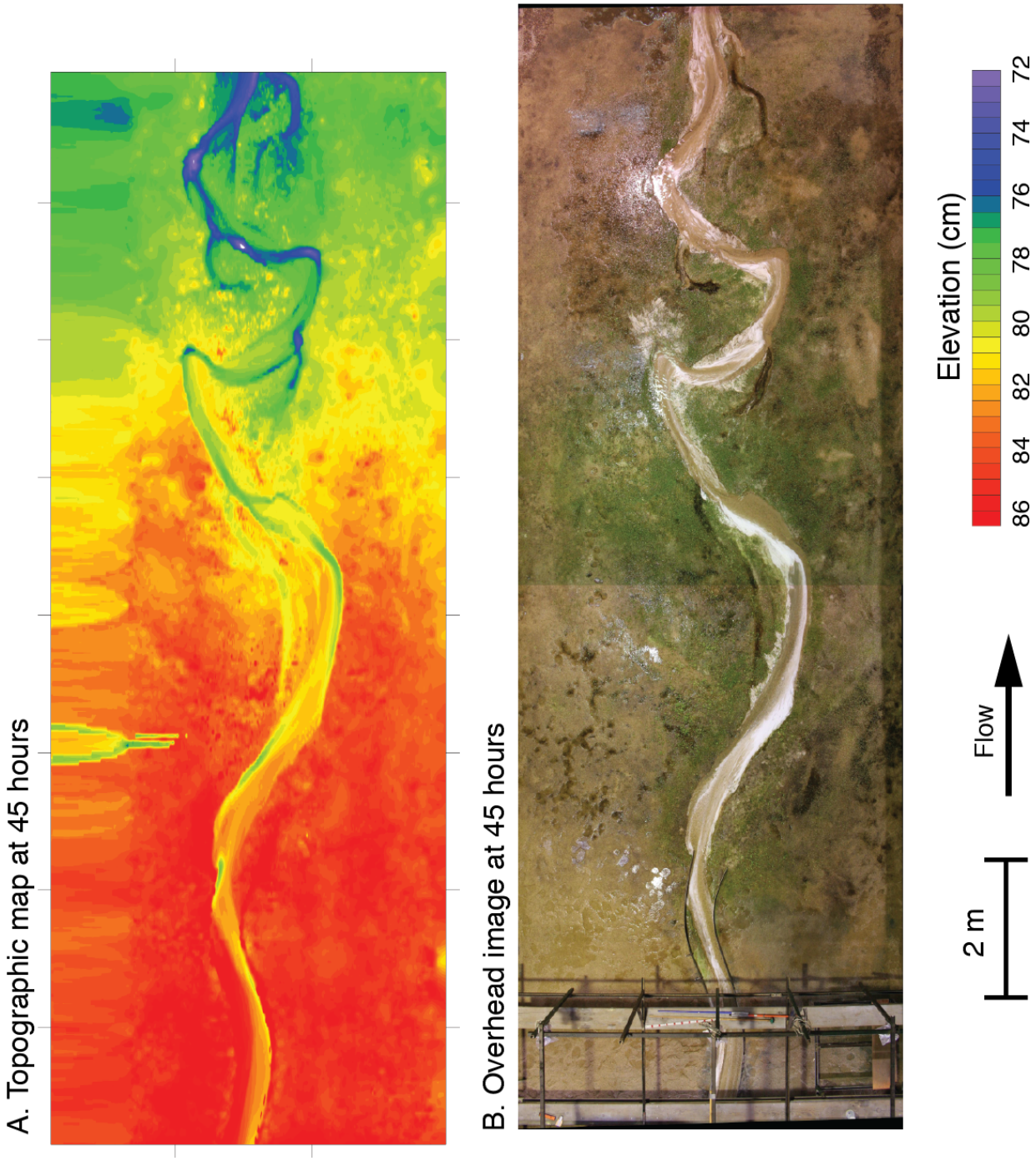


Figure D.8. Bed topography and overhead image at 45 hours.

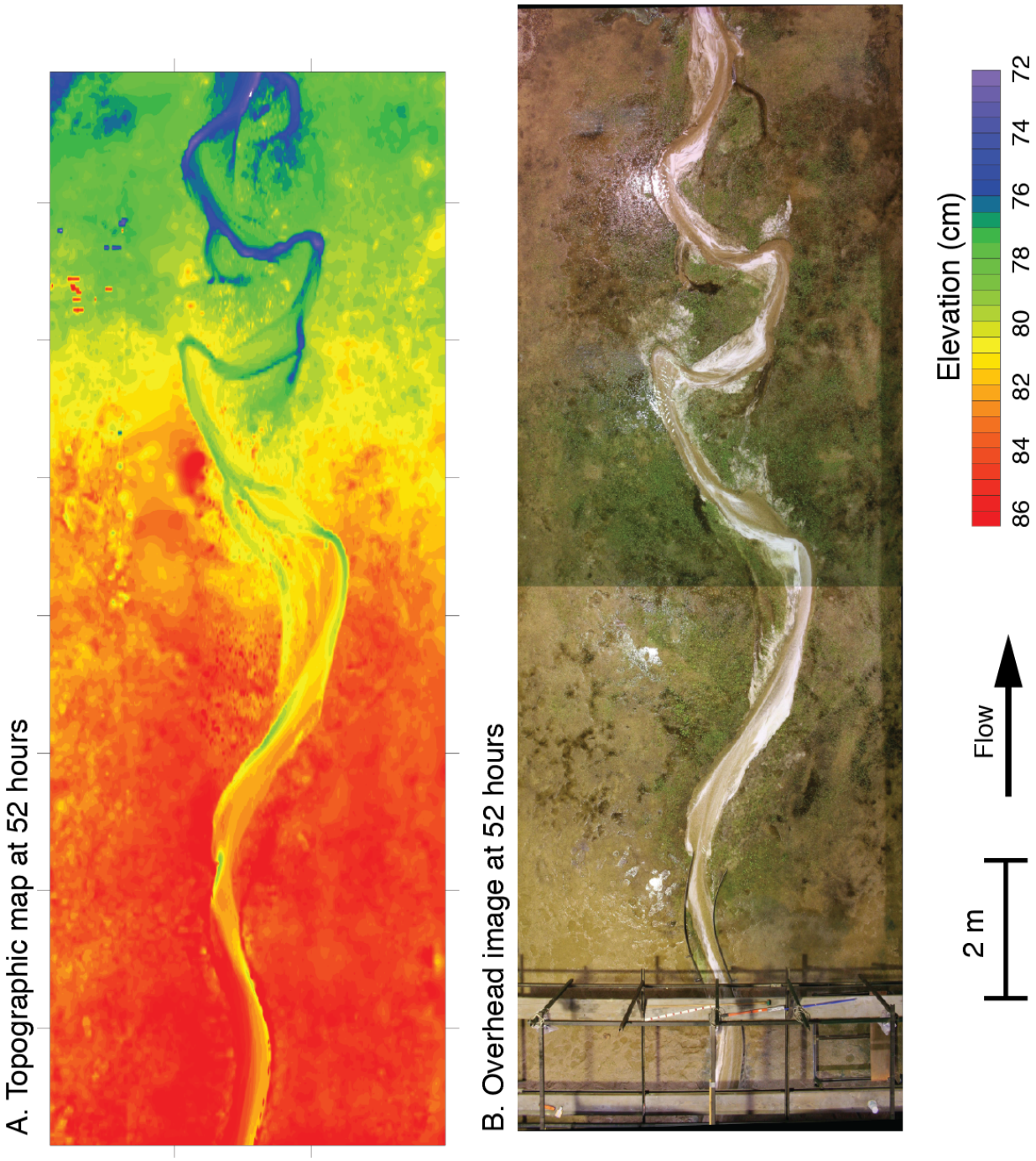


Figure D.9. Bed topography and overhead image at 52 hours.

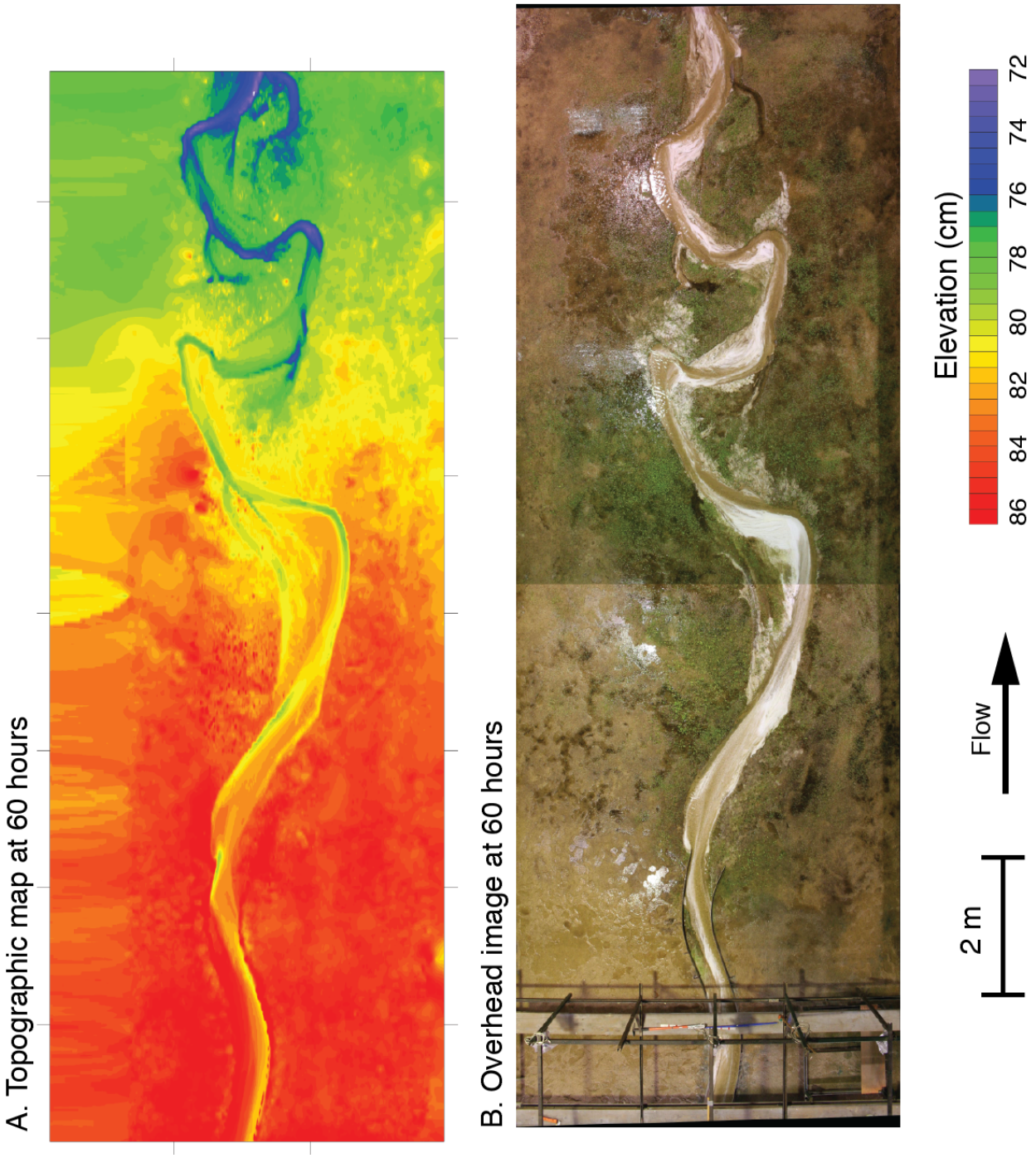


Figure D.10. Bed topography and overhead image at 60 hours.

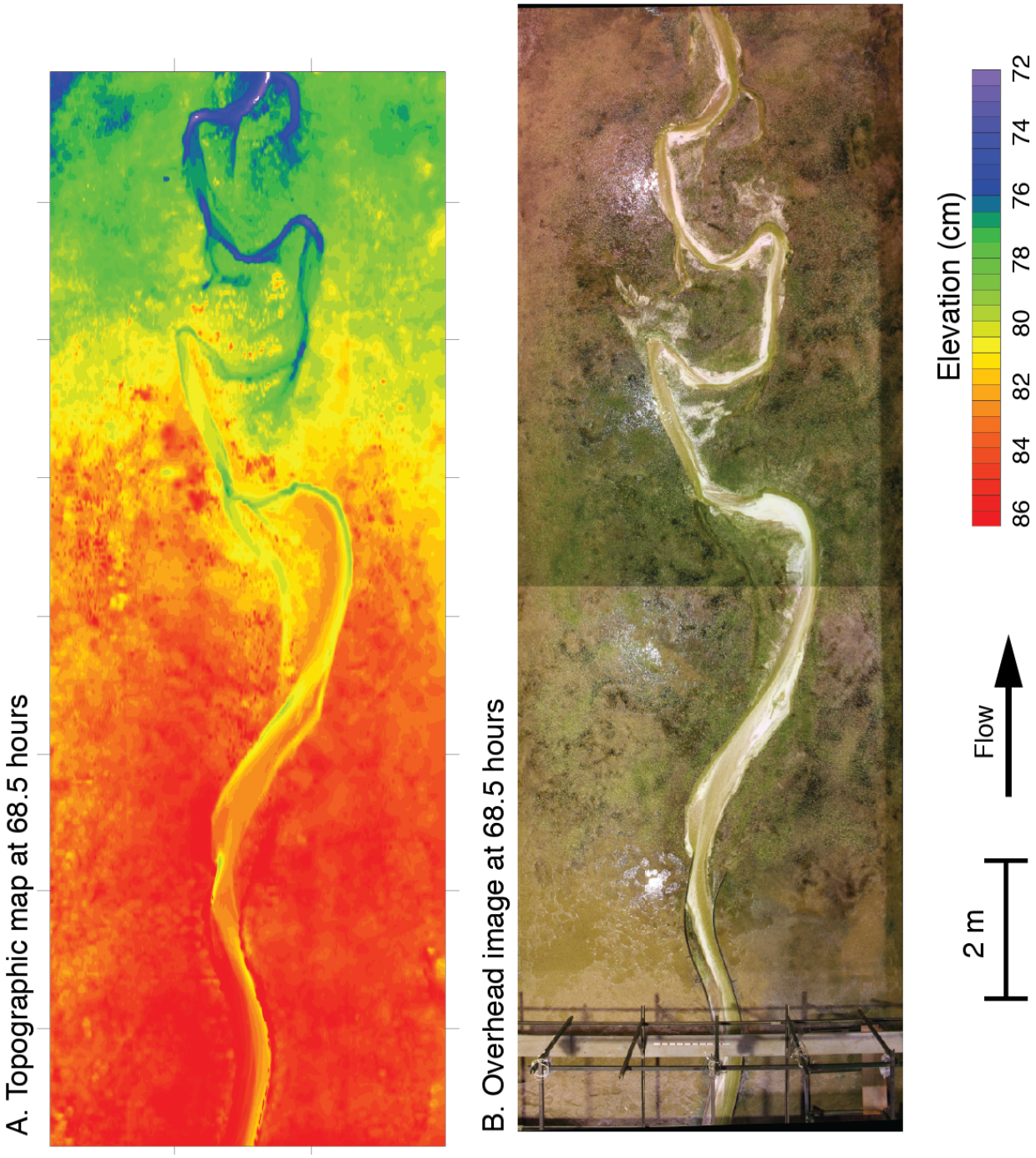


Figure D.11. Bed topography and overhead image at 68.5 hours.

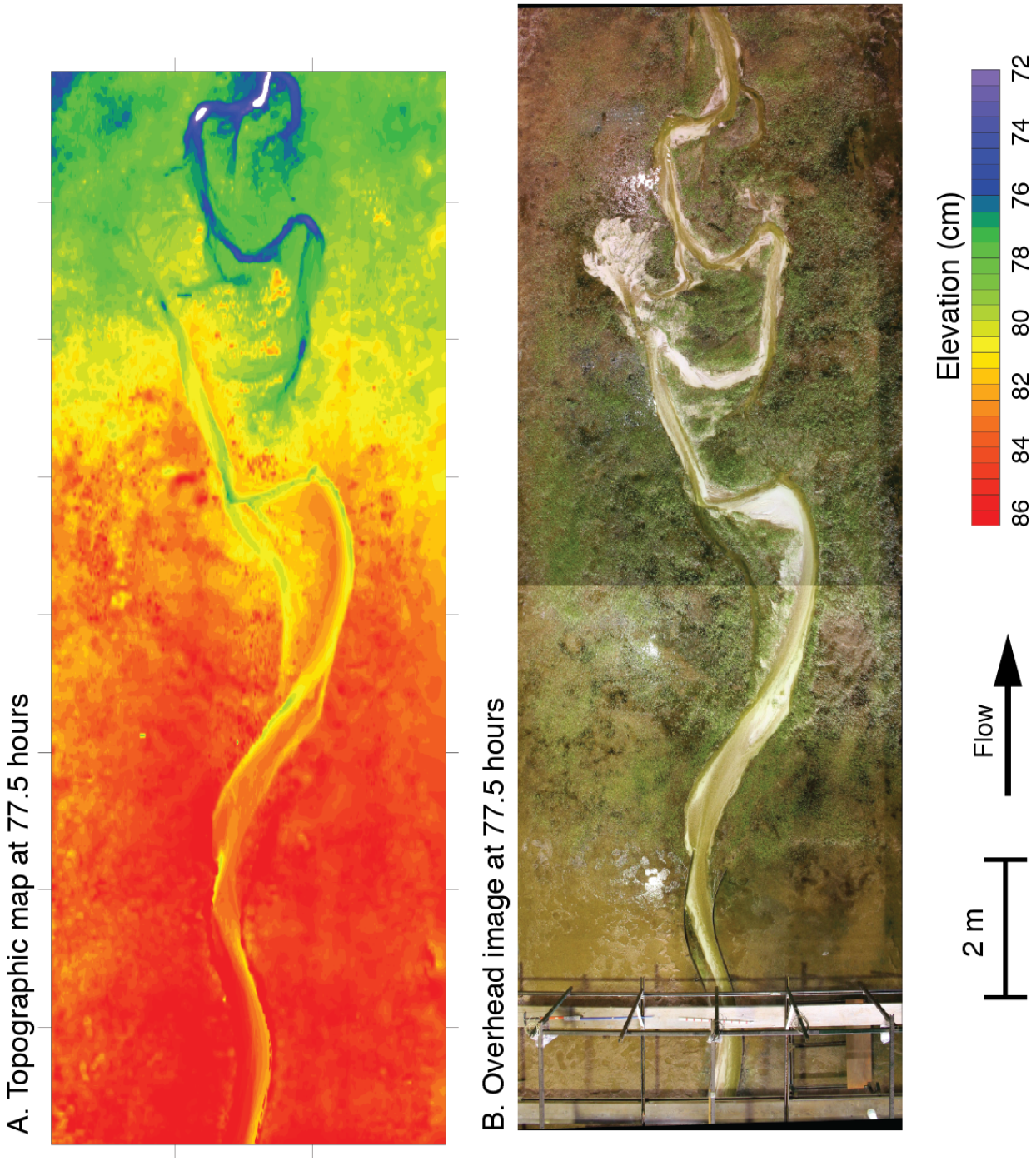


Figure D.12. Bed topography and overhead image at 77.5 hours.

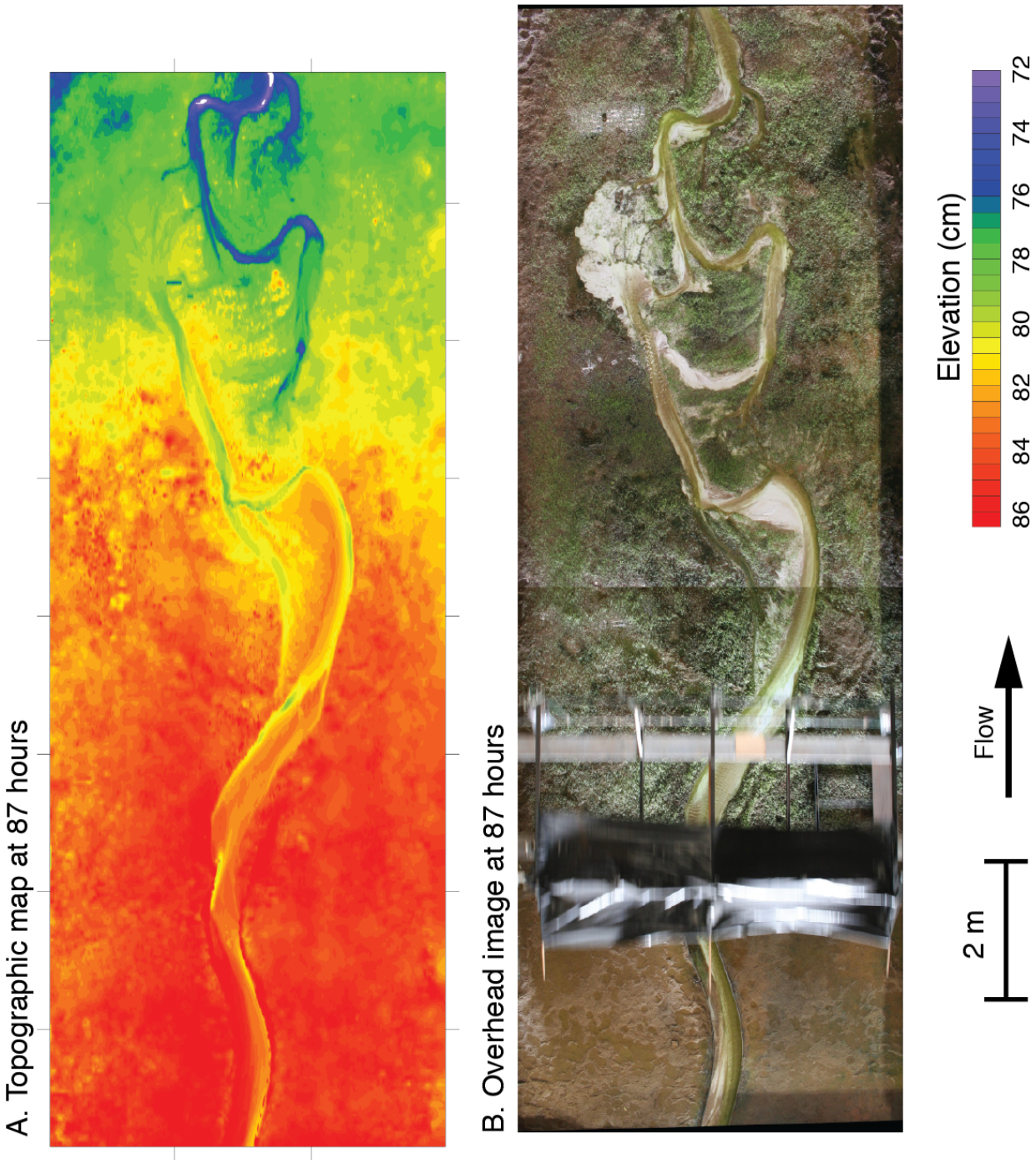


Figure D.13. Bed topography and overhead image at 87 hours.

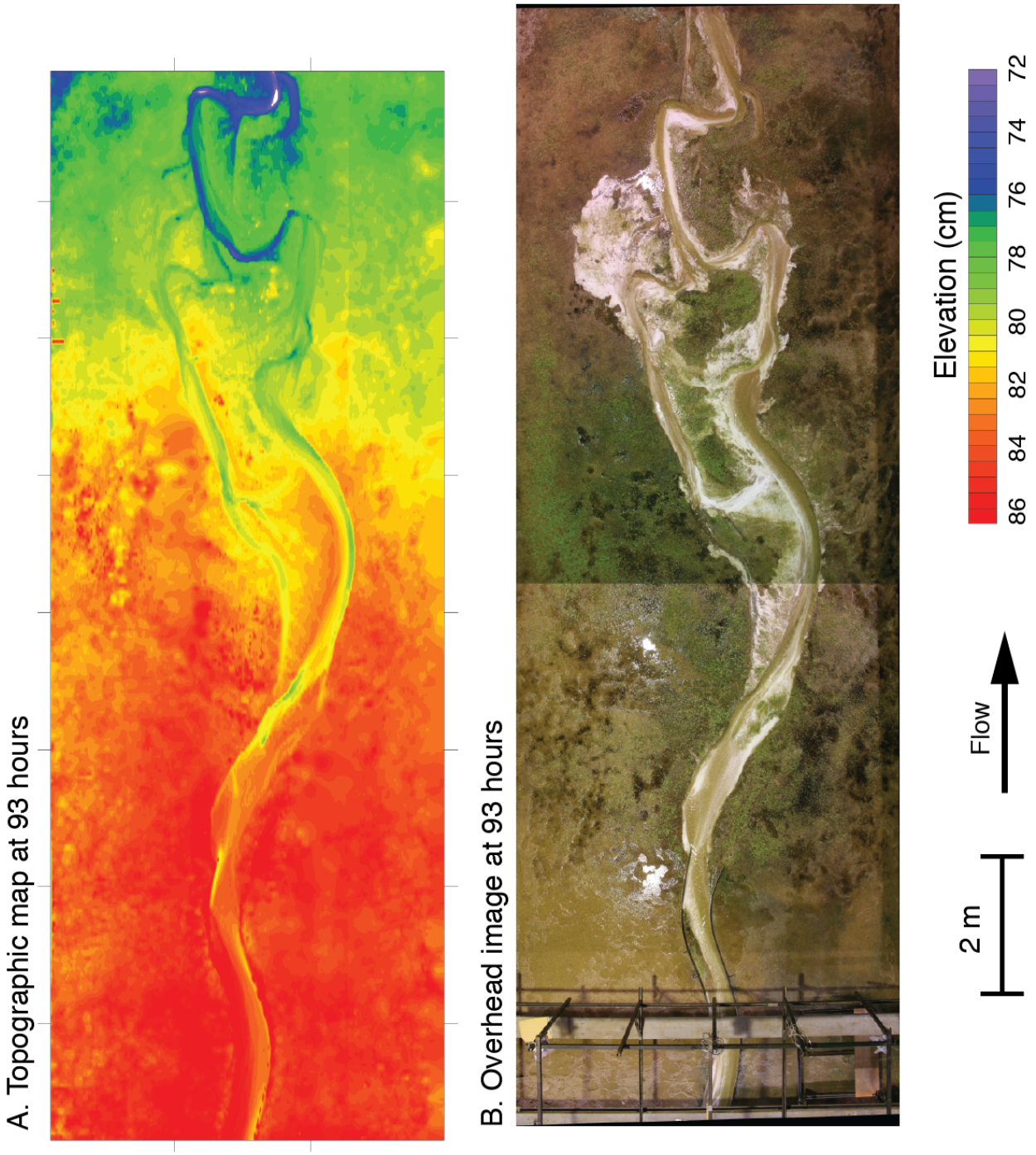


Figure D.14. Bed topography and overhead image at 93 hours.

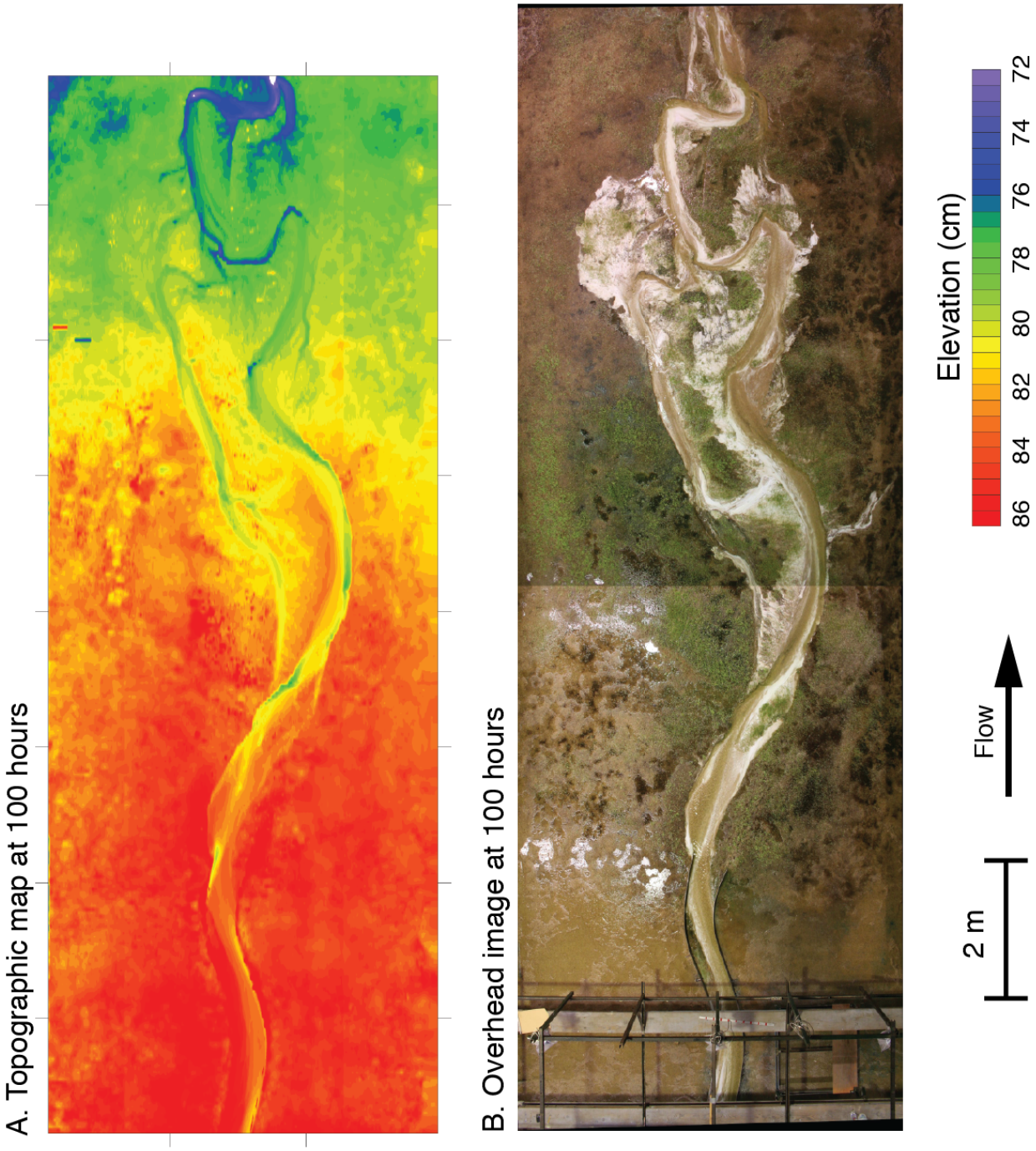


Figure D.15. Bed topography and overhead image at 100 hours.

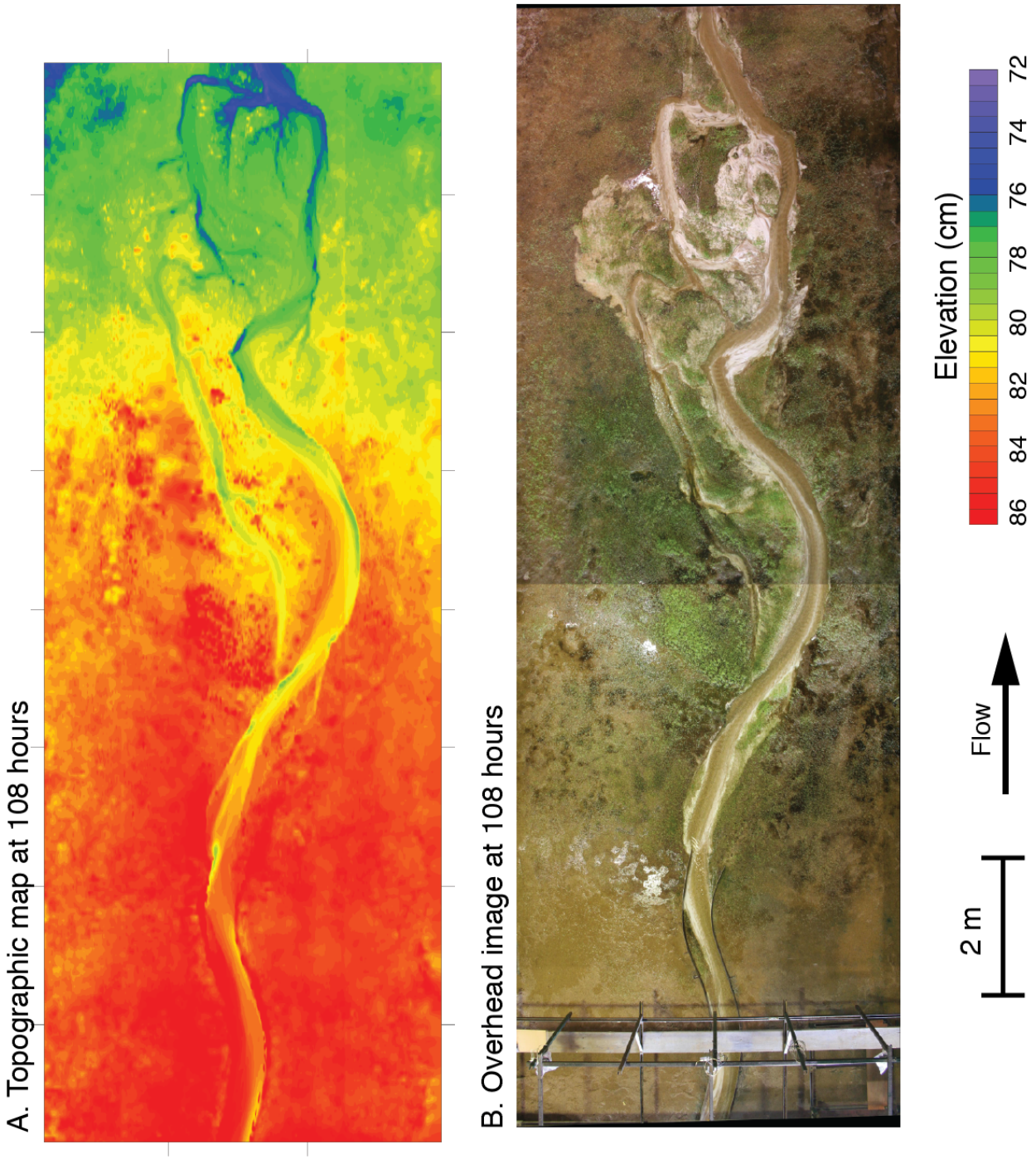


Figure D.16. Bed topography and overhead image at 108 hours.

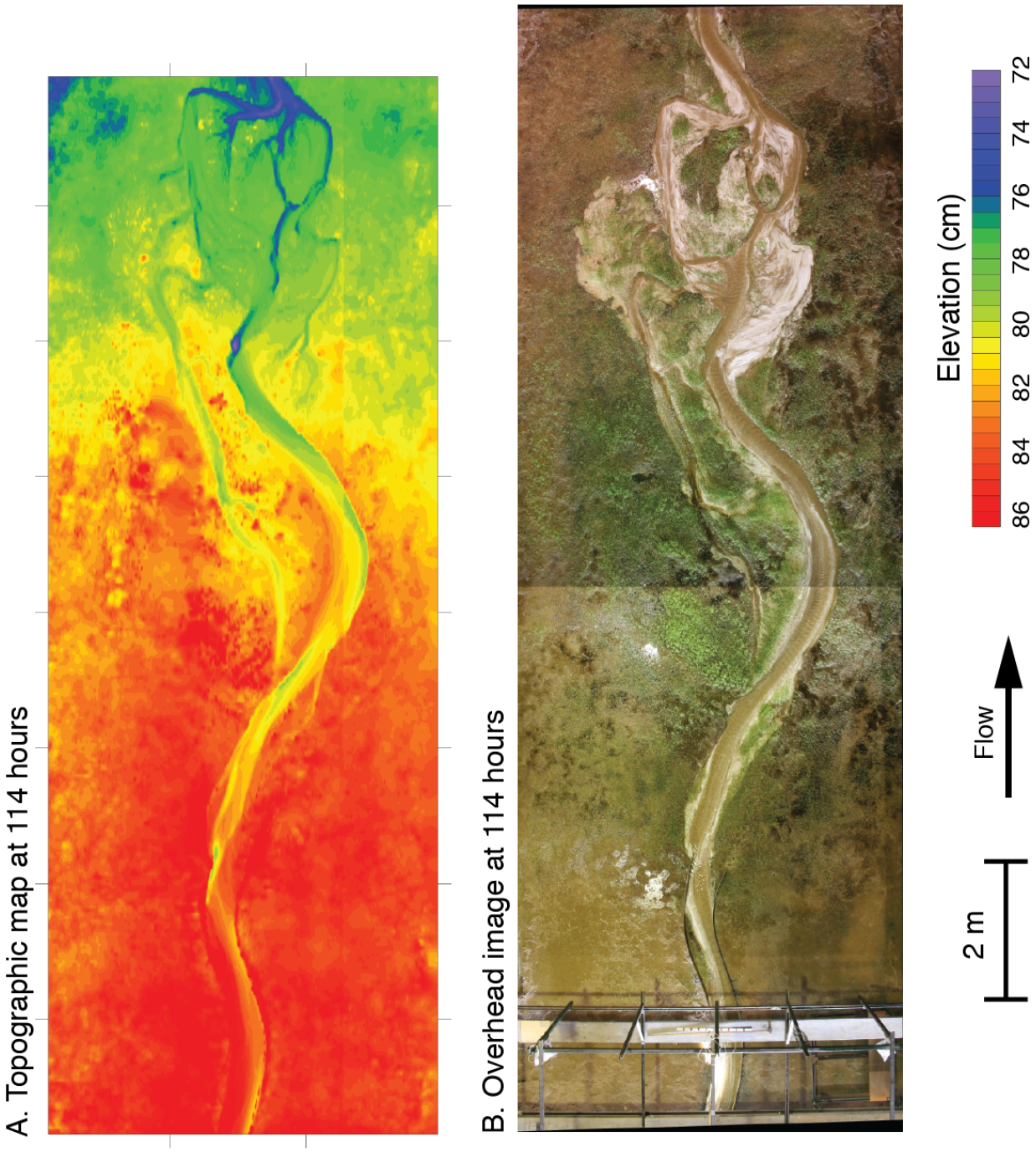


Figure D.17. Bed topography and overhead image at 114 hours.

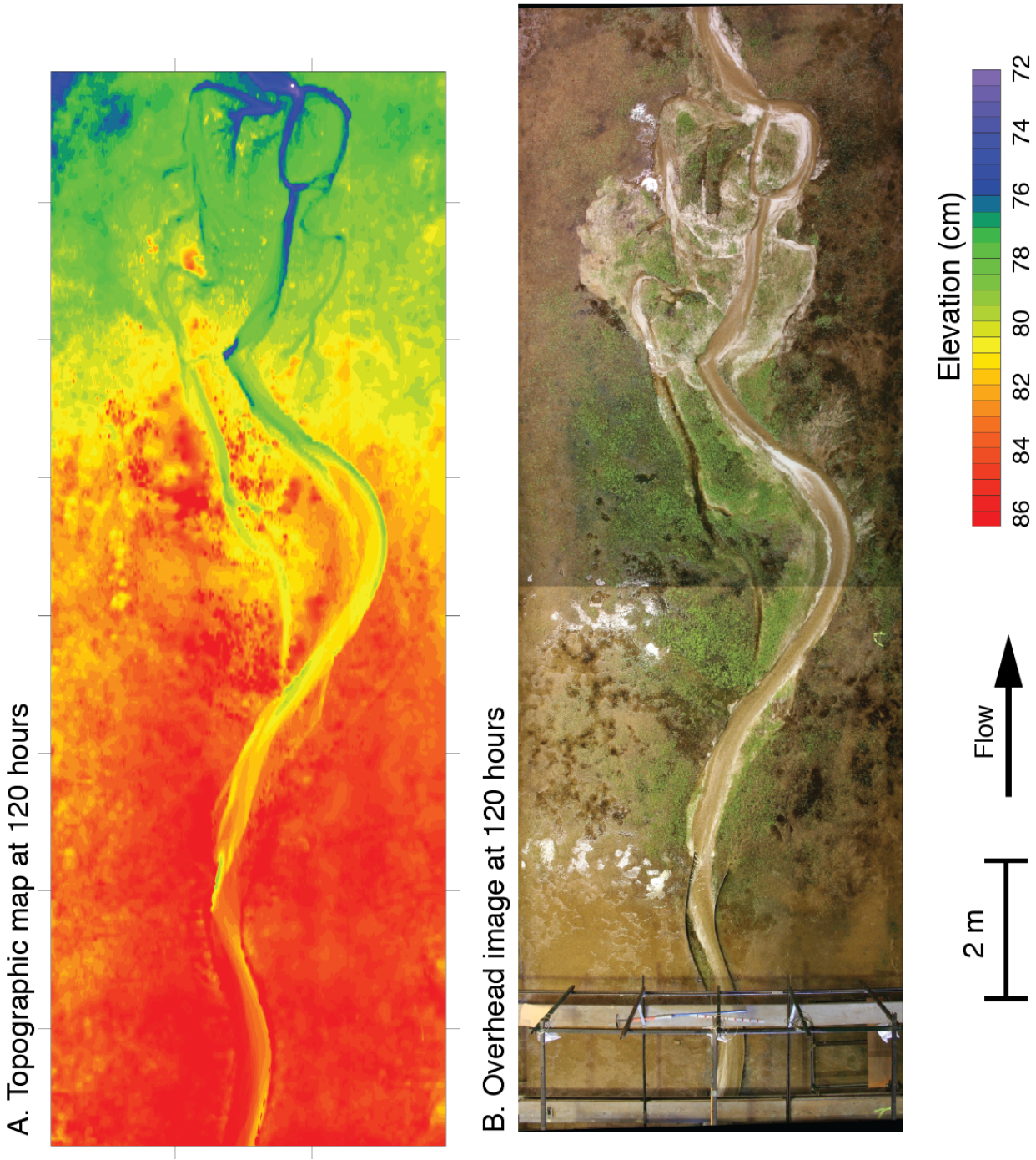


Figure D.18. Bed topography and overhead image at 120 hours.

## Appendix E-References used in the appendices


Aalto, R., Lauer, J. W. and Dietrich, W. E. (2008). Spatial and temporal dynamics of sediment accumulation and exchange along Strickland River floodplains (Papua New Guinea) over decadal-to-centenial timescales. Journal of Geophysical Research, 113, F01S04.

Allmendinger, N. E., Pizzuto, J. E., Potter, N., Johnson, T. E. and Hession, W. C. (2005). The influence of riparian vegetation on stream width, eastern Pennsylvania, USA. Geological Society of America Bulletin, 117(1), 229.

Andrews, E. D. (1984). Bed-material entrainment and hydraulic geometry of gravel-bed rivers in Colorado. Bulletin of the Geological Society of America, 95(3), 371-378.

Andrews, E. D. (1979). Hydraulic adjustment of the East Fork River, Wyoming to the supply of sediment. Adjustments of the Fluvial System. George Allen and Unwin, London, 69-94.

Andrews, E. D. (1994). Marginal bed load transport in a gravel bed stream, Sagehen Creek, California. Water Resources Research, 30(7), 2241-2250.

Beck, S., Melfi, D.A. & Yalamanchili, K. (1984). River Meandering, Lateral migration of the Genesee river, New York. pp. 510-7.

Beechie, T. J., Liermann, M., Pollock, M. M., Baker, S. and Davies, J. (2006). Channel pattern and river-floodplain dynamics in forested mountain river systems. Geomorphology, 78(1-2), 124-141.

Beeson, C. E. and Doyle, P. F. (1995) Comparison of bank erosion at vegetated and non-vegetated channel bends. JAWRA Journal of the American Water Resources Association, 31(6), 983-990.

Biedenharn, D.S. (1984). River Meandering, Channel response on the Little Tallahatchie River downstream of Sardis Dam. pp. 500-9.

Blacknell, C. (1982). Morphology and surface sedimentary features of point bars in Welsh gravel-bed rivers. Geological Magazine, 119(02), 181-192.

Bluck, B. J. (1971). Sedimentation in the meandering River Endrick, Edinburgh Geological Society.

Bridge, J.S. & Jarvis, J. (1976). Flow and sedimentary processes in the meandering river South Esk, Glen Clova, Scotland, Earth surface processes, 1(4), pp. 303-36.

Brierley, G. J. and Hickin, E. J. (1991). Channel planform as a non-controlling factor in fluvial sedimentology: the case of the Squamish River floodplain, British Columbia. Sedimentary Geology, 75(1-2), 67-83.

Carson, M. A. (1984). The meandering-braided river threshold: A reappraisal. Journal of Hydrology, 73, 315-334.

Charlton, F. G., Brown, P. M. and Benson, R. W. (1978). The hydraulic geometry of some gravel rivers in Britain, Hydraulics Research Station (Great Britain).

Church, M. and Rood, K. (1983). Catalogue of alluvial river channel regime data.

Clayton, J. A. (2010). Local sorting, bend curvature, and particle mobility in meandering gravel bed rivers. Water Resources Research, 56, W02601.

Clayton, J. A. and Pitlick, J. (2007). Spatial and temporal variations in bed load transport intensity in a gravel bed river bend. Water Resources Research, 43(2), W02426.

Constantine, C. R., Dunne, T. and Hanson, G. J. (2009). Examining the physical meaning of the bank erosion coefficient used in meander migration modeling. Geomorphology, 106(3-4), 242-252.

Darby, S. E., Rinaldi, M. and Dapporto, S. (2007). Coupled simulations of fluvial erosion and mass wasting for cohesive river banks. Journal of Geophysical Research, 112(F3).

Dietrich, W.E. & Smith, J.D., (1983). Influence of the point bar on flow through curved channels, Water Resources Research, 19(5), pp. 1173-92.
Dietrich, W. E. and Whiting, P. (1989). Boundary shear stress and sediment transport in river meanders of sand and gravel" in Ikeda, S. and Parker, G., (ed.) River Meandering, American Geophysical Union Water Resources Monograph. Washington DC, American Geophysical Union , 1-50.
Dunne, T., Dietrich, W. E., Humphrey, N. F. and Tubbs, D. W. (1981). Geologic and geomorphic implications for gravel supply. Proceedings of the Conference on Salmon-Spawning Gravel: A Renewable Resource in the Pacific Northwest, 75-100.
Elliott, J. G., and Gyetvai, S. (1999). Channel-pattern Adjustments and Geomorphic Characteristics of Elkhead Creek, Colorado, 1937-97, US Dept. of the Interior, US Geological Survey.
Emmett, W. W. (1972). The hydraulic geometry of some Alaskan streams south of the Yukon River. US Geological Survey Open File Report, 102.
Ferguson, R. and Ashworth, P. (1991). Slope-induced changes in channel character along a gravel-bed stream: The Allt Dubhaig, Scotland. Earth surface processes and landforms, 16(1), 65-82.
Forbes, D. L. (1983). Morphology and sedimentology of a sinuous gravel-bed channel system: lower Babbage River, Yukon coastal plain, Canada. Modern and ancient fluvial systems, 195-206.
Gay, G. R., Gay, H. H., Gay, W. H., Martinson, H. A., Meade, R. E. and Moody, J. A. (1998). Evolution of cutoffs across meander necks in Powder River, Montana, USA. Earth Surface Procceses and Landforms, 23, 651-662.
Gregory, K. J., Werritty, A., Lewin, J., Harvey, A. M., Macklin, M. G., Gregory, K. J., et al. (1997). Fluvial Geomorphology of Great Britain, Chapman & Hall London.
Griffin, E. R. and Smith, J. D. (2001). Analysis of vegetation controls on bank erosion rates, Clark Fork of the Columbia River, Deer Lodge Valley, Montana, US Department of the Interior, US Geological Survey.
Gustavson, T. C. (1978). Bed forms and stratification types of modern gravel meander lobes, Nueces River, Texas. Sedimentology, 25(3), 401-426.
Hession, W. C., Pizzuto, J. E., Johnson, T. E. and Horwitz, R. J. (2003). Influence of bank vegetation on channel morphology in rural and urban watersheds: Geology, v. 31.
Hey, R. D. and Thorne, C. R. (1986). Stable channels with mobile gravel beds. Journal of Hydraulic Engineering, 112(8), 671-689.
Hickin, E. J. (1988). Lateral migration rate of river bends" in Cheremisinoff, P. N. Chereminisoff, N. P. and Cheng, S. L., (ed.) Civil Engineering Practice Vol. 2: Hydraulics and Mechanics. Technomic, 419-445.
Hickin, E. J. and Nanson, G. C. (1975). The Character of channel migration on the Beatton River, Northeast British Columbia, Canada. Bulletin of the Geological Society of America, 86(4), 487-494.
Hickin, E. J. and Nanson, G. C. (1984). Lateral migration rates of river bends. Journal of Hydraulic Engineering, 110(11), 1557-1567.
Hooke, J. (2003). River meander behaviour and instability: a framework for analysis. Transactions of the Institute of British Geographers, 28(2), 238-253.
Hooke, J. M. (1995). River channel adjustment to meander cutoffs on the River Bollin and River Dane, northwest England. Geomorphology, 14(3), 235-253.

Ikeda, H. (1989). Sedimentary controls on channel migration and origin of point bars in sand-bedded meandering rivers. Water Resources Monograph, 12, 51-68.
Iseya, F. & Ikeda, H. (1989). Sedimentation in coarse-grained sand-bedded meanders: distinctive deposition of suspended sediment, Sedimentary Facies in the Active Plate Margin, pp. 81-112.
Juracek, K. E. (1999). Geomorphic effects of overflow dams on the lower Neosho River, Kansas, US Department of the Interior, US Geological Survey.
Juracek, K. E. and Perry, C. A. (2005). Gravel Sources for the Neosho River in Kansas, 2004.
Kellerhals, R., Neill, C. R. and Bray, D. I. 1972, Hydraulic and geomorphic characteristics of rivers in Alberta, Alberta Cooperative Research Program in Highway and River Engineering.
King, J. G., Emmett, W. W., Whiting, P. J., Kenworthy, R. P. and Barry, J. J. (2004). Sediment transport data and related information for selected coarse-bed streams and rivers in Idaho, US Department of Agriculture, Forest Service, Rocky Mountain Research Station.
Kleinhans, M. G. and van den Berg, J. H. (2010). River channel and bar patterns explained and predicted by an empirical and physics-based method. Earth Surface Processes and Landforms.
Kostohrys, J. and Sterin, B. B. (1996). Water resources of Birch Creek National Wild river, Alaska: stream gaging data from 1989 to 1994, US Bureau of Land Management, Alaska State Office.
Larsen, E. W. (1995). Mechanics and modeling of river meander migration. PhD Dissertation, UC Berkeley.
Lassettre, N. S., Piégay, H., Dufour, S. and Rollet, A. J. (2008). Decadal changes in distribution and frequency of wood in a free meandering river, the Ain River, France. Earth Surface Processes and Landforms, 33(7), 1098-1112.
Lauer, J. W. and Parker, G. (2008). Modeling framework for sediment deposition, storage, and evacuation in the floodplain of a meandering river: Application to the Clark Fork River, Montana. Water Resources Research, 44(8).
Lauer, J. W. and Parker, G. (2008). Net local removal of floodplain sediment by river meander migration. Geomorphology, 96(1-2), 123-149.
Leopold, L. B. (1973) River channel change with time: an example address as Retiring President of The Geological Society of America, Minneapolis, Minnesota, November 1972. Geological Society of America Bulletin, 84(6), 1845-1860.
Leopold, L. B. and Wolman, M. G. (1957). River channel patterns: Braided, meandering and straight. US Geological Survey Professional Paper 282-B, 282-B, 85 pp.
Levey, R. A. (1977). Bed-form distribution and internal stratification of coarse-grained point bars, Upper Congaree River, SC.
Lewin, J. (1976). Initiation of bed forms and meanders in coarse-grained sediment. Geological Society of America Bulletin, 87, 281-285.
Lewin, J. (1978). Meander development and floodplain sedimentation: A case study from mid-wales. Geological Journal, 13(1), 25-36.
Luchi, R., Hooke, J. M., Zolezzi, G. and Bertoldi, W. (2010). Width variations and mid-channel bar inception in meanders: River Bollin (UK). Geomorphology, 119(1-2), 1-8.
MacDonald, T. E., Parker, G., Leuthe, D. and Laboratory, S. A. F. H. (1991). Inventory and analysis of stream meander problems in Minnesota. Inventory and analysis of stream meander problems in Minnesota.

Marston, R. A., Girel, J., Pautou, G., Piegay, H., Bravard, J. P. and Arneson, C. (1995). Channel metamorphosis, floodplain disturbance, and vegetation development: Ain River, France. Geomorphology, 13(1-4), 121-131.
McGowen, J. H. and Garner, L. E. (1970). Physiographic features and stratification types of coarse grained point bars: modern and ancient examples. Sedimentology, 14, 77-111.
McKean, J. A., Isaak, D. J. and Wright, C. W. (2008). Geomorphic controls on salmon nesting patterns described by a new, narrow-beam terrestrial–aquatic lidar. Frontiers in Ecology and the Environment, 6(3), 125-130.
Micheli, E. R., Kirchner, J. W. and Larsen, E. W. (2004). Quantifying the effect of riparian forest versus agricultural vegetation on river meander migration rates, central Sacramento River, California, USA. River Research and Applications, 20(5), 537-548.
Micheli, E. R. and Kirchner, J. W. (2002). Effects of wet meadow riparian vegetation on streambank erosion. 2. Measurements of vegetated bank strength and consequences for failure mechanics. Earth Surface Processes and Landforms, 27, 687-697.
Nanson, G. C. (1980). A regional trend to meander migration. The Journal of Geology, 88(1), 100-108.
Osterkamp, W. R. (1978). Gradient, discharge, and particle size relations of alluvial channels in Kansas with observations on braiding. American Journal of Science, 278, 1253-1268.
Parker, G., Muto, T., Akamatsu, Y., Dietrich, W. E. and Lauer, J. W. (2008). Unravelling the conundrum of river response to rising sea-level from laboratory to field. Part II. The Fly-Strickland River system, Papua New Guinea. Sedimentology, 55(6), 1657-1686.
Piegay, H. and Gurnell, A. M. (1997). Large woody debris and river geomorphological pattern: examples from S.E. France and S. England. Geomorphology, 19, 99-116.
Rowland, J. C., Dietrich, W. E., Day, G. and Parker, G. (2009). Formation and maintenance of single□thread tie channels entering floodplain lakes: Observations from three diverse river systems. Journal of Geophysical Research, 114(F2).
Rozovskii, I.L., (1957). Flow of water in bends of open channels, Academy of Sciences of the Ukrainian SSR.
Sambrook Smith, G. H. and Ferguson, R. I. (1995). The gravel-sand transition along river channels. Journal of Sedimentary Research, 65, 423-430.
Schattner, I. (1962). The Lower Jordan Valley: a study in the fluviomorphology of an arid region, Magnes Press, Hebrew University.
Schumm, S. A., Dumont, J. F. and Holbrook, J. M. (2000). Active tectonics and alluvial rivers, Cambridge University Press.
Smalley, M. L., Emmett, W. W. and Wacker, A. M. (1994). Annual replenishment of bed material by sediment transport in the Wind River near Riverton, Wyoming, US Department of the Interior, US Geological Survey.
Smith, J. D. (2004). The role of riparian shrubs in preventing floodplain unraveling along the Clark Fork of the Columbia River in the Deer Lodge Valley, Montana" in Bennett, S. J. and Simon, A., (ed.) Riparian Vegetation and Fluvial Geomorphology, Water Sci. Appl. vol 8., 71-85.
Smith, V.B. (2012). Geomorphology of a coastal sand-bed river: Lower Trinity River, Texas, PhD Dissertation, University of Texas, Austin

Swanson, K. M., Watson, E., Aalto, R., Lauer, J. W., Bera, M. T., Marshall, A., et al. (2008). Sediment load and floodplain deposition rates: Comparison of the Fly and Strickland rivers, Papua New Guinea. Journal of Geophysical Research, 113(F1).
Thompson, A. (1986). Secondary flows and the pool-riffle unit: A case study of the processes of meander development. Earth Surface Processes and Landforms, 11(6), 631-641.
Thorne, C. R. and Lewin, J. (1979). Bank processes, bed material movement and planform development in a meandering river. Adjustments of the Fluvial System, 117-137.
Tonina, D. and McKean, J. A. (2010). Climate change impact on salmonid spawning in low-gradient streams in central Idaho, USA (J. Tao, Q. Chen and S. Y. Liong), ed. Proceedings of 9th International Conference on Hydroinformatics 2010; 7-11 September 2010.
Tooth, S., McCarthy, T.S., Brandt, D., Hancox, P.J. & Morris, R., (2002). Geological controls on the formation of alluvial meanders and floodplain wetlands: the example of the Klip River, eastern Free State, South Africa, Earth Surface Processes and Landforms, 27(8), pp. 797-815.van den Berg, J. H. 1995, Prediction of alluvial channel pattern of perennial rivers. Geomorphology, 12(4), 259-279.
Whiting, P. J. and Dietrich, W. E. (1991). Convective accelerations and boundary shear stress over a channel bar. Water Resources Research, 27(5), 783-796.
Williams, G. P. (1978). Bank-full discharge of rivers. Water Resources Research, 14(6), 1141-1154.
Williams, G. P. (1986). River meanders and channel size. Journal of Hydrology, 88, 147-164.